



TECHNISCHE
UNIVERSITÄT
WIEN
Vienna University of Technology

Institute of Chemical Engineering
Future Energy Technology



DISSERTATION

Temperature swing adsorption process scale up from bench to pilot scale

The ViennaGreenCO₂ pilot program

ausgeführt zum Zwecke der Erlangung des akademischen Grades eines
Doktors der technischen Wissenschaften Verfahrenstechnik unter der Leitung von

Univ.Prof. Dipl.-Ing. Dr.techn. Hermann Hofbauer
Dipl.Ing. Dr.techn. Gerhard Schöny

E166

Institut für Verfahrenstechnik, Umwelttechnik und technische Biowissenschaften

eingereicht an der Technischen Universität Wien
Fakultät für Maschinenwesen und Betriebswissenschaften

von

Dipl.-Ing. Johannes Fuchs
Matrikelnummer: 0525488
Polgarstraße 13/B/6, 1220 Wien

Wien, am 28.12. 2020

.....

ABSTRACT

Although, carbon capture and storage is not undisputed, it is more and more seen as inevitable to achieve climate targets of the Paris Climate Agreement. On the other side, what is broadly accepted is, that especially the capture part of CCS is a major challenge. CO₂ scrubbing by utilization of aqueous amine solutions is still seen as the current state of the art technology. But due to the utilization of a water-based liquid, some inherent drawbacks come with this technology. Besides the large energy demand required to achieve the temperature swing necessary for removal of the CO₂ and subsequent regeneration of the liquid, the process also suffers from additional emissions of harmful species, corrosion and fouling issues as well as high investment and operating costs.

Therefore, many studies in the past two decades focused on the identification of alternative paths for separation of CO₂. One emerging technology with high potential is temperature swing adsorption (TSA). Instead of a liquid solvent, TSA for CO₂ capture utilizes a solid sorbent (usually in form of a powder) which is circulated between an adsorption reactor, where CO₂ is loaded onto the sorbent, and a regenerator, where the CO₂ is released preferably in a concentrated form. The utilization of a solid sorbent has the potential to eliminate above mentioned drawbacks or to bring a significant improvement at least. Although, TSA is not new at all, the application of TSA for capture of CO₂ from large scale sources is novel and comes with many challenges. To fully exploit advantages of solid sorbents, a sophisticated process set-up is required.

In 2015 a novel TSA set-up based on multistage fluidized beds was presented by TU Wien and a prove of concept was delivered by continuous operation of a bench scale unit. Several parameter variations indicated highly promising process performance, but various limitations and uncertainties of results at bench scale hindered further process development.

Within this work, the design of a TSA pilot plant based on multistage fluidized beds for capture of CO₂ is elaborated. Although some of the advantages of a solid sorbent over a liquid amine solvent are evident, the handling of powdery material within a continuous process is more complicated. In investigations of the process sub systems the special requirements and challenges for the multistage fluidized bed columns, sorbent transport sections, and a heat recovery system are investigated, and design solutions are derived. An essential part of this work is the integration of detailed studies on the fluid-dynamic design of multistage fluidized bed systems, heat exchanger design, as well as experimental results from bench scale and modelling results. With the gained knowledge, a design strategy for a TSA pilot unit with a capture capacity of 1 ton/day is elaborated and the main equipment is dimensioned. Furthermore, an overview of results from detailed engineering, erection and commissioning phase are presented.

KURZFASSUNG

Die großtechnische Abscheidung von CO₂ aus Kraftwerks- und Industrieabgasen ist nicht unumstritten aber immer mehr als unumgänglich anzusehen, um die Ziele aus dem Pariser Klimaabkommen zu erreichen. Unabhängig von der politischen Diskussion ist jedoch allgemein anerkannt, dass speziell die Abscheidung von CO₂ aus verdünnten Abgasströmen eine große Herausforderung darstellt. Zwar gibt es mit der CO₂ Rauchgaswäsche mittels wässriger Aminlösung bereits eine ausgereifte Technologie, jedoch bringt diese einige Nachteile mit sich. Prozessbedingt ist der Energiebedarf für die Abscheidung von CO₂ nicht zuletzt aufgrund der hohen Wärmekapazität der eingesetzten Amin Lösung hoch. Neben dem hohen Energieverbrauch bedingt der Einsatz von wässrigen Aminlösungen aber auch zusätzliche Emissionen von potenziell gesundheitsgefährdenden Stoffen, führt zu Korrosionsproblemen und bedingt hohe Investitions- und Betriebskosten

Aus oben genannten Gründen beschäftigen sich viele Studien der letzten Jahre mit neuen Technologien zur CO₂ Abscheidung. Eine vielversprechende und oft zitierte Technologie ist die Abscheidung von CO₂ mittels Temperaturwechseladsorption (TSA). Im Gegensatz zur Aminwäsche, zirkuliert bei TSA ein pulverförmiger Feststoff zwischen einem Adsorptionsreaktor, wo das CO₂ aus dem Abgas aufgenommen wird und einem Regenerationsreaktor, wo das auf dem Feststoff gebundene CO₂ meist in konzentrierter Form wieder freigegeben wird. Der Einsatz eines Feststoffes anstelle der wässrigen Lösung bietet das Potential einerseits den Energiebedarf deutlich zu senken, und andererseits auch einige der obengenannten Probleme zu eliminieren oder zumindest deutliche Verbesserungen zu erzielen. TSA ist zwar kein grundlegend neuer Prozess und in verschiedenen Industriebereichen schon seit langem im Einsatz, der Einsatz der Technologie für die großtechnische CO₂ Abscheidung aus Industrie- und Kraftwerksabgasen birgt jedoch viele Herausforderungen, die ein gut durchdachtes Anlagenkonzept bedürfen.

Im Jahr 2015, wurde ein neuartiges Konzept zur Abscheidung von CO₂ mittels TSA in mehrstufigen Wirbelschichtreaktoren von der TU Wien vorgestellt und innerhalb einer eigens entwickelten Laboranlage erfolgreich demonstriert. Das neue Konzept konnte eine vielversprechende Abscheideleistung erzielen und wurde im Zuge zahlreicher Parametervariationen im Detail untersucht.

Im Zuge dieser Arbeit, wird das Design einer darauf basierenden TSA Pilotanlage erarbeitet und vorgestellt. Im Vergleich zu den flüssigen Aminlösungen, ist die Prozessführung mit pulverförmigen Adsorbentien jedoch deutlich komplizierter. Auf die damit verbundenen technologischen Herausforderungen wird im Detail eingegangen und Lösungen für die verschiedenen Subsysteme werden erarbeitet. Wesentlicher Bestandteil dieser Arbeit ist dabei die Zusammenführung von verschiedenen Detailuntersuchungen zur wirbelschichttechnischen Auslegung der Hauptkomponenten, Untersuchungen zum Wärmeübergang, sowie Ergebnissen von Laborexperimenten und Prozessmodellierung. Aus den gewonnenen Erkenntnissen der Detailuntersuchungen wird eine Designstrategie für eine TSA Pilotanlage mit einer Abscheidekapazität von einer Tonne CO₂ pro Tag abgeleitet und die Prozesshauptkomponenten dimensioniert. Des Weiteren wird ein Überblick über die Detailplanung der Anlage sowie Ergebnisse der Errichtungs- und Inbetriebnahme Phase präsentiert.

ACKNOWLEDGEMENT

Maybe the duration of my Ph.D. study and the time it took to finish this thesis is not an all-time record, but I can definitely say, that not a single of the past years was wasted time. This, I owe mainly to my former colleagues:

Gerhard Schöny, you were the one, who invited me to join the research group and you were the one who awakened my interest in process engineering. Without you, I would have spent 3 years, watching flywheels and I would have never known how it is to be part of real team. From the very beginning, when nobody even knew that we are onto something, until ViennaGreenCO₂, when suddenly dozens of people were working on the project, I always knew that I can rely on you, as a project leader, as an excellent scientist, engineer and colleague, but first of all as a friend. Therefore, I want to deeply thank you!

Another great thanks goes to you **Hermann Hofbauer** for giving me the possibility to work in the research group, but also for your support in all these years.

Egon Zehetner, Elisabeth Sonnleitner, Florian Dietrich, Florian Zerobin, Gerhard Hofer and Julius Pirkbauer, I want to thank you for the countless discussions we had in our projects. Without your contribution, the technology would not be where it is now. But even more important to me, is the fact, that with you, it never felt like working and I truly enjoyed being part of this team. Thank you for that!

At this point, I would also like to thank my other colleagues from the former CLC group **Karl Mayer, Michael Stollhof, Robert Pachler, Stefan Penthor and Stephan Piesenberger**. You were always open for discussions around our projects but also some of our legendary after work activities will be never forgotten.

Also, I want to thank the ViennaGreenCO₂ operating team for not giving up when we had to pass the valley of tears. Thank you, **Andreas Klingler, Benjamin Fleiß, Christoph Eder, Peter Adorjan, Stefan Arlt and Tobias Geißbüchler!**

Although, or just because you sometimes were a tough partner for negotiations during engineering and operation of the pilot, I would also like to thank you **Melina Infantino!**

Furthermore, I want to thank Bertsch Energy and **Otmar Bertsch** in particular, for the close cooperation in the ViennaGreenCO₂ project and for sharing the 3d model of the pilot plant presented in this thesis.

Finally, I want to express my greatest gratitude to my Family. I dedicate this work to my parents **Johann and Anita**, to my brother **Bernhard**, but first of all to **Janice, João and Giulia** my beloved wife and children.

TABLE OF CONTENTS

ABSTRACT	I
KURZFASSUNG	II
ACKNOWLEDGEMENT	III
TABLE OF CONTENTS	IV
1. INTRODUCTION	6
1.1 CLIMATE CHANGE MITIGATION	6
1.2 CARBON CAPTURE	8
1.3 PROBLEM DEFINITION	12
1.4 KEY OBJECTIVES AND ORGANIZATION OF THIS THESIS	14
2. BACKGROUND	16
2.1 FUNDAMENTALS OF FLUIDIZATION	16
2.2 ADSORPTION	22
2.3 MULTISTAGE FLUIDIZED BED TEMPERATURE SWING ADSORPTION	30
2.4 SUMMARY OF RESULTS FROM PREVIOUS STUDIES	41
3. PROCESS SCALE UP	45
3.1 GENERAL ASPECTS	45
3.2 TARGET APPLICATION – FULL SCALE TSA	45
3.3 TECHNOLOGICAL CHALLENGES FOR FULL SCALE TSA	46
3.4 LIMITATIONS AT BENCH SCALE	47
3.5 NEXT SCALE TSA	48
3.6 VIENNAGREENCO ₂ PILOT PROGRAM	49
3.7 DESIGN BASIS FOR THE TSA PILOT UNIT	51
4. TSA PILOT UNIT DESIGN PHILOSOPHY	61
4.1 MULTISTAGE FLUIDIZED BED COLUMN DESIGN	61
4.2 WATER CO-ADSORPTION	74
4.3 TRANSPORT SECTIONS AND GAS SEALING	76
4.4 LEAN/RICH HEAT EXCHANGE	87
5. PILOT UNIT REACTOR DESIGN	106
5.1 GENERAL PROCESS SET-UP AND KEY FIGURES	106
5.2 ADSORBER COLUMN	109
5.3 DESORBER COLUMN	113
5.4 LEAN/RICH HEAT EXCHANGE	119
5.5 PRE-REGENERATOR AND RICH RISER	120
5.6 LEAN TRANSPORT SECTION	123
5.7 REACTOR DESIGN OVERVIEW	124
5.8 DETAILED ENGINEERING	126

6. ERRECTION OF PILOT PLANT AND FIRST RESULTS.....	131
7. SUMMARY AND CONCLUSIONS.....	135
8. OUTLOOK.....	137
8.1 PRELIMINARY IMPLICATIONS ON FURTHER SCALE UP	137
8.2 OUTLOOK PILOT OPERATION AND DATA EVALUATION.....	138
NOTATION	140
LIST OF FIGURES.....	143
REFERENCES.....	146
LIST OF PUBLICATIONS	152
APPENDIX A – VIENNAGREENCO₂ P&IDS	153
APPENDIX B – PROCESS CONTROL SYSTEM.....	165

1. INTRODUCTION

1.1 CLIMATE CHANGE MITIGATION

1.1.1 Climate change

A huge amount of independent data clearly indicates an unequivocal temperature increase of our climate system, which is virtually certain caused by human activities. Atmospheric concentrations of carbon dioxide, methane and nitrous oxide, which are the most influential greenhouse gases (GHGs), have increased since the pre-industrial era and the atmospheric CO₂ concentration in particular increased to an 800 000 years all-time high. A correlation between greenhouse gas emissions and global warming is broadly seen as evident [1], [2] and a global temperature increase of approximately 1 °C within the last 100-150 years is already registered [3]. Global warming already has a big impact on various ecosystems and the current increase rate of approximately 0.2 °C per decade is alarming (see Figure 1-1). A further increase of the mean global surface temperature is expected to have tremendous negative effects on marine ecosystems, animals, and plants as well as on human beings. However, a substantial reduction of greenhouse gas emissions, can reduce global warming effects and limit its negative impact [4].

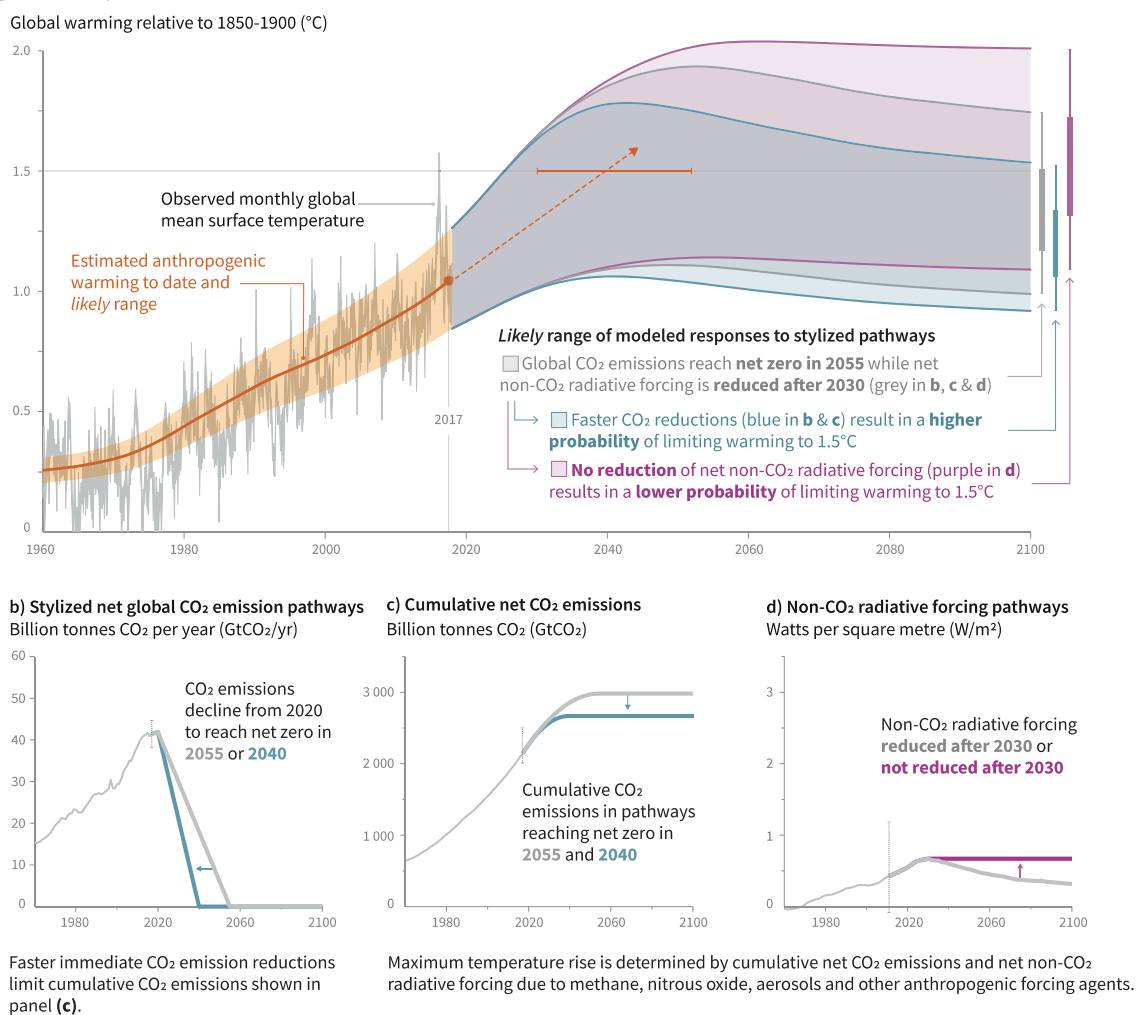


Figure 1-1: Observed and projected temperature change between 1900 and 2100 (taken from [3])

1.1.2 Mitigation of climate change

Even though, the existence of global warming and the role of GHGs has been broadly accepted and most countries committed to reduce their emissions in order to limit global warming to less than 2 °C in the Paris Agreement. The current development of GHG emissions shows some improvements in terms of reduced emission rates, but more substantial measures are required to reduce emissions and to limit global warming to 2 °C by the year 2100 [5].

The biggest contribution to the increase of GHG concentrations in the atmosphere is due to utilization of fossil fuels in the industry and energy sector. In addition, these emissions are growing further and further, because of the increasing economic output and growth of population [6]. However, climate models showed that a significant reduction of GHGs is needed as soon as possible, otherwise it will get more and more unlikely to achieve the 2 °C target or the overall costs for achieving the 2 °C target will increase drastically [7]. The international energy agency states, that global CO₂ emissions must be reduced to half of current levels until 2050 to limit the global temperature increase to 2 °C while energy consumption will increase significantly [6]. The European commission even defined the target of achieving net-zero emissions until 2050 within the EU [8]. This ambitious goal can only be achieved by a thoughtful catalogue of measures.

Looking at the different economic sectors, it can be seen, that the biggest share with 25 % of GHG emissions is related to the production of electricity and heat (see Figure 1-2). Furthermore, the energy demand from transport and buildings is expected to contribute more and more to the overall electricity demand. Most scenarios show that electricity will have to contribute to the reduction of GHG emissions in transport and emissions from buildings, so that electricity will almost double its share in final energy demand.

For that reasons, presented emission pathways for the 21st century are predicting, that especially emissions related to energy production need to be reduced to a fraction of current levels in order to achieve the 2 °C goal. The “Energy Roadmap 2050” of the European commission assumes a reduction of GHG emissions in the energy sector by over 80 % [4].

A large share of emissions is related to agriculture, forestry and other land use (AFOLU), however, the industry sector with 20 % share of direct emissions and 11 % indirect emissions is the second largest source of GHG emissions. A significant part of these emissions is not only related to burning of fossil fuels but to the technical processes itself like in steel or cement production. For numerous processes CO₂ emissions are not expected to be reduced significantly without extensive measures.

CCS is seen as bridge technology, which could help to ease the transition from fossil fuels to renewable energies. Furthermore, CCS is currently the most promising or only opportunity for several industry sectors to significantly reduce their CO₂ emissions.

This work deals with the development of a novel CO₂ capture technology. In the following, an overview of existing capture technologies as well as a closer look on the benchmark technology and the novel CO₂ capture technology will be given.

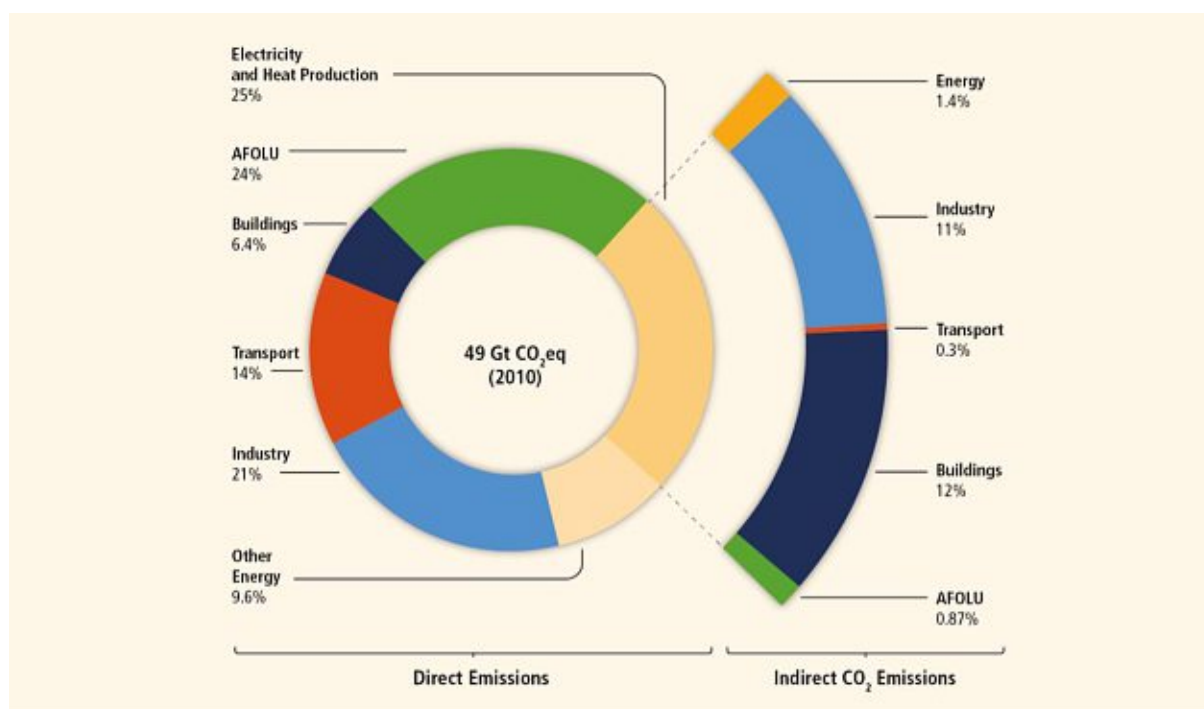


Figure 1-2: GHG emissions by economic sectors (taken from [7])

1.2 CARBON CAPTURE

1.2.1 General aspects

Carbon capture and storage (CCS) refers to several technologies that are used to obtain a preferably pure CO₂ stream, which is then liquefied, transported and sequestered in geological storages. With CCS it is at least theoretically possible to continue to utilize fossil fuels without the negative impact of CO₂ on the climate. The utilization of renewables like biomass in combination with CCS could even enable below zero emission power generation. CCS plays a substantial role in different emission scenarios for the 21st century [6], [9], [10]. However, for the intended long term storage of CO₂, potential negative effects are uncertain and the public acceptance is not guaranteed [11]. On the other hand, climate change is and will be one of the biggest challenges of our time and long-term storage of CO₂ is believed to be an important part of the transition towards a more sustainable future.

Looking at the complete CCS chain from CO₂ capture, transport, and storage of the CO₂, the main cost share is contributed by the capture part. In a CCS chain, around 75 % of total costs are estimated for the capture of CO₂ from a diluted off gas stream and currently an increase of electricity costs in the range of 50 % is assumed for power generation with CCS [12].

In parallel to CCS, there is also research activity in the field of carbon capture and utilization (CCU). In a CCU process chain, the captured CO₂ is used as a feedstock for chemical synthesis, for fertilization in agriculture, or food industry for example. However, the potential CO₂ demand is too low to be considered as a single solution. However, in some extent, CCU might be a good supplement to CCS. Nevertheless, the capture of CO₂ is again the main cost driver, which makes the technology viable or not.

1.2.2 CO₂ capture processes

In literature, various capture technologies can be found and a lot of research in different fields is currently ongoing. Most of the CO₂ capture processes can be categorized as follows (see: Figure 1-3):

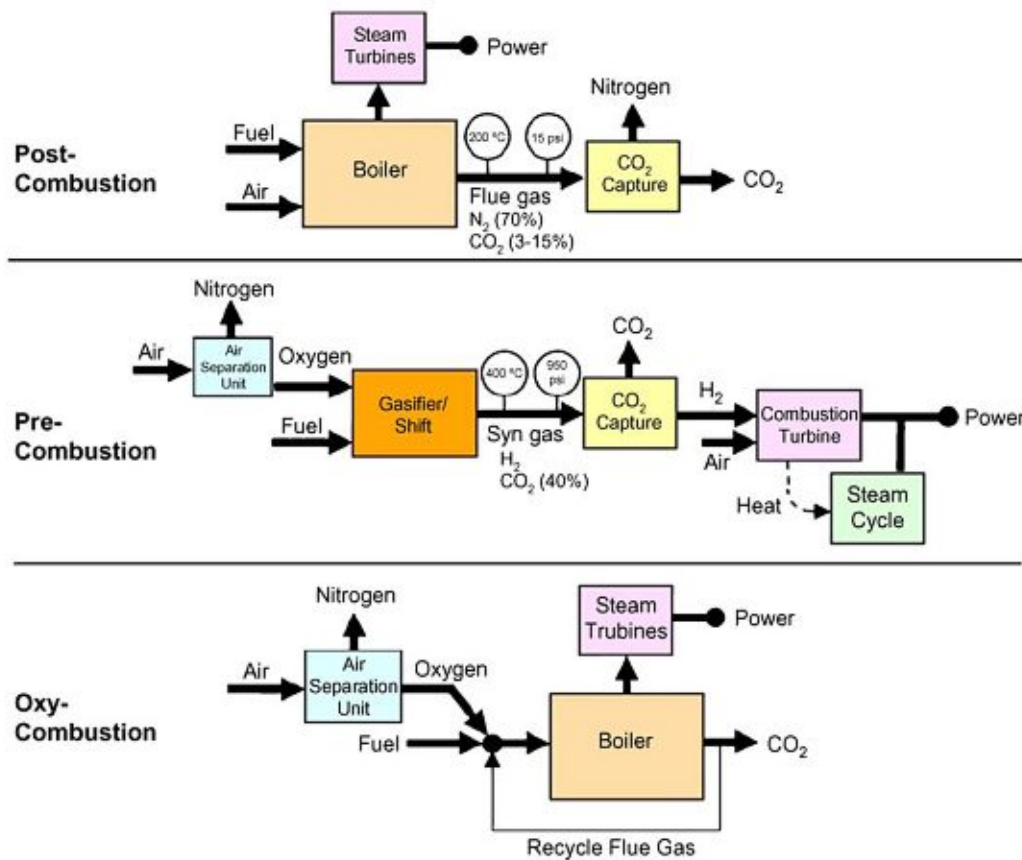


Figure 1-3: Overview of CO₂ capture processes (taken from [13])

Post-combustion processes

The term post-combustion capture refers to the point in the process chain, where the CO₂ is captured. In combustion processes, where the fuel is combusted with air the off-gas CO₂ concentration typically lies in the range of 3-15 Vol-%. This diluted CO₂ stream is then directed to the capture unit where the CO₂ is separated from the rest of the flue gas. A post combustion capture process has minimum interference with the flue gas source (e.g.: on the power plant) and the main advantage is that it can be retrofitted to existing infrastructures. Another advantage is, that the technology can also be used in the industry sector like in the production of cement or other processes with considerable amounts of CO₂ in the off-gas stream.

Pre-combustion processes

In a pre-combustion CO₂ capture process, the fuel is converted to a mixture of mainly CO₂ and H₂ within a gasification or reforming step. After separation of CO₂, the H₂ can be used for power generation or as feedstock for other processes.

Oxy-fuel processes

Oxy-fuel processes are characterized in that the fuel is combusted in a mixture of O₂ and flue gas recycle for temperature control and thus in absence of nitrogen. Without nitrogen present in the combustion process, the resulting flue gas consists mainly of CO₂ and H₂O. In order to obtain the oxygen for combustion an oxy-fuel process requires an air separation unit (e.g.: cryogenic air separator) which is primary responsible for the energy demand related to the capture of CO₂.

CO₂ Absorption

In a CO₂ absorption process, a liquid solvent (mostly an aqueous amine solution) is brought into contact with the flue gas within the absorber column where the solvent selectively takes up CO₂ from the flue gas. The absorption of CO₂ can be divided into 3 steps: The first step is the dissolution of CO₂ in the aqueous solvent, the second step is the diffusion of the CO₂ within the solvent and the third step is the reaction of the dissolved amine with the dissolved CO₂. The overall process is mainly limited by diffusion, therefore, the adsorber is filled with packings to increase the surface area at one hand, but also to achieve thin solvent films and short diffusion paths at the other hand. The unloaded or lean solvent is fed at the top of the absorber column, from where it flows down over the packing to the bottom of the column. The flue gas is in counter current flow to the solvent flow. On the way from bottom to the top of the column, the flue gas CO₂ concentration is more and more reduced, while the solvent gets more and more loaded with CO₂ on the way from top to the bottom of the column. At the bottom of the absorber column, the loaded or rich solvent is extracted and directed to the regenerator. In the regenerator two mechanisms force the CO₂ release from the solvent: The regenerator is operated at elevated temperatures compared to the absorber at which the solvent has reduced capacity for CO₂ and further the regenerator is stripped with steam which lowers the partial pressure of CO₂ and helps to regenerate the solvent. Also, steam is used to obtain the desired temperature within the regenerator.

The CO₂ capture capacity of an absorption process is determined by the delta CO₂ loading of the solvent and the solvent circulation rate. A common range for the delta CO₂ loading is below 10 wt% CO₂ referred to the mass flow of solvent. Thus, a huge solvent mass flow is required to capture a certain amount of CO₂. Furthermore, this mass flow of solvent has to be continuously heated and cooled to achieve the desired temperature ranges of absorber and regenerator, which requires a good heat integration with heat recovery from lean and transfer to the rich solvent for example. Absorption of CO₂ with aqueous amine solvents is the current state of the art in post combustion CO₂ capture and has already been implemented at commercial scale (e.g.: Boundary dam combined SO₂ and CO₂ removal from a coal fired power plant – see Figure 1-4)

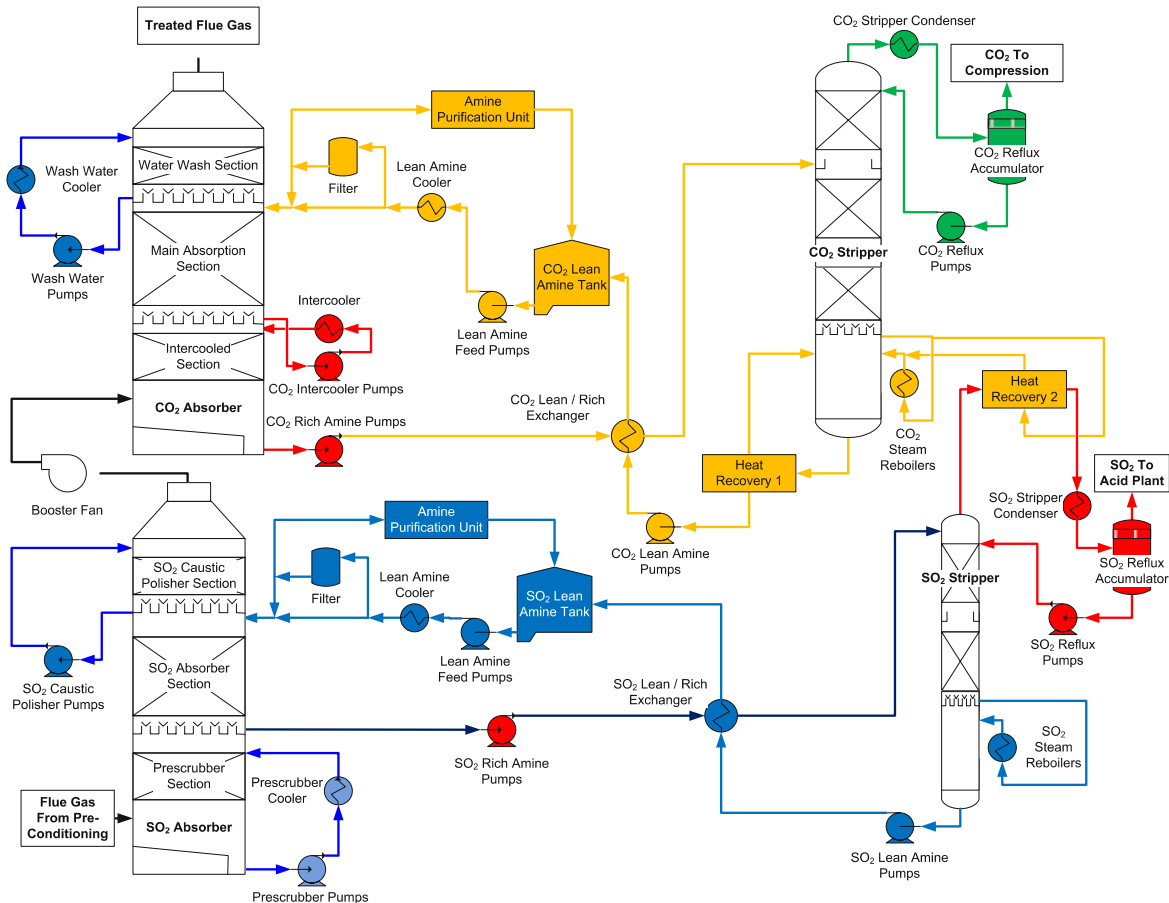


Figure 1-4: Cansolv process line-up for the SaskPower BD3 CCS project (taken from [14])

Despite the relatively high level of development, absorption of CO₂ with aqueous amine solvents has some inherent disadvantages [15], [16]:

- **Energy demand**

A state-of-the-art CO₂ absorption process with aqueous amine solvents has a relative high energy demand for the regeneration of the solvent, which is at least partially caused by the relatively high heat capacity of the water-based solvent and evaporation of the liquid during regeneration. The energy demand for capture of CO₂ with a liquid amine absorption process is reported to be in the range between 3 and 5 GJ/ton of CO₂ captured ([17]–[19]). Whereby deviations in the level of heat integration as well as valuation of electrical energy leads to hardly comparable results.

- **Capital costs**

Because of diffusion and dissolution limitations, a high surface area for the contact between gas and solvent has to be provided. Thus, the columns are usually quite big in order to treat the required amount of flue gas. Furthermore, the corrosive nature of liquid solvents requires utilization of high-grade material. Also, significant effort needs to be put into pre- and post-treatment, which all together results in high investment costs.

- **Fugitive emissions and degradation**

Various amine solvents like monoethanolamine (MEA), diethanolamine (DEA), methyldiethanolamine (MDEA), aminomethylpropanal (AMP) and others, as well as blends of different amine compounds have been proposed for CO₂ absorption [20]. MEA is the most studied amine because of its relatively low production costs and high CO₂ capacity at low CO₂ partial pressure. However, all the studied amines show thermal degradation and/or partially irreversible chemical deactivation or degradation under the presence of components like O₂, NO_x and SO_x. For a process where MEA is utilized, around 10 % of total capture costs are related to solvent make-up that is required to compensate for solvent degradation and to maintain a certain level of solvent activity [21]. Furthermore, degradation products often lead to corrosion and fouling issues, or form harmful emissions like nitrosamines, nitramines, aldehydes and other species. [16], [22].

CO₂ Adsorption

The number of studied CO₂ capture technologies is growing year by year and many innovative processes have been proposed or demonstrated. This is also reflected by the number of patents or scientific publications [23], [24]. One very promising and frequently mentioned process for the capture of CO₂ is adsorption [25]–[28]. Adsorption of other species than CO₂ is a well-known technology and has been applied in various chemical processes. The utilization of solid sorbents for the capture of CO₂ instead of a liquid potentially has some promising advantages:

- The heat capacity of solid sorbents is significantly lower compared to solvents used in state-of-the-art CO₂ absorption processes. Thus, the energy demand for heating and cooling of the CO₂ carrier is theoretically lower compared to liquid amine processes. [29]–[31].
- Especially for solid sorbents, where the functionalization is chemically bonded to the solid carrier, a considerable reduction of volatile organic compound (VOC) emissions can be expected.
- Issues with corrosion, fouling and foaming and the consequently necessity of foaming inhibitors and high-grade materials could be potentially eliminated [32].
- Depending on the structure and size of a solid sorbent, it can provide a very high surface to volume ratio. Thus, fast kinetics can be expected, which can have positive effects on plant size and capital costs.

1.3 PROBLEM DEFINITION

Amine scrubbing is seen as the state-of-the-art technology for post combustion capture of CO₂. Despite the maturity of the process, it is still very energy intensive. Also, capital expenses and other operational expenses (solvent make-up, maintenance costs, necessary post treatment of gas streams etc.) are leading to high specific capture costs. Solid sorbent CO₂ capture has been identified as promising technology for further reduction of the overall CO₂ capture costs. While a lot of research has been carried out on development of sorbent materials only a few studies deal with reactor and process design in detail [29], [33]–[35]. However, compared to a liquid, solid sorbents are more difficult to handle within the process (except for batch operation in fixed beds, which leads to other disadvantages). Thus, development of the process line-up and reactor design, is one of the biggest challenges for the commercial readiness of the technology.

In 2011, researchers from the Future Energy Technology Group at TU Wien proposed an innovative temperature swing adsorption (TSA) process, based on multistage fluidized beds [36] and a bench scale unit (BSU) was designed and built. Continuous operation with synthetic flue gas mixtures was successfully demonstrated [37]. The utilized amine impregnated silica sorbent showed excellent kinetics and high delta loadings under lab conditions with synthetically mixed flue gases. A basic description of the BSU can be found in chapter 2.3.3, for more details it is referred to literature [37]–[39].

With the BSU a first proof of concept has been delivered. However, many important questions regarding the economic and technological scale-up potentials of the solid sorbent CO₂ capture process remained unanswered. For a lab scale TSA plant in general, two important factors can potentially affect the process behavior either in a negative or positive way, which reduces the transferability of results from lab scale to large scale:

- **Fluid dynamics:** Scaling of fluidized beds is a delicate task. One of the main challenges for the TSA technology lies in the scale up of the multistage fluidized bed columns. As the scale up would have to be achieved mainly by increasing the cross section of the fluidized beds and hardly by increasing their height (to limit the pressure drop of the beds), the aspect ratio of the fluidized beds would be completely different which leads to different issues. For example: the wall friction potentially strongly affects the process at lab scale, while achieving a proper gas and sorbent distribution is likely to be one of the main fluid dynamic challenges at large scale.
- **Heat losses:** Especially when it comes to the energy demand of a process, one has to be aware, that the volume to surface ratio of a plant drastically changes with scale and heat losses of a lab scale plant are unproportionally higher than they would be at larger scale, which makes accurate predictions difficult.

However, for the BSU in particular, not only these two factors are hindering the further development of the technology. Also design parameters changed during development of the technology and certain design aspects of the BSU turned out inappropriate. So that for example, insufficient heat exchange surface is limiting the controllability of process temperatures which results in a reduced capture performance. Furthermore, the process control system is not suitable for unattended long term operation, which makes longer test runs at stable conditions complicated. Also, the general design framework of the BSU does not allow for certain design modifications without creating a huge effort. For the above-mentioned reasons, further development of the multistage fluidized bed temperature swing adsorption process (MStFB-TSA) should be combined with a scale up of the reactor system.

With a target scaling factor from lab scale to commercial scale of approximately 50 000 (see 3.5) one single scaling step is unrealistic, so that most likely several intermediate scaling steps will be required, before the technology can be considered as commercially available.

With increasing scale of a research plant, also project costs are increasing. Thus, a reasonable scaling factor needs to be found, which delivers a good tradeoff between quality of the gained results and the investment risk. Furthermore, current limitations need to be identified and overcome to maximize the

overall process performance. Drawbacks of the technology shall be compensated as much as possible and potential benefits shall be further elaborated and exploited.

1.4 KEY OBJECTIVES AND ORGANIZATION OF THIS THESIS

To enable further development of the novel MStFB-TSA process, a pilot plant shall be designed and operated. For the design of the plant the focus lies on gathering the required tools, the required knowledge, and the required operating experience to bring this technology further.

Although, potentially not all relevant questions can be answered in a pilot phase, key objectives are defined as follows:

Reduction of process energy demand

The expectation of a reduction of the energy demand for separation of CO₂ compared to the state-of-the-art technology (CO₂ scrubbing with aqueous amines) is valid since the heat capacity of solid sorbents is considerably lower. However, this advantage does not eliminate the need for an advanced heat integration of the process. Especially heat recovery from the lean sorbent stream is crucial for the process. Therefore, a suitable heat recovery system shall be selected and implemented.

Maximization of CO₂ capture performance

One of the main cost drivers for CO₂ capture technologies are the relatively high capital expenses. Huge amounts of flue gas are to be treated in an adsorption column. Therefore, one aims for high gas velocities, which can lead to kinetic limitations or fluid-dynamic limitations (e.g.: transport of sorbent, sorbent entrainment). However, also heat exchange limitations can occur if the gas throughput, and thus the overall load, is increased. To maximize the plant throughput, potential limitations shall be identified and preferably eliminated.

Model development

One of the most important tools for process engineering is a process model, capable of delivering reliable predictions. Within the pilot phase, an existing process model shall be refined with the aid of several pre-studies before it is used to derive the heat and mass balance required for the pilot design. Furthermore, results from experiments with the pilot plant will be later used for model validation. Although, model development is not part of this thesis, the pilot unit has to be equipped with sufficient instrumentation to allow for validation of certain data points.

Sorbent development

Although, a large number of sorbent materials for capture of CO₂ from large scale sources have been suggested, only a small fraction was tested under realistic conditions. Within the pilot program, suitable sorbent materials shall be identified and tested with real flue gas in the pilot unit.

To meet these main objectives, several different workstreams have been defined. In particular, the overall scale-up of the multistage fluidized bed temperature swing adsorption CO₂ capture process can be divided into following main tasks:

- Pre-studies at bench scale
- Fluidization engineering and scale up of columns
- Heat transfer investigations and heat exchanger design
- Optimization of process line up
- Process modelling
- Reactor design
- Detail engineering

Due to the relatively large scope, the above-mentioned tasks have been divided within a whole project team. Some of the detailed investigations are presented in several research papers and other theses. Although, the author contributed significantly to most of the above-mentioned tasks, this work mainly deals with the elaboration of an optimized process line up and the crosslinks between the detailed investigations as well as on elaboration of the pilot unit reactor design.

Chapter 2 provides a brief introduction into fundamentals of fluidization and adsorption as well as to the most relevant background of multistage fluidized bed temperature swing adsorption which was developed in the Zero Emissions workgroup at TU Wien.

Within **Chapter 3** a reasonable scaling step is elaborated and a design basis for the pilot unit is found.

Chapter 4 explains the design philosophy for the TSA pilot plant, while special attention is paid to the process line up outside of the two main reactors. The unique challenges for the sorbent transport system are discussed and design solutions are elaborated.

In **chapter 5**, the main dimensions of the TSA pilot unit are derived and presented. Furthermore, important design considerations are explained.

Chapter 6 summarizes construction and commissioning phase and briefly presents first results from operation.

2. BACKGROUND

2.1 FUNDAMENTALS OF FLUIDIZATION

2.1.1 General aspects

A Fluidized bed can be seen as a suspension of solid particles in a gas or liquid, whereby the suspension shows liquidlike behaviour (see Figure 2-1). Compared to other technical possibilities used to bring solid particles in contact with a gas, fluidization shows very particular characteristics, which are exploited in numerous processes. In the following a short summary of the most important theory of fluidized bed applications is given.

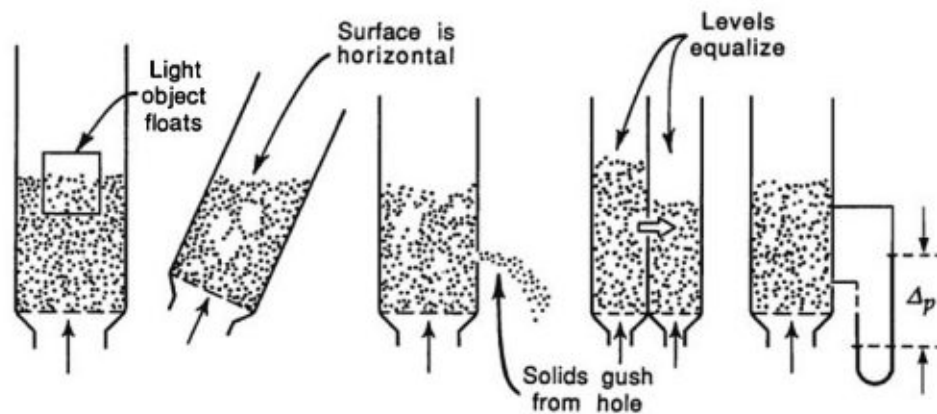


Figure 2-1: liquidlike behaviour of a fluidized bed (taken from [40])

2.1.2 Minimum fluidization velocity and fluidized bed existence range

Figure 2-2 shows the existence range of fluidized beds. In the simplest set-up a fluidized bed reactor consists of a containment for the particles and a gas distributor. Without any fluid flow (gas or liquid), as well as for small gas flows, the particles remain as a fixed bed with the height L_m and without movement (see Figure 2-2(a)). For increasing gas velocity, the drag force on the particle is getting higher and higher, until the bed expands to L_{mf} and fluidization of the particles is established (see Figure 2-2(b)). A further increase of the fluid velocity leads either to bubbling fluidization (Figure 2-2(d)), which is common for fluidization with gas, or to a homogenous distribution of the particles in a liquid system with the height L_f (Figure 2-2(c)). For better readability of this document, the term fluidized bed within this document refers to gas fluidized beds only. If the gas velocity is further increased, at a certain velocity the reactor will start to entrain particles. Independent of the height of the reactor, this point is reached as soon as the gas velocity exceeds the terminal velocity of a single particle. Before the terminal velocity is reached and the fluidized bed starts to entrain particles, formation of a turbulent regime with some special properties is possible (see Figure 2-2(g)). Depending on the form factor of the fluidized beds, special forms of bubbling beds can occur like the formation of slugs in deep bed with a relatively small cross section (see Figure 2-2(e) and (f)). At gas velocities above the terminal velocity of the particles a lean phase fluidization with pneumatic transport of the particles is formed (see Figure 2-2(h)).

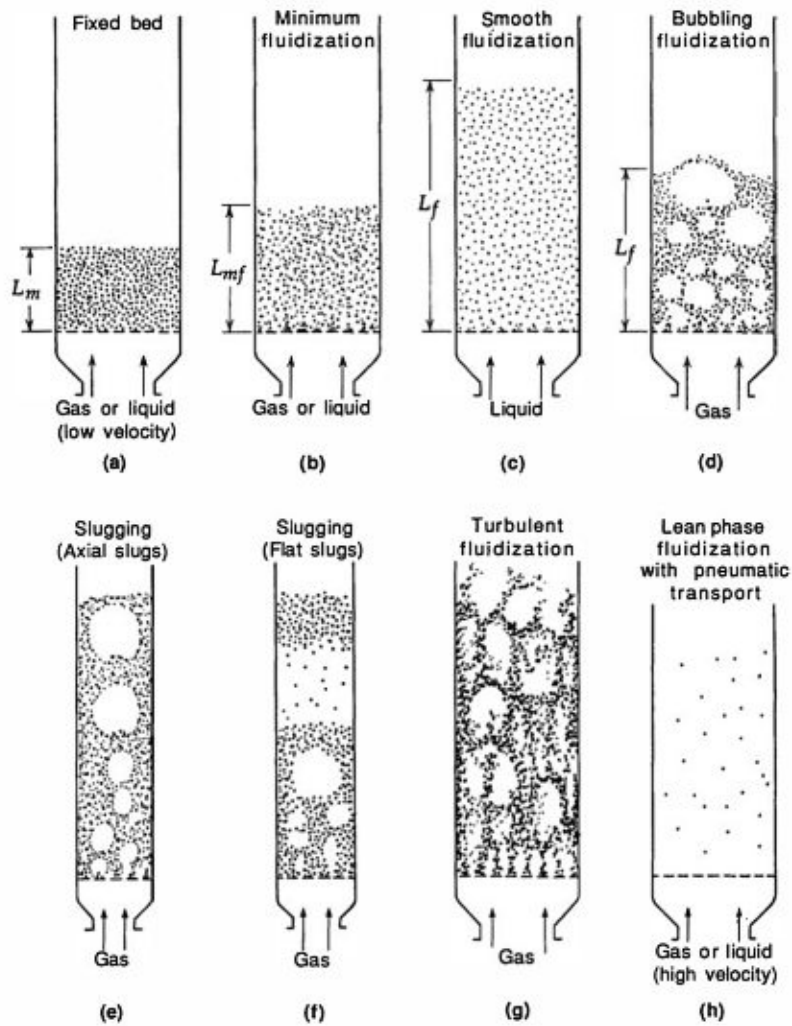


Figure 2-2: Fixed bed, fluidized bed, pneumatic/hydraulic transport (taken from [40])

2.1.3 Particle classification

Besides of the influence from the operating conditions, the behavior of a fluidized bed is strongly depending on the utilized particles. Especially the particle size or size distribution as well as the particle density play an important role. But also, other factors have to be considered when designing a fluidized bed. In the following the most important particle parameters are introduced.

Particle size

For several calculations, assumption of a perfectly spherical particle, with the particle diameter to describe its size is a common approximation. However, particles in practical applications of course deviate from the ideal sphere. Therefore, equivalent diameters have been introduced. The most common equivalent diameters are listed in Table 2-1.

Table 2-1: Equivalent particle diameters

Symbol	Name	Equation
d_p	Sieve diameter	-
d_s	Surface equivalent diameter	$d_s = \sqrt{\frac{A_P}{\pi}}$ (Equation 2-1)
d_v	Volume equivalent diameter	$d_v = \sqrt[3]{\frac{6 \cdot V_P}{\pi}}$ (Equation 2-2)
d_{sv}	Sauter diameter (diameter of a sphere with the same volume to surface ratio)	$d_{sv} = \frac{d_v^3}{d_s^2} = 6 \cdot \frac{V_P}{A_P}$ (Equation 2-3)

Technically used bed materials are not ideally uniform, thus instead of a single particle size, the particle size distribution (PSD) is often used to characterize a bed material batch.

The PSD can be measured automated for example via laser diffraction with fully automated dispersion in air or within a liquid. However, the PSD of a sorbent material sometimes is also determined with sieve or microscopic analyses.

Particle form factor

A frequently used further parameter for fluidized bed engineering is the particle form factor, which is defined by (Equation 2-4). An ideally spherical particle would have a form factor of 1 while the theoretical opposite of a sphere (e.g.: an infinite long and thin, needle like shape) would have a form factor of 0. Most practically used bed materials have a form factor in the range between 0.6 and 1.

$$\phi_P = \left(\frac{d_v}{d_s}\right)^2 \quad (\text{Equation 2-4})$$

Particle density

The **true density** of a particle is the quotient of dry mass of the particle to the volume of the particle without consideration of the pore volume.

$$\rho_{true} = \frac{m_P}{V_S} \quad (\text{Equation 2-5})$$

Particles utilized in typical fluidized bed applications often have a significant pore volume. This pore volume reduces the apparent density which is relevant for calculations around fluidization engineering. The **apparent density** is the ratio of dry mass of a particle to the total volume including pores of the particle.

$$\rho_P = \frac{m_P}{V_P} = \frac{m_P}{V_{Pore} + V_S} \quad (\text{Equation 2-6})$$

The **bulk density** is measured with a standardized procedure, where a bulk material is filled into a container with defined volume. The bulk density is then calculated by the quotient of the mass of the loosely packed material within the container to the volume of the container.

Depending on the procedure of the filling, the measured values can fluctuate significantly. However, it is a very common and cheap method for characterization of a bulk material.

Geldart particle classification

As already indicated, fluidized bed behavior strongly depends on the utilized particles. For a basic classification and gross predictions of the fluidization behavior, the particle classification according to Geldart is commonly used. Based on observations of various authors, Geldart defined 4 groups of particles, while candidates from each group showed similar behavior [41]. The empirically derived definition of the 4 groups is shown in a graph of density difference (particle to gas) over particle size. (see Figure 2-3)

Group C usually stands for very small particles which are hardly fluidizable like flour. For group C particles, the cohesive force between particles lets them stick together which promotes channeling and prevents proper fluidization.

Group A particles usually form an expanding homogenous phase above minimum fluidization condition which transforms into a bubbling bed only at higher gas velocities. Group A is typical for bed materials used in fluid catalytic cracking (FCC).

For group B particles (commonly described as sand-like material), the role of cohesive forces is further reduced. In contrast to group A, bubbling behavior starts almost right above minimum fluidization velocity. A large number of practical applications utilizes group B particles.

Group D stands for large or dense particles which can show spouting behavior. Group D is mostly relevant for food processing (fluidization of rice, peas, coffee etc.)

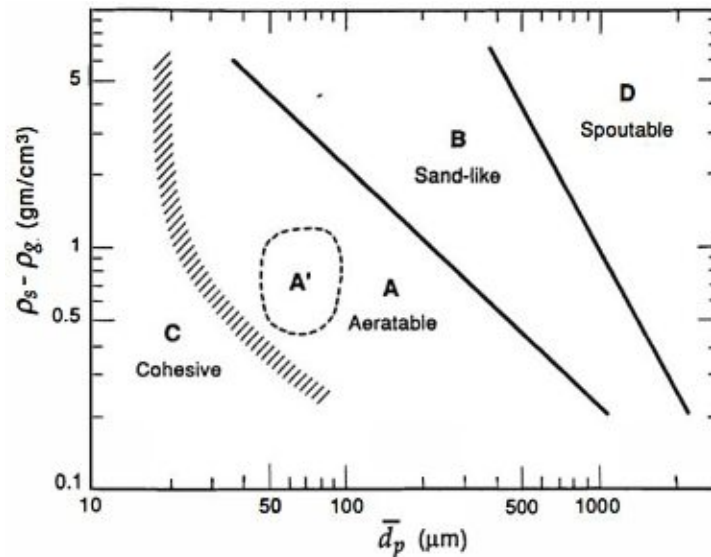


Figure 2-3 Geldart particle classification (taken from [40])

2.1.4 Pressure drop in fluidized beds

When a gas is fed to a vessel containing a fluidizable bulk material, a very characteristic behaviour can be observed. Starting from zero flow, the gas must pass through the void of the bulk material. This gas flow range with increasing pressure drop and without particle movement defines the fixed bed existence range. With increasing gas flow, the pressure drop increases until it is just as high to balance the weight of the bulk material (see Figure 2-4). At this point, the fixed bed expands, and minimum fluidization velocity (u_{MF}) is reached. A further increase of the gas velocity does not result in a significant increase of the pressure drop over the bed. Only at higher gas flows, the total pressure drop rises again because of additional frictional forces due to start of transport.

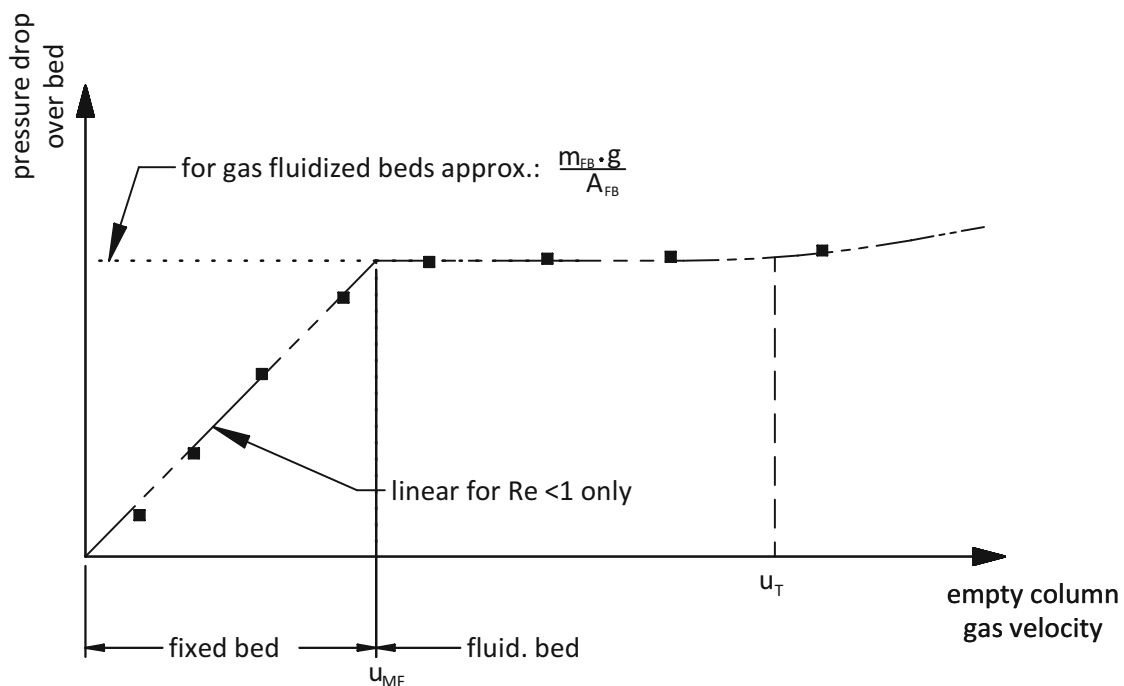


Figure 2-4 pressure drop of a fixed/fluidized bed

2.1.5 Heat transfer in fluidized beds

Fluidized beds are well known for excellent heat transfer. However, this simple statement is not very useful for the design of a fluidized bed application. Good knowledge of heat transfer rates is required to provide/extract heat sufficiently to/from the process without adding to much margin on the heat transfer surface. However, compared to heat exchange from gas to a wall, the heat exchange between a fluidized bed and a heated/cooled wall is more complex and a huge range of heat transfer rates is possible. Basic mechanism of heat transfer in fluidized beds, as well as the most important influencing factors are presented in the following. For more detailed aspects of fluidized bed heat transfer, it is referred to literature [42]–[47].

Basically, the overall heat transfer between a fluidized bed and an immersed surface is the combination of 3 mechanism: heat transfer by radiation, particle convective heat transfer and gas convective heat transfer. Depending on the operating conditions, and the utilized bed material, each of the three mechanism can be dominating. While the gas convective heat transfer is the governing mechanism for rather large particles and thus high gas flow rates, radiation of course plays a big role only at high temperatures. In the context of this work, where operating temperatures are well below 500 °C and particle size does not exceed 1mm the dominating mechanism is the particle convective heat transfer. In contrast to fixed bed heat exchange, where the limiting factor is the heat conduction of the bulk, in a fluidized bed the particle movement and mixing of the bed eliminates this limitation, which drastically improves the overall heat transfer. For a short time, single particles are in direct contact with the heat exchange surface, where heat is exchanged. As they are transported away from the heat exchange surface and mixed with the other particles, the heat is “transported” with the particles reducing the temperature gradients of the fluidized bed and improving the overall heat transfer coefficient. This behaviour is described in the packet-renewal model introduced by Mickley and Fairbanks [48].

Various other authors studied heat transfer in fluidized beds under different conditions and several models or model adaptations for the estimation of fluidized bed heat transfer coefficients have been suggested ([45][46][47]). In general, all studies report a strong dependence of the heat transfer coefficient on the operating gas flow. However, also the particle size has a huge impact on the maximum achievable heat transfer, which is indicated in Figure 2-5.

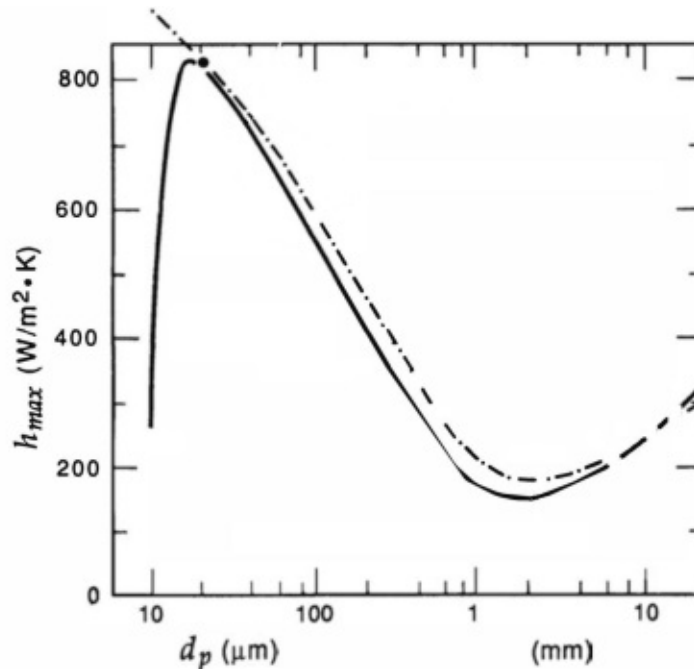


Figure 2-5: effect of the particle size on fluidized bed heat transfer (adapted from [40])

A well-known method for a first estimate of the maximum achievable heat transfer coefficient without consideration at which gas flow this maximum occurs, was given by Zadbrosky [44]:

$$h_{MAX} = 35.8 \cdot \rho_P^{0.2} \cdot \lambda_G^{0.6} \cdot d_{SV}^{-0.36} \quad \text{Equation 2-7}$$

2.2 ADSORPTION

2.2.1 General aspects

The utilization of powders with healing effects due to their adsorption activity can be traced back to the oldest records of human history. However, the scientific research in the field of adsorption started back in the 18th century with investigations of activated carbon e.g. for purification of water. In the early 19th century activated carbon was first-time used for the industrial purification of sugar. The patents of Ostrejko in 1900 for the industrial production of activated carbon led to a significant progress of adsorption technologies [49].

Within the 20th century adsorption processes became more and more important for various separation tasks in different industry sectors. And still, adsorption shows a steady increasing importance ([49]). In the following, a brief introduction to basic concepts of adsorption will be given.

2.2.2 Definitions

Adsorption is the accumulation of molecules from a gaseous or liquid phase on the surface of a solid while the reversal process, the release of the molecules, is called desorption or regeneration (see Figure 2-6). The gaseous or liquid molecule, which is to be adsorbed, is called adsorptive in its free state and adsorpt in its bound state. The unloaded solid is called adsorbent or sorbent, while the

composition of adsorbent and adsorpt is called adsorbate. The adsorptive in its non-bound state has a higher enthalpy than in its adsorbed state. Thus, adsorption is an exothermic process. The desorption, or the release of adsorbed components from the adsorbent, is then of course an endothermic process. Adsorption is thus usually promoted at lower temperatures and/or high partial pressure of the adsorptive while desorption happens preferably at higher temperatures and/or low partial pressure of the adsorptive.

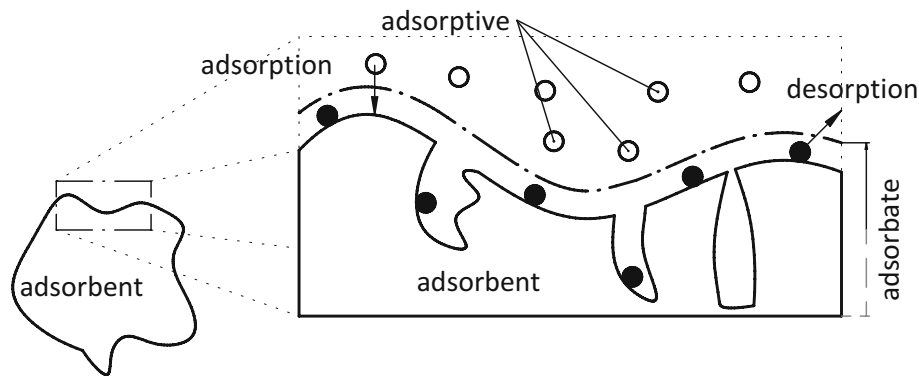


Figure 2-6: Definition of terms

Adsorption can be differentiated in adsorption in liquid or gaseous phase. Although it is the same process, there are some differences like the influence of pressure for adsorption in liquid phases is almost negligible, while the influence on adsorption in a gaseous phase is significant. However, adsorption in the context of this work refers to adsorption from gaseous phase only with a focus on adsorption of CO₂.

2.2.3 Sorbent materials

A huge effort has been made in the field of adsorbent development and many potential candidates have been proposed for temperature swing adsorption (TSA). Besides, zeolites, metal organic frameworks, various carbon based sorbents, also countless functionalized sorbents have been studied with regard to their suitability for CO₂ capture processes [25], [32], [50]. In order to exploit previously discussed potential benefits of solid sorbents over the state-of-the-art CO₂ scrubbing process, various sorbent properties can play an important role. Besides a high CO₂ adsorption capacity also high selectivity towards CO₂, fast kinetics, mechanical, chemical and thermal stability, low energy demand for regeneration as well as low sorbent costs are desired attributes for a sorbent [26]. Unfortunately, available sorbent materials, usually do not combine all these attributes in one, which requires a good compromise for selection of a sorbent. In contrast to CO₂ absorption, where CO₂ is dissolved in a solvent, in an adsorption process, CO₂ is bound to the surface of a solid. Depending on the type of interaction between adsorbent and adsorptive, two different forms of adsorption are differentiated: adsorption where chemical reactions between adsorbent and adsorptive are the dominant factor is called chemisorption. In case of mainly physical interaction between adsorbent and adsorptive, like van der Waals forces or an ionic bond, it is referred to physisorption. For physisorption the heat of adsorption typically lies in the range of -25 to -50 kJ·mol⁻¹, and between -60 to -90 kJ·mol⁻¹ for chemisorption [26]. Since adsorption takes place on the surface of the sorbent in both cases, chemisorbents and physisorbents require a high surface area to reach relevant CO₂ capacities. For

porous materials, the inner surface of a particle is much higher compared to the particle outer surface. Thus, most of the adsorption activity is taking place on the inner surface of an adsorbent. Therefore, in terms of capacity, a high inner surface area is desirable. However, for increasing inner surface area, the average pore size of a particle is reduced necessarily and depending on the molecule size of the adsorptive it comes to limitations or at least to slower adsorption rates due to a higher diffusion resistance [49]. Depending on their pore size, sorbent material can also be distinguished in:

- **Microporous sorbents**
The pore size of microporous sorbents is in the range of the size of a molecule. Microporous sorbents are either crystalline with a very narrow pore size distribution or amorphous with a broader pore size distribution. Zeolites and metal organic frameworks (MOFs) are assigned to crystalline sorbents, while carbon molecular sieves and microporous polymers are amorphous sorbents. Gas separation with microporous sorbents can be achieved either via equilibrium, kinetic or molecular sieving mechanisms [51].
- **Mesoporous sorbents**
Mesoporous sorbents usually have a pore size in the range from 2 to 50 nm. Because of the larger pore size, higher mass transfer rates can be achieved. However, at pressure levels relevant for post combustion CO₂ capture, the capacity of mesoporous sorbents can be considered as low compared to other types.

But also, the particle size of a sorbent material is a governing factor for adsorption. The smaller the particles are, the faster the mass transport from gas phase to the solid, which can be explained by shorter diffusion paths [49]. However, the sorbent particle size also influences fluidization behavior (see 2.1) and can limit the gas flow that can be treated in praxis.

In literature hundreds of different sorbent materials are assessed regarding their suitability for capture of CO₂ [26], [52]–[59]. Figure 2-7 gives a quick overview of CO₂ sorbents, their rough range of CO₂ capacity and the corresponding range of operating temperature. In the following some of the most important sorbent types are shortly discussed. For more detailed information it is primarily referred to the following review papers [25], [26], [60].

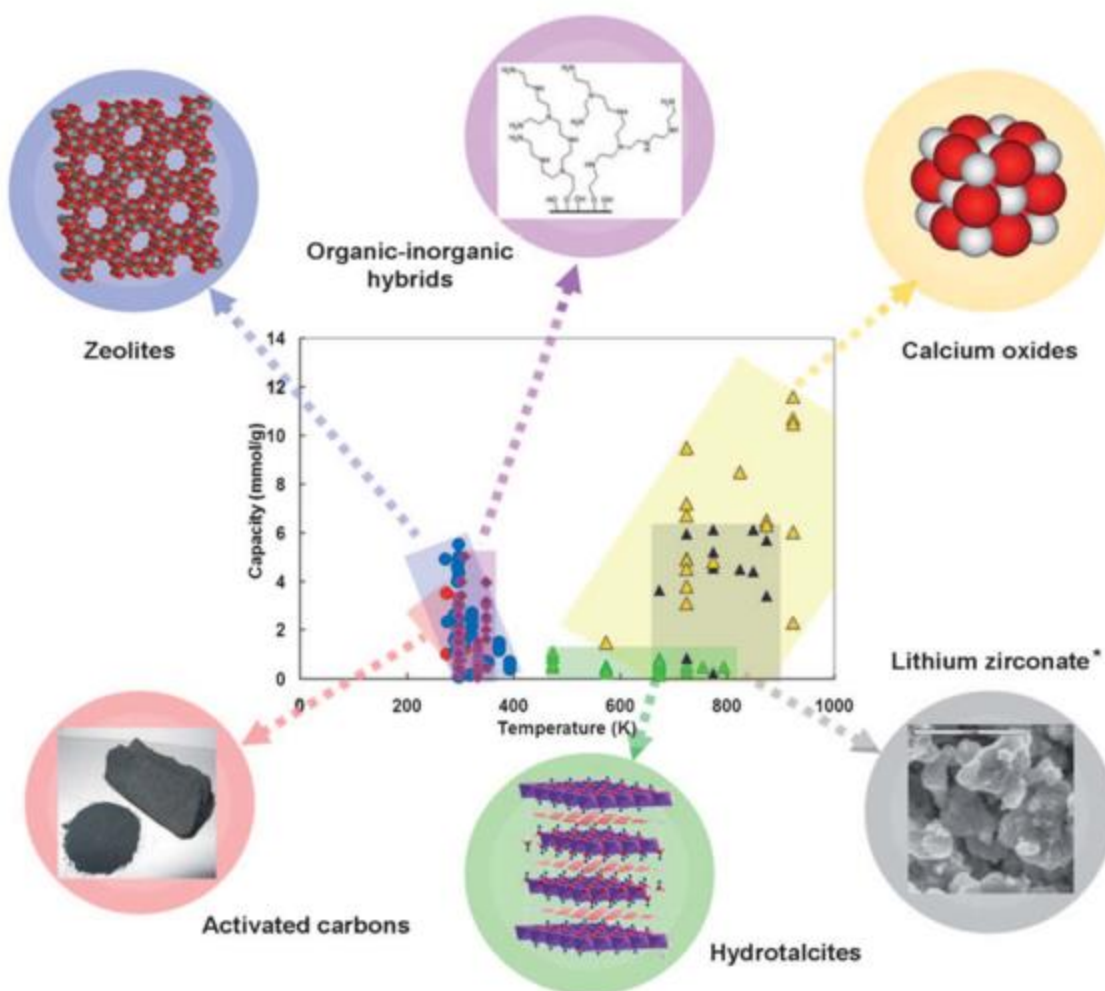


Figure 2-7: Overview of sorbent CO₂ capacities and operating temperature range (taken from [25])

Activated carbons

Depending on the organic raw material and the manufacturing process, activated carbon-based sorbents can be either assigned to microporous or mesoporous sorbents. Activated carbon-based sorbents have the advantage of relatively high availability at comparably low costs. For that reason, many studies focus on activated carbon-based sorbents from different organic material as well as on modification of such [25], [60], [61].

Zeolites are either naturally occurring or synthetically manufactured porous crystalline aluminosilicates. Over 170 different zeolites are indexed by the International Zeolite Association. Zeolites typically feature fast kinetics and good regenerability with low degradation [25]. Zeolites have high CO₂ adsorption capacities at relatively low temperatures, which requires much effort in cooling of the gas which is to be treated. Furthermore, zeolites show preferred adsorption of water, which drastically reduces their CO₂ adsorption capacity and requires deep drying of the feed gas. Also the relatively low selectivity towards adsorption of CO₂ leads to impurities in the separated CO₂ [60]. An example for isotherms for Zeolite 13X is given in Figure 2-8.

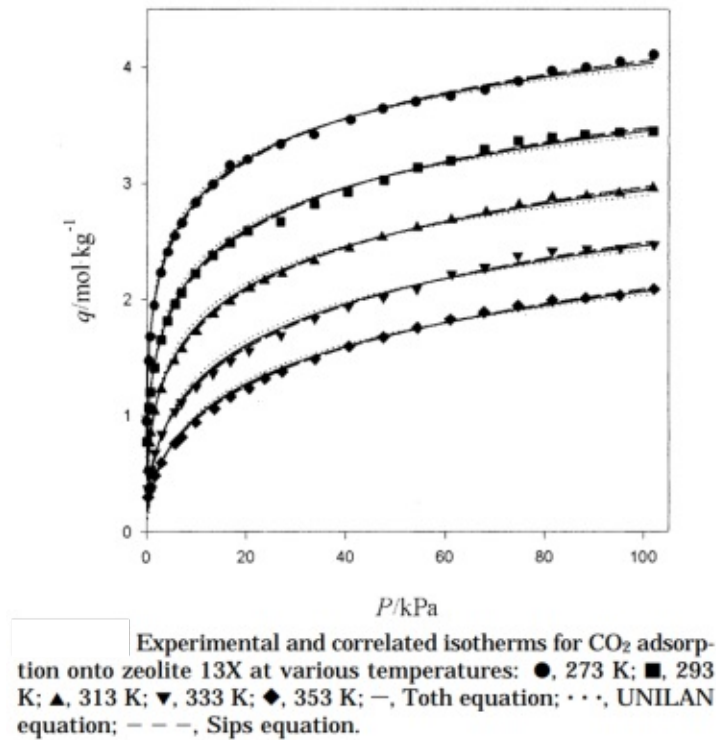


Figure 2-8: CO₂ Adsorption isotherms for zeolite 13X (taken from [62])

Metal organic frameworks (MOFs) are porous sorbents constructed from transition metal ions and bridging organic ligands ([60]). Although relatively high adsorption capacities are reported for certain MOFs, these capacities are usually reached only at high CO₂ partial pressure, which makes application of MOFs for dilute CO₂ streams at ambient pressure (like most flue gases from thermal power plants) difficult. Furthermore, MOFs have a high adsorption affinity towards H₂O which reduces their CO₂ capacity as well as the selectivity for CO₂.

Amine functionalized sorbents

In contrast to physisorbents where CO₂ is bonded to the surface with relatively weak van der Waals forces or ionic bonds only, amine functionalized sorbents bind CO₂ molecules by means of a chemical reaction. This at one hand results in a higher selectivity compared to most physical sorbents. However, this comes with the price of higher regeneration demands, since the adsorption enthalpy increases to the level of the chemical reaction enthalpy. Figure 2-9 shows the reaction of primary amines with CO₂ forming carbamate. However, the same reaction mechanism is presumed for the reaction of secondary and hindered amines with CO₂. This formation of carbamate, which is also referred to as Zwitterion Mechanism, is a two-step reaction, where the CO₂ molecule first reacts with the amine to form a zwitterion, and then deprotonation by a base (B), which can be another amine, H₂O or OH⁻. Under dry conditions, where H₂O and OH⁻ is absent, the stoichiometry for this reaction is 0.5 mol CO₂ per mol N, while it theoretically doubles in presence of H₂O (at humid conditions) [25].

The reaction mechanism for CO₂ and tertiary amines is different: In the first step, the tertiary amine dissociates H₂O to form OH⁻, which then reacts with CO₂ to bicarbonate. The last step is an ionic bond between the protonated amine and bicarbonate (see Figure 2-10) [25].

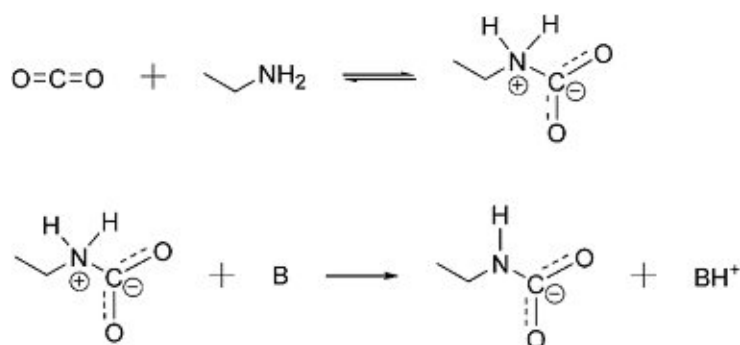


Figure 2-9: Carbamate formation by reaction of CO₂ with primary, secondary or hindered amines (taken from [25])

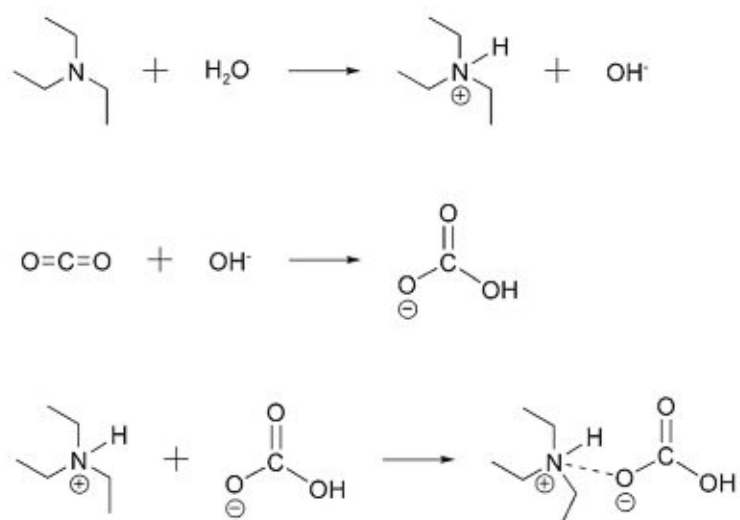


Figure 2-10: Mechanism for the reaction of CO₂ and tertiary amines (taken from [25])

Various amine compounds like Monoethanolamine (MEA), Diethanolamine (DEA), Polyethylenimine (PEI) and many others have been tested for sorbent functionalization. The functionalization is either achieved by impregnation of a carrier like porous silica or covalent bonding to a solid support ([26]). A widely studied approach is the impregnation of PEI on porous silica. An exemplary comparison of the adsorption and desorption capacity of a 50 % PEI impregnated silica with zeolite 13X is given in Figure 2-11. What can be seen in Figure 2-11 is the dependency of the loading on the adsorption temperature. However, contrary to the general tendency, that the adsorption capacity increases with decreasing temperature, the amine impregnated silica showed reduced capacity at the lower adsorption temperature. This is an effect, which was also observed in laboratory experiments at TU Wien with amine impregnated sorbents, below a temperature of 50-60 °C reaction rates are too low to reach equilibrium within a reasonable time frame.

Besides impregnation of a solid carrier with an amine solution another way to immobilize the functional group on the carrier is achieved by a covalent bond between amine and carrier, which is referred to as grafting method. While impregnated materials show significant evaporation of residuals from the impregnation process and leaching or volatilization of amines, grafted materials have the advantage of a stronger bond between the carrier and the amine functionalization [32].

Apart from amine leaching, different degradation mechanism can affect the sorbent uptake capacity in a negative way. For PEI based sorbents, Drage et al. [63] observed the formation of urea at a temperature of 130 °C, which however, is prevented in the presence of steam. One important degradation mechanism for amine functionalized sorbents is oxidative degradation, which occurs at elevated temperatures in presence of oxygen (see Figure 2-12). In an experimental assessment of the thermal stability of Lewatit VP OC 1065, Sonnleitner et al. [50] observed a mass loss when exposed to air already at 90 °C, which became more severe at 110 °C. However, also typical flue gas contaminants as SO₂ and NO_x have the potential to irreversibly react and degrade amine functionalized sorbents [64].

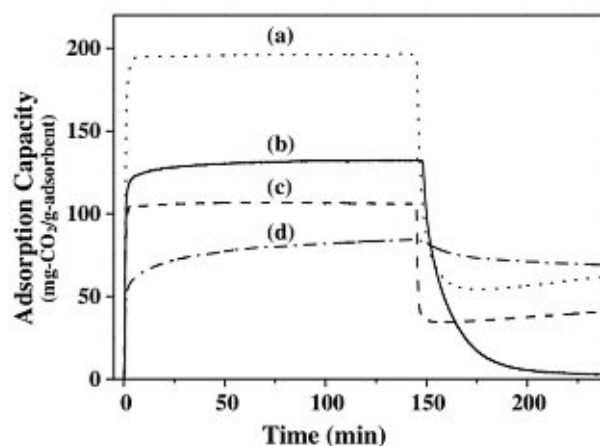


Figure 2-11: Comparison of adsorption-desorption performance with 100 % CO₂ feed gas between zeolite 13X and 50 % PEI impregnated porous silica. ((a): zeolite 13X at 25 °C; (b): KIT-60-PEI-50 at 75 °C; (c): zeolite 13X at 75 °C; (d): KIT-60-PEI-50 at 25 °C) (taken from [65])

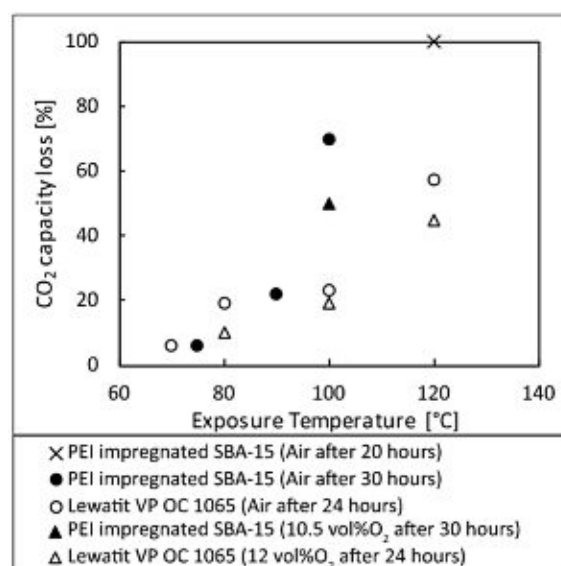


Figure 2-12: CO₂ capacity loss of amine functionalized sorbents as a function of exposure time and temperature in presence of oxygen (taken from [66])

Many of the workstreams in sorbent development are focussed not only on maximization of CO₂ uptake capacity, but also on improvements of cyclic stability, avoidance of amine emissions and degradation products, as well as in cost optimizations (e.g.: [27], [67]).

2.2.4 Thermodynamics of adsorption

When an adsorptive molecule is adsorbed its energy gets reduced compared to its free state in the gaseous phase. Thus, adsorption is an exothermic process. For desorption or regeneration of the adsorbent energy needs to be provided to reverse the process. If not hindered by other mechanisms, adsorption happens preferably at lower temperatures, while desorption is promoted at higher temperatures. Furthermore, the concentration or partial pressure of the adsorptive in the surrounding atmosphere has a large influence on adsorption from gaseous phases. Generally speaking, the higher the partial pressure of the adsorptive, the higher is the adsorption capacity.

Thus, for a basic characterization of an adsorbent material, it is commonly tested at varying temperatures and partial pressures of the adsorptive. For a certain adsorptive partial pressure and adsorbent temperature, adsorption and desorption takes place until the rate of adsorption equals the rate of desorption and equilibrium between the gaseous phase and the sorbent material is reached.

An indicator for the amount of gas in mol that can be adsorbed per kg of adsorbent material at a certain temperature and adsorptive partial pressure is the adsorption loading β . A common presentation of the connection between adsorption loading and temperature or partial pressure is done in form of adsorption isotherms. An example of adsorption isotherms is shown in Figure 2-13. These rather typical isotherms for chemisorbents, that show a steep increase of the adsorption capacity at low partial pressures and a saturation-like behavior at higher partial pressures. What can also be seen, is the strong correlation between temperature and adsorption capacity. For a certain partial pressure, the adsorption capacity is significantly higher at lower temperatures. However, for certain combinations of adsorbent material and adsorptive the shape of the isotherms can differ considerably from those shown in Figure 2-13.

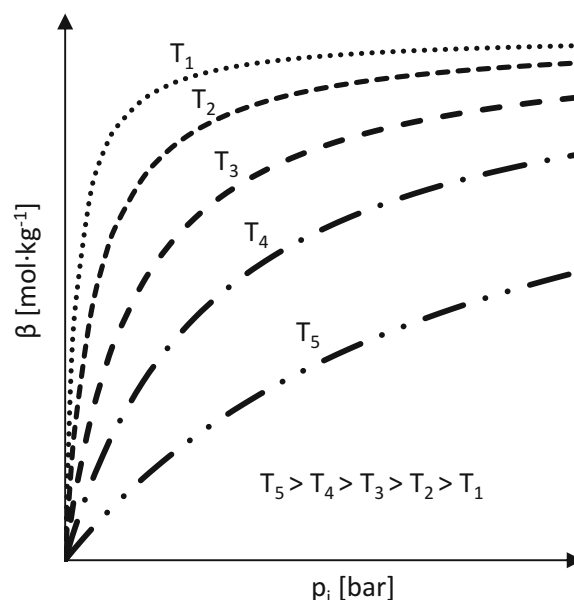


Figure 2-13: Adsorption isotherms

Figure 2-14 shows the extended BET (Brunauer, Emmet and Teller) classification of isotherms. Type I isotherms like also shown in Figure 2-13 are characterized by a steep increase of the adsorption capacity at low partial pressure and a flattening at higher partial pressures which indicates a maximum loading. Type II isotherms are similar to type I, with the difference, that a higher partial pressure leads

to multi-layer adsorption and adsorptive condensation on the particles, which is reflected in the second increase of the adsorption capacity. For combinations of adsorbent materials and adsorptive where pore condensation occurs, hysteresis effects can be observed, which is shown typically for type IV and V isotherms. Depending on the adsorbent and the adsorption conditions special forms of adsorption isotherms like shown in Figure 2-14 (Type III and VI) can be observed, but in the context of this work, only type I isotherms are relevant.

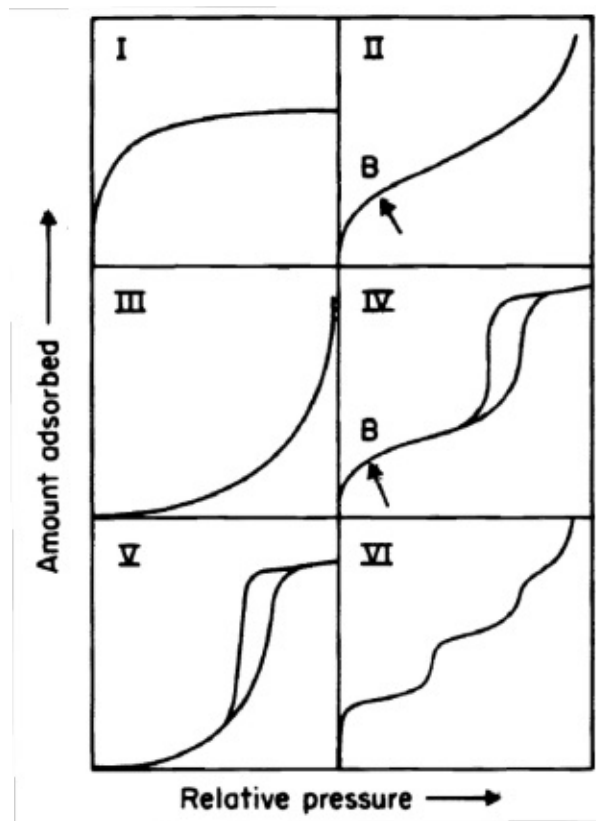


Figure 2-14: Classification of isotherms (taken from [68])

2.3 MULTISTAGE FLUIDIZED BED TEMPERATURE SWING ADSORPTION

2.3.1 Regeneration strategies

Temperature swing adsorption implicates, that the only mechanism for adsorption and desorption is the temperature swing between the two sub-processes, while for pressure swing adsorption it is only the change of partial pressure, which promotes adsorption and regeneration. However, in practical applications it is mostly a mixture of both mechanisms. Some processes are closer to the one extreme and some are closer to the other. What is given for all continuous adsorption processes is, that the sorbent is loaded at a certain partial pressure and temperature and regenerated at certain pressure and temperature. The question is, which conditions are favorable for a certain adsorbent and a certain capture task.

For a simplified adsorber with ideal plug flow and countercurrent flow scheme of gas and sorbent (Figure 2-15) and a defined capture task (e.g.: 90 % capture from a flue gas containing 4 Vol-% of CO₂), the adsorption process has following constraints:

- The maximum achievable rich sorbent loading is limited by the equilibrium loading at adsorber temperature which corresponds to the CO₂ partial pressure of the flue gas feed.
- The minimum required lean loading is defined by the equilibrium loading at adsorber temperature which corresponds to the CO₂ partial pressure at the adsorber outlet.

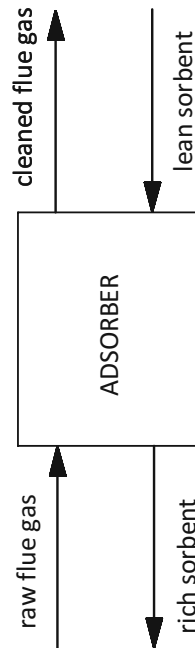


Figure 2-15: Counter current adsorption

However, these two limitations are representing limitations of an ideal system assuming ideal counter-current flow in the adsorber and equilibrium conditions. This in turn for a real application means that the rich sorbent loading will be lower than estimated by this assessment and the required lean loading needs to be lower than in this estimation in order to fulfil the capture task.

Nevertheless, this estimation roughly defines incoming and outgoing sorbent loading of the desorber and is sufficient for a basic assessment of different regeneration strategies.

Temperature driven regeneration in pure CO₂ atmosphere

One possible way of regenerating the sorbent material, is to simply heat it up. As the CO₂ capacity of the sorbent is reduced for increasing temperatures, the sorbent can be regenerated without the aid of a stripping gas. Both, self-fluidising regenerator concepts, where the released amount of gas exceeds the minimum fluidization velocity as well as fluidized bed reactors where the outlet gas is recycled to serve for fluidization of the sorbent can be found in literature [69], [70]. Assuming, that only the sorbent gets transported from the adsorber to the regenerator and no gas slip occurs, then the only gas present in the regenerator would be the released gas from the sorbent, which theoretically would

be pure CO₂ (if other adsorbed species are neglected). Looking at the CO₂ isotherms shown in Figure 2-16 it is possible to estimate the maximal achievable CO₂ loading of the adsorbent leaving the adsorber as described previously.

On the regeneration side, approximately pure CO₂ is assumed which is in this case translated to 100kPa partial pressure of CO₂, as roughly atmospheric conditions are expected. With a regeneration temperature of 100 °C, this would lead to a relatively high lean loading, which limits the performance of the adsorber, where the CO₂ concentration in the gas is supposed to be well below 1 Vol-% (assuming 4 Vol-% in the feed gas and 90 % CO₂ removal). Furthermore, the high lean loading would result in a low delta loading between lean and rich sorbent and thus to a high required sorbent circulation rate.

In contrast to the adsorber, where a relatively high gradient of CO₂ partial pressure is required by definition of the capture task (90 % CO₂ removal), regeneration without a stripping gas would result in almost no CO₂ partial pressure gradient.

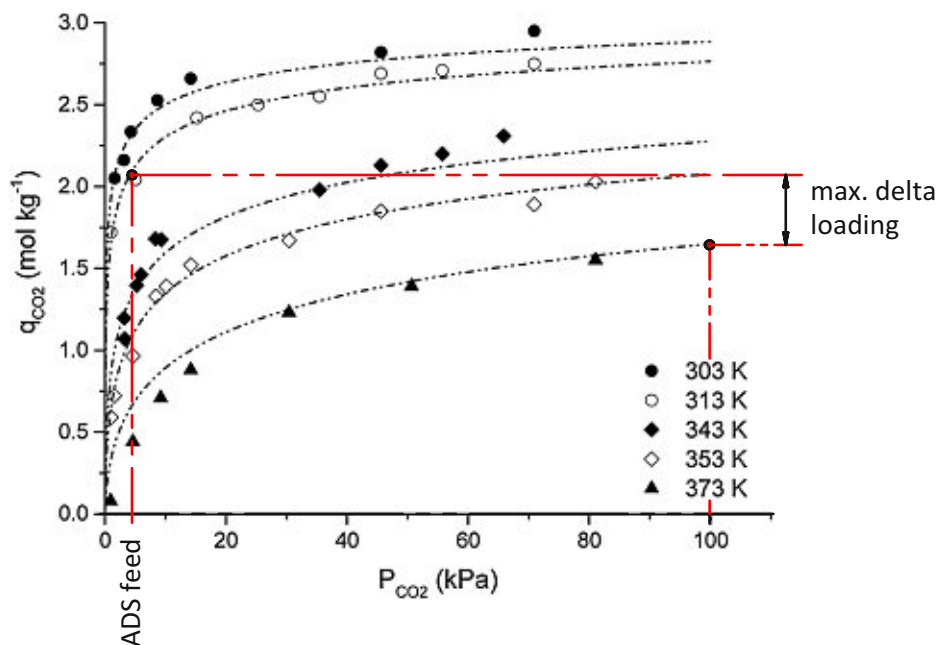


Figure 2-16: Lewatit VP OC1065 adsorption isotherms: Regeneration in CO₂ atmosphere (adapted from [71])

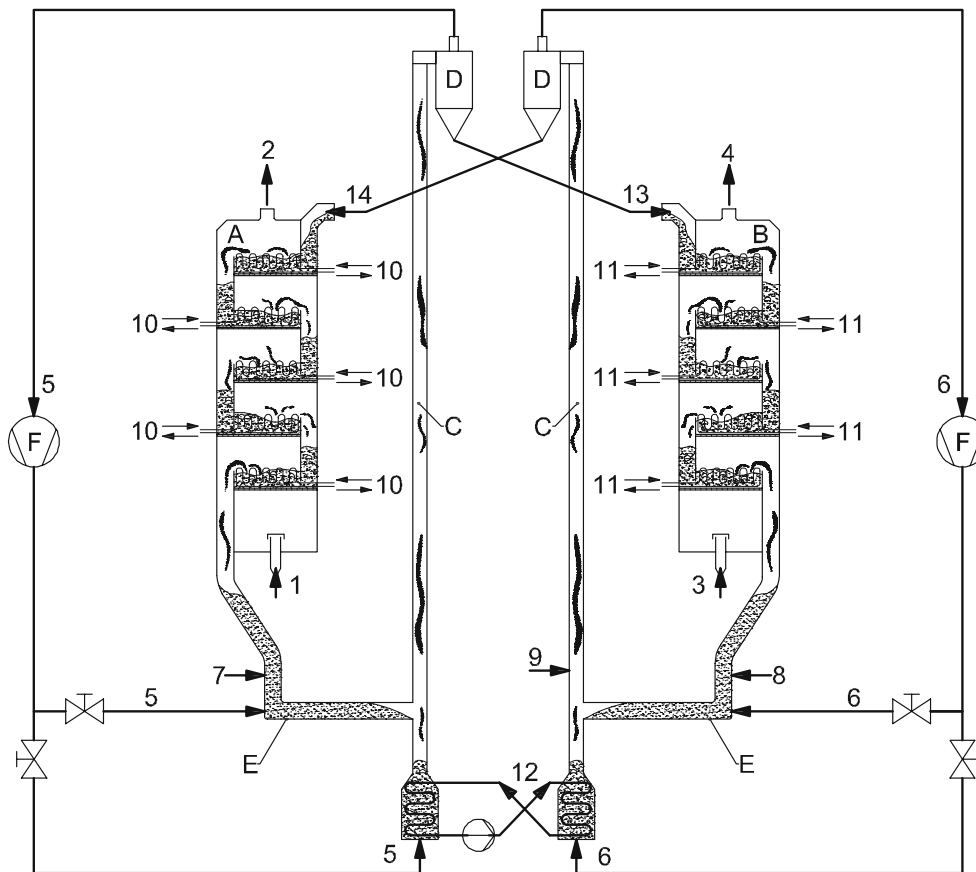
Regeneration with the aid of a stripping agent

In order to reduce the lean sorbent loading to levels which are favorable for deep removal of CO₂ in the upper adsorber stages it is possible to increase the sorbent temperature or to reduce the partial pressure of CO₂ in the regenerator. Since adsorbent degradation and energy demand considerations are limiting the sorbent temperature at a certain level, a further reduction of the lean sorbent CO₂ loading can only be achieved by lowering the partial pressure of CO₂ in the surrounding atmosphere. This in turn is possible by lowering the absolute pressure within the desorber or with the aid of a stripping gas. The utilization of a stripping agent will result not only in a reduced CO₂ partial pressure but also in a gradient of the CO₂ partial pressure over the regenerator. Assuming that the stripping gas

is injected at the bottom of the regenerator, more and more CO₂ is released over the height of the regenerator, leading to the maximum CO₂ partial pressure at the top of the reactor. However, in a single stage fluidized bed regenerator the stripping gas is not exploited effectively. Due to the excellent mixing behavior of fluidized beds, the sorbent loading would equalize to some extent which lowers the overall driving force for regeneration. Thus, if a stripping gas (e.g. steam) is utilized, a counter current flow pattern is highly beneficial also for regeneration of the sorbent.

2.3.2 Multistage fluidized bed temperature swing adsorption process

A novel concept for CO₂ capture based on temperature swing adsorption (TSA) utilizing multistage fluidized beds has been developed (see Figure 2-17). The process consists of two interconnected multistage fluidized bed columns. The adsorber as well as the desorber consist of five individual stages. Each stage is equipped with a heat exchanger, a weir plate and a downcomer. Following the sorbent cycle, the regenerated or lean sorbent enters the adsorber column (A) at the top (14). Then the sorbent passes each adsorber stage from top to the bottom of the column. On its way, the sorbent is more and more loaded with CO₂ from the flue gas (1) which serves as fluidization gas. The CO₂ loading of the particles increases from top to the bottom. The CO₂ concentration in the fluidization gas decreases from bottom to top. The sorbent is extracted from the lowermost stage of the adsorber to the transport riser (C). At the top of the transport riser, it is separated in a gas/solid separator (D) and directed to the uppermost stage of the desorber (B, 13), while the transport gas is recycled (5). In contrast to the adsorber, which is operated at temperatures in the range of 40-70 °C, the desorber is operated at elevated temperatures to promote regeneration of the particles. In order to reduce the process heat demand, a lean/rich heat exchanger (12) is incorporated at the bottom of the transport risers. Steam (3) serves to lower the partial pressure of CO₂ in the desorber as well as fluidization gas. Similar to the adsorber, the desorber also consists of five stages, each equipped with a heat exchanger (11), a wear plate and a downcomer. On the way from top of the desorber column to the bottom, the sorbent is regenerated. As adsorption is an exothermic reaction, the adsorber is cooled (10) to maintain the required operating temperature. While the heat of reaction and the required sensible heat to obtain the desired temperature-swing needs to be removed from the adsorber, heat is provided via the fluidized bed heat exchangers to the desorber, to enable the regeneration of the adsorbent.



- | | |
|--------------------------------|--|
| A ... adsorber | 4 ... CO ₂ enriched stripping gas |
| B ... desorber | 5 ... recirculation gas (CO ₂) |
| C ... riser | 6 ... recirculation gas (clean flue gas) |
| D ... gas-solid separator | 7 ... purge gas (CO ₂) |
| E ... L-valve | 8 ... purge gas (steam) |
| F ... recirculation compressor | 9 ... dilution stream (raw flue gas) |
| 1 ... raw flue gas | 10... Adsorber stage cooling |
| 2 ... clean flue gas | 11... Desorber stage heating |
| 3 ... stripping gas (steam) | 12... lean-rich heat exchange |
| | 13... high loaded solids |
| | 14... regenerated solids |

Figure 2-17: Basic scheme of double loop staged fluidized bed system for continuous TSA (taken from [36])

Pröll et al. [36] showed, that with the multistage fluidized bed process set-up, benefits of fluidized beds like excellent gas/solid contact and high heat transfer rates can be fully exploited whilst maintaining a net counter current flow pattern between gas and sorbent. In contrast to a single stage fluidized bed reactor, where the CO₂ content of the exiting gas stream and the loading of the exiting solid stream is in a direct relation because of the almost ideal solids mixing within the fluidized bed, a multistage system fluidized bed column uncouples this direct connection between these two variables. This in turn enables deep CO₂ removal from flue gases and high delta loadings between the rich and the lean sorbent stream at the same time (see Figure 2-18). Pröll et al. [36] showed, that this setup is superior over single stage configurations, as it leads to significantly lower process energy demands. Furthermore, Pirklbauer et al. [72] showed that the ideal stage configuration for such a process setup

depends on the CO₂ partial pressure in the raw flue gas as well as on the relative amount of CO₂ that needs to be separated.

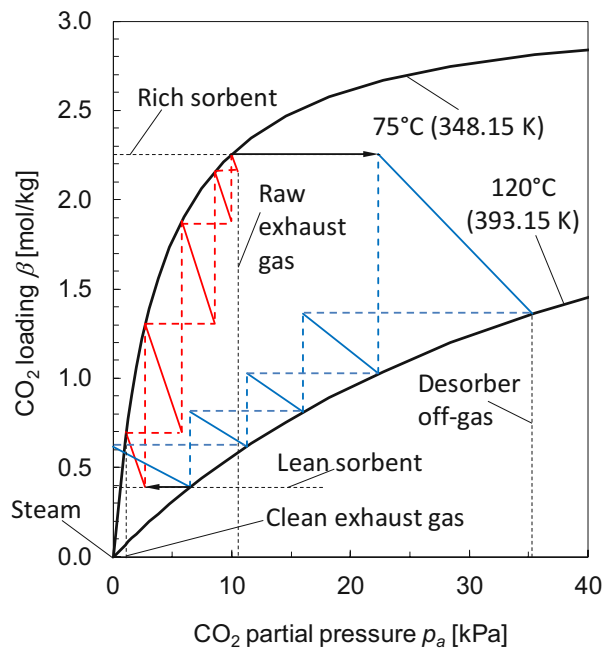
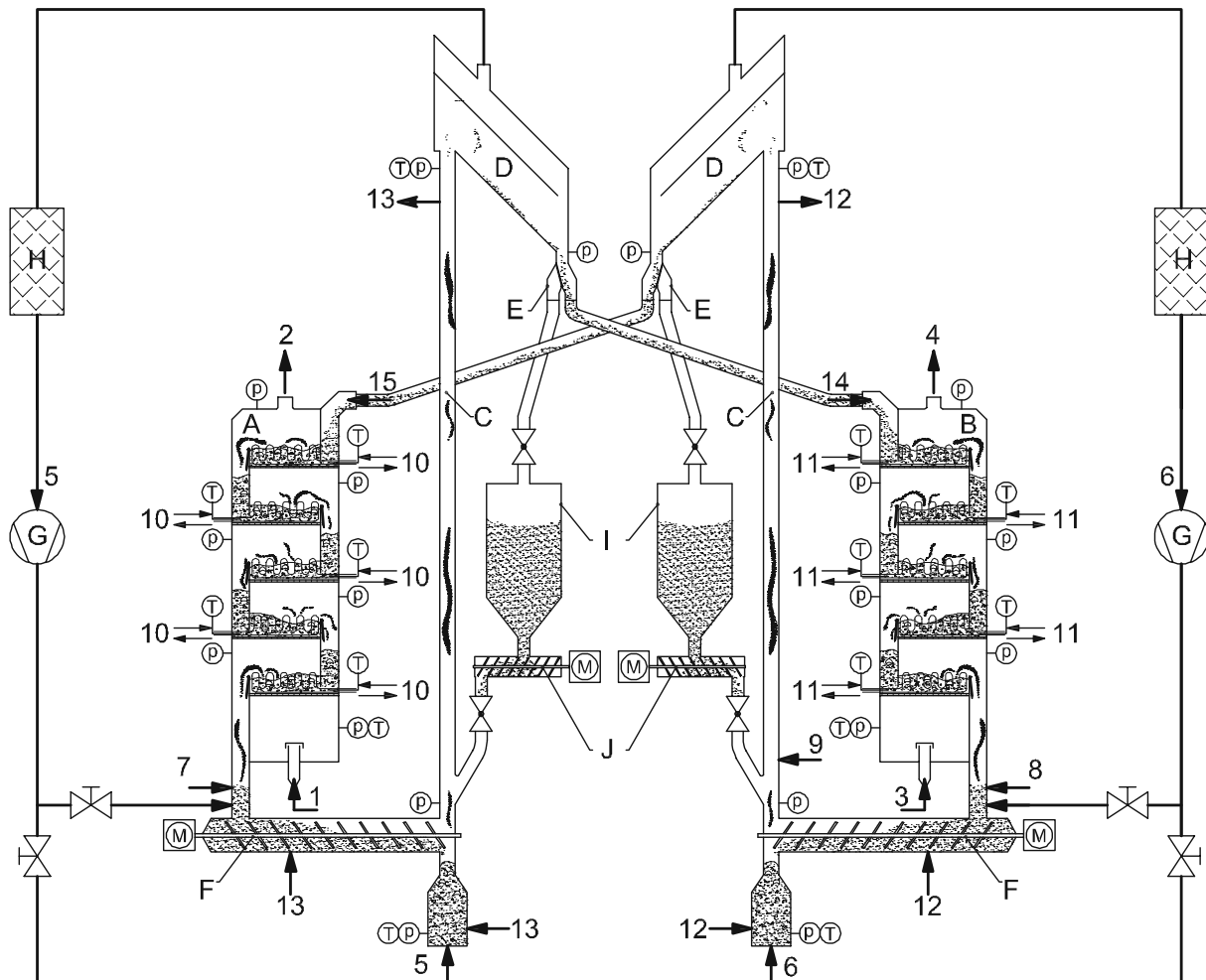


Figure 2-18: Illustration of CO₂ loadings in a multistage fluidized bed TSA process for adsorption at 75°C and regeneration at 120°C, at approx. 10 Vol-% CO₂, utilizing an amine impregnated silica sorbent (taken from [36])

2.3.3 MStFB-TSA bench scale unit

Based on a fluid dynamic design study of the multistage fluidized bed system and comprehensive modelling of the process, a bench scale unit (BSU) was designed and built to deliver a first proof of concept [37], [38]. Figure 2-19 shows the schematic set-up of the BSU. In accordance with the previously proposed process set-up, the BSU consists of two interconnected multistage fluidized bed columns with 5 stages each and two transport sections. In order to understand the current state of development especially in terms of reactor design, the design of the BSU is presented in the following. The most important design parameters are summarized in Table 2-2.



- | | | |
|-------------------------------|---|--|
| A ... adsorber | 1 ... raw flue gas | 11... desorber stage heating |
| B ... desorber | 2 ... clean flue gas | 12... riser cooling |
| C ... riser | 3 ... stripping gas (N ₂ , steam) | 13... riser heating |
| D ... gas-solid separator | 4 ... CO ₂ enriched stripping gas | 14... CO ₂ loaded adsorbent |
| E ... solids directing flap | 5 ... recirculation gas | 15... regenerated adsorbent |
| F ... bottom screw conveyor | 6 ... recirculation gas | |
| G ... recycle-gas blower | 7 ... purge gas (N ₂ , CO ₂) | Ⓟ ... pressure sensor |
| H ... particle filter | 8 ... purge gas (N ₂ , steam) | Ⓣ ... temperature sensor |
| I ... adsorbent tank | 9 ... dilution stream (N ₂) | Ⓜ ... driving motor |
| J ... adsorbent feeding screw | 10... adsorber stage cooling | |

Figure 2-19: Multistage fluidized bed TSA bench scale unit (taken from [37])

Adsorber

The adsorber column is a five-stage fluidized bed column with an inner diameter of 150mm and a stage height of approximately 210mm. Each stage of the adsorber (see Figure 2-20) is equipped with an exchangeable weir plate and gas distributor. The exchangeable weir plate allows to run experiments with varying adsorbent inventory per stage and to enable modifications of the downcomer geometry. An exchange of the gas distributor plate can be necessary to adapt the unit for a different gas velocity or for a different adsorbent. The stage heat exchanger is made of a 6mm copper tube and provides a heat exchange surface of 37840mm², which is connected to a water/glycol cooling cycle. As operating temperature and pressure are relatively low, part of the adsorber is made of borosilicate glass to allow for visual observation of the fluid dynamic behavior of the fluidized beds during CO₂ capture operation

and to facilitate potential troubleshooting during commissioning of the unit. Temperature is measured within the dense phase of each fluidized bed stage, as well as in the wind box of the column.

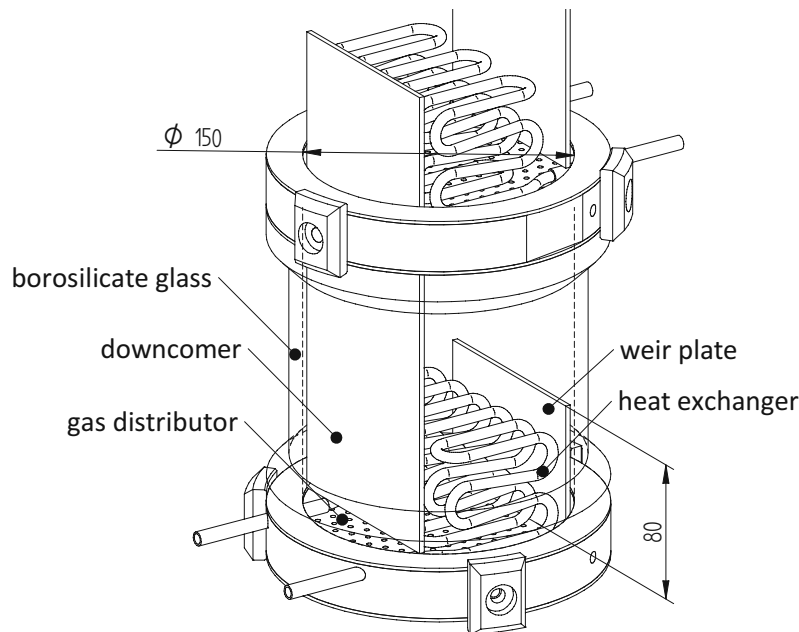


Figure 2-20: Bench scale unit: adsorber stage design

Desorber

Similar to the design of the adsorber, the desorber also consists of five individual fluidized bed stages. However, the cross section of the desorber is reduced to lower the consumption of stripping steam for regeneration and fluidization of the sorbent. Each equipped with exchangeable gas distributor and weir plate. The copper tube heat exchangers provide a heat exchange surface of 25260mm² per stage. But in contrast to the adsorber, the desorber features double walled heating jackets to avoid condensation due to heat losses. Each double walled heating jacket is connected in series with the respective stage heat exchanger which is connected to a thermal oil heating system. Because of the small size of the unit, the contribution of the heated wall on the overall heat transfer cannot be neglected. Assuming the height of the dense phase of the fluidized bed with 80mm and neglecting the wall area of the heating jacket within the freeboards, additional 27600mm² heat exchange surface per stage can be assumed for the double wall. Visual monitoring of the fluidized beds is not possible because of the desorber design. Thus, the operator has to fully rely on the differential pressure measurements over each stage as an indicator for the state of the fluidized bed. Similar to the adsorber, each desorber stage also features a temperature sensor within the dense phase of the fluidized beds.

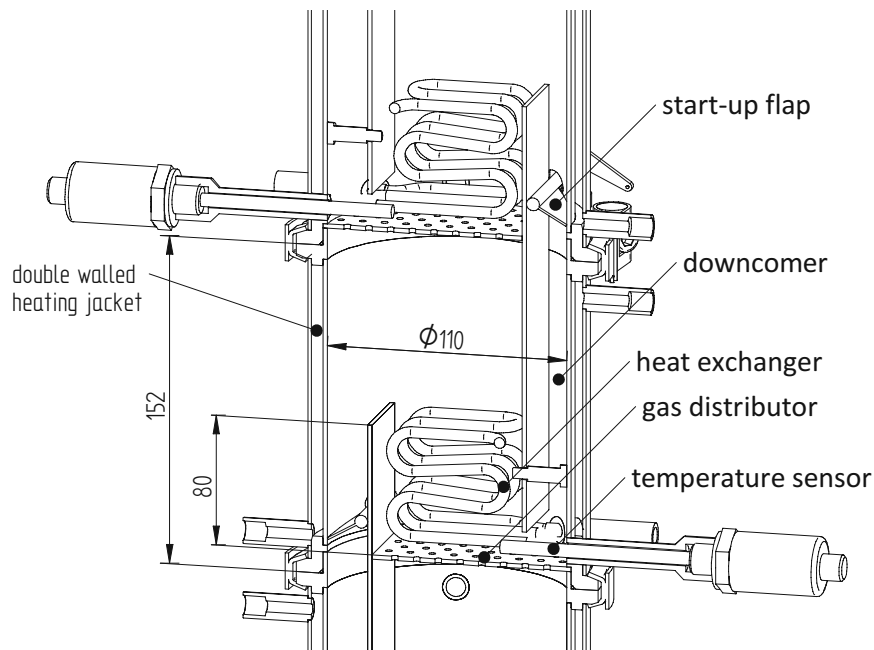


Figure 2-21 Bench scale unit: desorber stage design

Transport sections

As described above, the adsorbent enters at the respective top stage of adsorber and desorber where it is brought into contact with the fluidization gas in counter current flow. At the bottom of the adsorber and desorber column, the sorbent is continuously extracted from the lower most stages by means of screw conveyors with variable frequency drives. These bottom screw conveyors (BSC) feed the adsorbent to the bottom section of the transport risers (see Figure 2-22). The transport risers are fluidized with recycled gas entering over a bubble cap in the bottom of the risers. The whole transport section from screw conveyor inlet to particle separator inlet is double walled to enable active heating or cooling in this area. The bottom section of the risers has a bigger cross section (DN40) compared to the transport section (DN25) above. The reduced gas velocity in the bottom section of the riser causes an increased sorbent hold-up and improves the heat transfer from the walls to the adsorbent. At the top of the transport risers, the particles are entering the particle separators. These are a combination of gravitational and impact separators, where the solids velocity is reduced in the first part before the solids are deflected downwards by a baffle plate. Because of their relatively high surface area and subsequent heat losses, the particle separators are insulated and can be trace heated to avoid condensation. After the particle separators, the solids can be directed either to the column or back to the storage tank, by means of a flap valve located below the separators. Furthermore, adsorbent from the storage tank can be fed to the system during operation over a nozzle in the bottom section of the transport risers. These two options for sorbent extraction and feed allow for a partial exchange of the sorbent material during operation, for example to exchange degraded material or to compensate material losses due to attrition. Temperature can be measured in the bottom section as well as in the transport section of the risers.

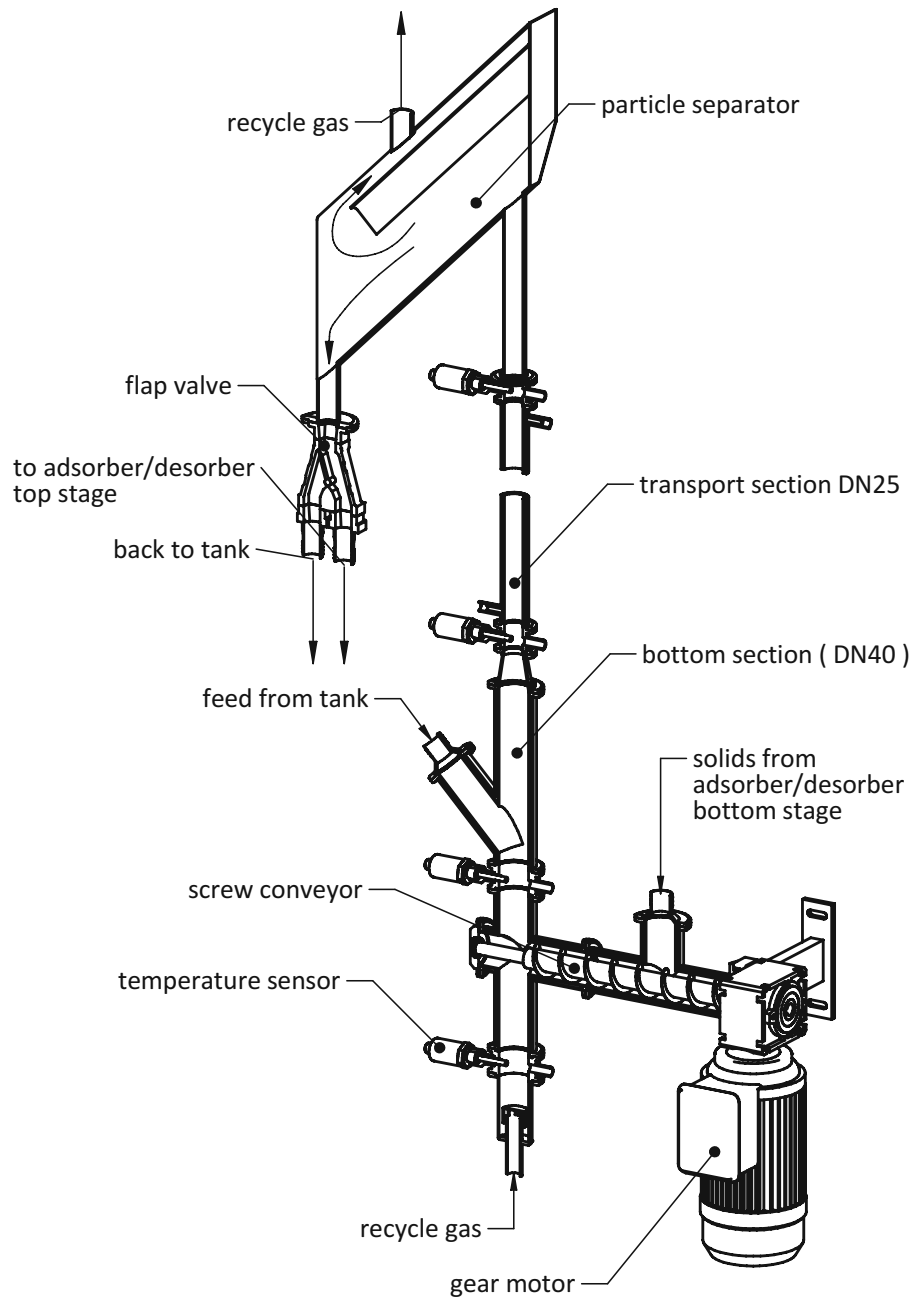


Figure 2-22 Bench scale unit: sorbent transport section design

Table 2-2 Bench scale unit specifications

adsorber column		
column diameter	150	[mm]
number of stages	5	[-]
weir height	80(40/60)	[mm]
total stage height	207	[mm]
design operating temperature	75	[°C]
feeding gas components	N ₂ , CO ₂ , H ₂ O, air, flue-gas [-]	
design gas flow rate (y _{N₂} = 95 % _{Vol.} , y _{CO₂} = 5 % _{Vol.})	15.8	[Nm ³ h ⁻¹]
design CO ₂ capture efficiency	90	[%]
design CO ₂ capture rate	34	[kg day ⁻¹]
desorber column		
column diameter	110	[mm]
number of stages	5	[-]
weir height	80(40/60)	[mm]
total stage height	152	[mm]
design operating temperature	120	[°C]
feeding gas components	N ₂ , H ₂ O, air [-]	
design gas feeding rate (steam)	8	[kg h ⁻¹]
design gas feeding rate (N ₂)	10	[Nm ³ h ⁻¹]

Definition of performance parameters:

In the following, the parameters used to measure the performance of the TSA CO₂ capture process are defined:

- The **capture efficiency** is defined as the ratio between volumetric standard flow rate of captured CO₂ to the volumetric standard flow rate of the total CO₂ feed:

$$\eta_{captured} = 100 \cdot \frac{\dot{V}_{CO_2,captured}}{\dot{V}_{CO_2,in}} = 100 \cdot \frac{\dot{V}_{CO_2,ADS,in} - \dot{V}_{CO_2,ADS,out}}{\dot{V}_{CO_2,ADS,in}} \quad \text{Equation 2-8}$$

If leakages from or to the column are neglected, the capture efficiency can be calculated as follows:

$$\eta_{captured} = 100 \cdot \left(1 - \frac{c_{CO_2,ADS,out} * (1 - c_{CO_2,ADS,in})}{c_{CO_2,ADS,in} * (1 - c_{CO_2,ADS,out})}\right) \quad \text{Equation 2-9}$$

- Another frequently used performance parameter is the **dynamic sorbent loading**, which is defined as follows:

$$dSl = \frac{\dot{m}_{CO_2,captured}}{\dot{m}_{Sorbent}} * 100 \quad \text{Equation 2-10}$$

2.4 SUMMARY OF RESULTS FROM PREVIOUS STUDIES

Since design and operation of multistage stage fluidized beds is a challenge already without adsorption activity, fluid-dynamic operability of the BSU had to be proven first. Therefore, dedicated cold flow experiments have been conducted with the actual adsorber column and the fluid dynamic behaviour was studied ([37], [73]). One major challenge for multistage fluidized beds lies in the sorbent flow and inventory control. Within these studies important experience for design and operation was gained and the fluid-dynamic feasibility was proven. Furthermore, the influence of operating parameters on the sorbent hold up in the individual stages was studied and a design and operating strategy for sorbent inventory control was elaborated.

After the fluid-dynamic feasibility under cold conditions was proven, first capture operation with a 50 % PEI impregnated porous silica sorbent material under dry conditions (N_2 as stripping agent) was achieved in 2013. Schöny [37] showed that the multistage fluidized bed adsorber is capable of very deep CO_2 removal which is indicated in the data log of one of the first experiments with the BSU (see Figure 2-23). In this experiment, the sorbent was circulated without CO_2 feed for approx. 1 hour to heat up the system. Thus, the sorbent can be considered as fully regenerated. At timestamp 1:05 CO_2 was added, which is followed by an immediate increase of adsorber temperatures. However, a breakthrough of CO_2 at the outlet of the adsorber was delayed by roughly 20-30 minutes, which already indicates fast kinetics and no significant gas bypass at the prevailing operating conditions.

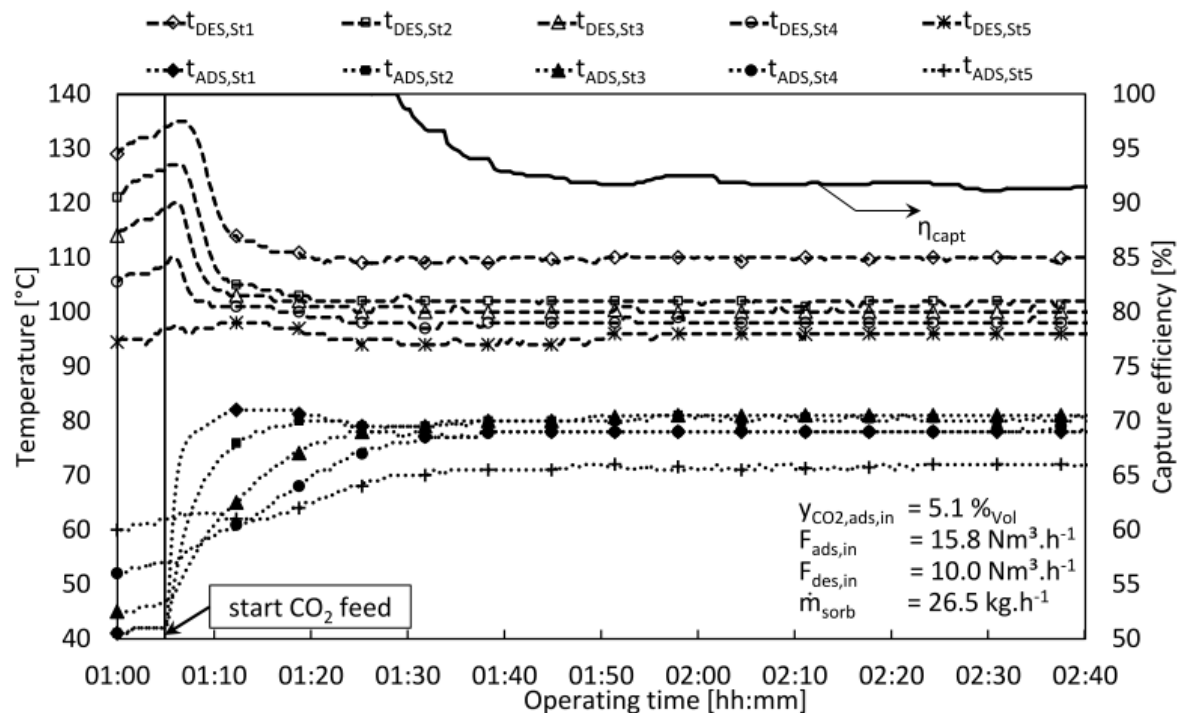


Figure 2-23: Data log of BSU experiment with N_2/CO_2 mixture (taken from [37])

In the further course of technology development, several parameter variations were conducted. Besides operation with steam as stripping and fluidization gas for the desorber, [38] varied parameter

like the dew point of the adsorber feed gas, sorbent circulation rate, the relative and absolute CO₂ feed, as well as the stage inventories.

Figure 2-24 shows a variation of the sorbent circulation rate at bench scale. On the left side of Figure 2-24, stage temperatures are shown, while the right side presents the dynamic sorbent loading and the capture rate over the sorbent circulation rate. Although, this variation was done with nitrogen as stripping and fluidization gas for the desorber, it shows the general tendency, that with a higher sorbent circulation rate the capture rate was increased to some extent. However, insufficient heat exchange led to a reduced temperature swing between both reactors, so that the dynamic sorbent loading was affected in a negative way, which finally limited the capture rate of the plant. A similar behavior was observed when the CO₂ content in the simulated flue gas, which was fed to the adsorber column, was varied (see Figure 2-25). Since a higher CO₂ concentration increases the driving force for adsorption, the capture rate gets first increased but levels as soon as the temperature swing cannot be maintained anymore due to heat transfer limitations.

With the amine functionalized sorbents, tested in the BSU, also the role of humidity was identified as crucial for the process. It was shown that a significant amount of water is co-adsorbed by the sorbent material. Depending on the relative humidity in both columns, a net transport of water occurs either from adsorber to desorber or in the opposite direction. The exact heat of reaction for the observed water co-adsorption was not determined but for Lewatit VP OC 1065, it is reported to lie in the range of the water condensation enthalpy [71] and is therefore significant for the process heat management.

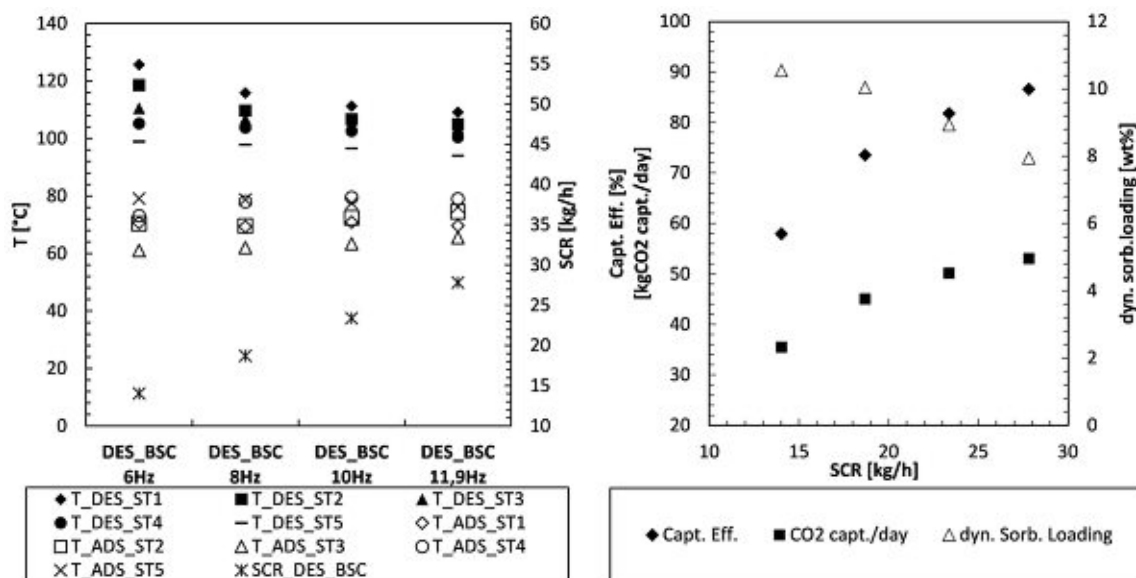


Figure 2-24: Variation of sorbent circulation rate under dry conditions (desorber operated with nitrogen) at bench scale (taken from [38])

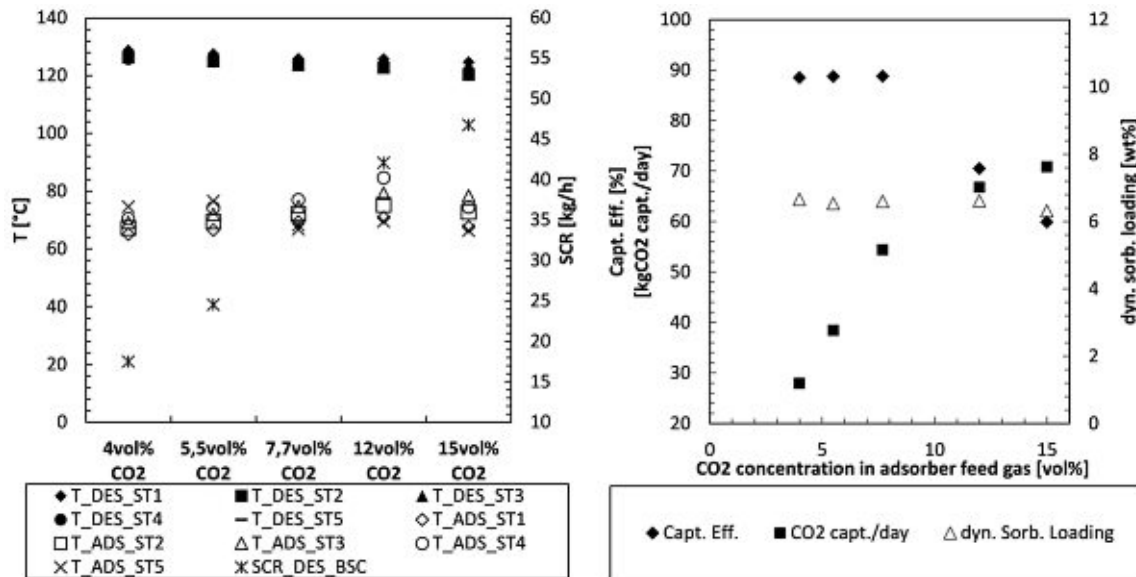


Figure 2-25: Variation of CO₂ content in adsorber at bench scale (taken from [38])

Another important milestone was reached by conduction of two 120-hour test runs to assess the cyclic stability of two different sorbent materials (see Table 2-3). While experiment A was conducted with the previously utilized impregnated silica, experiment B was conducted with a commercially available ion exchange resin called Lewatit VP OC1065 by Lanxess, which is further described in Chapter 3.

Table 2-3: 120h test run conditions (taken from [66])

	experiment A	experiment B	unit
flue gas flow rate	16.8	16.8	[Nm ³ ·h ⁻¹]
N ₂ flow rate	8.9	8.9	[Nm ³ ·h ⁻¹]
CO ₂ flow rate	0.7	0.7	[Nm ³ ·h ⁻¹]
pressurized air flow rate	7.2	7.2	[Nm ³ ·h ⁻¹]
adsorber steam flow	0	0.6	[kg·h ⁻¹]
flue gas O ₂ concentration	9	9	[Vol-%]
flue gas CO ₂ concentration	4.2	4.2	[Vol-%]
target adsorber operating temperature	70-75	45-50	[°C]
stripping steam feeding rate	8.5	8.5	[kg·h ⁻¹]
target desorber operating temperature	120-125	100-105	[°C]
sorbent inventory	6	4.9	[kg]

For both test runs, the sorbent circulation rate was tuned within the first hours of operation to achieve around 90 % capture efficiency in both cases. After this initial tuning, the conditions were kept constant. Sorbent A showed a slightly higher initial CO₂ capacity and required less sorbent circulation rate than Sorbent B (Sorbent A: 13.5 kg·h⁻¹; Sorbent B: 15.4 kg·h⁻¹). However, based on the continuous measurement of performance parameters as well as on process emission measurements [66] a significant degradation of Sorbent A over the course of the test run was identified. The loss of

adsorption capacity over 100 h for sorbent A was 3.48 wt%, which is 20 times higher than for Sorbent B (0.16 wt%). Furthermore, the porous silica adsorbent did show significant attrition which was reflected by an entrainment rate of $3.31 \text{ g}\cdot\text{h}^{-1}$, while the loss rate for Sorbent B was less than $0.5 \text{ g}\cdot\text{h}^{-1}$.

Although, the bench scale unit experiments enabled to gain design and operating knowledge for the multistage TSA process, various limitations at bench scale hindered further development of this technology. In the following section, the observed limitations will be identified, and process scale up considerations and main challenges will be discussed.

3. PROCESS SCALE UP

3.1 GENERAL ASPECTS

As discussed previously, CO₂ scrubbing by means of absorption with liquid amine solvents has some drawbacks and various new technologies have been introduced for capture of CO₂ [74]. Many of them are very promising and might be superior compared to the state of the art. But most of these technologies are still in a relatively early stage of development and have been demonstrated, if at all, only at small scale.

Depending on the technological field, large CO₂ stationary sources have an average CO₂ emission of up to 4 MtCO₂ per source and year (coal fired power plants). Gas fired power plants typically lie in the range of 1 MtCO₂ per source and year, which is also the rough order of magnitude for average large cement production sites and production in petrochemical industry (e.g.: Ethylene production) as well as refineries [75].

While a target application is expected somewhere in the range of 10⁶ tons of captured CO₂ per year, solid sorbent processes are currently evaluated several orders of magnitude below that at lab or pilot scale (e.g.: [34], [35], [76]). This large gap between the current stage of development and the target application most likely requires several upscaling steps.

Temperature swing adsorption has been identified as a very promising emerging technology [60]. A large share of TSA related publications in literature is focused on adsorbent development while the reactor design is often disregarded. However, the past years frequently showed that promising adsorbent materials with high adsorption capacities on paper often perform completely different when they are used in continuous operation at realistic conditions. Zeolite 13X for example showed significant attrition in fluidization tests [50]. Furthermore, different adsorbent materials, sometimes require their own reactor or process design to perform well. Thus, adsorbent development and reactor design should go hand in hand.

For the TSA process design developed at TU Wien, the proof of concept was delivered, and promising sorbent materials have been selected and tested. The bench scale unit enabled to gain a general understanding of the process and relevant connections between operating as well as design parameters and the process performance (see chapter 2).

However, at the stage of lab scale testing not all of many important questions can be answered with the required precision. Especially, when it comes to economic figures like capture costs per ton relatively huge uncertainties have to be taken into account. This is mainly attributed to high relative heat losses and some compromises in design that are necessary at small scale. Thus, tests at a larger scale are necessary to develop this technology further.

3.2 TARGET APPLICATION – FULL SCALE TSA

From the logical perspective, it would make sense to replace power plants and industrial plants with high specific CO₂ emissions against technologies with lower specific CO₂ emissions instead or in addition to application of carbon capture measures. Furthermore, it is thermodynamically easier and

would make more sense to separate CO₂ from sources with higher CO₂ concentration, instead of separation from sources with low concentrations. But for the question if carbon capture and/or CCS makes sense at all, and what should be the target application a lot of factors play together. For some regions it can make sense to separate CO₂ from air, while coal fired power plants with a relatively high CO₂ concentration in their flue gas are still in operation without separation of CO₂ in a different region. In any case, it makes sense to think about potential target applications of a technology in an early stage already. Which means identifying of advantages and disadvantages of the developed TSA technology compared to other separation technologies. One specific advantage of the multistage TSA process is, that high dynamic sorbent loadings are achieved even at low CO₂ concentrations.

Another aspect of CCS, if applied to power generation, is the reduction of the overall efficiency of power generation. Since heat and electrical power for the capture process is indirectly supplied by the fuel, which is burnt, either the electrical net output gets reduced or more fuel has to be provided (if possible) to maintain the same output. This efficiency drop is directly coupled to the specific CO₂ emissions of the fuel. The higher the specific CO₂ emission of the fuel, the higher is the drop in efficiency for a certain reduction of emitted CO₂. For fuels with high specific CO₂ emissions like coal the drop of net efficiency is therefore significantly higher than for fuels with low specific CO₂ emissions like natural gas. Therefore, it is expected, that there will be a future market for this technology in combination with gas-fired power plants.

Without limiting the technology to this field, the target application has therefore been defined as follows:

CO₂ feed concentration: 4 Vol-%

Target capture efficiency: 90 %

Target capture rate: 1 Mtpa

3.3 TECHNOLOGICAL CHALLENGES FOR FULL SCALE TSA

Despite the promising performance of the TSA bench scale unit, many technological challenges need to be overcome before the technology is considered as commercially available. Among others, these are some of them:

- **Adsorbent development:** The utilized adsorbent has a huge impact on many parts of the process. The particle size for example influences the fluid dynamic behaviour of the fluidized beds, but also kinetics of adsorption and the heat transfer coefficient. The type of adsorbent will also have a big impact on process performance, emissions, as well as on the heating and cooling demand and the final energy demand and costs for separation of CO₂. Since a significant share of operating costs will potentially be attributed to sorbent make-up, sorbent stability will also play a big role. Therefore, the optimal sorbent, which delivers the best compromise for all these factors needs to be identified.
- **Model development:** To allow for reliable predictions of important process parameters, a good model is indispensable. A process model can be a powerful tool not only for the design of a plant, but also for further improvements and optimization of operating parameters. Huge

effort was made to develop models capable of predicting process performance under varying conditions [61], [72], [77]–[79]. However, these models are based on many assumptions and many measurements like measurement of the CO₂ uptake capacity, water uptake, heat capacity and many more. Thus, actual results, might deviate from model predictions. If a model is used for design of a large-scale plant, these deviations can cause a significant financial damage. Therefore, process models need to be validated and if required adapted with actual results from operation at most realistic conditions.

- Process design: To fully exploit the advantages of solid sorbents, an optimized process design will be required. Small changes of the set-up and thoughtful heat integration measures can make a decisive difference in terms of energy consumption or other key performance indicators.
- Identification and control of process emissions: To decide on if and which pre- and or post treatment of the flue gas and CO₂ will be required, good knowledge of process emissions will be required. Furthermore, operating conditions will have a big impact on process emissions as well. This could mean, that the optimum operating parameters for the capture task only, might not match the optimum operating parameters for emission control. The challenge will be to find the best compromise between many factors. Therefore, an extensive study will be required to understand mechanisms of sorbent degradation and process emissions.
- Reactor design: One of the biggest challenges for TSA is the development of a suitable reactor design, which provides optimized process performance at low footprint, low operating costs and low capital expenditure. Temperature swing adsorption for separation of CO₂ is promising. However, compared to a liquid amine system, the reactors and the sorbent transport between and within the main reactors is much more complicated, which will create many challenges for upscaling.

3.4 LIMITATIONS AT BENCH SCALE

As indicated previously, the multistage fluidized bed temperature swing adsorption lab scale unit presented in Chapter 2 provided an excellent opportunity to assess the process performance under varying conditions and to get a basic understanding of the process. However, there are some limitations that make further process development difficult. The main limitations are listed here:

- Heat transfer limitations: due to the small size of the lab scale unit, one has to face limitations in terms of manufacturability. With respect to the bench scale unit this means, that it was not possible to fit the same specific heat transfer surface per bed volume as it would be potentially possible in a larger scale unit. This lack of heat transfer surface limits temperature control during operation
- Heat losses: the smaller a plant is, the higher its surface to volume ratio. Thus, a lab scale unit usually has disproportional heat losses, which needs to be considered in the evaluation of process performance. However, if the share of heat losses is getting higher and higher, compensation of heat losses for evaluation of process performance is more and more inaccurate.
- Wall effects: For the fluid dynamic design of a large-scale unit, wall effects only play a minor role, while for a plant of the size of the bench scale unit it becomes very important and can strongly impact the fluid dynamic behaviour.

- Long-term operation experience: Despite the relatively extensive experiments conducted with the lab scale unit, it was not designed for long term operation. Especially the relatively low level of process automation requires many operator interactions, which results in unstable operating conditions. This in turn complicates certain investigations and reduces the quality of gained results.

3.5 NEXT SCALE TSA

Due to limitations at lab scale further process development requires investigations at larger scale. This leads to the question: What scaling factor should be applied to overcome the discussed limitations. Depending on the operating point, a scaling factor of approx. 50 000 would be required to reach the target capture capacity of a commercial unit with the design of the bench scale unit presented in Chapter 2. It is obvious, that it is not reasonable to apply a scaling factor that high. But on the other hand, it is also not reasonable to make too small steps in scaling. In the end, the choice of a scaling factor is a tradeoff between investment risk, quality of gained results and the overall development time. Clear optimum steps for scaling cannot be identified, but for this technology the following steps are seen reasonable:

- Lab scale (50 kg/day = 18 t/year; see 2.3.3)
A lab scale plant enables a relatively fast basic assessment of process performance under varying conditions at low investment and operating costs. Furthermore, continuous tests at lab scale represent an excellent supplement to TGA tests for adsorbent screening and development.
- Pilot scale (1 t/day = 365 t/year)
The aim of a pilot program in this context is not to demonstrate a final design of the technology but to enable further development of the technology. The aim is to provide a tool which can answer remaining questions, which cannot be answered at lab scale. The pilot scale unit should provide sufficient operating flexibility to enable a comprehensive experimental campaign to gain a deepened understanding of the process and to allow for model refinement and more precise predictions of process performance at the next scaling level. Therefore, it is required to overcome at least partially above-mentioned limitations.
- Demonstration scale (100 t/day = 36500 t year)
After completion of the pilot program, it should be clear already how core components (e.g.: adsorber, desorber, transport and heat exchange equipment) should look like for a demonstration plant and how they are designed to obtain a certain process performance. Ideally, a demonstration scale unit would prove the commercial readiness of the technology at minimized investment risk. Thus, any critical design questions should be answered at this scale already. This means that the demonstration should rather be a down-scale of the commercial scale than a scale up of the pilot unit. The demonstration plant should deliver concrete figures for all relevant process performance indicators like: capture efficiency, capture costs, sorbent initial costs and make up costs, process emissions etc. to allow for well-founded decisions for the future of the technology.

- Commercial scale (1 000 000 t/year; see Chapter 3.1)
Besides the actual process performance and a comparison to other available technologies, many factors as well as the political situation will play a role for the final decision if a commercial scale TSA plant will be realized or not.

3.6 VIENNA GREEN CO₂ PILOT PROGRAM

ViennaGreenCO₂ is a flagship-project, co-funded by the Austrian Climate and Energy Fund, which was started in 2014 together with a consortium of industry partners and the University of Natural Resources and Life Sciences with TU-Wien as consortium leader.

The project leads the way to demonstration of the TSA CO₂ capture technology by investigation of the technology at pilot scale. A pilot plant is designed with focus on scalability and built at the site of the biomass combined heat and power (CHP) plant Vienna/Simmering. Tests with real combustion exhaust gas over several hundreds of hours will be conducted. The design, construction and operation of the pilot plant is accompanied by focused research activities regarding the basic process performance (existing laboratory unit) fluid dynamics (cold flow model of the pilot plant), low temperature fluidized bed heat transfer and heat exchanger design (heat transfer test facility), mathematical modelling of the TSA system, overall process simulation and optimized heat integration. The outcome of the pilot scale experimental campaigns constitutes the basis for solid techno-economic evaluation of the proposed technology.

An additional aspect of the flagship project is the investigation of the possibility to locally supply captured CO₂ to vegetable farms in Vienna/Simmering for greenhouse fertilization (see Figure 3-1). This would save transport effort and costs compared to the current situation, where the farmers buy technical CO₂ from distant fossil sources. If the CO₂ utilization route is technically feasible, this may create a niche situation for sustainable operation of a next scale CO₂ capture demonstration unit at the Vienna site beyond the proposed project. However, this thesis will focus on the development of the TSA CO₂ capture technology only.

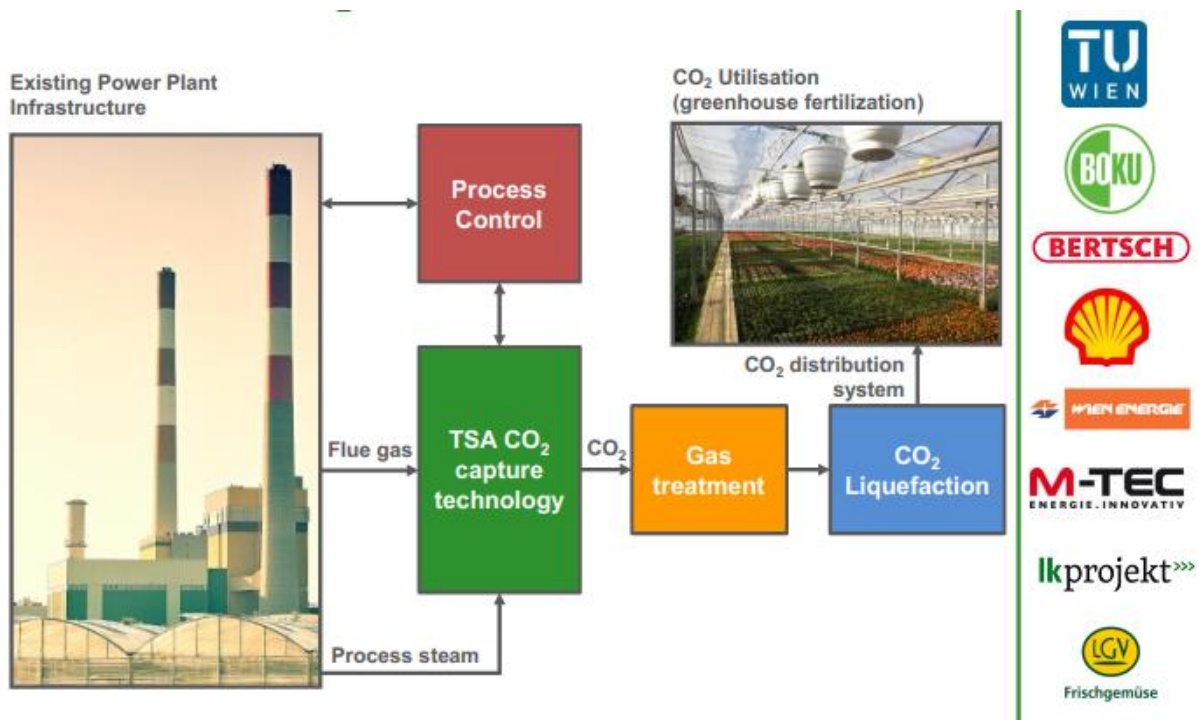


Figure 3-1: ViennaGreenCO₂ project

3.6.1 Main tasks

Following main tasks have been defined:

- **Definition of design basis**

Within the ViennaGreenCO₂ pilot project, a one-of-a-kind CO₂ capture plant shall be designed, erected, and operated. This pilot unit shall be designed in a way, that certain operating conditions can be achieved, while also the efficiency of the process is demonstrated. This requires clear definition of targets, requirements, and operating conditions in a design basis before the actual design process starts.
- **Process engineering**

Process engineering for TSA is an iterative process, starting with process flow diagrams (PFD) and the most basic TSA set-up, which consists of an adsorber, a desorber and the transport sections (e.g.: two risers) in between. With the aid of process modelling and accompanying experiments at bench scale, the set-up shall be improved and trimmed to meet defined requirements at the best compromise possible. After final PFDs are determined, all relevant process data shall be derived in form of a heat and material balance (HMB), which will be the major input for reactor design.
- **Reactor design**

With the design basis, process flow diagrams and the heat and material balance, required inputs for the reactor design are defined. The challenge is to implement a reactor design, which considers many technical aspects at the same time. The adsorber for example needs to allow for a certain gas through put. But at the same time, a certain sorbent mass flow and a certain

heat exchange needs to be ensured as well, while these factors potentially have some mutual interference. With design criteria from literature as well as with the aid of dedicated investigations, a reactor design shall be found which features continuous and stable operation at design conditions.

- Detail design, erection, and commissioning

As soon as the basic reactor design is completed, which in this case means that the geometry of everything that is in contact with the sorbent is specified, remaining details of the whole plant design need to be elaborated. Besides equipment specification and the production of manufacturing drawings, an HSE study shall be conducted to ensure safe operation of the plant. As the ViennaGreenCO₂ pilot is to be erected in an industrial environment, it requires a permit by the authorities. Thus, relevant regulations need to be considered as well in the design of the pilot unit. After erection and commissioning of the plant, one further challenge will be to find the right procedures for startup of the plant. Therefore, startup planning has to be carried out relatively early, since it could reveal required features of the process setup.

- Operation

The process will be investigated in an extensive experimental campaign. Within this campaign, the influence of main operating parameters like flue gas flow, stripping steam flow rate, adsorbent circulation rate and others will be studied in a thorough parameter variation. Long term operation will deliver precious results for adsorbent stability and process emissions. Gained results from operation will be used to close the feedback-loop for model development as well as for a techno-economic assessment of sub-units of the process and the whole TSA set up. With a significantly improved ratio of heat losses vs. process heat demand, economic figures will be predicted with increased accuracy compared to bench scale.

3.7 DESIGN BASIS FOR THE TSA PILOT UNIT

3.7.1 Key Objectives for pilot program

The main objective of the pilot program is to demonstrate the technology in long-term operation at relevant scale and varying operating parameters. But the true rationale behind this is, that there are many open questions, which have to be answered for further upscaling.

Model development is a workstream which is part of the TSA development since the very beginning. A process model can be a powerful tool not only for design of a plant but also for optimization during operation. The process model which served process design of the bench scale unit presented in Chapter 2 is a mathematical equilibrium model which is based on measured CO₂ adsorption isotherms. These isotherms represent the equilibrium loading of CO₂ on the sorbent for a certain temperature and partial pressure. The assumption, that adsorption and desorption reach equilibrium in the continuous process is a rough approximation at best. But the actual process behavior can deviate significantly from equilibrium conditions. Different mechanism like insufficient gas to solid contact or diffusion limitations can lead to such deviations. However, also the sorbent characteristics itself can

change in presence of other gas components like water vapor. In order to validate the ability of the model to predict the process behavior and or to improve the model, dedicated experiments with the bench scale unit and other experimental set-ups have to be conducted. In the next step, the process model will be used to derive most important process data in form of a heat and mass balance.

Literature in the field of TSA highlights the significant reduction of the **process energy demand** which is to be expected when a solid sorbent replaces its liquid counterpart. At a first glance, a reduction of the energy demand looks obvious, since the solid sorbent features a significantly lower heat capacity compared to the water-based solvent. However, it is still to prove if this can be exploited advantageously.

Degradation of the sorbent material and other mechanism will very likely lead to **process emissions**. One aim of the pilot program is to identify and quantify preferably all gaseous and aqueous emissions from the process and to study the mechanism leading to them. Good knowledge of process emissions is important for the further development of the process and to identify potentially required pre- and or post-treatment of the flue gas or the captured CO₂.

Adsorbent stability will play a major role for the process assessment since a significant share of operating costs is expected to be attributed to sorbent make-up. Within the scope of the pilot campaign, selected sorbent materials shall be assessed regarding their mechanical stability as well as their CO₂ capacity over a large number of cycles. Experimental results shall be the input for a techno-economic assessment which delivers the required sorbent make up rate.

Another important objective of the pilot program is to perform focused tests with regards to **CO₂ purity and a potential gas slip** between the two columns in general. A strategy to avoid unwanted gas slips shall be elaborated, implemented, and tested in the pilot unit.

Circulating multistage fluidized beds require a rather complex reactor design. The sorbent transport to and within the columns as well as sorbent distribution will be one of the major challenges for large scale plants. One objective of this pilot program is to **gain design expertise** required to deal with the special challenges of this technology. Furthermore, the pilot unit shall provide the framework to de-risk equipment design (e.g.: a certain heat exchanger design) at relatively low costs.

The final aim is the assessment of expected **total capture costs per ton of CO₂**, which indirectly includes all previously mentioned points, that is going to be of highest interest for the decision makers.

3.7.2 Key requirements for pilot unit

It is obvious, that not all detailed requirements for the pilot unit can be mentioned in this context. However, the most important requirements for the ViennaGreenCO₂ pilot unit are listed here:

- Sufficient heat transfer

At bench scale, heat transfer limitations frequently resulted in either too low or too high operating temperatures. Independent setting of operating conditions was often not possible, which made the evaluation of parameter variations very difficult. To have good control of process temperatures and to overcome limitations in terms of heat transfer, which have been observed in the bench scale unit, an optimized fluidized bed heat exchanger design is required. Since large surface areas are required to provide or extract the heat to/from the process, densely packed heat exchanger bundles are expected to be required for sufficient temperature control. For a precise design of the heat exchanger bundles, it is required to investigate influencing parameters on the heat exchange coefficient like: tube diameter, bundle geometry, particle size and operating conditions in particular.

- Long term operation

For the assessment of long-term effects like adsorbent degradation and process emissions, the plant needs to be operated for at least several hundred or thousand adsorption and regeneration cycles at stable conditions. Stable conditions means at one hand, that the plant itself has to provide stable operating conditions (temperatures, sorbent circulation rate etc.) and on the other hand, that the host site should provide flue gas of constant composition as well.

- Possibility to assess co-adsorption of water at realistic conditions

Most sorbent materials for capture of CO₂ can adsorb a significant amount of water, whereby the adsorption capacity is, similar to CO₂ adsorption, depending on the water content and the temperature of the surrounding gas composition. This means, depending on the conditions in adsorber and desorber, water transport takes place either in this or the other direction (see also [37], [66]). As adsorption and desorption of water requires or releases the heat of reaction, the heat exchanger duty of both columns can be influenced significantly. However, the impact of water co-adsorption needs to be investigated further in order to reduce any negative impact as much as possible or to even exploit its impact on the heat balance. Besides experiments at lab scale, an assessment at pilot scale under realistic conditions shall take place. In order to fully understand influencing parameters, the pilot unit shall feature good control of the operating conditions with regard to water adsorption.

- Reduced adsorber footprint

At pilot scale, the plant footprint will not make a significant difference in total project costs, the complex instrumentation and the disproportional design costs are larger cost drivers. But at full scale, the size of the plant will be one of the main cost factors. Therefore, the adsorber gas velocity shall be maximized already at pilot scale to enable the assessment of potential limitations already at this stage of development. While first experiments at bench scale have been conducted with approximately 0.3m/s, the pilot unit shall allow for conducting experiments with gas velocities of up to 1m/s in the adsorber.

- Flue gas feed variation

Even though, multistage fluidized bed temperature swing adsorption might have its main advantages at lower CO₂ feed concentrations, the pilot unit set-up should feature a broad flue gas feed variation so that the feed concentration can be controlled as well as the total flue gas flow.

- Assessment and implementation of lean/rich heat exchange

A system for exchange of sensible heat between the hot lean and the cold rich sorbent stream has the potential to significantly reduce the overall process energy demand [36], [78]. However, due to the utilization of solids instead of a liquid, the design of the required heat exchangers is more challenging. As part of this work, a suitable design shall be identified, developed, and tested.

- High CO₂ purity and advanced gas sealing measures

In solid sorbent systems, gas sealing between different subsections of the process cannot be achieved as easily as it is the case for liquids. However, the requirements for gas sealing are similar. The separated CO₂ should be of high purity especially with regards to O₂ traces in order to avoid equipment corrosion issues downstream to the CO₂ compression unit. Furthermore, an oxygen slip from the adsorber to sections of the process with higher temperature could cause oxidative degradation of the sorbent which reduces its CO₂ capacity [80]. Among other reasons, it is therefore important to elaborate and test suitable measures for gas sealing of different sections of the process.

- Minimization of steam demand

The steam feed to the desorber serves for two purposes: On the one hand it is the fluidization gas for the fluidized beds of the desorber and on the other, it serves as a stripping gas which reduces the partial pressure of CO₂ and promotes regeneration of the sorbent. One important task is to design the desorber in a way, that both functions are optimized. That means, that the steam feed is at the optimum for stripping and enough for proper fluidization at the same time.

- Instrumentation and analytical equipment

In order to get the best output from the experimental campaign, it is crucial to equip the pilot unit with adequate instrumentation and analytical equipment. Various online measurements of flows, temperature, pressure, and gas compositions but also offline analyses in the lab can provide additional information for model validation and can even help to improve the process models. Minimum requirement for the pilot unit's instrumentation is to enable a full assessment of cooling and heating duties in all relevant sections of the pilot unit as well as the closure of the CO₂ mass balance.

3.7.3 Key challenges for the design of the pilot unit reactor design

- Selection of a suitable adsorbent material

The selection of a sorbent material has of course the biggest impact on the whole process. Not only CO₂ adsorption isotherms have an impact on the process. Also, other important parameters like fluid-

dynamic characteristics, water uptake, adsorbent stability (mechanical, thermal, chemical) and sorbent related emissions (e.g. amine evaporation of impregnated sorbents, dust emissions) are influencing the overall process performance and of course also the required reactor design. The challenge is to select a sorbent material, which delivers a good compromise of all these key performance indicators and to find a suitable process and reactor design which results in lowest possible total capture costs.

- Matching of fluid-dynamically optimal design with the thermodynamically optimal design

Theoretically, it is possible to design a process model which combines adsorption models (including mechanisms like equilibrium CO₂ loadings, kinetic effects, water co-adsorption etc.), heat exchange models, and fluid-dynamic mechanism in one big model. If such a model would exist and would be able to converge and to deliver a solution for certain optimization tasks, it would be easier to derive an optimized set-up. However, in praxis this is not the case. The process model available (see [36], [78]) is capable of optimizing the thermodynamic main figure of the process only (like sorbent circulation rate and desorber stripping steam rate). Therefore, one of the biggest challenges is to elaborate a design which can be operated at the thermodynamic optimum conditions, while also the conditions for fluidization and heat exchange are favorable.

- Lean/rich heat exchange

Heat recovery from the hot lean sorbent which is transported from desorber to adsorber is essential to reduce the overall heat demand of the process. Lean/rich heat exchangers are common in liquid amine systems where they can be implemented rather easily. Plate heat exchangers as used for lean/rich heat exchange in amine scrubbing plants are featuring high specific surface areas, and the solvent can be pumped efficiently in counter current flow. For solid sorbents it is much more complicated. The sorbent cannot flow through a heat exchanger easily or only with a special design and direct heat exchange from lean to rich sorbent without a heat carrier medium is hardly possible. Therefore, the challenge is to find a design, which features high heat recovery rates at low costs (capital costs and operational costs).

- Downcomer design

The TSA set-up presented in Chapter 2 principally consists of 12 interconnected fluidized beds: 5 bubbling fluidized beds in the adsorber, 5 bubbling fluidized beds in the desorber, and two transport risers. What connects all these fluidized beds is the superimposed sorbent circulation rate. Each section of the sorbent cycle needs to follow so that in- and outcoming flow of sorbent material matches for each section in steady state condition. What sounds obvious, is a big challenge for a multistage fluidized bed system. If just one link in this chain fails, the whole sorbent inventory distribution gets disturbed, which can lead to a loss of gas sealing, entrainment of the sorbent, condensation issues etc. Therefore, the downcomers from stage to stage require special attention in the design phase. Furthermore, it might be advantageous not only to avoid emptying or overfilling of stages by matching of the SCR of all sections, but also to actively control the transport behavior from stage to stage in order to achieve an intended inventory shift.

3.7.4 Host site and capture task

General remarks

For further development of the TSA technology at pilot scale, it is important to select a host site, which is, in the first place, in operation. Although many thermal power plants in the region of Vienna would be able to provide flue gas in the desired composition and the required utilities for operation, not all of them are in continuous operation. The expansion of renewable energies caused many natural gas power plants to change their way of operation. Instead of providing base load capacity, natural gas power plants are more and more used to balance out peaks in the short and mid-term energy demand. This would lead to frequent start-stop operation of the TSA pilot unit and most likely to fluctuating flue gas compositions, which makes the assessment of long-term effects (e.g.: adsorbent stability) very difficult. Therefore, a power plant needs to be selected, which delivers flue gas and other required utilities preferably all over the year and with constant quality.

Simmering biomass power plant

The combined heat and power plant Simmering is a plant owned by the companies Wien Energie and Österreichische Bundesforste AG and was commissioned in 2006. It was the biggest biomass plant in Europe at that time. Although the plant is theoretically certified for waste incineration as well, it is operated with forest wood chips only.

Figure 3-2 shows a simplified plant overview: Starting at the left side, the wood chips are transported from the forest to the site by trucks and loaded into the hopper. From there, a conveying system is feeding the woodchips into a storage tank and further to the dosing system of the boiler. At design load, roughly 24 t/h are incinerated in the circulating fluidized bed boiler. The circulating fluidized bed boiler has a thermal output of 66 MW which roughly corresponds to 73 t/h of steam at 520 °C and 120 bar. The steam turbine downstream of the boiler produces up to 24.5 MW electrical energy if district heat is not required and up to 17.5 MW in co-generation ([81]). Downstream of the boiler, an ammonia dosing system and an SCR unit helps to minimize nitrous oxides emissions and the baghouse filter reduces dust emissions to acceptable limits. Finally, the flue gas is vented by an ID fan upstream of the stack.

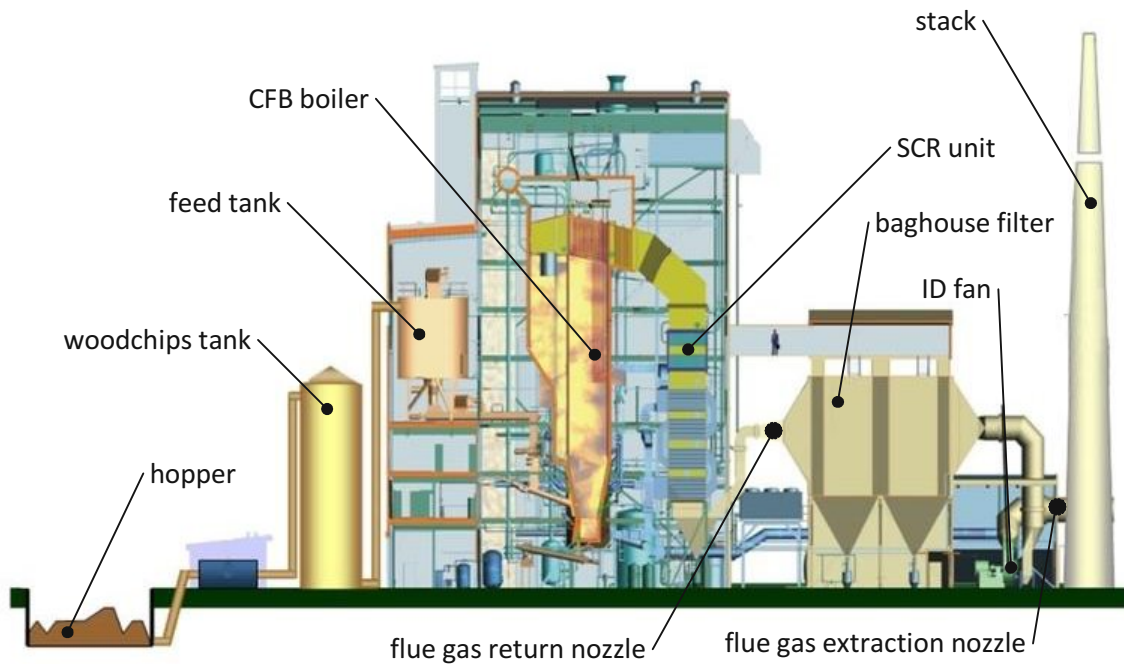


Figure 3-2: Simmering biomass power plant (adapted from [81])

Due to subsidies, the mean feed in tariff for electricity from renewable energies, like from biomass, was in the past 10 years many times higher than the actual price on the electricity market [82]. For plant owners it is therefore profitable to operate these power plants as much as possible. Thus, the biomass power plant Simmering achieves a relatively high average operating time of 7500 full load hours per year, which makes it highly attractive as flue gas source for the TSA pilot unit [81].

Fluegas and utilities supply

Figure 3-3 shows the carbon dioxide, moisture, and oxygen content of the flue gas from the Simmering Biomass plant in the period from April 1st, 2015 to February 29, 2016. As can be seen, the oxygen content sometimes peaks to 21 Vol-%, this represents upset conditions where no combustion is occurring. For the design of the TSA pilot unit, it was decided to take the arithmetic averages of the main reactive species (CO_2 and H_2O) during the available operating period presented above. Some datapoints with high O_2 concentration were removed to have average values that are realistic for the normal operating conditions. However, the flue gas cooler, which will be required to control the dew point of the flue gas, will be designed to be able to handle the highest water concentration registered to be 25.1 Vol-%. Furthermore, trace component values have been gathered during an analysis of the flue gas in February 2016. These values are displayed in Table 3-1.

As indicated in Figure 3-2, the flue gas will be extracted downstream of the ID-fan (flue gas extraction nozzle) and after it has passed the TSA pilot unit, it will be returned upstream of the baghouse filter (flue gas return nozzle). This brings the advantage, that the pressure difference between these points can be exploited to (help) feed the flue gas towards the pilot unit and the baghouse filter serves as an additional barrier for potential dust emissions from the TSA pilot unit. Flue gas extraction and return pressures can be found in Table 3-1 as well.

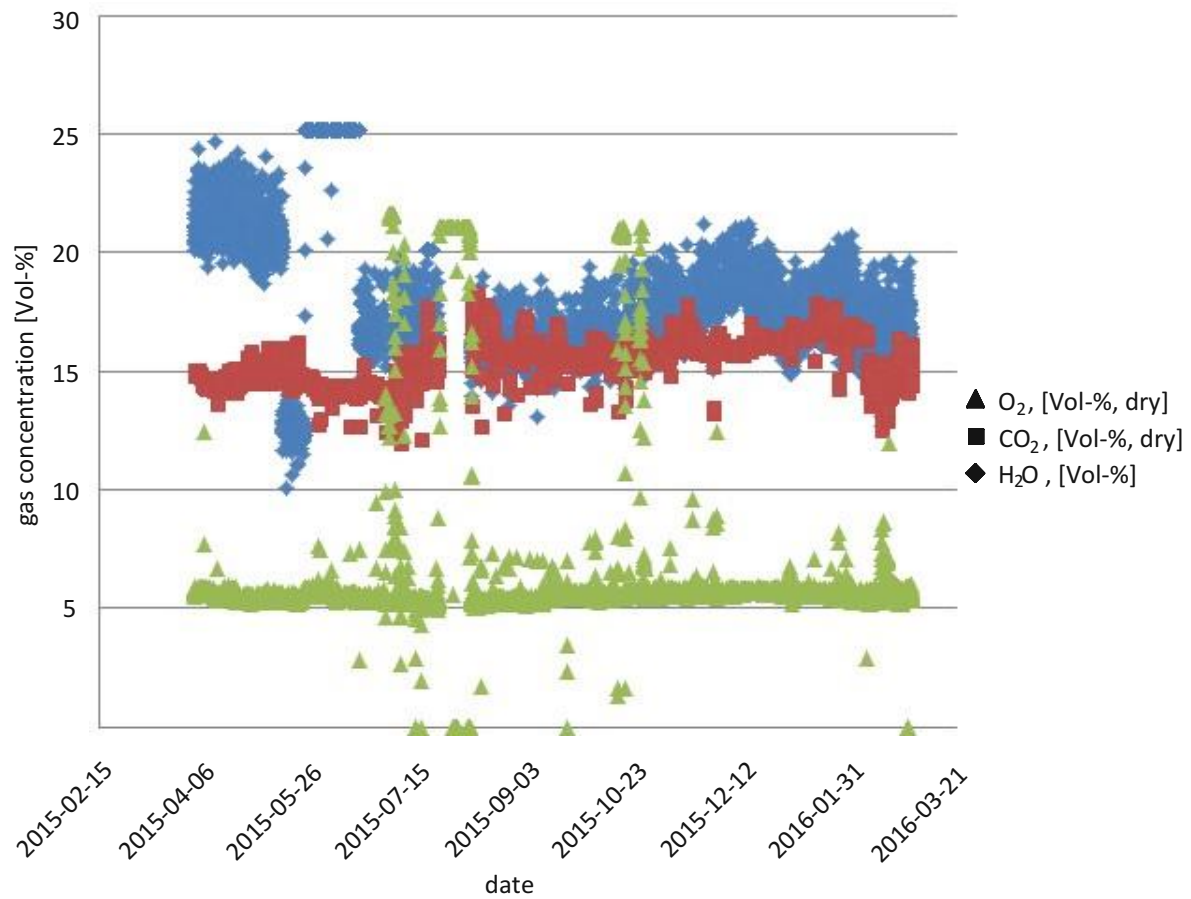


Figure 3-3: Flue gas H₂O, CO₂ and O₂ concentration at Simmering biomass power plant (measured between Feb. 2015 and Mar. 2016)

Table 3-1: Simmering biomass power plant raw flue gas composition summary

pressure at extraction nozzle	-1.5	mbar(g)
pressure at return nozzle	-35	mbar(g)
temperature	150	°C
H ₂ O (avg.)	18.0	Vol-%
H ₂ O (max.)	25.1	Vol-%
CO ₂ (avg., dry basis)	15.5	Vol-%
N ₂ (dry basis)	balance	Vol-%
O ₂ (dry basis)	5.9	Vol-%
HF (dry basis)	1.1	ppmv
SO ₃ (dry basis)	0.02	ppmv
SO ₂ (dry basis)	0.04	ppmv
HCl (dry basis)	0.03	ppmv
NO ₂ (dry basis)	3.7	ppmv
NH ₃ (dry basis)	4.52	ppmv

Compared with the defined target values (see chapter 3.2), one can see, that the CO₂ concentration of the flue gas is much higher. However, the CO₂ feed concentration can be reduced rather easily with a recycle of cleaned flue gas. On the other side, an increase of the CO₂ feed concentration would be much more complicated. Thus, the relatively high CO₂ concentration in the raw flue gas in combination with a flue gas recycle provides a broad operating window.

Nevertheless, for the design of the pilot plant a capture task with low CO₂ feed concentration was defined (see Table 3-2).

Table 3-2: Capture task for ViennaGreenCO₂ pilot unit

CO₂ feed concentration:	4	Vol-%
CO₂ removal:	90	%
CO₂ capture rate:	1000	Kg/day
adsorber pressure drop	<50	mbar

Besides the flue gas, the TSA pilot unit will be supplied with required utilities like instrument air, cooling water, electrical power, nitrogen and steam.

The host site provides saturated steam at 9 bar(g) which will be used for steam fluidization in the desorber as well as for heat exchange via immersed tube bundles. In order to avoid thermal degradation of the sorbent material, the medium pressure steam needs to be partially depressurized and brought to saturation conditions before it is injected to the process. For adsorber heat exchanger design, a maximum cooling water temperature of 20 °C will be considered.

3.7.5 Adsorbent selection

At low CO₂ partial pressure, the adsorption capacity of activated carbons is relatively low, and zeolites are, as already indicated in 2.2.3, sensitive to humidity which is to be expected in most flue gasses. Therefore, a pre-selection of amine functionalized sorbents has been made for ViennaGreenCO₂, which still delivers a high number of potential candidates.

Not every sorbent material which delivers a good performance in a TGA, can meet the expectations in a continuous process. For several reasons, the sorbent performance within the continuous process can deviate significantly from lab tests. For the ViennaGreenCO₂ pilot plant two promising adsorbent materials have been investigated by [66]. Both sorbents are amine functionalized, while one sorbent is a custom-made silica based porous carrier material with an impregnation of polyethyleneimine, the other sorbent consists of a polystyrene matrix with covalently bound benzylamine and is commercially available as Lewatit VP OC1065. Despite of a relatively high initial performance of the PEI impregnated sorbent, the commercially available adsorbent Lewatit VP OC1065 delivered the better compromise with regards to long term CO₂ capacity and adsorbent stability. For detailed information on the experimental campaign and the corresponding results, it is referred to the work of Dietrich [66].

In the following, the most important adsorbent parameters are listed in Table 3-3. Some of these values are subject to fluctuations, as they are depending on the water content.

Table 3-3: Properties of Lewatit VP OC1065

adsorbent type	Lewatit VP OC 1065	
matrix	crosslinked polystyrene	
functional group	benzylamine	
adsorbent size (Sauter diameter)	676	μm
adsorbent bulk density	550	$\text{kg}\cdot\text{m}^{-3}$
fixed bed voidage	0.43	-
particle density	965	$\text{kg}\cdot\text{m}^{-3}$
minimum fluidization velocity (measured with air at ambient conditions)	0.13	$\text{m}\cdot\text{s}^{-1}$

4. TSA PILOT UNIT DESIGN PHILOSOPHY

4.1 MULTISTAGE FLUIDIZED BED COLUMN DESIGN

4.1.1 General aspects

The multistage fluidized bed concept has proven its advantages especially on the adsorption side of the process (see 2.3). The fluidized beds enable relatively high heat transfer rates, while the multistage design effectively uncouples the adsorber off gas concentration from the maximum achievable CO₂ loading on the rich sorbent. But for the desorber the multistage fluidized bed columns can bring major advantages as well if the equipment is designed properly (see also chapter 2.3). In the following design considerations for the pilot unit adsorber and desorber are discussed.

Problem definition

As indicated in chapter 3, a TSA process at full scale will have to treat a huge amount of flue gas, which in turn will require a huge adsorber. At lab and pilot scale a 20 % bigger adsorber for example will only have a minor impact on total project costs, but at full scale equipment size will be a major cost driver. Therefore, one of the main targets in process development is a reduction of the adsorber size, or maximization of its capacity. However, if the load on the adsorber is increased (e.g. by increasing the gas velocity) this can lead to different limitations:

- **Fluid-dynamic limitations:** More capture capacity tendentially requires more sorbent circulation to maintain the same capture efficiency, which can be a fluid dynamic challenge. But with increasing gas velocity also the impact on pressure profiles, fluidized bed density, particle attrition and entrainment behaviour need to be considered in the design.
- **Regeneration limitations:** To achieve the defined capture task, the lean sorbent loading needs to be relatively low. But more load on the adsorber, automatically creates more load on the regeneration side of the process, which can lead to limitations if not considered in design.
- **Heat exchange limitations:** Experiments at bench scale clearly showed, that insufficient heat transfer can be a major limitation for process performance. The bench scale unit achieved target sorbent circulation rate and did not indicate significant kinetic limitations. But adsorption and regeneration temperatures could have not been controlled properly which led to reduced delta CO₂ loading and therefore a reduced capture performance. The same limitation is to be expected for large scale plants if the installed heat transfer surface is too low. On the other hand, immersed heat exchanger bundles can significantly affect the fluid dynamic design of a plant, which can lead to further limitations there.
- **Kinetic limitations:** Assuming, that all fluid-dynamic issues are resolved, the sorbent is regenerated to the required extend and temperatures are at target values, then kinetic limitations can still hinder a further increase of the gas velocity. Depending on where the limitation occurs (e.g.: mass transfer from the gas phase to the particles, diffusion limitations etc.) an adaptation of the fluid dynamic design could for example help to partially overcome the limitation.

However, the main challenge for TSA process development is that all potential limitations are connected. An optimization at one side can likely make things worse on the other. Thus, TSA process and reactor design always requires seeing the big picture and not only one aspect of the design. Since previous experiments at lab scale did not indicate kinetic limitations, the focus of the following section lies on elimination of the observed limitations in heat exchange and fluid-dynamics as well as on optimizations regarding thermodynamics of adsorption.

4.1.2 Fluidized bed heat exchange

Fluidized beds are well known for excellent heat transfer between particles and immersed heat exchangers. However, depending on particle properties and fluidization conditions a broad range of heat transfer rates is possible. While rather small particles within the Geldart A classification can reach up to $1000\text{W/m}^2\text{K}$, bigger particles often only provide a fraction of this value. Fluidized bed heat exchange is one of the major challenges for TSA. Thus, knowledge of achievable heat transfer rates for a certain sorbent material and certain operating conditions is crucial to provide a design with preferably just as much as required heat transfer surface.

One more challenge is, that the adsorber is intended to be operated at relatively high superficial gas velocities and the heat exchange bundle will locally cause even higher gas velocities. Thus, the fluidized bed will expand significantly, and the bed porosity increases. This can reduce the heat transfer coefficient at one hand but increases the bed volume at almost constant pressure drop, which allows for more heat exchange surface within the fluidized bed. The challenge is to find a heat exchanger geometry, which provides a high heat exchange surface per fluidized bed volume and a high heat transfer coefficient, without creating fluid dynamic issues.

In literature different equations for estimation of the achievable heat transfer rate in dependence on bed material and operating conditions exist. A commonly used equation for estimation of the maximum achievable heat transfer rate is given by [44], while others predict the achievable heat transfer rate in dependence on the fluidization conditions [83]–[85]. However, predictions often significantly deviate from each other. Figure 4-1 shows predictions according to literature equations for exemplary particle properties and fluidization conditions. Although estimation of the maximum achievable heat transfer coefficient acc. to Zabrodsky is not a function of the gas velocity, its value is shown in Figure 4-1 as well.

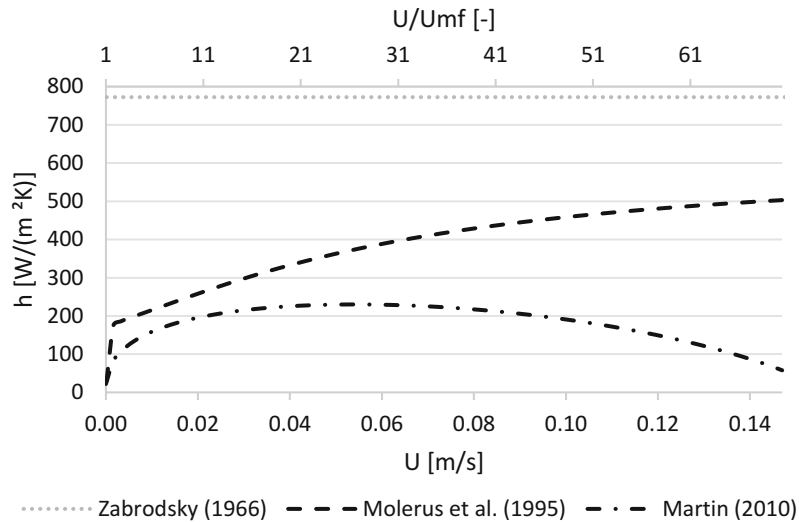


Figure 4-1: Exemplary calculation of heat transfer rates using literature equations ([44], [84], [85]), calculated for copper particles with a mean diameter of 50 μ m and air as fluidization gas at ambient conditions

Considering the relatively large discrepancies of literature predictions and the importance of fluidized bed heat exchange for the TSA process it was decided to conduct dedicated experiments with the actual sorbent material and relevant bundle configurations and operating conditions. In the following, the methodology and results of these tests are presented and discussed shortly. For more detailed information and further results it is referred to other publications. Publications by Hofer et al. [86]–[88] focus on heat transfer in the fluidized beds, while the fluid dynamic impact of heat exchanger bundles on bed expansion is studied within the scope of a thesis written by Zehetner [89].

Heat transfer measurements

Since precise knowledge of the achievable heat transfer rate is crucial for the design of a TSA plant, dedicated measurements with the actual sorbent material Lewatit VP OC1065 have been conducted in a heat transfer measurement test rig (see Figure 4-2). The test rig mainly consists of a rectangular channel with a cross section of 200 x 400 mm² in which the sorbent material can be fluidized. Within the fluidized bed area of the test rig, different heat exchange probes can be introduced. Besides an exchangeable gas distributor, also the Perspex plates at front and rear, which act as bundle support, can be exchanged. Thus, different heat exchanger configurations can be tested.

The measuring principle is as follows: a temperature controller for the electrical heating cartridge ensures a constant temperature of the heat transfer probe (see Figure 4-3). The electrical power, which is provided to maintain a set-temperature of e.g.: 50 °C is constantly monitored. In the surrounding of the heat transfer probe, the fluidized bed temperature is measured to obtain a reference for calculation of the temperature difference.

Due to the selection of PMMA as material for the support of the copper body, heat conduction is relatively low and was neglected. Thus, the active heat exchange surface can be calculated with the known diameter and length of the copper body. With the measured temperature difference, electrical power consumption and the known geometry, the heat transfer coefficient can be calculated. The heat

transfer coefficient derived with this method represents mainly the particle convective heat transfer, since the measurement is done at approximately ambient temperature which means no significant heat exchange by radiation and due to the small particle size, gas convective heat transfer plays only a minor role as well.

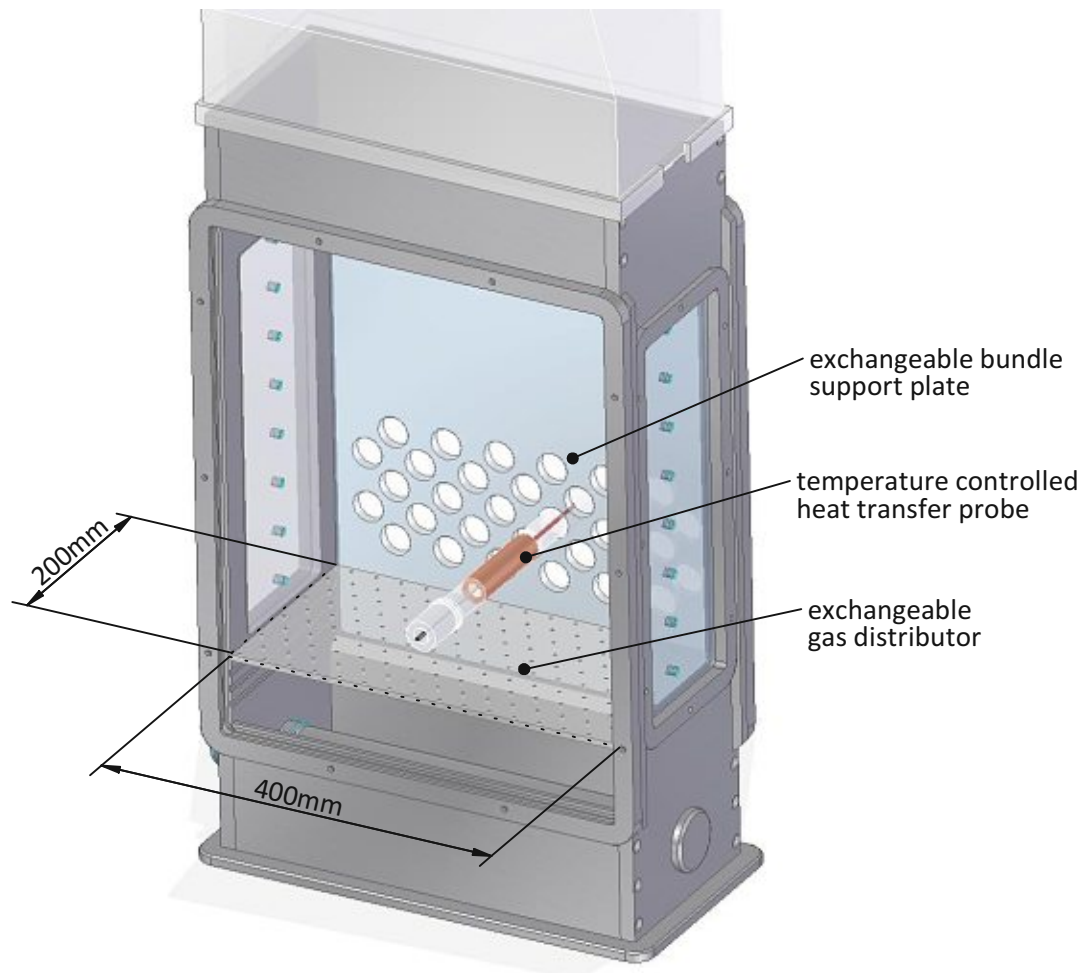


Figure 4-2: Heat transfer measurement test rig

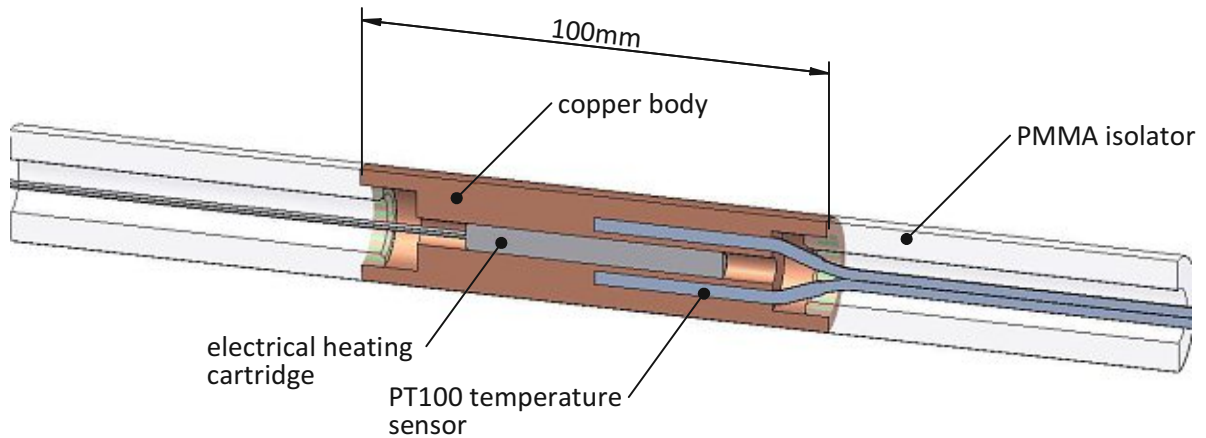


Figure 4-3: Heat transfer probe

Besides single tube measurements, the test rig was equipped with different tube bundle geometries and operating parameters as expected in adsorber and desorber. For the bundle configurations the position of the heat transfer probe was varied, while unheated dummies were used to simulate the fluid dynamic effects of a real bundle configuration. In the following, results for the bundle geometries which were finally selected for the pilot unit will be presented only. For further results it is again referred to the work of Hofer et al. [86]–[88], [90].

4.1.2.1.1 Adsorber stage heat exchanger

Since adsorption is an exothermic reaction, the adsorber needs to be cooled in order to maintain the operating temperatures. Despite the relatively high heat transfer rates which can be achieved in fluidized bed applications, heat exchange is still a challenge for the process. Stage heat exchangers have to be optimized in a way, that operating temperatures can be controlled precisely even at increased load for the adsorber. With the aid of an iteration which was based on literature equations for heat transfer rates, the estimated cooling demand, the estimated cooling water temperatures and estimates for the bed expansion the required heat transfer surface was calculated and a bundle geometry was selected. A bare tube bundle with **a triangular pitch of 38 mm and an outer tube diameter of 20 mm** was selected. With this geometry a variation of the fluidization velocity was performed, and the corresponding heat transfer coefficients were measured within the heat transfer measurement test rig. Results for this variation can be found in Figure 4-4. As indicated previously one aim of the pilot program is to increase the adsorber gas velocity as much as possible. However, increased gas velocity results in more load on the heat exchangers as well. The selected gas velocity range is a result from various considerations and a trade-off between the gas velocity dependence of the cooling demand and the amount of heat exchange surface, which can be fitted within the fluidized beds and bed expansion effects.

As indicated in Figure 4-4 the heat transfer coefficient for this configuration has been measured at various locations within the bundle. The individual results are named according to their position within the bundle. The tag 0/0 refers to the tube in the centre of the bundle. The first number is the position in horizontal direction and the second the vertical position, with the centre of the bundle as origin. However, in the range of a gas velocity between 0.3 and 0.9 $\text{m}\cdot\text{s}^{-1}$, which is the relevant range for the adsorber, the difference of the heat transfer coefficient between the individual positions was not significant. But a slight dependence on the gas velocity was observed. In particular, the heat transfer rate showed a slight trend to lower values for higher gas velocities. However, for the design of the pilot unit adsorber, the correlation between gas velocity and heat transfer rate was neglected and a mean value of $203 \text{ W}\cdot\text{m}^{-2}\cdot\text{K}^{-1}$ at a gas velocity of $0.7 \text{ m}\cdot\text{s}^{-1}$ was derived for further calculations.

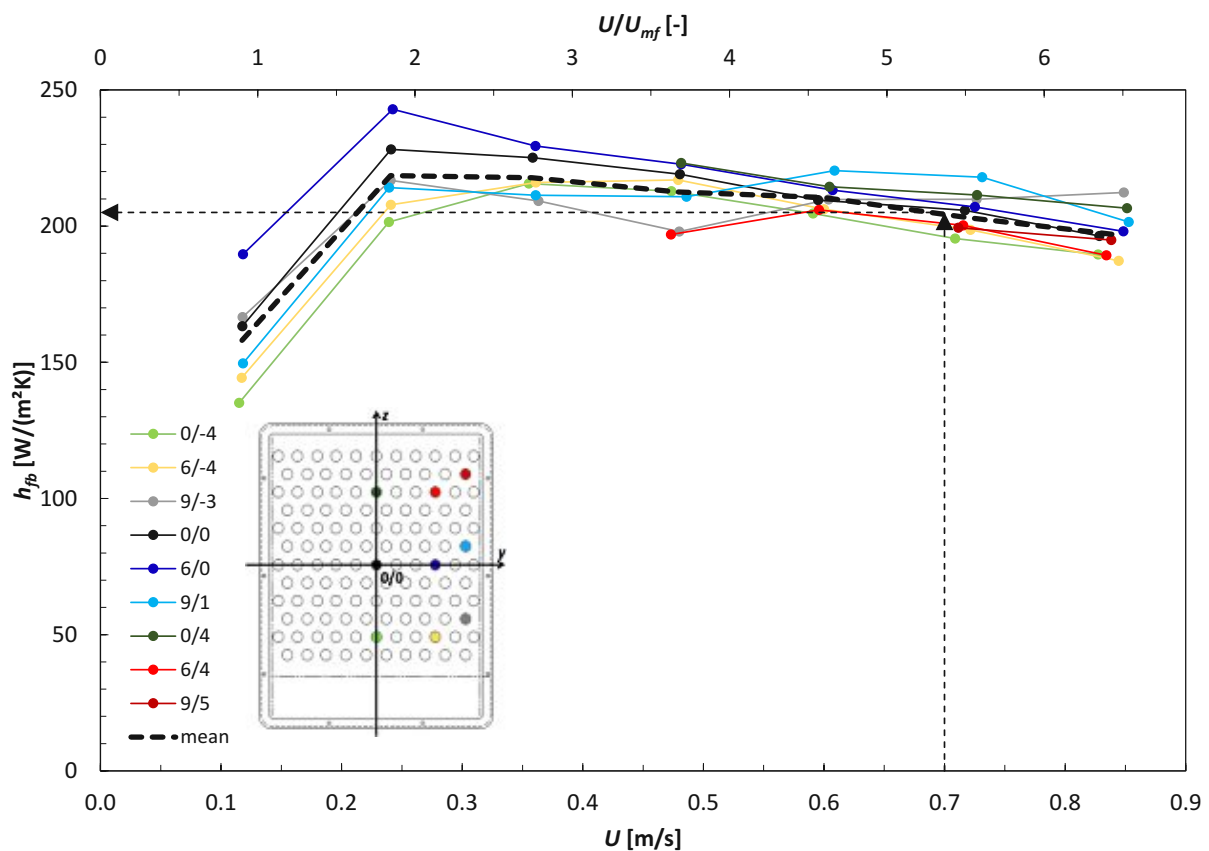


Figure 4-4: Measured heat transfer rates for varying superficial gas velocities at indicated locations of adsorber stage heat exchanger

4.1.2.1.2 Desorber stage heat exchanger

In contrast to the adsorber, where the treated gas flow is maximized, optimization of the energy demand aims for low stripping steam rates and therefore low fluidization. It is important to know, that there is a thermodynamic optimum for the stripping steam rate which is not necessarily the optimum from a fluid-dynamic point of view and most likely also not optimal for fluidized bed heat exchange. Preliminary simulations indicate that the optimal specific stripping steam rate from a thermodynamic point of view is below 1 kilogram of steam per kilogram of captured CO₂. Translated to the expected cross section of the adsorber, the desorber would not even be fluidized with that specific stripping steam rate. Thus, the cross section of the desorber needs to be much smaller compared to the adsorber. On the other side, the fluidized beds need to offer enough room for the heat exchangers. Therefore, if the cross section of the desorber gets reduced, the bed height and the pressure drop of the column needs to be increased to provide enough space for integration of the required heat exchange surface.

Since the bed height and the pressure drop cannot be increased at will, the fluidization number is additionally reduced to rather low numbers in order to achieve the desired specific steam rates. For the heat transfer measurements, this means, that the desorber has to be operated close to minimum fluidization conditions. Therefore, the investigated range of fluidization numbers was chosen between zero and two. Since, fitting of the required heat transfer surface within the fluidized beds of the desorber is even more challenging (compared to the adsorber) a narrower bundle **pitch of 30 mm** (triangular) and an outer **tube diameter of 16 mm** was chosen. This increases the specific heat exchange surface per bed volume at one hand, and on the other hand the smaller tube diameter tendentially provides slightly higher heat transfer coefficients [91]. Additionally, the reduced cross-sectional open area of the bundle increases the gas velocity locally and moves the local u/u_{mf} to higher values (if related to empty column cross section).

Since the test rig was not designed for operation with steam as fluidization gas, compressed air was used for all test runs. For the adsorber heat exchange measurements the influence of the different gas composition and temperature is expected to be very low and was therefore neglected. However, for the desorber stage heat exchanger a direct transfer of results at cold conditions with air is not possible. Therefore, results with the same fluidization numbers have been considered as good approximation of hot conditions with steam in the desorber.

It was shown that the achievable heat transfer coefficients are in the range of about 40 to 220 W·m⁻²·K⁻¹ (see Figure 4-5). The results clearly indicate that heat transfer strongly depends on the fluidization gas velocity and the tube location within the fluidized bed. While relatively low heat transfer rates were measured close to the wall of the test rig, the heat transfer tends to increase when moving towards the center of the fluidized bed. As this result is most likely attributed to the low fluidization and bad gas distribution, a set-up with modified gas distributors was investigated as well, which showed an improvement. But a relatively strong dependence of the heat transfer coefficient on the tube position and gas velocity as well was still observed. Thus, it was decided to calculate a weighted heat transfer coefficient from the average heat transfer coefficients measured in the wall and the core region of the bed (see Table 4-1). The weighting of the results is based on preliminary desorber geometries. Thus, the weighted results are not fully transferrable to other column geometries.

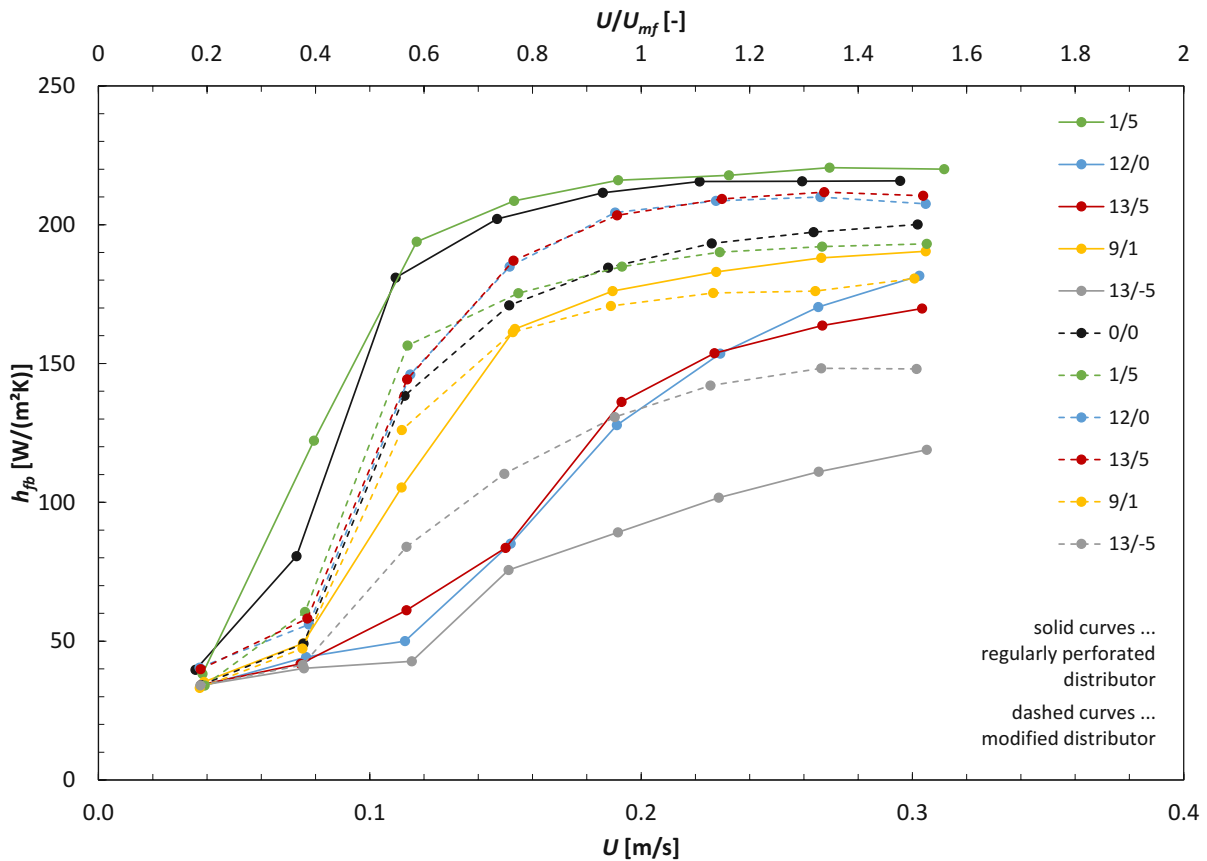


Figure 4-5: Measured heat transfer rates for varying superficial gas velocities at indicated locations of desorber stage heat exchanger.

U [m/s]	$h_{fb} [\text{W}\cdot\text{m}^{-2}\cdot\text{K}^{-1}]$					
	y=0mm	y=140mm	y=200mm	core zone	wall zone	weighted
0.15	188	170	88	179	129	143
0.19	197	187	126	192	156	166
0.23	203	195	141	199	168	177
0.27	207	201	151	204	176	184
0.31	209	204	158	206	181	188

Table 4-1: Measured and weighted heat transfer coefficients for desorber heat exchanger

Bed expansion

For fluidization of the adsorber either an additional or an existing blower of the host plant needs to overcome the pressure drop of the column. To limit the additionally required electric power for this blower, the pressure drop of the column should be kept as small as possible. But still the required heat transfer surface needs to be fit within the fluidized beds. If the heat exchangers are not fully immersed, the apparent heat transfer rates are drastically reduced. If the fluidized beds are much higher than the heat exchange bundle, the pressure drop might be higher than necessary. Thus, a relation between pressure drop, height of the fluidized bed (dense phase), gas velocity and bundle geometry needs to be found. But for the desorber as well, which is fluidized with steam the total pressure drop plays an

important role. The higher the pressure drop is, the more complicated gets gas sealing. Also, the sorbent transport from stage to stage can be affected in a negative way if the pressure drop per stage gets too high. Therefore, dedicated experiments with the actual heat exchanger geometries of adsorber and desorber have been performed to gather information of the dense phase bed height for a certain pressure drop and fluidization condition. In the scope of these experiments, different bed materials have been tested with 2 different heat exchange bundles in a cold flow model. A comparison with the model developed by Löffstrand et al. [92] showed good agreement within certain boundaries. The experiments in detail are presented in the scope of [89].

However, for the design of the ViennaGreenCO₂ pilot unit, the specific pressure drop per meter of fluidized bed height for varying gas velocities in the adsorber was directly measured with the actual sorbent material (Lewatit VP OC1065) for the piloting campaign. In accordance to the conducted heat exchange tests an outer tube diameter of 20mm was selected for the adsorber cold flow model and two different tube bundle pitches have been tested. The narrower bundle of both featured a triangular pitch of 38.4 mm while the other was wider with a triangular pitch of 48 mm.

The variation of the gas velocity in the adsorber cold flow model showed a strong impact on bed expansion which was higher for the narrower pitch. The desired empty column gas velocity of 1m/s resulted in partial formation of a dense phase above the heat exchange section. Subsequently, an optimization strategy for the narrow tube bundle would be either a reduction of the inventory or a higher tube bundle (if more heat exchange surface is required). Although, the heat transfer coefficient would potentially be reduced, the total heat transfer could be increased by this method. But since also the particle residence time is affected by the inventory, and sufficient heat transfer surface is provided by both bundle geometries, the wider pitch was selected and further increased by 2mm to a **50mm triangular pitch** for manufacturing reasons. The impact of the slightly wider pitch on the previously derived heat transfer coefficient was estimated to be relatively low in the desired gas velocity range of the adsorber. In this very case the heat transfer coefficient is most likely underestimated with the slightly narrower pitch used in the heat transfer tests. Thus, the derived value of 203 W/m²K is seen as conservative estimate for the bundle design. For the estimated gas velocity at design and high load, following specific pressure drops have been derived:

Table 4-2: Specific adsorber bed pressure drop

adsorber specific pressure drop	design load	high load	
superficial gas velocity	0.73	1.04	m·s ⁻¹
specific solid pressure drop	30.1	22.5	mbar·m _{bed} ⁻¹

Since the desorber requires a different downcomer design (see chapter 4.1.3), which is relatively challenging from a fluid-dynamic point of view, a 1:1 multistage cold flow model has been constructed and tested at relevant operating conditions. Besides other results, following stage pressure drops for design and high load have been derived from these experiments:

Table 4-3: Desorber stage pressure drop

desorber bed pressure drop	design load	high load	
mean gas velocity in desorber	0.33	0.47	m·s ⁻¹
stage pressure drop incl. gas distributor	26.6	28.0	mbar

In general, there are many possibilities to solve the heat transfer challenge of TSA but there are also as many things to consider. Smaller particles for example would improve heat transfer (within certain boundaries) but would at some time lead to limitations of the gas throughput of the adsorber design due to the different fluid-dynamic behaviour. Therefore, heat transfer in the context of TSA cannot be studied independently from other design issues and it is always part of an optimization task with a large number of variables. The sorbent selection made in chapter 3 significantly reduced the degrees of freedom for the fluidized bed heat exchange design. So that with the derived heat exchange coefficients and bed expansion data for adsorber and desorber the required inputs for the heat exchanger design calculations are defined.

For the pilot unit design, sufficient margin on the heat exchange design shall compensate remaining uncertainties and avoid potential limitations in heat exchange. Finally, the instrumentation of the pilot unit should allow to assess the performance of the fluidized bed heat exchangers further to allow for more precise calculations at large scale.

4.1.3 Downcomer design

Multistage fluidized bed temperature swing adsorption requires sorbent flow downwards from stage to stage to achieve the beneficial counter current flow of sorbent and gas. If the gas passes through the multistage fluidized bed column from bottom to the top of the column, the pressure at the bottom is of course higher than at the top. Thus, the downwards flow of sorbent has to be established against the prevailing pressure gradient. This downward flow of the sorbent is achieved with a downcomer that connects one stage with the stage below. Downcomers can have different configurations at the inlet and outlet (see Figure 4-6). In practice, many different design solutions, as well as hybrids of the shown types are possible, and many designs are able to fulfil the main task of transporting sorbent material downwards against the prevailing pressure gradient. However, it is a very delicate task to design a downcomer for certain operating conditions, and the stable operating window is usually rather limited. If the pressure balance over the downcomer gets disturbed, blockages or other undesired operating states can occur. Any downcomer requires that the bed material at the bottom of the downcomer gets transported away from the downcomer into the next fluidized bed. This is achieved either with external aeration or by directing the downcomer directly into the fluidized bed. For self-aerated downcomer as shown in Figure 4-6, bottom type (4), the transport characteristic is mainly defined by the geometry of the downcomer and the operating conditions of the fluidized beds. Actively aerated downcomer (see Figure 4-6: bottom type (1),(2) and(3)) feature the possibility to affect the transport behaviour with the flow of aeration gas. However, any additional control loop also increases the process complexity. Thus, a closer look at the requirements of the downcomer is necessary to come to a well-founded decision.

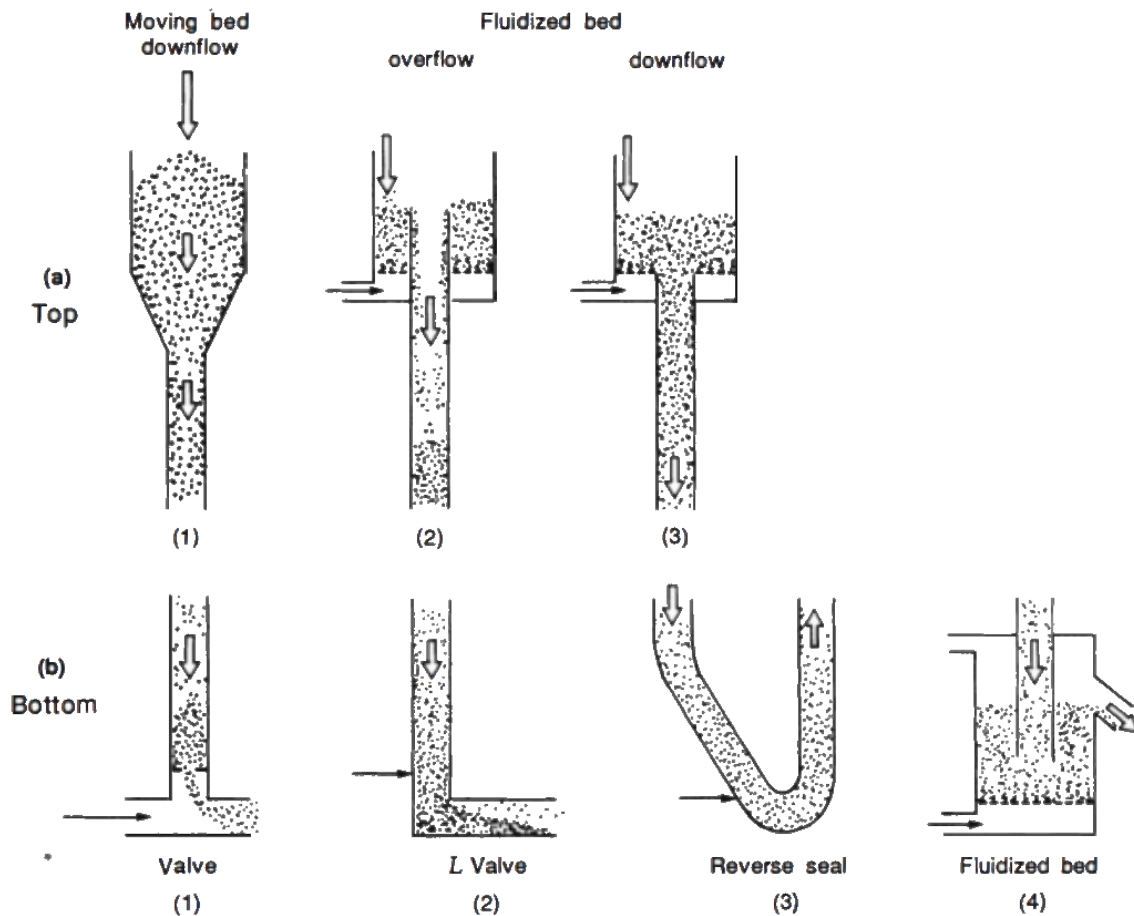


Figure 4-6: Downcomer configurations (taken from [40])

Assuming aerated downcomers for adsorber and desorber, the requirements on the downcomer systems are different, while one of the most important differences is, which gas would be used for aeration. In order to achieve high CO_2 purities, the only acceptable gas on the desorber side is either CO_2 or steam, while the adsorber would allow for compositions of air, N_2 , raw flue gas and cleaned flue gas. One more important circumstance is, that any introduced gas has an impact on the partial pressure of CO_2 and H_2O in the column. This impact might not be very significant on the adsorber side, since the amount of treated gas is much higher than the expected aeration demand for the downcomer. However, on the desorber side, the fluidization gas flows are much lower, while the aeration demand stays in the same range as for the adsorber column, because the same sorbent circulation/throughput has to be maintained in each downcomer. Assuming almost pure steam in the lowermost stage, and a gas composition with a significant CO_2 content in the outlet, the desorber is expected to have a strong concentration gradient which makes the selection of an applicable aeration gas composition even more complicated. If too much steam is used, the energy demand of the process might be affected in a negative way while too much CO_2 in the aeration gas would disturb regeneration of the sorbent. Therefore, self-aerated downcomer are the preferred design solution on the desorber side, while the increased flexibility of an externally aerated downcomer is preferred on the adsorption side of the process. Since a downcomer is strongly affected by the prevailing pressure difference and the fluidization conditions of the bed at the downcomer bottom, also the gas distributor design requires

special attention. For proper gas distribution over the cross section of the fluidized bed and to ensure uniform fluidization of the bed, a gas distributor should have a significant share of the total pressure drop of bed and distributor. However, since the downcomer must balance the pressure difference of two fluidized beds and the gas distributor, the pressure drop from the distributor has to be considered in the downcomer design as well. A distributor design with too much pressure difference can lead to malfunction of the downcomer (e.g. throughput limitation and subsequent flooding of the downcomer).

Both downcomer types as well as gas distributors have been investigated in detailed cold flow modelling studies [89], [93]. The final downcomer design and the geometry of gas distributors is presented in Chapter 5.

4.1.4 Optimum stripping steam rate

As indicated previously, the steam introduced into the desorber serves two purposes. One is to achieve fluidization conditions and the other is to promote regeneration of the sorbent material by lowering the CO₂ partial pressure in the column. However, introduced steam also relates to the energy demand. A too low stripping steam rate would result in more heating duty in order to fulfil the capture task, while over-stripping also increases the overall process energy demand. Therefore, a simulation-based assessment of the influence of the stripping steam rate was made. Pirklbauer et al. [72] found, that there is a minimum stripping steam rate below which, the capture task cannot be fulfilled with the given boundary conditions (e.g.: 90% capture from a flue gas with 4 Vol-% CO₂), and that there is an optimum stripping steam rate, at which the process energy demand reaches a minimum. This optimum stripping steam rate (saturated steam at desorber temperature) is depending on the stage configuration (number of stages in adsorber and desorber) and the extend of heat recovery between lean and rich sorbent stream if applied. The influence of the stage configuration on the optimum stripping steam rate is shown in Figure 4-7, while the correlation between stripping steam rate, lean/rich heat recovery rate and the total energy demand of the process is presented in Figure 4-8. One can see that the optimum stripping steam rate generally decreases for stage configurations with higher stage numbers as well as for increasing lean/rich heat recovery rate.

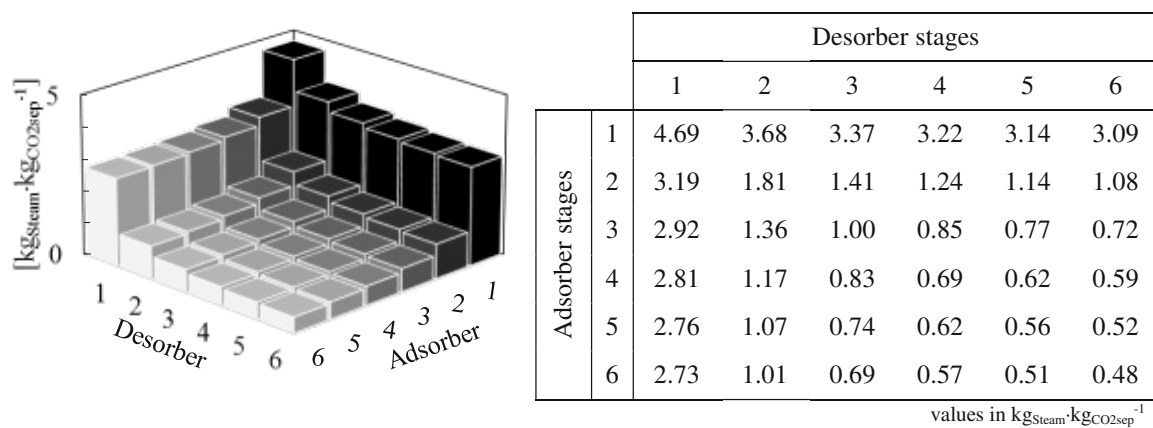


Figure 4-7: Specific stripping steam demand at optimal total energy demand dependent on number of stages in adsorber and desorber (taken from [72])

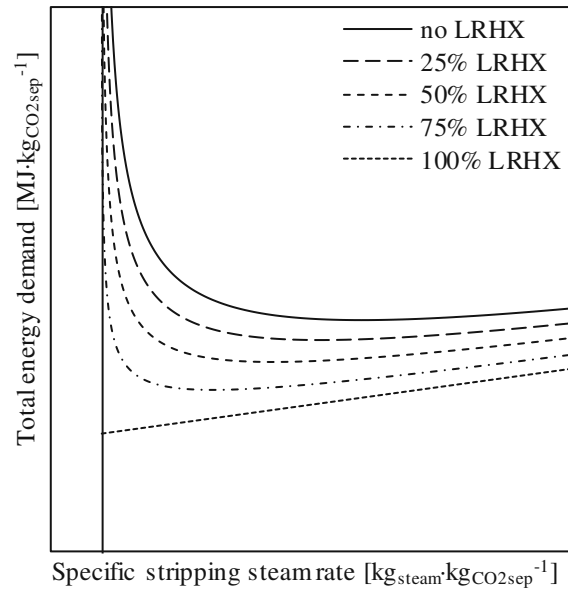


Figure 4-8: Influence of lean/rich heat exchange and stripping steam rate on the total energy demand (taken from [72])

4.1.5 Required number of stages and column pressure drop

As discussed previously, the main advantage of a multistage fluidized bed column is the high heat transfer coefficient and good gas to solids contact combined with a counter current flow pattern. However, with a multistage fluidized bed column, counter current flow is achieved only partially. The actual flow pattern can be compared to individual stirring reactors connected in series. The higher the number of stages, the closer it gets towards ideal counter current flow. But practically this of course cannot be reached. This leads to the question, what is a reasonable number of stages. By adaptation of an existing process model which was first introduced by [37], Pirklbauer et al. [72], [78] studied the impact of the stage configuration of the multistage TSA process on the energy demand for CO₂ capture. The authors showed that the energy demand for CO₂ capture decreases with increasing number of fluidized bed stages in the adsorber and desorber. However, the reduction steps are getting smaller and smaller for higher stage numbers (see Figure 4-9). Since each stage increases process complexity and investment costs, a clear optimum stage configuration cannot be defined with the current knowledge.

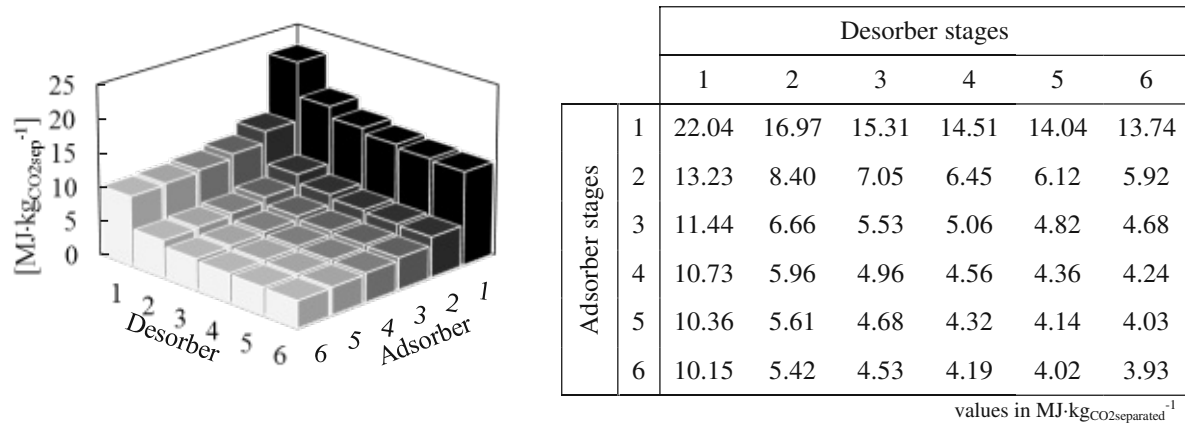


Figure 4-9: Effect of stage configurations on process energy demand (taken from [72])

A configuration with a five stage adsorber and a five stage desorber was selected for the TSA pilot unit, which is, based on the current knowledge, seen as a reasonable compromise between plant complexity and the gain in efficiency. In future a more detailed assessment with inclusion of a CAPEX estimation for each stage configuration should help to find the optimum stage configuration for a certain capture task with this technology.

4.2 WATER CO-ADSORPTION

The presence of water can have a strong effect on the performance of the TSA CO₂ capture process, which has been observed in early experiments with the bench scale unit already [37], [38]. Depending on the type of sorbent, the water adsorption capacity can be comparably high. For Zeolite 13X for example, a water adsorption capacity, which is much higher than the adsorption capacity for CO₂ was reported [77], which even hinders adsorption of CO₂ in presence of water. In almost any potential applications of TSA for capture of CO₂, a significant amount of water has to be expected in the gas stream which is to be treated. Amine functionalized sorbents are reported to be more tolerant to water moisture and should even increase capacity for CO₂ in presence of water due to a different stoichiometry (formation of bicarbonate). However, in practice this enhancement was not confirmed by all studies [94]. A detailed investigation of the effect of moisture on the adsorption of CO₂ with Lewatit VP OC1065 was conducted by Veneman et al. [71]. Within this study, it was shown, that water adsorption is mainly a function of the relative humidity in the gas phase (see Figure 4-10) and the H₂O adsorption enthalpy is close to the condensation heat of water (43 kJ·mol⁻¹).

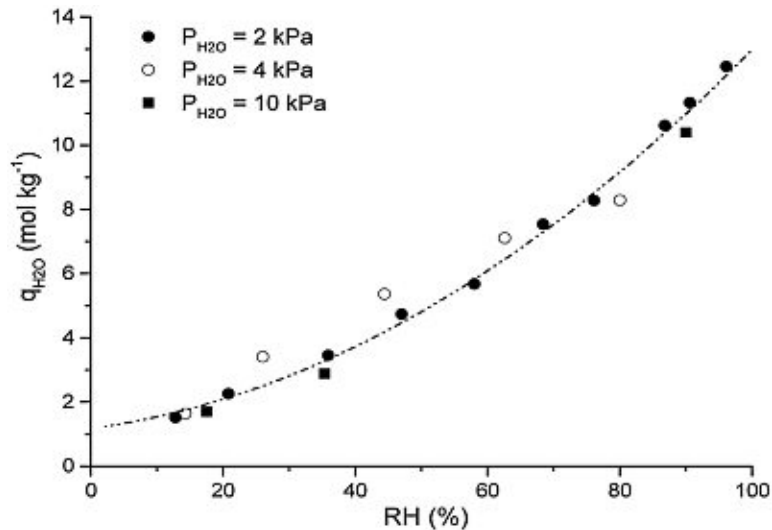


Figure 4-10: H₂O adsorption capacity of Lewatit VP OC 1065 plotted against the relative humidity (RH) in the gas phase (taken from [71])

Water co-adsorption within the adsorber increases the cooling demand of the adsorber and adds a parasitic load for heating and regenerating the sorbent. Therefore, [71] concluded, that the dew point of the incoming gas should be lowered to limit co-adsorption of water. However, co-adsorption can be influenced from regeneration side as well. By adjusting the relative humidity in the desorber, the H₂O loading of the incoming sorbent in the adsorber can be increased, which in turn reduces the uptake in the adsorber. The influence of the relative humidity in adsorber and desorber on the required heating and cooling demand in both columns, as well as on the temperature distribution in the columns and capture performance has been assessed in dedicated experiments with the bench scale unit. The detailed results are summarized in the work of Dietrich [66]. Dietrich showed that adsorption of water in the adsorber can be prevented by increasing the relative humidity in the desorber. With a further increase of the relative humidity in the desorber, the water transport was even reversed, so that water was adsorbed in the desorber and released in the adsorber. Since the enthalpy for water adsorption lies in the range of the condensation enthalpy (approximately 40 kJ·mol⁻¹), this net transport of water from the desorber to the adsorber significantly reduced the heating duty of the desorber and the cooling duty of the adsorber as well.

Furthermore, it should be mentioned, that sorbent materials can tend to electrostatic charging, which is strongly depending on the water content of the sorbent. In various cold flow experiments, as well as in continuous operation at bench scale low relative humidity frequently caused electrostatic charging of the particles, which significantly influences its fluidization behaviour.

From thermodynamic point of view, the average humidity in the system should be as low as possible, to avoid an increase of the apparent heat capacity of the sorbent. However, to avoid electrostatic charging of the sorbent and to exploit the positive effect of water transport on the heating and cooling demand of the process, water co-adsorption should be enabled to some extent. As the positive effect on the heating and cooling demand requires a net transport of water from desorber to adsorber, two measures are thinkable to achieve this. At one hand, the dew point of the incoming flue gas to the adsorber can be lowered by cooling and separation of condensed water and on the other hand, the relative humidity in the desorber can be influenced by introduction of more stripping steam (which slightly increases the average H₂O content of the gas) or by lowering the operating temperature closer

to the dew point (100 % relative humidity) of the gas. Since both can have a strong influence on the fluid dynamic behaviour of the fluidized beds as well as on sorbent regeneration, in practice a good compromise needs to be found.

For the TSA pilot unit, a combined approach is chosen: On the adsorption side, a flue gas cooler with sufficient margin shall allow to adjust the dew point of the incoming gas within a broad range, while on the regeneration side, the equipment will be designed for a wide range of stripping steam flow and operating temperature, which directly influences the relative humidity. The optimum operating conditions are to be found with the aid of parameter variations with the pilot unit and accompanying refinement of the process models regarding water co-adsorption which is to be expected in upcoming experiments with the pilot unit.

4.3 TRANSPORT SECTIONS AND GAS SEALING

4.3.1 General aspects

A lot of required process engineering is not related to the two main reactors but to the rest of the process. A thoughtful set-up, or a clever heat integration for example can play a crucial role for the future of the process. For optimizations discussed in this chapter, a starting point is defined by the process set-up shown in Figure 4-11 which is similar to the process set-up of the bench scale unit (see Chapter 2). The set-up mainly consists of two multistage fluidized bed reactors for adsorption and regeneration which are connected via two transport sections. The transport sections feature L-valves for pneumatic control of the sorbent circulation rate, a transport riser with lean/rich heat exchange in the lower section and a particle separator at the top of the riser. In this basic set-up, the riser gas is recycled by a blower.

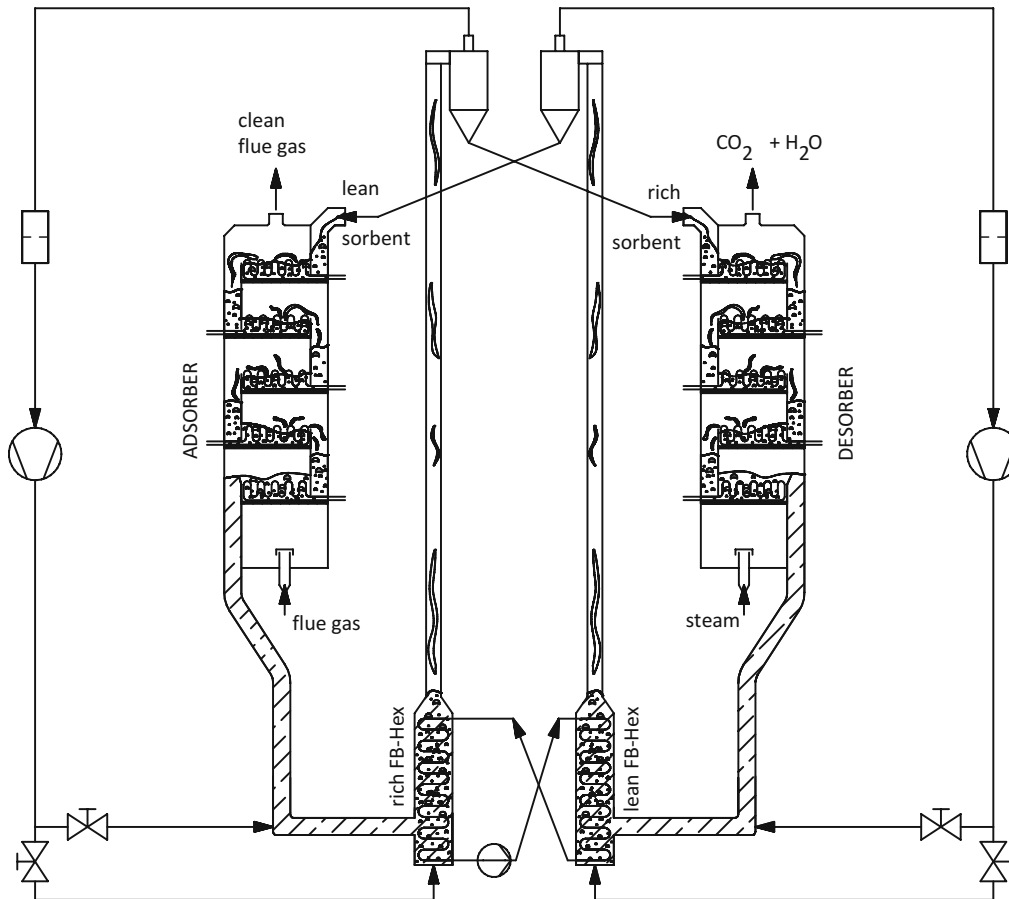


Figure 4-11: Basic TSA process set-up

In this chapter, gas sealing strategies and a thermodynamically improved riser set-up are elaborated. But, to understand gas sealing challenges and to derive appropriate measures, requirements and design details of the transport sections must be discussed first.

Within the multistage fluidized bed columns, sorbent flow in both columns is from top to bottom. Which in turn means, that the sorbent must be lifted at some part as well. Although other possibilities would exist, pneumatic risers are considered as a robust state of the art design solution for this task. Furthermore, pneumatic transport risers are scalable and are providing a broad operating window, which makes them the first choice for circulating fluidized bed systems and in this case also for the TSA pilot plant.

If the allowable pressure drop over the fluidized bed columns is held constant, then scale-up of the process is possible only by increasing the cross section rather than the height of the fluidized beds. Thus, the aspect ratio of adsorber and desorber will significantly change with the scale of the process. At full scale, the adsorber would have a huge cross section but would be relatively low in height. A TSA design with columns positioned above each other as suggested by [37] would be a reasonable way to eliminate one of the two transport risers and to reduce the footprint of a large scale TSA plant [37]. However, even then at least one transport riser is required for a continuous TSA process.

At pilot scale such a design would lead to a plant with high overall height and a relatively low footprint. However, due to expected static issues (wind loads) the increase of costs due to the increased height

would outweigh the reduction of footprint. Thus, for the design of the ViennaGreenCO₂ pilot plant a system with two transport risers and with the columns next to each other was chosen.

Once the sorbent stream is lifted by the transport riser, gas and sorbent needs to be separated, which is in this case done by gravitational separators (cyclones would be possible as well). Within the gravitational separators, the velocity of gas and solids gets reduced. As a result, the sorbent will fall to the bottom, while the gas is extracted at the top of the separator. A deflector plate avoids a direct bypass of particles towards the gas outlet.

The sorbent outlet of the gas/solid separator is connected to the sorbent inlet of the respective column. Three possible sorbent inlet details are shown in Figure 4-12. In the set-up on the left side of Figure 4-12 (a), the sorbent material is introduced directly into the dense phase of the fluidized bed. For this scenario, a certain filling level in the connecting pipe will establish. This filling level is mainly depending on the pressure difference between particle separator and the column inlet. Operation of the bench scale plant showed that the particle separator and sorbent inlet can be operated stably if a certain gas flow in particle flow direction is allowed. If this gas flow is avoided by setting the pressure at the sorbent inlet of the column higher than the pressure in the particle separator bridging and blockages can occur. An L-Valve type inlet with a nozzle for an actively controlled gas flow (Figure 4-12 (b)) would create additional measures to influence the sorbent transport at this potential bottleneck of the system. However, a self-balancing system without the need for active control is preferred to keep the systems complexity and costs as low as possible. A third option would be to feed the sorbent within the freeboard of the column (Figure 4-12 (c)). However, for deeper fluidized beds, as they are expected in the desorber, this could easily lead to bypasses towards the downcomer and the stage below. For the above-mentioned reasons an inlet design as shown in Figure 4-12 (a) is considered for the pilot unit.

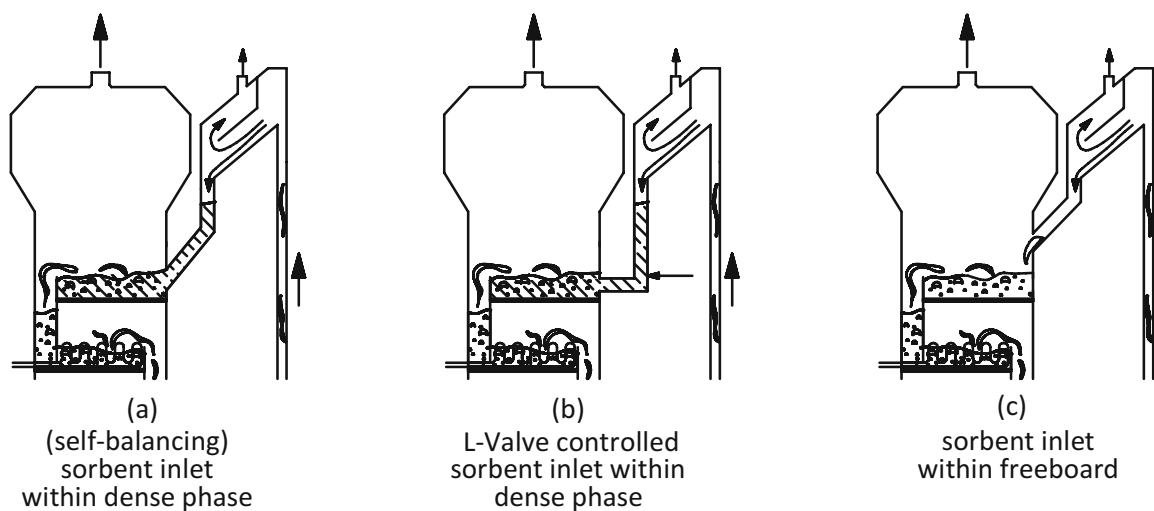


Figure 4-12: Different sorbent inlet details

4.3.2 Gas slip mechanism

In a TSA process set-up as shown in **Fehler! Verweisquelle konnte nicht gefunden werden.**, the pressure profiles are crucial for proper sorbent transport and fluidization of the columns but also for gas sealing between the columns. Key requirement on a separation process for CO₂ is deep removal in the adsorber and a high CO₂ purity (water content neglected) at the desorber outlet. This means, the sorbent material needs to be circulated between adsorber and desorber, but the gas streams of both columns need to be separated. However, since a bulk material is used, and other species than CO₂ might even get co-adsorbed by the sorbent, a direct or indirect gas slip will occur. So, the question is how this gas slip can be avoided or reduced to an acceptable level.

But to resolve this issue, it is important to understand the mechanism first.

For sorbent material, which is flowing in a pipe, like it is the case at the in- and outlet of adsorber and desorber, 3 different gas slip mechanism can be distinguished:

- Gas transported within the void of the moving bulk material
Characteristically for this mechanism is, that this gas flow will not result in a pressure drop between two points with a certain distance in flow direction. The gas is just dragged within the free space between the particles.
- Gas flow through the moving bulk material
If a pressure difference is applied over a moving bed regime, a gas flow relative to the flow of the bulk material will occur. Reversely, this means that a superimposed gas flow through a moving bulk material results in a pressure gradient.
- Gas co-adsorbed (and transported) on the sorbent
Depending on the selectivity of the utilized adsorbent, certain species other than CO₂ will get adsorbed. This co-adsorption will lead to an indirect gas slip from one column to the other.

As the gas flow which is induced by a pressure difference is superimposed to the gas, which is transported with the void of the bulk material, it makes sense to assess the mechanism in combination. Figure 4-13 shows the impact of a pressure difference in flow direction of the bulk material. For equal pressure at in- and outlet of the pipe section, the amount of gas that is dragged with the void can be easily estimated by the product of volumetric sorbent flow times the voidage of the moving bed. While a positive pressure difference would even increase the gas slip, a negative pressure difference would reduce the transported amount of gas. If the pressure difference is further adjusted to more negative values, it is possible to eliminate the gas slip with the void of the bulk material.

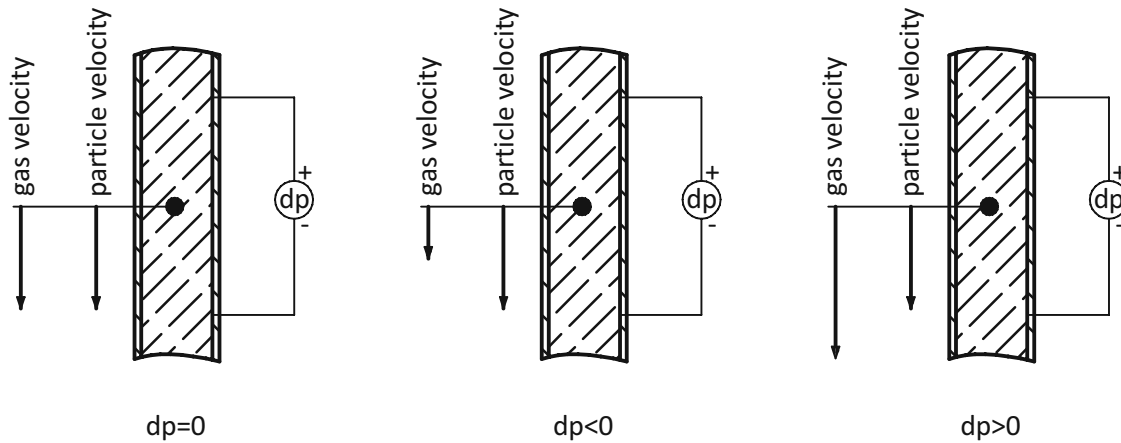


Figure 4-13: Superimposed gas flow in moving bed regime

Thus, if co-adsorption is neglected, the net gas slip from and into the columns can be avoided if the pressure profile of the system is adjusted accordingly.

4.3.3 Gas sealing requirements

Each transport section (lean and rich side) features two points where preferred gas sealing measures can be applied:

- Lean and rich standpipe (below the columns)
For control of the sorbent flow, both columns require a regulating element, which can be a pneumatic or mechanical device (L-valve, screw conveyor etc.). Above this regulating element a moving bed section is formed in the standpipe, which connects the column sorbent outlet and the sorbent flow control valve.
- Lean and rich particle separator standpipe (standpipe between particle separator and column sorbent inlet)
As shown in Figure 4-12 a second moving bed section can be established between particle separator and column inlet. However, as indicated previously, gas sealing at this location might lead to blockages. Since a blockage at this position can lead to major issues as soon as the function of the particle separator is affected, and particles are entrained towards the recycle blower (see **Fehler! Verweisquelle konnte nicht gefunden werden.**).

However, before actual measures are discussed, it should be defined which sections have to be sealed against each other, since some possible leakage scenarios might be acceptable. Furthermore, it is hardly possible, to completely avoid any gas slip in the moving bed sections. Practically, a gas flow can only be reduced to a certain extend.

Leakages at the rich standpipe

Assuming atmospheric conditions at the gas outlet of the columns, the highest-pressure points are to be expected at the lower most stages of the columns. Therefore, and without any countermeasures, a gas slip from the column sorbent outlet towards the respective transport riser would occur. If the transport riser gas is implemented as a closed recycle as shown in **Fehler! Verweisquelle konnte nicht gefunden werden.**, then any gas slip from the column sorbent outlet towards the riser would finally end at the top of the other column to fulfil the mass balance over the transport riser. Furthermore, the rich transport system will not only feature the function of sorbent transport, but also allow to pre-heat the sorbent. It is likely that the pre-heating of the material will lead to a partial regeneration and formation of an $\text{CO}_2/\text{H}_2\text{O}$ atmosphere.

A leakage of flue gas, which is fed to the adsorber, towards the rich riser must be avoided for two reasons:

- Sorbent degradation
The oxygen content of the flue gas in combination with elevated temperatures in the rich transport section will cause degradation of the sorbent material
- CO_2 purity
The sorbent material is partially regenerated at the elevated temperatures prevailing in the rich transport section. The CO_2 which is released in the transport section will finally be combined with the desorber off gas. Any contamination with flue gas should therefore be avoided.

In a leakage scenario against flow direction, a $\text{CO}_2/\text{H}_2\text{O}$ mixture, which is released from the sorbent due to heat up, would flow upwards the standpipe and would potentially cause a parasitic loading on the sorbent. But apart from potential losses in process performance, this scenario seems more acceptable compared to a flue gas leak towards the hot sections of the rich transport system, if the net flow is reduced to a minimum.

Leakages at the rich particle separator standpipe

As indicated previously, the sorbent material is expected to get partially regenerated within the rich transport system. This means, that a certain amount of CO_2 and potentially water vapor is continuously released from the sorbent material. If gas leakage from the adsorber towards the rich transport system is avoided effectively, this CO_2 gas stream can and should be combined with the desorber off gas stream.

At the desorber particle separator standpipe, gas sealing is hard to achieve without creating potential blockages of the standpipe. Gas sealing in the particle separator standpipe can only be achieved if a pressure gradient against sorbent flow direction is established. But operation at bench scale showed, that a negative pressure gradient easily leads to blockages if it is not controlled precisely. At bench scale, stable operation was achieved by a flow control valve in the gas side outlet of the particle separator. With this control valve, the particle separator was set to a pressure, which was slightly above the pressure in the column top stage. This measure efficiently eliminated previously observed blockages of the particle separator standpipes, by allowing a small amount of gas to flow with the particles into the column. However, careful setting of this pressure difference is required, since from

multistage adsorption point of view, this gas flow should be as small as possible, and other issues like: formation of large bubbles in the uppermost stage and entrainment can be generated.

A requirement to allow this small gas flow with the particle flow, is that the gas of the rich riser system is practically free of contaminants like O₂ and N₂ and therefore compatible with the uppermost stage of the desorber (which is achieved by sealing the adsorber standpipe against flue gas leaks). But for the configuration indicated in **Fehler! Verweisquelle konnte nicht gefunden werden.**, the maximum amount of gas that can be allowed to flow with the sorbent is limited by the amount of gas, that is released within the transport system. In this configuration, the gas flow is a result of desorption within the riser and potentially not at the fluid dynamic optimum. Furthermore, during start-up no gas is released in the transport section, and an alternative source for this gas needs to be found.

Leakages at the lean particle separator standpipe

Similar to the rich particle separator standpipe, leakages against flow direction (from the adsorber into the lean riser section), as well as zero net gas flow would likely lead to blockages of the lean particle separator standpipe. Thus, a small gas flow with sorbent flow direction would be favorable to avoid blockages of the standpipe. However, in the lean transport section no gas is released from the particles and if the lean riser gas is operated in a closed recycle, the amount of gas, which is allowed to flow with the particles in the lean particle separator standpipe would have to be introduced from an external source into the lean transport section. Furthermore, a gas composition, which is acceptable in the lean riser itself as well as in the adsorber off-gas needs to be chosen (e.g.: recycle of adsorber off gas)

Leakages at the lean standpipe

Assuming, within the lean transport section the material is cooled to some extent, a leakage of desorber fluidization steam can be critical in terms of condensation. On the other side, any leakage of oxygen from the lean riser gas towards the desorber would cause degradation and needs to be avoided. At the desorber sorbent outlet, a small leakage of fluidization steam downwards to the lean riser is the more acceptable scenario. But the pressure profile needs to be adjusted in a way that this leakage is reduced to a minimum and condensation needs to be avoided (e.g.: by introduction of a purge and/or dilution gas stream).

4.3.4 Transport sections as dedicated adsorption/desorption stages

As discussed previously, gas sealing requirements would allow for leakages from the riser system towards the columns via the respective particle separators if the transport gas is compatible with the column off-gas. The additional benefit of this scenario would be a more robust sorbent transport behavior from the particle separators to adsorber and desorber.

From a thermodynamic point of view, the transport sections could be adapted to dedicated adsorption/desorption sections if the recycle of the transport gas is changed accordingly. Figure 4-14 shows a thermodynamically optimized set-up, where the column off gas is used as a transport gas for the respective pneumatic risers. Taking a slipstream of the column off gas for fluidization of the transport risers makes them an additional step of the counter current flow pattern of adsorber and desorber. In this set-up, the lean riser can be seen as the 6th stage of the adsorber, while the rich riser

acts as first regeneration step if heat is supplied. Although, the transport sections need independent gas flows and will not be as effective as an additional column stage, the benefit comes at very low costs, since the recycle blower is required anyway.

Furthermore, the gas flow in sorbent flow direction at the particle separator standpipes is uncoupled from the gas release in transport section and can be adjusted to its fluid-dynamic optimum, by adjustment of the pressure difference between particle separator and uppermost stage of the column.

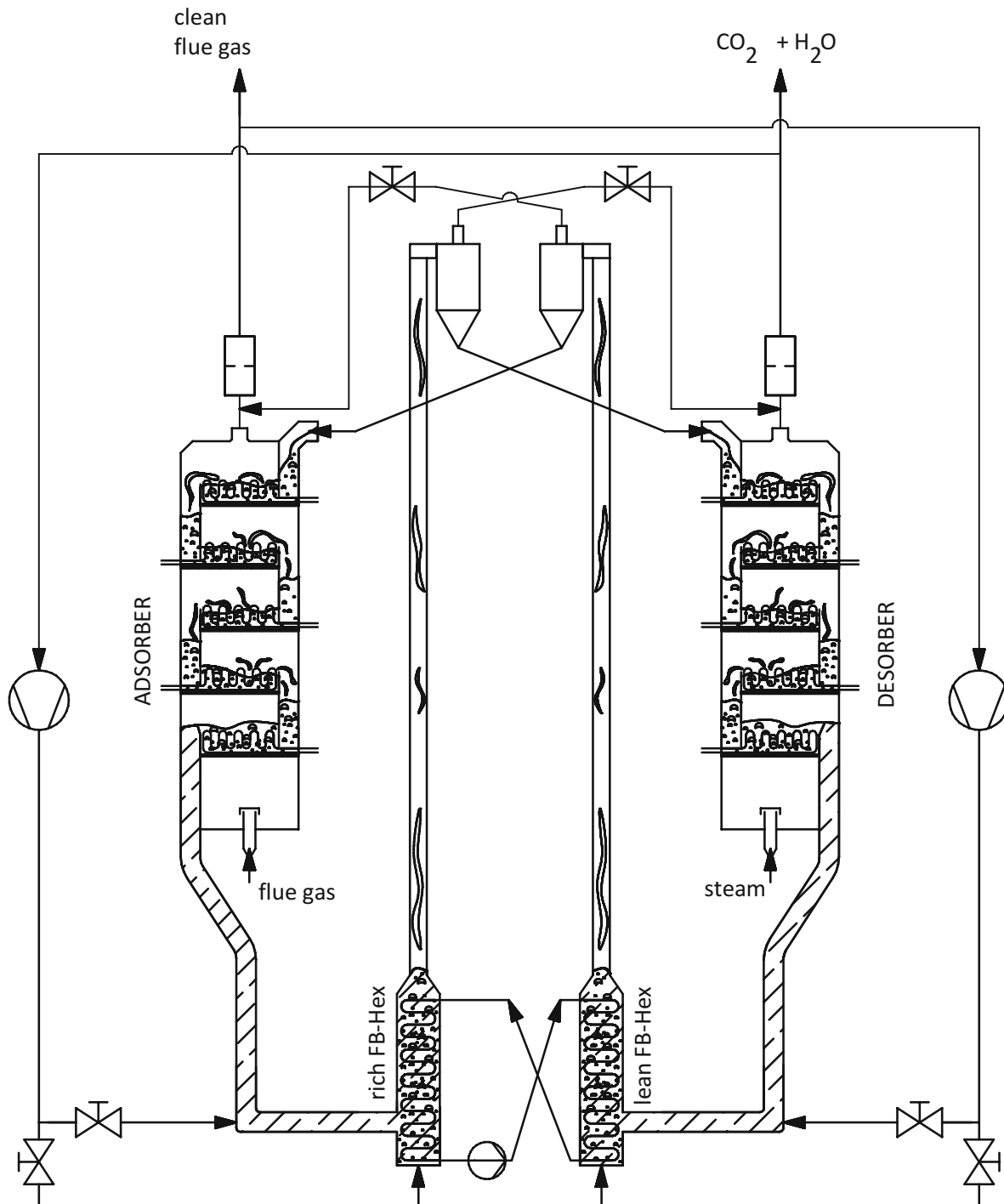


Figure 4-14: Transport risers as dedicated adsorption/desorption stages

4.3.5 Sorbent flow control

One key requirement for the previously discussed gas sealing measures is that adsorber and desorber standpipes are always filled with sorbent material. As soon as one of the standpipe empties, the flow resistance for the gas will drop to practically zero and a huge amount of gas can pass. Thus, an active control element for the sorbent flow is required at the bottom of each standpipe which ensures the desired sorbent flow at one hand and avoids emptying of the downcomer at the other. While one of the control elements will be used to set the desired sorbent circulation rate, the other will have to follow in order to maintain the sorbent inventory share between adsorber and desorber and to avoid that one of the standpipes empties (see also findings of Schöny et al. [73], [95]).

Within the bench scale unit, L-valves showed good controllability of the sorbent flow within certain pressure differentials between in- and outlet of the L-valve [66]. Since the pressure drop over the adsorber is required to be rather low (~50 mbar), a L-valve will be used also to control the sorbent flow at the rich standpipe of the pilot unit. To achieve gas velocities required for fluidization of the desorber and to avoid excessive stripping steam consumption, the desorber tendentially requires higher fluidized beds with lower cross section compared to the adsorber. Thus, at the desorber standpipe, a significantly higher difference in pressure is expected, which potentially could cause problems for a pneumatic L-valve. Therefore, a mechanical slide valve has been chosen to control the sorbent flow at the lean standpipe. Zehetner [89] presents a detailed study on the control behaviour of both control elements.

4.3.6 Concluding gas sealing measures

Finally, the requirements on gas sealing can be summarized as shown in Table 4-4.

Table 4-4: Gas sealing requirements summary

	in sorbent flow direction	against sorbent flow direction
rich standpipe	leakage not acceptable (degradation and reduction of CO₂ purity)	small flow acceptable
lean standpipe	small flow acceptable if condensation is avoided	leakage not acceptable (degradation and reduction of CO₂ purity)
rich particle separator standpipe	small flow acceptable	fluid dynamically undesired (blockages)
lean particle separator standpipe	small flow acceptable	fluid dynamically undesired (blockages)

As discussed previously, the sorbent flow within the standpipes drags gas in the void of the bulk material. In addition to this, a pressure gradient in flow direction causes a superimposed gas flow, that is dependent on the flow resistance of the bulk material. In reality, the voidage and the flow resistance

of the bulk material will change with operating conditions. However, for the assessment of general tendencies a constant voidage and flow resistance is assumed.

For this assumption, the amount of gas that is transported with the void of the bulk material is proportional to the sorbent flow rate. To reduce this gas flow, a pressure gradient against flow direction can be applied. Depending on operating and design conditions, this method can reduce, eliminate, or even reverse the net gas slip in the moving bed by replacement through a purge gas.

In principle there are 4 different options to reduce or eliminate this net gas flow:

Reduction of inlet pressure

The inlet pressure of adsorber and desorber standpipe is a result of the pressure drop over the columns if approximately atmospheric conditions are assumed at the top of the columns. A lower column pressure drop would not necessarily eliminate a gas slip, but it would simplify gas sealing. However, the pressure drop of the columns is a result of many other design considerations (e.g. a certain bed height, which is proportional to the bed pressure drop can be required to fit sufficient heat exchange surface at limited cross section).

Increase of outlet pressure

The pressure gradient in the standpipe can be reduced if the outlet pressure of the standpipe is increased. This could for instance be achieved in the outlet of the rich L-valve by adding a flow restriction downstream to the desorber. However, this in turn makes it more difficult to seal the lean L-Valve. A different way to achieve an increase of the outlet pressure of the rich L-valve is to intentionally increase the pressure drop of the transport section between rich L-valve and desorber. This can be achieved by a dense fluidized bed in the bottom of the rich riser which can be combined with a fluidized bed heat exchanger in the bottom section of the riser.

Standpipe length

The standpipe length does not necessarily affect the pressure difference between in- and outlet of the standpipe but influences the pressure gradient ($\text{Pa}\cdot\text{m}^{-1}$) and thus the overall flow resistance for a superimposed gas flow. Therefore, from a gas sealing point of view, the standpipes should be as long as possible. However, there needs to be tradeoff between gas sealing and overall height of the plant.

Purge gas introduction

Another measure for gas sealing is the introduction of a purge gas stream (see Figure 4-15). With introduction of a purge gas stream the shape of the pressure profile can be adjusted actively (see Figure 4-15, right side). Below the purge gas introduction point, the net gas flow would be even increased compared to the situation without purge gas, but the gas can be replaced by the purge gas if a certain negative pressure gradient is achieved above the introduction point. Therefore, the introduction of a purge gas is no actual gas sealing measure, but a measure which allows to replace harmful leakages (e.g. O_2) with a gas which is more acceptable.

At the desorber standpipe, without any counter measures, the steam used for fluidization of the desorber would flow with the sorbent flow towards the lean riser. Furthermore, a superimposed flow through the sorbent bulk would occur, which is caused by the pressure difference between desorber

first stage and lean riser. This slip of steam would lead to condensation issues in the colder lean riser section and needs to be avoided as much as possible. Purge gas introduction within the lean standpipe can create sufficient back pressure for the steam to avoid this steam slip. However, a gas composition which does not create problems in the downflow section needs to be chosen, which is in this case a recycle of the adsorber off gas. While this gas is compatible with the lean riser, it must be avoided, that the purge gas enters the desorber, as it would lead to contamination of the CO₂ product as well as increased oxidative degradation of the sorbent. Therefore the control strategy for the lean standpipe is as follows: Instead of avoiding 100 % of the potential steam slip only a small amount of purge gas is introduced at the lean standpipe, which is enough to avoid condensation issues, but not enough to risk a return flow of the purge gas.

At the rich standpipe, the situation is different: Condensation issues in a leak case are not to be expected, but again oxidative degradation and contamination would be the consequence, which needs to be avoided. At the rich standpipe, the adsorber pressure difference between adsorber and rich riser is significantly lower, and a L-valve with actively controlled aeration flow comes to use for sorbent flow control. In a certain range the sorbent flow of a L-valve is proportional to aeration gas flow which is introduced at the elbow of the L-valve. The aeration of the L-valve has an effect, which is similar to the previously described purge gas introduction, but this effect cannot be exploited exclusively for gas sealing purposes as it is foreseen for sorbent flow control primarily. Especially at low load conditions when low sorbent flow is required, the reduced L-valve aeration cannot meet gas sealing requirements. But the L-valve can be designed to partially avoid a gas slip from the adsorber to the rich riser at least at design conditions.

Additionally, to the sealing effect of the L-valve itself, a purge gas introduction upstream of the L-valve comes to use for further avoidance of a gas slip from the adsorber. Differently to the lean standpipe gas compositions of CO₂ and H₂O (to avoid contamination of the CO₂ product and to avoid oxidative degradation) are preferred, which is achieved by recirculation of desorber off gas.

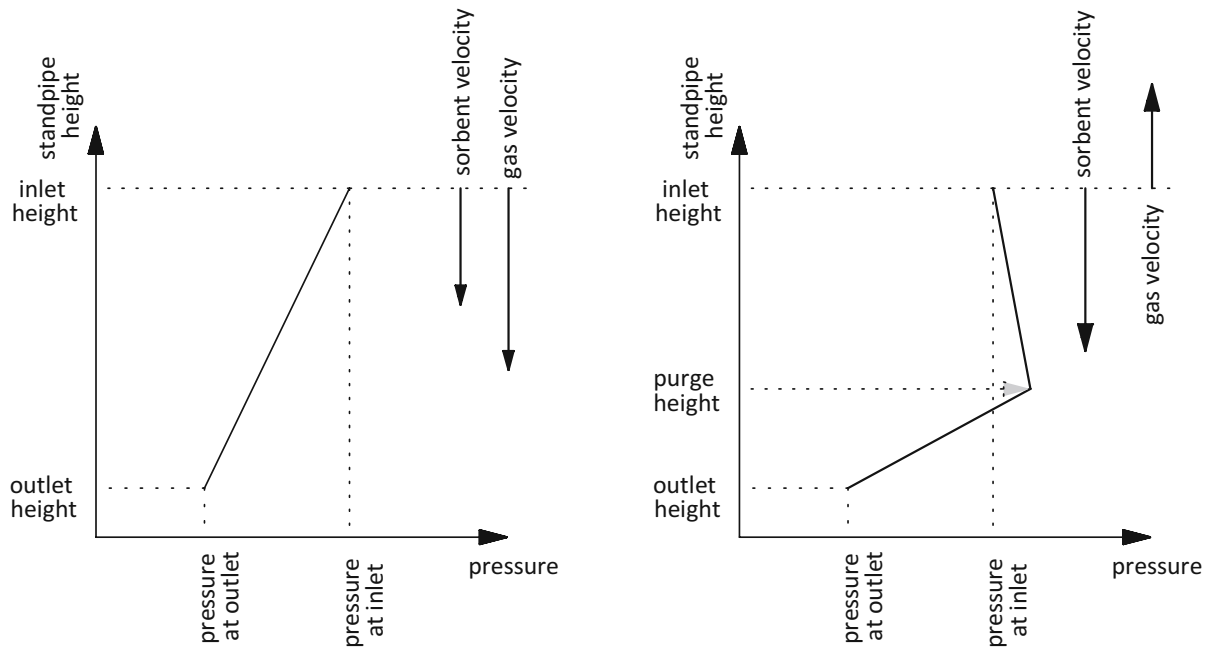


Figure 4-15: Standpipe pressure profiles with and without purge gas introduction

4.4 LEAN/RICH HEAT EXCHANGE

4.4.1 General aspects

A significant share of the TSA process energy demand is related to heating and cooling of the adsorbent. Pröll et al. calculated, that heating and cooling accounts for 20 % of the total multistage TSA process heat demand [36]. Sonnleitner et al. [50] measured a heat capacity of $1.58 \text{ kJ}\cdot\text{kg}^{-1}\cdot\text{K}^{-1}$ for Lewatit VP OC1065, which is compared to aqueous amines (e.g.: $4 \text{ kJ}\cdot\text{kg}^{-1}\cdot\text{K}^{-1}$ for 30 wt% MEA solvent [18]) relatively low. However, most of the sensible heat in a liquid amine process can be recovered with a lean/rich heat exchanger (see Figure 1-4). Liquid/liquid heat exchange with plate heat exchangers can reach several thousand $\text{W}\cdot\text{K}^{-1}\cdot\text{m}^{-2}$, which results in low required heat exchange surfaces. Furthermore, liquid/liquid heat exchangers costs per square meter are rather low, compared to other heat exchangers and a direct heat exchange between lean and rich solvent is possible. This means that the often-discussed disadvantage of the higher heat capacity of solvents in liquid amine systems is at least partially compensated by the comparably low costs for the heat recovery between lean (hot) and rich (cold) solvent streams.

Similar to amine scrubbing systems, a lean/rich heat exchange can also be realized in combination with the TSA process. Within the lean/rich heat exchanger, the temperature difference between regenerated and loaded adsorbent material is exploited to transfer sensible heat between both material streams. The heat recovery rate is defined as:

$$\eta_{HR} = \frac{T_{SORB\ DES\ IN} - T_{SORB\ ADS\ OUT}}{T_{SORB\ DES\ OUT} - T_{SORB\ ADS\ OUT}} \cdot 100$$

Equation 4-1

This means that, if the adsorbent is heated up in the lean rich heat exchanger so that it enters the desorber column at the same temperature as it exits the desorber, the heat recovery rate calculates to 100 %. If the temperature at the desorber inlet equals to the mean adsorber stage temperature, the heat recovery rate is 0 %. Lean/rich heat exchange reduces both, the heating demand within the desorber as well as the cooling demand within the adsorber column as the temperatures of both material streams approach the desired operating temperatures within the contactors.

Compared to liquid amine systems, the exchange of heat between rich and lean solid sorbent, is more challenging. This is mainly because a bulk material is more complicated to handle compared to a liquid. Practically, it is not possible to achieve a material transport within pipes by application of a pressure difference only, as it is the case for liquids or gases. While a solvent can be pumped efficiently from one point in the process to the other, or even through a heat exchanger in any direction, bulk material streams need to be transported with more complicated and mostly less efficient systems like screw or belt conveyors, bucket elevators, pneumatic transport risers or similar systems.

4.4.2 Basic assessment of potential lean/rich heat exchange setups for TSA

In order to overcome the previously discussed drawback and to maintain the competitiveness of the TSA process, a suitable lean/rich heat exchange system needs to be identified. Several concepts have been evaluated with respect to their suitability for the TSA process. The following gives a conclusive summary of the investigated set-ups.

Fluidized bed heat exchangers within riser bottom section

By increasing the diameter of the bottom section of the transport risers, it is possible to form dense phases with increased particle residence time. Such a dense phase can provide a relatively high heat transfer coefficient compared to the transport section. By application of indirect heat exchangers within the bottom regions of the transport risers and by utilization of a heat carrier medium that is circulated between both heat exchangers (see **Fehler! Verweisquelle konnte nicht gefunden werden.**), part of the sensible heat can be recovered.

As described in Chapter 2, heat exchange between a fluidized bed and an immersed surface can be separated in three main mechanism. In low temperature applications like TSA, radiation heat can be neglected, and gas convective heat transfer would become more important only for bigger particles. Thus, the particle convective heat transfer plays the biggest role in this case. Particle convective heat transfer describes the short direct contact between particles and a heated or cooled surface and the subsequent “transport of heat” into the fluidized bed by particle movement. Therefore, this heat transfer mechanism depends strongly on the particle movement or mixing of the fluidized bed.

For a well-mixed fluidized bed, the achievable heat transfer coefficient is relatively high, but the temperature of the sorbent within the dense phase is also relatively uniform. Consequently, the maximum heat exchange in this configuration is limited and the adsorbent material within both beds can at the best reach the mean temperature difference between the operating temperature in the adsorber and the desorber column. Hence, the sensible heat that can be recovered from the regenerated adsorbent material is theoretically limited to 50 %, where the ΔT for heat exchange approaches zero.

Ideally, the adsorbent flow should be like a plug flow. Then, the heat carrier medium flow can be realized in counter-current flow to the adsorbent flow. Which would theoretically allow for heat recovery rates of up to 100 %. However, achieving the desired high heat transfer rates of a fluidized bed whilst having a plug flow behaviour to allow for higher heat recovery rates is hardly possible. So that a reasonable compromise between flow pattern and achievable heat transfer coefficient needs to be identified.

Another issue of fluidized bed lean/rich heat exchange is the required blower power. For higher heat recovery rates, the required heat exchange surface increases. As the heat transfer surface that can be fit within a fluidized bed is limited, the bed volume needs to increase at a certain point. This means either more pressure drop, if the bed height increases or more flow if the fluidized bed increases in width or depth. For high heat recovery rates, the electrical power consumption of the blower might overweigh the reduction of the heating and cooling demand of the sorbent.

Moving bed lean/rich heat exchange

Compared to fluidized bed heat exchange, moving bed heat exchangers can provide only a fraction of the achievable heat transfer coefficient. On the other side, moving bed heat exchangers can be operated at low operating costs, since gas for fluidization is not needed. Furthermore, a high specific heat exchange surface per heat exchanger volume can be fitted in a moving bed heat exchanger, which potentially compensates the disadvantage of the lower heat transfer coefficient.

One critical requirement for application of a moving bed heat exchanger is sufficient height, as the material needs to flow through the heat exchanger by gravitation only. This means, that also the direction of flow is not freely selectable and has to be top down always. Another requirement is sufficient filling and a proper flow distribution over the cross section of the heat exchanger, which is usually achieved with a special outlet geometry and a control element for the sorbent flow, installed at the outlet of the heat exchanger. For the TSA process, the sorbent flow at the adsorber and desorber outlet needs to be controlled anyway. To avoid additional equipment for control of the moving bed heat exchanger filling level, the moving bed heat exchangers can be installed between adsorber or desorber outlet and the respective flow control element (see Figure 4-16). To ensure good gas sealing between adsorber and desorber, this moving bed sections need to be filled anyway. The moving bed heat exchangers would only increase the inventory in this section.

With a proper outlet geometry, the flow pattern of the sorbent material within the moving bed heat exchangers can be considered as plug flow. Thus, if the heat carrier medium is flowing through the heat exchanger from bottom to top, an indirect counter current heat exchange can be established, which theoretically allows for heat recovery rates of up to 100 %. However, in practice a reasonable trade-off between heat transfer surface and heat recovery rate needs to be defined.

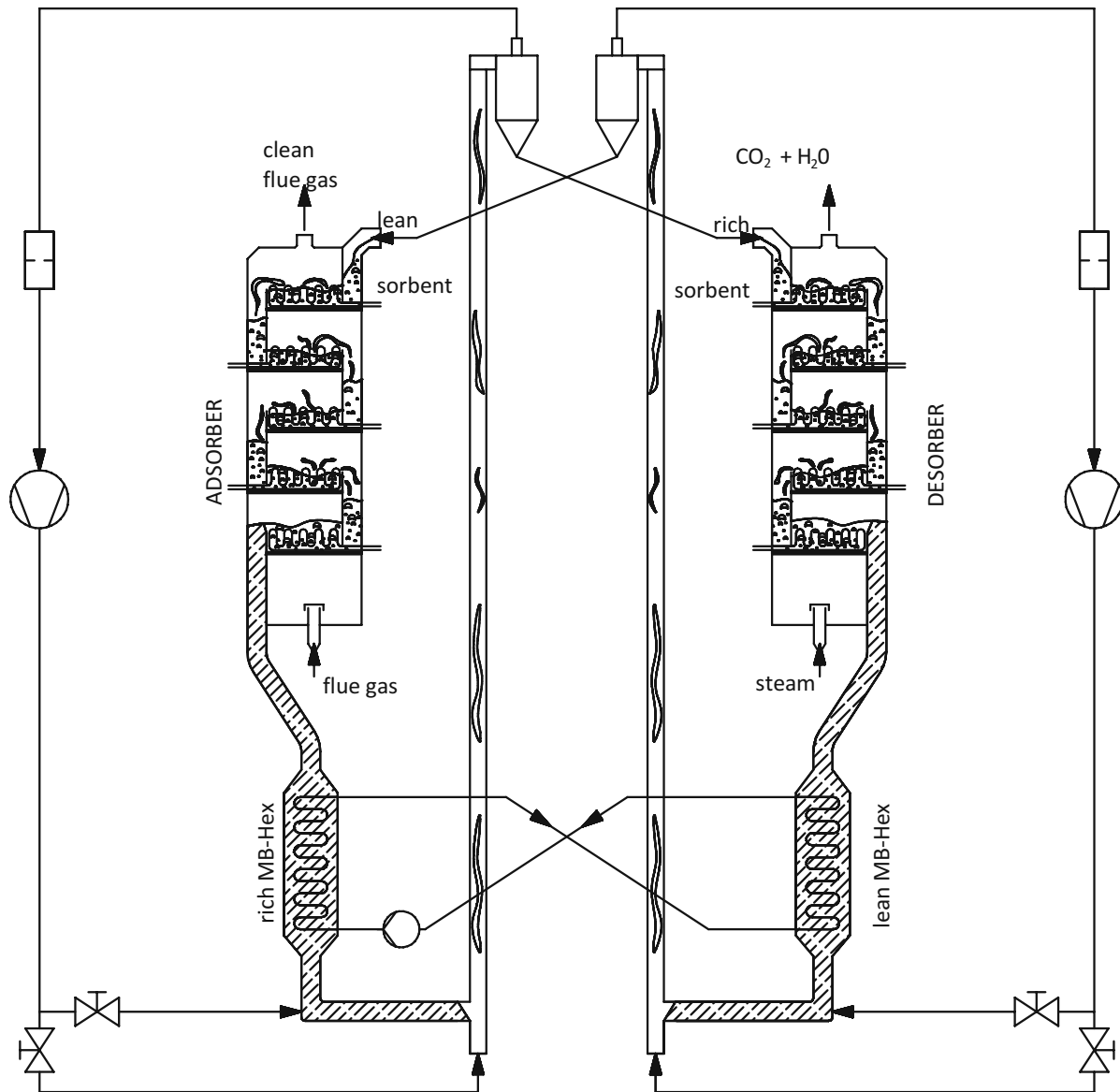


Figure 4-16: Moving bed lean/rich heat exchange

Combination of moving bed heat exchanger and fluidized bed heat exchanger within riser bottom section

As discussed previously, a fluidized bed lean/rich heat exchanger within the bottom section of the transport riser features a relatively high heat transfer coefficient but requires more blower pressure increase and/or flow, which adds to the energy demand of the process. Especially if the total flow to the riser has to increase, the transport riser efficiency is also reduced. However, a favourable case might be, if the blower is sized for optimum flow in the transport risers, while only the pressure drop is increased by the fluidized bed heat exchanger. Therefore, the transport risers would be operated

economically, while the high heat transfer rate of the fluidized bed is exploited at relatively low operating costs.

As the applicable heat transfer surface is limited to some extent, an additional moving bed heat exchange could be connected in series to the fluidized bed heat exchangers to enable higher heat recovery rates.

If the fluidized bed heat exchangers are considered as continuous stirred tank heat exchangers, and the moving bed heat exchangers as counter current heat exchangers, this combined set-up is beneficial especially at lower targets for the heat recovery rate. Compared to a moving bed lean/rich heat exchanger set-up an additional fluidized bed heat exchanger can reduce the total required heat exchange surface significantly. At higher heat recovery targets, the fluidized bed heat exchanger delivers only a minor part of the total recovered heat if it is considered as continuous stirred tank heat exchanger.

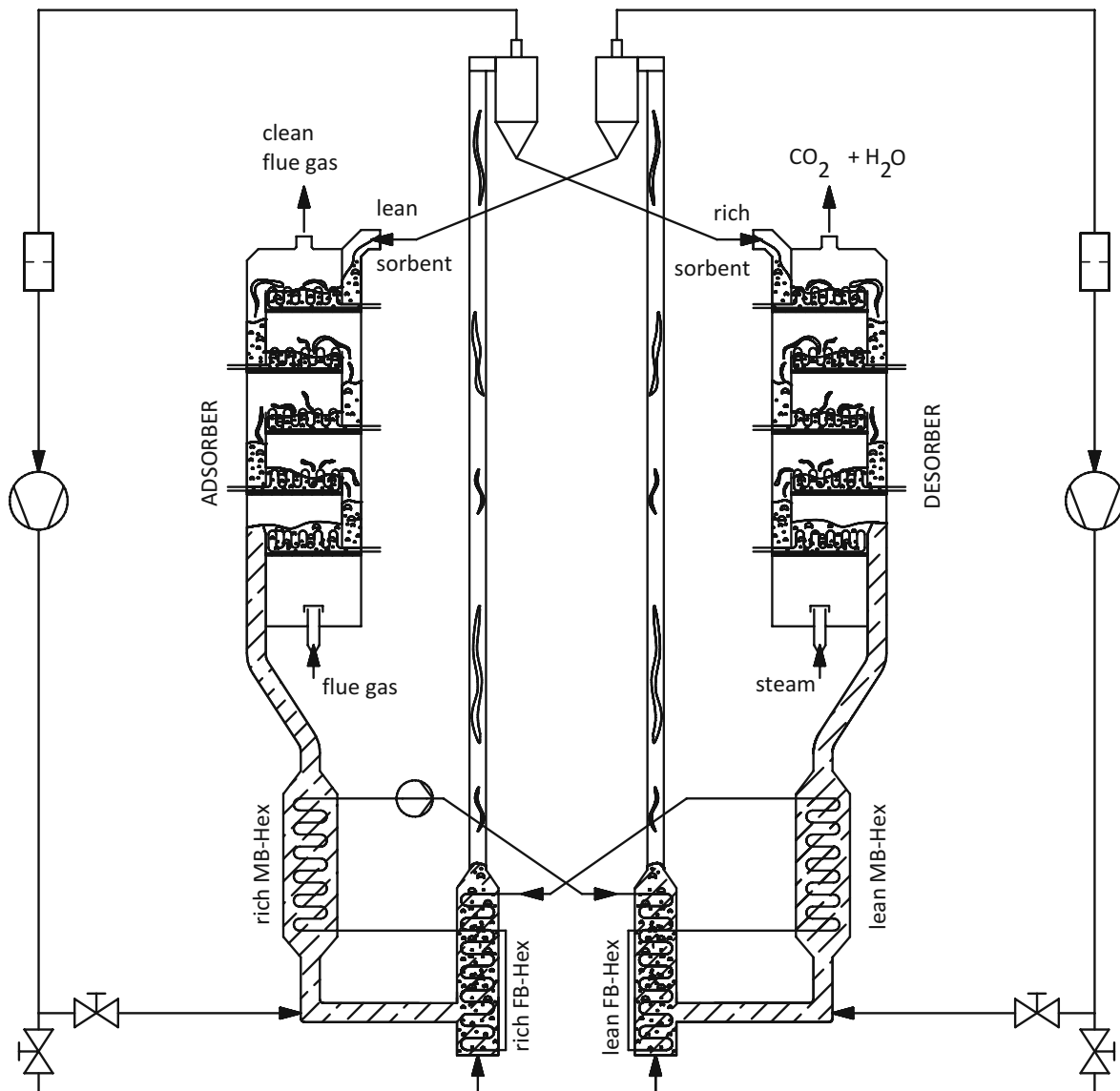


Figure 4-17: Combination of moving bed and fluidized bed lean/rich heat exchanger

Adsorption and desorption activity within lean/rich heat exchangers

In the standpipe below the adsorber, the rich sorbent is considered to be more or less in equilibrium with the surrounding gas phase. This means that the gas composition as well as the particle CO₂ and H₂O loading will adapt accordingly. As soon as the sorbent material enters the rich heat exchanger and gets heated it will release CO₂ and H₂O until equilibrium with the gas phase is reached again. On the one hand, desorption of H₂O and CO₂ requires latent heat and therefore influences the temperature levels of the in- and outlet streams as well as the achievable heat recovery rate of the heat exchangers. On the other hand, this gas release has to be taken into account for the heat exchanger design, so that it does not cause operational problems. Especially the flow direction of the released gas is important. If the released CO₂ and/or H₂O (partially) flows back towards the adsorber, it could be adsorbed again by the colder adsorbent, which could cause a parasitic loading within the rich heat exchanger. If CO₂ and or H₂O flows upstream to the adsorber, the temperature within the heat exchanger inlet would increase because of the subsequent adsorption activity, which would then reduce the achievable heat recovery rate of the lean/rich heat exchange set-up.

Regarding the release of adsorbed CO₂ and H₂O, the fluidized bed heat exchanger is less critical, because the gas release is relatively small, compared to the fluidization gas flow. Furthermore, the fluidization gas flow forces the released gas to flow into the right direction. Thus, the previously mentioned parasitic loading is not relevant in a fluidized rich lean/heat exchanger

For the moving bed heat exchanger set-up, it is more challenging to design it in a way, that a back flow of the released gas is minimized. For the installation position indicated in Figure 4-16, the whole pressure profile of this transport section from adsorber to desorber needs to be taken into account. The pressure at the adsorber sorbent outlet results from the adsorber design and the current load and stage inventories. Thus, the transport section needs to be designed in a way that the pressure at the rich standpipe, upstream the rich heat exchanger is well balanced to avoid superimposed gas flows in the standpipes or in the heat exchanger. However, also a gas flow from the adsorber downwards is not acceptable, as this would cause O₂ and N₂ contaminations of the CO₂ product.

Thus, only a very small window for operation is available, in which both, the parasitic CO₂ loading and the CO₂ product contaminations are within an acceptable range.

Both, the fluidized lean/rich heat exchange set-up as well as the proposed moving bed lean/rich heat exchange require an investigation on the achievable heat transfer coefficient in such set-ups, in order to allow for a more detailed assessment of these set-ups.

However, the bigger uncertainty of this basic assessment comes from the moving bed lean/rich heat exchange set-ups. For fluidized bed heat exchange, at least some experimental data with the desired bed material is available from the adsorber and desorber stage heat exchangers. However, for moving bed heat exchange, heat transfer measurements and additional investigations of following points are required to identify a thoughtful heat exchanger design:

- **Heat exchanger type:** Several different moving bed heat exchanger designs can be found on the market. Plate heat exchangers are broadly used for heating/cooling of polymers, fertilizers, oil seeds, etc. However, in the context of TSA, the requirements may deviate, so that other designs might become more attractive.

- **In- and outlet geometry:** At the inlet of a moving bed heat exchanger, the sorbent material needs to be distributed over the whole cross section and at the outlet the cross section is reduced again by an outlet cone. Depending on the sorbent material, different cone designs might be necessary to ensure an even distribution of the sorbent flow.

4.4.3 *Moving bed heat transfer measurement in single pipe*

The previously discussed moving bed heat exchanger design aspects can have a great impact on the performance and the costs of this equipment. However, before these aspects can be investigated in detail, it is necessary to get a rough estimation of the required heat transfer surface. For this preliminary estimation, at least some experimental data with the actual sorbent material is required. Therefore, it was decided to conduct moving bed heat transfer measurements in a very simple set-up in order to get an idea of the basic correlations.

Experimental setup

As can be seen in Figure 4-18, the setup consists of a hopper, which is filled with sorbent material, and feeds a heated, vertical pipe. The sorbent material utilized during this experiment was Lewatit VP OC 1065 and the same material, which was chosen for the pilot unit (see chapter 3.7). The sorbent flow rate through the pipe was controlled by a screw conveyor located at the bottom of the pipe. For heating, a temperature-controlled water cycle, which flows from bottom to top through the double wall of the pipe was implemented. The screw conveyor was calibrated with a method, where the transported mass of sorbent was measured in a specific timeframe for various screw conveyor speeds. The sorbent inlet and outlet temperatures as well as the temperature of the heated water cycle was measured using PT-100 1/3 DIN B-class type temperature sensors. The water flow was adjusted to 120 l/h, which is compared to the sorbent mass flow (see Table 4-5) and with regard to the higher heat capacity, high enough to neglect the temperature difference between water inlet and outlet in good approximation.

While the pipe length was constant at 500 mm, 3 different pipe diameters have been tested. The inner diameter of the pipe was 12, 15 and 21 mm.

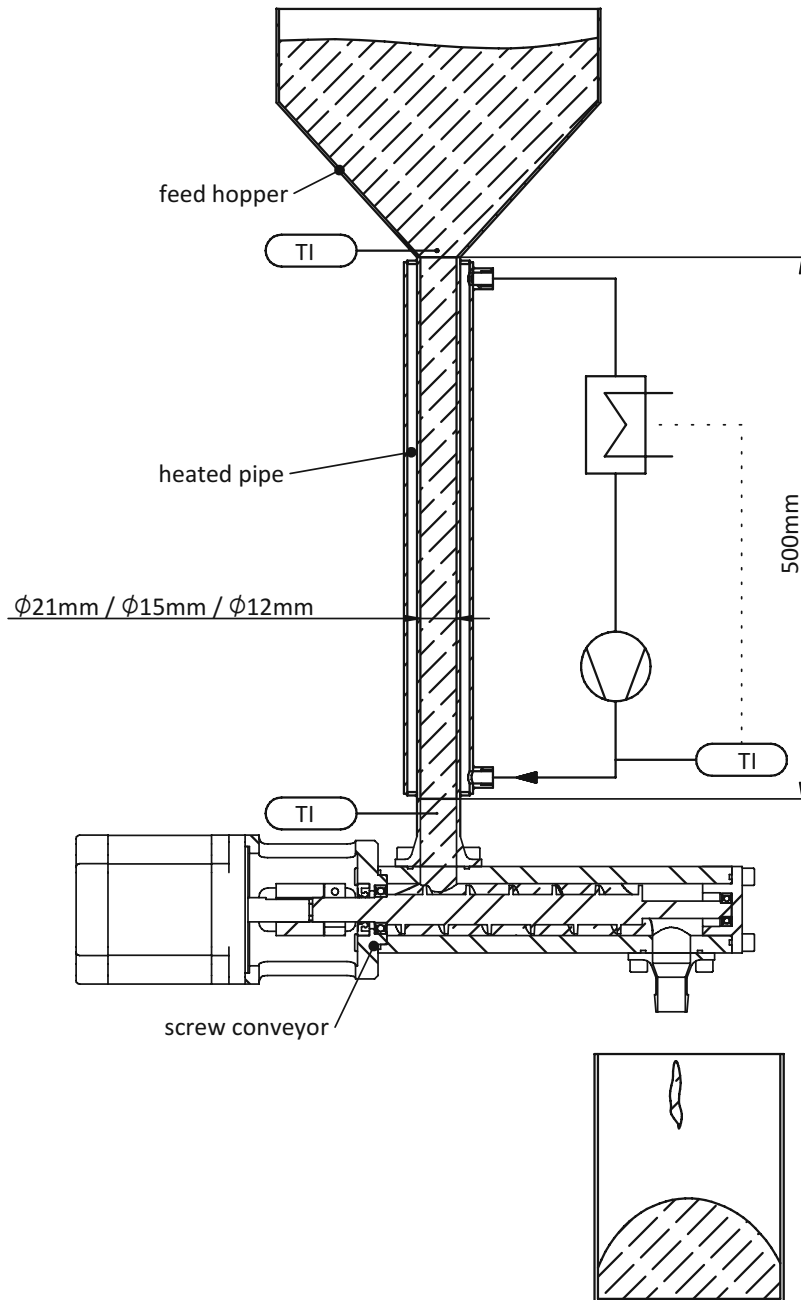


Figure 4-18: Experimental setup for single pipe moving bed heat transfer measurements

Experimental results

The heat transfer rate was calculated according to the equation below:

$$q = \dot{m}_{\text{Sorbent}} * c_{p,\text{Sorbent}} * (T_{\text{in,Sorbent}} - T_{\text{out,Sorbent}}) \quad \text{Equation 4-2}$$

The heat capacity of the sorbent was estimated at $1.5 \text{ kJ} \cdot (\text{kg} \cdot \text{K})^{-1}$. As mentioned above, isothermal conditions were assumed at the pipe wall, the temperature of which was assumed equal to the water temperature. The temperature difference required for the determination of the heat transfer coefficient was calculated as follows:

$$\Delta T = \frac{(T_{\text{water}} - T_{\text{in,Sorbent}}) - (T_{\text{Water}} - T_{\text{out,Sorbent}})}{\ln \frac{T_{\text{water}} - T_{\text{in,Sorbent}}}{T_{\text{Water}} - T_{\text{out,Sorbent}}}} \quad \text{Equation 4-3}$$

Together with the heat transfer surface area, the heat transfer coefficient was calculated:

$$h = \frac{q}{A * \Delta T} \quad \text{Equation 4-4}$$

As shown in Table 4-5, experiments were carried out with three different pipe diameters at three different solids flow rates.

pipe diameter	heat transfer surface [mm ²]	solids flow rate [kg·h ⁻¹]	water temperature [°C]	solids inlet temperature [°C]	solids outlet temperature [°C]	heat transfer coefficient [W·m ⁻² ·K ⁻¹]
12,0	18849,6	1,3	53,9	19,7	43,7	34,7
		2,5	54,3	19,5	40,2	49,2
		3,6	54,0	23,3	39,3	58,6
15,0	23561,9	1,3	53,4	22,3	45,8	32,0
		2,6	53,1	22,0	42,1	47,6
		4,1	52,0	17,8	36,9	58,4
21,0	32986,7	1,2	54,2	25,9	43,6	15,0
		2,2	54,3	25,5	43,4	27,2
		3,6	54,3	24,6	42,6	42,1

Table 4-5: Summary of results gained from single pipe moving bed heat transfer measurements

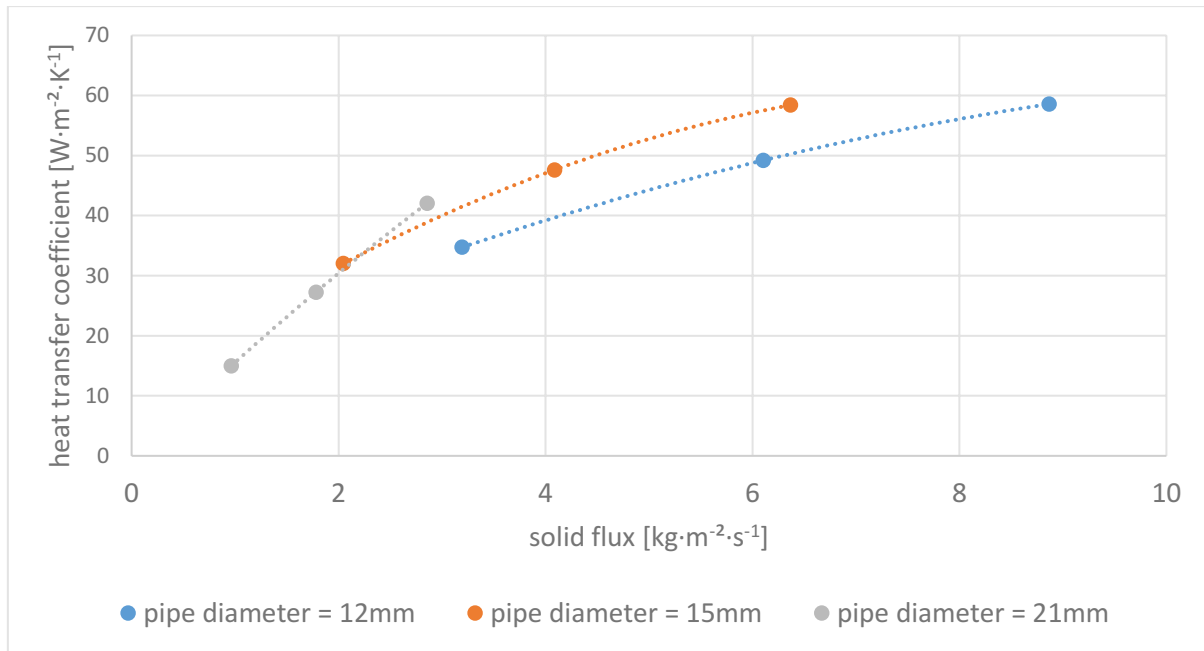


Figure 4-19: Summary of results gained from single pipe moving bed heat transfer measurements

As can be seen in Table 4-5, the heat transfer coefficient of all pipes investigated in this experimental series increases with increasing solids throughput. However, it should be noted that differently to the pipes with 12 mm or 15 mm diameter, a radially uneven temperature of the sorbent was observed at the end of the pipe with a diameter of 21 mm, when the stick out of the temperature probe was varied, which indicates insufficient mixing of particles in the radial direction of the 21 mm pipe and thus less confidence in the determination of the heat transfer coefficient in the current setup.

The representation of the heat transfer coefficient over the solid flux suggests a behaviour, which is less dependent on the pipe diameter, but more on the solid flux in the pipe, which was also observed by Niegsch et al [96]. However, one explanation for the observed behaviour could also be following: The total heat transfer coefficient can be separated in the heat transfer coefficient from wall to the 'first layer' of particles and in a coefficient for heat conduction from the first layer into the moving bed. It is expected that the heat transfer from the wall to the 'first layer' of particles, is always relatively high. But at lower solid flux, the heat conduction into the bed itself limits the achievable total heat transfer coefficient, while it plays a smaller role at higher solid fluxes.

For a heat exchanger set-up as shown in Figure 4-18, where the bulk is flowing in a small channel, the channel width probably is the main influencing parameter, as it directly affects the apparent heat conduction resistance of the bulk. Anyway, for a given sorbent mass flow rate and a given heat exchange surface, a tall and thin heat exchanger with narrow flow channels would be preferable.

Within the tested mass flow range, the sorbent material was flowing smoothly even through the 12mm pipe so that even a further reduction of the pipe diameter seemed possible. This would have the advantage of a reduced specific sorbent inventory and a potential further increase of the heat transfer coefficient.

4.4.4 Basic assessment of moving bed heat exchanger designs

Pillow plate moving bed heat exchanger

Plate heat exchangers are broadly used for gaseous and liquid mediums and offer a very high specific surface area (heat exchange surface per volume) combined with a good scalability.

It is also possible to utilize plate heat exchangers for heat exchange between a gas or a liquid and a bulk material. There the bulk material is transported by gravitation in moving bed regime through the heat exchanger. This kind of heat exchangers are already commonly utilized for various heating/cooling tasks of different bulk materials like oil-seeds, polymers, food products, fertilizers etc. (see Figure 4-20).

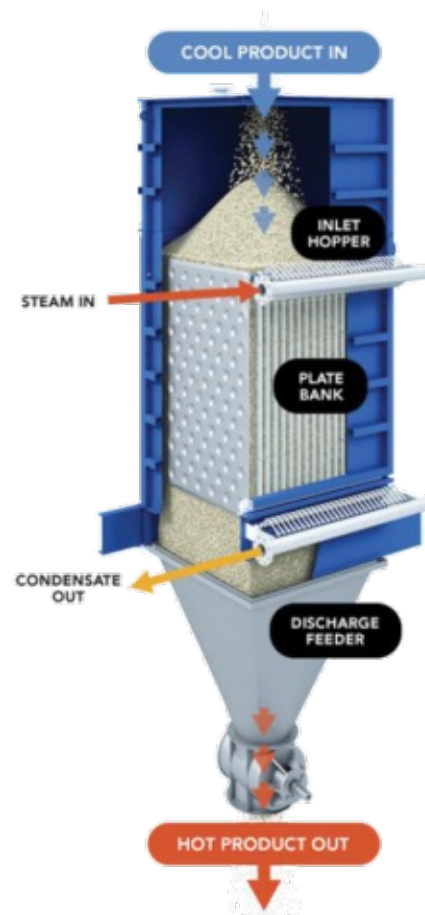


Figure 4-20: Moving bed plate heat exchanger (taken from [97])

Pillow plate heat exchangers are for example utilized in the chemical industry as condensers, where they can be found in a relatively broad range of size.

Furthermore, the pressure design of this equipment might get important at larger scale. In the TSA process, the sorbent side is at very low pressure ($\ll 500$ mbar), while the heating/cooling medium side has to be designed for at least several bar if water is assumed as heating/cooling medium. The pillow plate design allows for scaling without implications on the wall thickness of the plates while the shell of the heat exchanger has to be designed for the sorbent side design pressure only.

Shell & tube moving bed heat exchanger

Other manufacturers in the field of polymer production and further processing offer shell and tube type heat exchangers for application in heating or cooling of bulk materials (see Figure 4-21). Similar to the previously described plate heat exchanger, the bulk material enters the heat exchanger at the top. Then the bulk material flows through the pipes of a bundle from top to bottom by gravitation in moving bed regime. The heating or cooling medium is connected to the shell, which surrounds the pipe bundle. In order to take advantage of the previously discussed increased heat transfer coefficient, the pipes should be rather small in diameter, which also has a positive effect on the specific sorbent inventory of the heat exchanger. On the other hand, with decreasing pipe diameter, the specific material input as well as the effort for welding of the increased quantity of pipes increases.

In contrast to the plate heat exchanger design, the wall thickness of the shell has to be significantly higher because the shell of the heat exchanger has to be designed for the pressure of the heating/cooling medium. For rather small heat exchangers, this design has the advantage of minimum requirements on the machinery of a manufacturer, which might have a positive effect on costs. However, at larger scale this design requires a significantly higher material input, which potentially makes it unattractive for bigger plants.

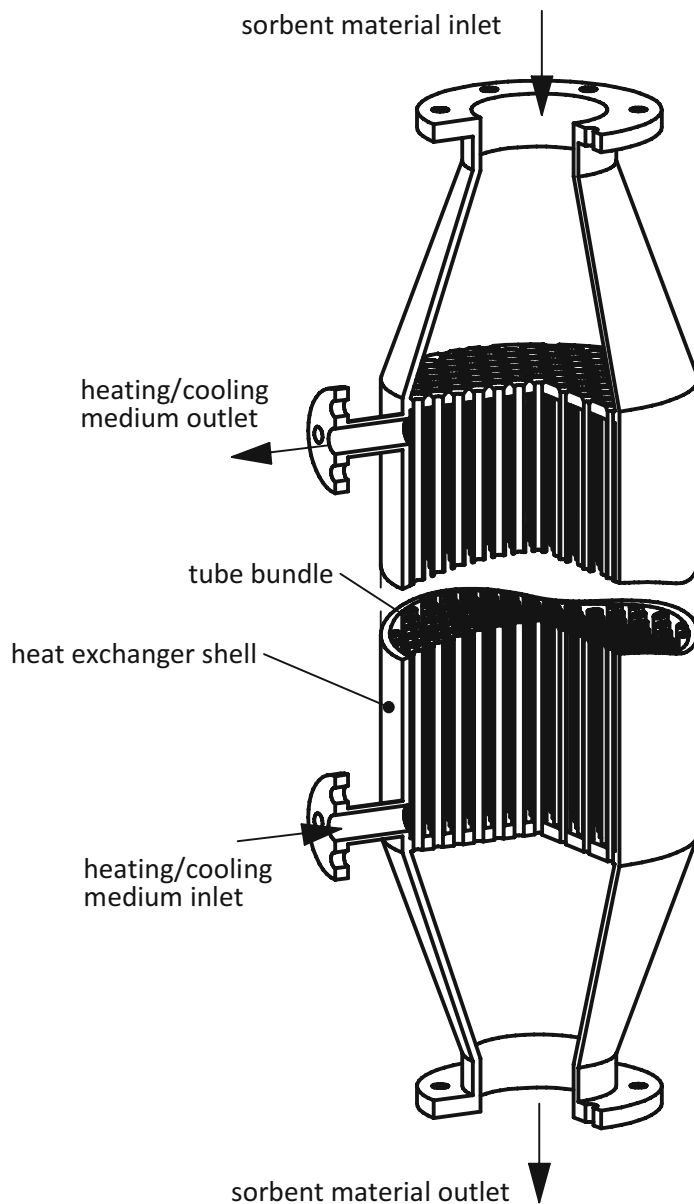


Figure 4-21: Vertical tube bundle moving bed heat exchanger

Finned tube moving bed heat exchanger

Another potential heat exchanger design for moving bed lean/rich heat exchange would be a finned tube bundle heat exchanger (see Figure 4-22). In contrast to the previously discussed shell & tube heat exchanger, the heating/cooling medium would flow through the tube bundle while the sorbent material is again transported by gravitation but through the shell of the heat exchanger where it passes the fins of the tubes. One major advantage of finned tubes is that they are relatively cheap in terms of costs per square meter of heat exchange surface.

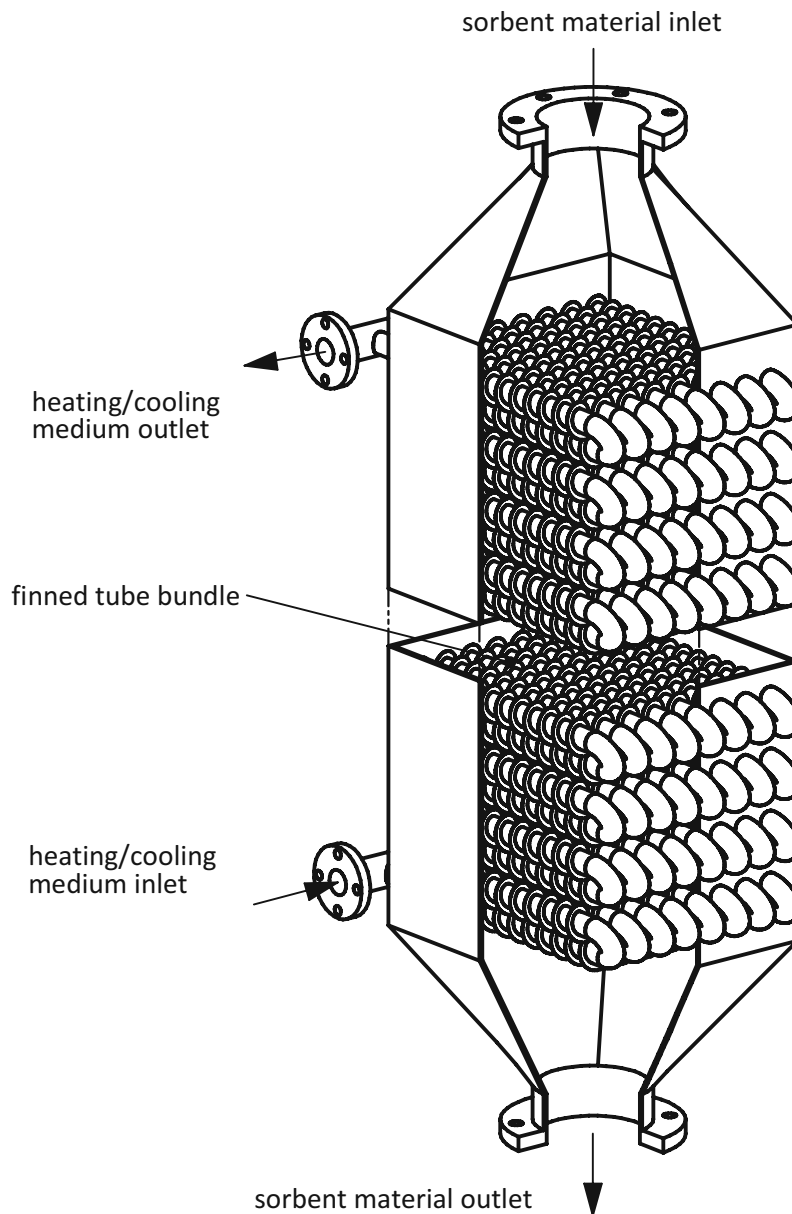


Figure 4-22: Finned tube moving bed heat exchanger

Comparison between different lean/rich heat exchanger designs

At this early stage of development, it is hardly possible to make a reliable assessment of the discussed set-ups, as this requires much more data before the most suitable set-up can be identified. However, even at this early stage some basic statements are possible if the set-ups are compared regarding these key performance indicators:

Specific sorbent inventory: First estimations indicated that the lean/rich heat exchangers most likely have a significant contribution to the total sorbent inventory of the TSA process. The sorbent inventory has a direct impact on the costs for the sorbent material, but on the other hand the sorbent inventory of a specific equipment, also influences the residence time within this equipment. The higher the

residence time is at elevated temperature the more degradation can be expected. Therefore, it is desired to reduce the sorbent inventory as much as possible (see Table 4-6).

Specific heat exchanger weight: At small scale, costs for material are only a minor share of the total costs of an equipment. The costs for machining or welding and engineering are much higher and the complexity of the design itself has the biggest impact on the costs. However, for large-scale applications, there is a relatively good correlation between the weight of an equipment and its manufacturing costs. Thus, it makes sense to assess the different heat exchanger set-ups regarding their specific heat exchanger weight (see Table 4-6).

Specific heat exchanger volume: As the lean/rich heat exchange system for TSA will have a significant impact on the total footprint and total height of the process, it also makes sense to start with a first assessment of the heat exchanger size.

As the different heat exchanger types most likely feature different heat transfer coefficient, the mentioned parameters should be related to the estimated heat transfer coefficient. As a higher heat transfer coefficient would reduce the required surface and thus would also reduce the inventory, weight and volume of the heat exchanger. The basic assessment of moving bed heat transfer coefficients presented in 4.4.3, indicate a correlation between the sorbent flux and the achievable heat transfer coefficient, whereby higher heat transfer coefficients are achieved at a higher flux. However, in practice, the sorbent flux for a fixed amount of heat transfer surface can only be influenced by the aspect ratio of the heat exchanger, while a long heat exchanger with low cross section would be preferred. Since, the whole steel structure of the overall plant is affected by this equipment, there are certain limits for the height of the moving bed heat exchangers. Therefore, for this first comparison, a relatively low solid flux was assumed and a heat transfer coefficient of $30 \text{ W}\cdot\text{m}^{-2}\cdot\text{K}^{-1}$ for all moving bed heat exchangers was chosen. Furthermore, following additional assumptions have been made:

- **Pillow plate moving bed heat exchanger:** A single plate of a pillow plate heat exchanger consists of two metal sheets, which are welded together on the sides and with a certain pattern in the middle of the sheets. After that, the pillows are formed by water under high pressure. With knowledge of the thickness of these metal sheets, the weight per square meter can be calculated easily. A vendor quote for a pillow plate heat exchanger with 50 m^2 considers 1.5 mm as wall thickness for a single sheet. The mean thickness of a single pillow plate was assumed 4.5 mm and the mean gap between two pillow plates was assumed with 5.5 mm, which results in a pitch of 10 mm. The inlet and outlet geometry as well as the weight of the heat exchanger shell was not considered.
- **Shell & tube moving bed heat exchanger:** For this assessment, tubes with an inner diameter of 12 mm and a wall thickness of 1.5 mm have been considered which allows for an estimation of the tube weight per square meter. However, due to a lack of data for the pitch of the tube bundle it was not possible to estimate the heat exchanger volume. Also, the shell and the in- and outlet geometry was not taken into account.

- **Finned tube moving bed heat exchanger:** For the assessment of the finned tube heat exchangers, tubes with 30 mm outer diameter and a wall thickness of 1.5 mm were assumed. In contrast to the other heat exchangers, two different fin geometries have been considered to assess the impact of the fin pitch. The fin cross section was $9 \times 0.4 \text{ mm}^2$ for both, while the quantity of fins per meter was varied from 200 to 300. For the sorbent inventory and heat exchanger volume estimation a triangular pitch of 50 mm was assumed for the tube bundle. The selection of the tubes and the fin geometry is based on a vendor quote for a gas/liquid heat exchanger. Again, only the bundle itself was considered for this estimation.
- Furthermore, a **fluidized bed heat exchanger** was added to this comparison as a reference. For this heat exchanger, a plain tube bundle with 16 mm tubes (outer diameter) and a triangular pitch of 50 mm was considered. The actual heat transfer coefficient of a fluidized bed heat exchanger depends on many parameters. However, for this assessment with the actual sorbent material for the pilot program and low fluidization in bubbling regime, a value of $200 \text{ W} \cdot \text{m}^{-2} \cdot \text{K}^{-1}$ was chosen (calculated maximum acc. to Zabrodsky: $220 \text{ W} \cdot \text{m}^{-2} \cdot \text{K}^{-1}$ [44], see also 4.1.2)

Table 4-6 shows the results of this assessment. Since the heat exchanger performance parameters are not directly comparable due to different heat transfer coefficients the specific representation in Table 4-6 is standardized with the corresponding heat transfer coefficient as well. It can be seen, that without further optimizations the vertical shell and tube heat exchanger design, as well as the pillow plate heat exchanger are showing disadvantages in the specific weight of the heat exchanger. With the assumptions made, only the finned tube heat exchange design would potentially reach as low specific heat exchanger weights as it is expected for a fluidized bed heat exchanger but without the previously discussed drawback of sorbent mixing and without electrical power demand for a blower. Thus, at this stage of development a finned tube heat exchanger was identified to be the most promising design for application in lean/rich heat exchange within the TSA process. Especially with a high quantity of fins per meter, this design would feature a very low specific sorbent inventory and specific heat exchanger weight. However, in order to prove the assumptions made, it is necessary to conduct further tests with the actual geometries.

Table 4-6: comparison of lean/rich heat exchange set-ups

	moving bed plate heat exchanger	vertical shell and tube type heat exchanger	moving bed finned tube heat exchanger 200 fins/m	moving bed finned tube heat exchanger 300 fins/m	fluidized bed heat exchanger
spec. sorbent inventory [$l \cdot m^{-2}$]	2,8	3,0	2,7	1,8	13,5
spec. heat exchanger volume [$l \cdot m^{-2}$]	5	-	4,0	2,9	16,2
spec. weight of heat exchanger [$kg \cdot m^{-2}$]	12	13	3,4	2,7	22,2
heat transfer coefficient [$W \cdot m^{-2} \cdot K^{-1}$]	30	30	30	30	200
spec. sorbent inventory [$l \cdot (kW \cdot K^{-1})^{-1}$]	92	100	91	59	68
spec. weight of heat exch. [$kg \cdot (kW \cdot K^{-1})^{-1}$]	400	439	113	91	111
spec. heat exchanger volume [$l \cdot (kW \cdot K^{-1})^{-1}$]	167	-	134	97	81

4.4.5 Finned tube moving bed heat exchanger tests

Cold flow model tests

As stated above, a finned tube heat exchanger is seen as a promising heat exchanger design for application in lean/rich heat exchange of the TSA process. To prove made assumptions, and to gather experience for designing this equipment at larger scale, it was decided to build two cold flow models with commercially available finned tubes. One heat exchanger model was built with 200 fins per meter (see Figure 4-23) and the other with 300 fins per meter. The fin cross section with $9 \times 0.4 \text{ mm}^2$ as well as the tubes ($D30 \times 1.5 \text{ mm}$) and the bundle pitch were the same for both heat exchangers. Both cold flow models of the heat exchangers have been tested, however the detailed results can be found in a different thesis [89].

The main conclusions of these tests are as follows:

- The fin quantity per meter did not show any impact on the flow distribution through the bundle. Both geometries could be tested successfully in a broad range of solid flux. From a fluid dynamic point of view, the preferred geometry with 300 fins per meter is suitable for the tested sorbent material. Even a further increase of the fin quantity could be possible but was not tested in the scope of this experimental campaign.
- The angle of the outlet cone influences the sorbent flow distribution through the heat exchanger bundle. An outlet cone with 45° was identified as good compromise between sorbent inventory of the cone and a good flow distribution.

- The inlet cone of the heat exchanger is less critical and should be designed in accordance to the angle of repose of the sorbent material.
- Above the tubes a stagnant zone forms, where no sorbent movement was observed. On the one hand, this will most likely reduce the overall heat transfer coefficient of the heat exchanger and needs to be compensated with additional surface and on the other hand, this could also lead to increased thermal degradation of this remaining material.

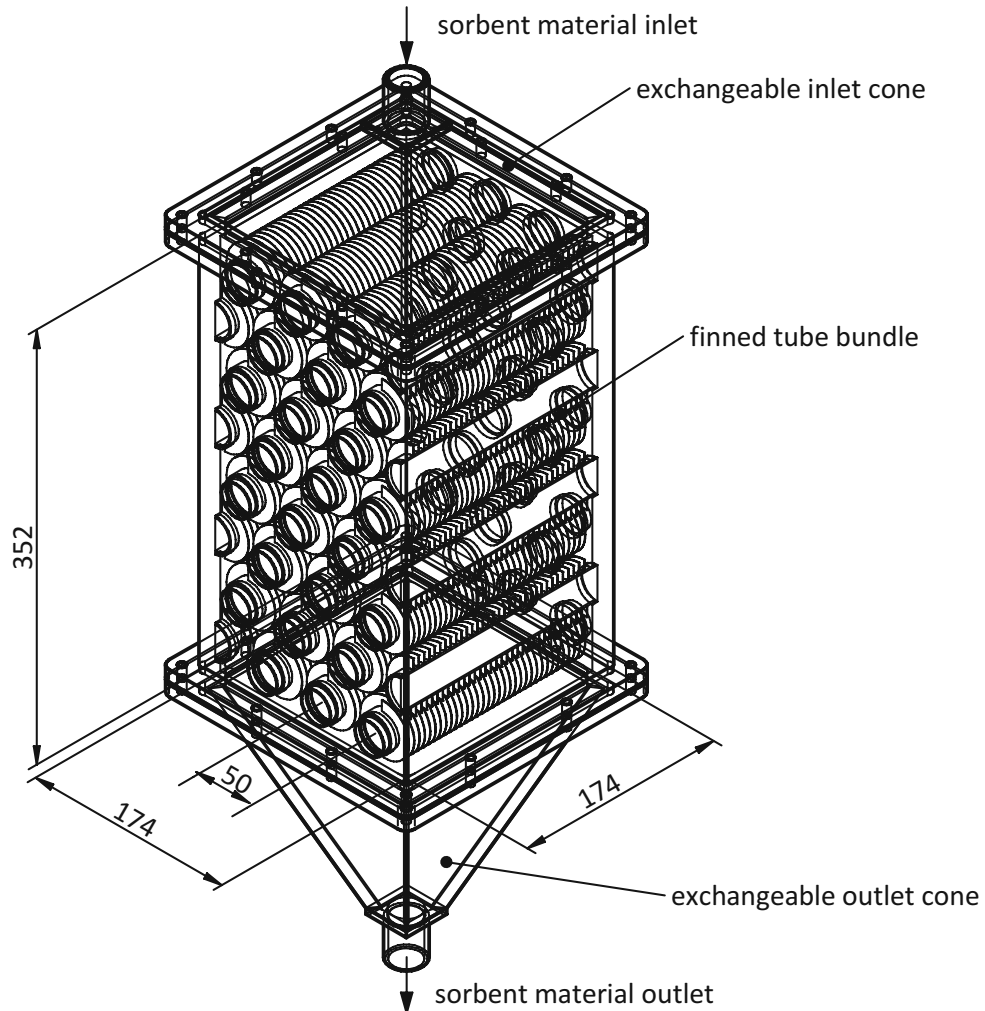


Figure 4-23: Finned tube moving bed heat exchanger cold flow model

Tests within continuous process

As discussed previously, especially the rich heat exchanger of a lean/rich heat exchange system is a critical piece of equipment in a TSA process, as adsorption and desorption activities might influence the performance of the heat exchanger. Therefore, 2 different finned tube heat exchangers with approximately equal heat exchange surface but different fin geometry have been designed and integrated in the TSA bench scale unit. To allow for independent control of temperatures at lean and rich sorbent side, no actual lean/rich heat exchange was realized. Instead of a heat carrier medium connecting the two heat exchangers, only a simulated heat exchange via independent cooling a heating media was established. Continuous tests within the bench scale unit could not confirm the expected

heat transfer coefficient of $30 \text{ W}\cdot\text{m}^{-2}\cdot\text{K}^{-1}$. The lean heat exchanger reached heat transfer coefficients in the range of $13\text{-}18 \text{ W}\cdot\text{m}^{-2}\cdot\text{K}^{-1}$, while the rich heat exchanger showed even lower results ($7 \text{ W}\cdot\text{m}^{-2}\cdot\text{K}^{-1}$). The experimental set-up as well as results and conclusions in detail are presented in [66].

Since a commercially available finned tube geometry was selected and the available height for installation of the heat exchangers in the bench scale unit was limited, the resulting aspect ratio of the heat exchanger was not optimal. This resulted in rather low sorbent fluxes which could explain the low heat transfer coefficients. A reason for the difference between rich and lean heat exchanger could be desorption activity observed during heat up in the rich heat exchanger. Depending on the operating temperature of the rich heat exchanger, it was observed that significant amounts of gas are released which can have a negative effect on the controllability of the L-valve or can lead to blockages of the rich standpipe.

Although, the heat transfer coefficient was below expectations, the tests were successful in terms of general operability of the heat exchangers and control of sorbent temperature. It has been proven, that a finned tube moving bed heat exchanger is suitable for lean/rich heat exchange within the TSA process. However, some open questions still have to be answered, before a more detailed assessment can be done to finally compare capital expenses and operational expenses with the actual heat recovery. This comparison will finally trigger the decision, if such a lean/rich heat exchange system is realized or not in potential large scale applications. Within the pilot program a lean/rich heat exchange system with finned tube moving bed heat exchangers will be demonstrated. This will deliver precious experience in operating these heat exchangers. But in order to maximize the scientific output of the pilot program it is important to design the system in a way that it can be operated flexible and that it allows to answer critical questions like the following:

- Is there a parasitic load on the rich heat exchanger due to CO_2 and/or H_2O adsorption/desorption activities and how can it be avoided?
- What is the influence of the rich heat exchanger on the gas sealing between adsorber and desorber?
- How does the rich heat exchanger influence the L-valve operation and is it possible to decouple the L-valve transport rate from the heat exchanger gas release?
- Confirmation of the expected increase of the heat transfer coefficient at higher solid flux.
- Is it possible to operate the lean heat exchanger without running into condensation issues?

Although, these questions cannot be answered in the scope of this thesis, the pilot unit equipment and instrumentation needs to allow for an assessment for upcoming investigations.

5. PILOT UNIT REACTOR DESIGN

5.1 GENERAL PROCESS SET-UP AND KEY FIGURES

As indicated before, the design of the pilot plant is not just a result of a capture performance maximization. It is still a research plant which is primarily intended for technology development. Therefore, compared to a commercial plant many design aspects might be solved differently.

Based on the design philosophy (see chapter 4) and the design basis for the pilot unit (see chapter 3), a process set-up was elaborated. Until the final version was found, countless changes of the piping and instrumentation diagrams were necessary to account for all requirements on the pilot unit. Figure 5-1 shows a simplified process scheme which represents a major outcome from various investigations made in the scope of the whole project. For better overview, equipment like auxiliary heat exchangers and instrumentation are not indicated. In contrast to the piping and instrumentation diagrams which can be found in Appendix A, only the main process equipment is shown in Figure 5-1.

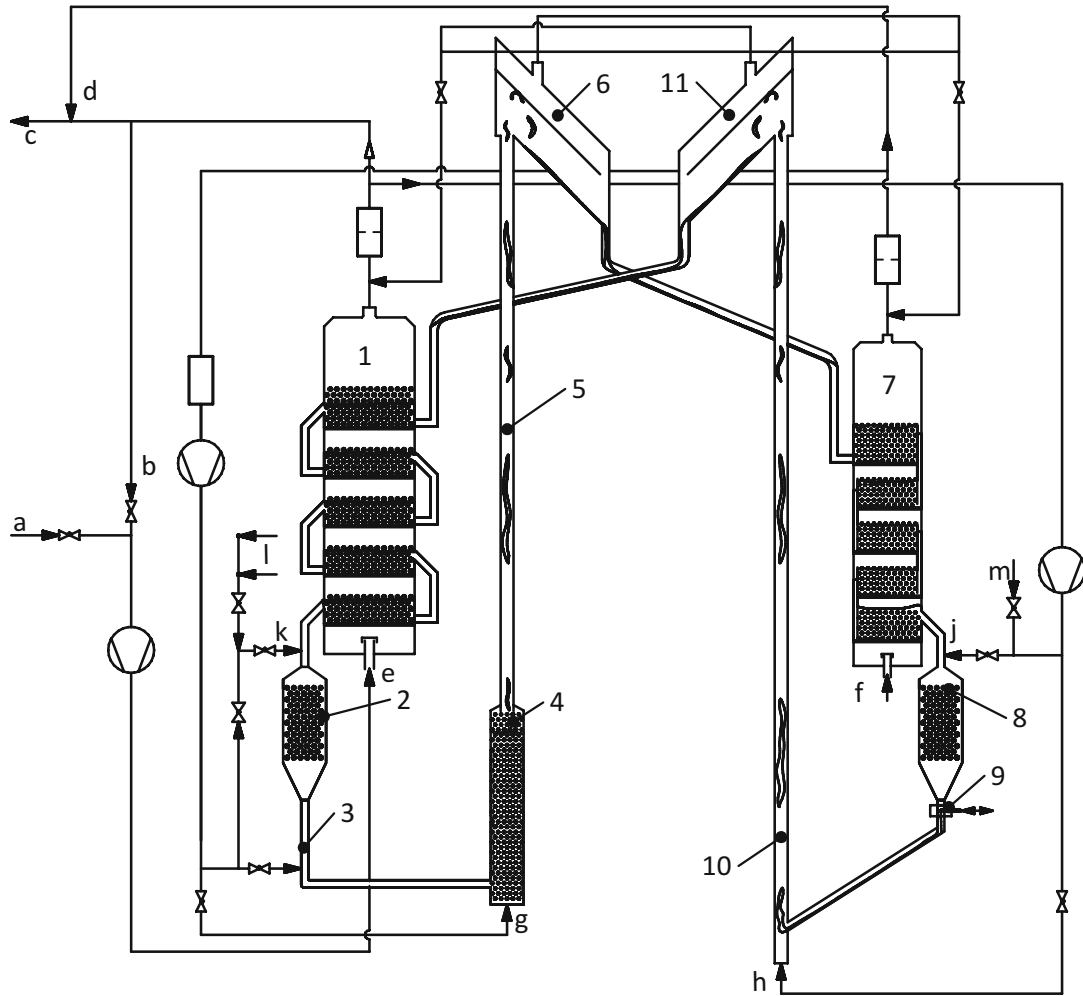
The process set-up consists of two fluidized bed columns (adsorber (1) and desorber (7)) with five stages each. Each stage features a gas-distributor, a stage heat exchanger and a downcomer. In contrast to the adsorber which features actively controlled external downcomers, the top to bottom transport of sorbent in the desorber is established with internal (self-aerated) downcomers. After loading of the sorbent within the adsorber, the sorbent is flowing through the rich heat exchanger (2), which simulates a partial heat recovery from the lean side by heating the sorbent with steam. On the rich sorbent side, an L-valve (3) is used to control the sorbent flow from the rich heat exchanger towards the pre-regenerator (4). The pre-regenerator is a bubbling fluidized bed heat exchanger operated with steam as heating medium, where the sorbent is further heated and partially regenerated. At the top of the pre-regenerator the smaller cross section of the rich riser leads to pneumatic transport (5) of the sorbent towards the rich particle separator (6). There, the sorbent is separated from the gas and enters the uppermost stage of the desorber. The desorber (7) is fluidized with steam (f), which promotes regeneration of the sorbent by reducing the partial pressure of CO₂. At the bottom stage of the desorber, the lean sorbent is extracted and directed to the lean heat exchanger (8). For independent tests, an actual lean/rich heat exchange is not realized but can be simulated by adjusting the cooling water flow to the lean heat exchanger or the steam flow to the rich heat exchanger (2). In contrast to the L-valve on the rich sorbent side, the lean sorbent flow is controlled via a mechanical slide valve (9). Since cooling of the lean sorbent requires only removal of sensible heat (on the rich side sensible and latent heat is provided), the lean heat exchanger is able to cool the sorbent sufficiently so that it can be directed right into the transport section of the lean riser (10). After separation of gas and solids in the lean particle separator, the sorbent cycle is closed, when the sorbent enters the fifth stage of the adsorber. In order to be flexible in terms of CO₂ concentration at the adsorber feed (e), raw flue gas from the host site (a) is mixed with a slip stream of cleaned flue gas which is recycled (b). The desorber off gas, which mainly consists of steam and CO₂ is cooled, separated from condensate and directed back to the host site (d, c). Table 5-1 summarizes the most important key figures for 3 different load cases, which are used for the pilot unit design. As defined in the capture task (see 3.7.4), the pilot unit design CO₂ capture capacity is 1t/day at a feed concentration of 4 Vol-% CO₂. The target operating temperature of the adsorber is 50 °C, while the desorber shall be operated

at 115 °C. Especially for the desorber temperature, strong effects on co-adsorption are expected. Since the uptake and release of water on the sorbent depends on the relative humidity (see also [71]), small variations of the temperature of the desorber which is operated with steam, potentially has a strong effect on the net water transport between adsorber and desorber. Therefore, a potential deviation of the desorber temperature in order to optimize the process in terms of water transport should be assessed in the upcoming experiments.

Contrary to reported heat capacities of $1.58 \text{ kJ}\cdot\text{kg}^{-1}\cdot\text{K}^{-1}$ [50] and $1.5 \text{ kJ}\cdot\text{kg}^{-1}\cdot\text{K}^{-1}$ [71], a heat capacity of $2.25 \text{ kJ}\cdot\text{kg}^{-1}\cdot\text{K}^{-1}$ was used for the design of the pilot unit. This is explained, by the expected average water and CO_2 content of the sorbent, which increases the apparent heat capacity. Also, the bulk density of $550 \text{ kg}\cdot\text{m}^{-3}$ is a value, which takes the H_2O and CO_2 content into account. By directly measuring the bulk density of rich sorbent from bench scale experiments a realistic value was derived. The adsorption enthalpies given in Table 5-1 have been derived from TGA tests with the sorbent material.

Beside fluid-dynamic investigations ([89], [98]) on downcomer, bed expansion, gas distributors, pressure profiles and more, extensive process modelling with a simulation tool which was elaborated and refined ([72], [78]), as well as a large number of experiments with the existing bench scale unit ([37], [38], [66], [99]) had a big impact on these process schemes. Furthermore, extensive investigations on heat transfer ([86]–[88], [90]) enabled to solve the iterative task of fitting sufficient heat transfer surface in a column without knowing the impact on the fluid-dynamics.

Within this chapter, some of the crosslinks between these detailed studies are explained and the final pilot unit design is elaborated.



- | | | | |
|---|-------------------------|----|-------------------------|
| 1 | adsorber | 7 | desorber |
| 2 | rich heat exchanger | 8 | lean heat exchanger |
| 3 | L-valve | 9 | slide valve |
| 4 | pre-regenerator | 10 | lean transport riser |
| 5 | rich transport riser | 11 | lean particle separator |
| 6 | rich particle separator | | |

Figure 5-1: Final ViennaGreenCO₂ process scheme (simplified)

Table 5-1: Main operating figures

Load cases	Low load	Design load	High load	Unit
CO₂ capture target				
CO ₂ capture capacity	29.6 (0.7)	41.7 (1.0)	59.5 (1.4)	kg·h ⁻¹ (t·day ⁻¹)
target CO ₂ capture efficiency	90			%
CO ₂ feed concentration	4.0			%-Vol.
operating gas velocity in adsorber inlet	0.52	0.73	1.04	m·s ⁻¹
specific stripping steam feeding rate	0.42	0.3	0.3	kg·kg _{CO₂,capt} ⁻¹
lean sorbent circulation rate	393	591	845	kg·h ⁻¹
TSA operation				
adsorber operating temperature	50			°C
desorber operating temperature	115			°C
pre-desorber operating temperature	115			°C
adsorbent properties				
adsorbent type	Lewatit VP OC 1065			
adsorbent size (Sauter diameter)	676			µm
adsorbent bulk density (BSU samples)	550			kg·m ⁻³
assumed fixed bed voidage	0.43			-
derived particle density	965			kg·m ⁻³
heat capacity (conservative design value)	2.25			kJ (kg·K) ⁻¹
CO ₂ adsorption enthalpy @ 50°C (adsorber)	-75.92			kJ mol ⁻¹
CO ₂ adsorption enthalpy @ 115°C (desorber)	-95.00			kJ mol ⁻¹
utilities				
steam feed saturation pressure	4.2	4.2	4.7	bar(a)
steam feed saturation temperature	145	145	149	°C
assumed internal CW temperature in ADS	32	32	34	°C

5.2 ADSORBER COLUMN

The major aim for the adsorber column design was the maximization of the adsorber gas velocity without facing limitations in mass transfer, heat transfer, or in the fluid-dynamic design of the reactor. If a fixed CO₂ feed concentration is assumed, the gas velocity is proportional to the heat exchange load of the adsorber stages. Therefore, a higher gas velocity would require more heat exchange surface (if the effect on the heat transfer coefficient is neglected). By several iterations with simulation data for the heat exchanger load, experimental data for bed expansion and the heat transfer coefficient, as well as experimental data from bench scale unit operation a superficial design load gas velocity of around 0.7 m·s⁻¹ was defined. Furthermore, a high load case with a superficial gas velocity of 1 m·s⁻¹ was defined. For this load case, potential mass transfer limitations can occur since bench scale unit operation was not possible at this velocity and the respective operating experience and data is lacking. However, the fluid dynamic design as well as the heat exchanger design of the whole plant was

adopted for this high load case. Future experiments will help to identify and assess potential limitations at high load.

Important fluid-dynamic figures and the adsorber main dimensions are summarized in Table 5-2. A cold flow model of the adsorber enabled direct investigation of bed expansion at different velocities under the influence of the heat exchange bundle. From these tests results for the specific pressure drop, bed height, inventory and others have been derived. Since the specific pressure drop at high load is significantly lower, the same inventory results in more fluidized bed height. However, the design of the adsorber allows for a variation of the inventory per stage. In upcoming experiments, this influence shall be assessed in order to define the required inventories for both load cases.

The freeboard height is a result of two considerations. At the one hand, entrainment to the subsequent stage or entrainment from the top stage to the off-gas line should be avoided, whereby slight entrainment from stage to stage is less critical. On the other hand, there is a minimum standpipe height for the external downcomers. Since the downcomer approximately needs to balance the pressure drop of two fluidized beds and the gas distributor, the minimum filling level of the downcomer standpipe is calculated by the quotient of the pressure difference between downcomer inlet and outlet and the maximal allowable specific pressure drop per meter of the moving bed, which is less or equal to the specific pressure drop per meter at minimum fluidization conditions (approx. 54mbar). The freeboard height given in Table 5-2 provides sufficient margin for both criteria.

Stages 2-5 have been equipped with perforated plates (1033 holes with $\varnothing 4.5$ mm) as gas distributor, which results in a relative pressure drop in the range of 10-20 % of bed pressure drop, depending on load case. The design is a tradeoff between maximum pressure drop at high load and sufficient gas distribution at start-up and potential low load cases. Since the holes are several times bigger than the mean particle size, the sorbent is weeping through the distributor during a shutdown. This behavior is intended for emptying reasons. However, a weeping gas distributor at the bottom stage would fill the wind box with sorbent which is an issue. Therefore, stage 1 is equipped with a non-weeping distributor with 169 Tuyere nozzles with 6 ($\varnothing 4.5$ mm) holes each. Details on the adsorber gas distributor design are summarized in the work of Zehetner [89].

Table 5-2: Fluid-dynamic key figures and main dimensions of the adsorber column

	Design load	High load	Unit
fluid-dynamics			
minimum fluidization velocity (calculated acc.to Grace [100])	0.16	0.16	m·s ⁻¹
fluidization number (empty column)	4.6	6.6	-
superficial gas velocity (adsorber feed)	0.73	1.04	m·s ⁻¹
main dimensions column			
cross section of empty column	0.26		m ²
side length of quadratic column cross section	0.513		m
average bed height in stages	0.25	0.3	m
average freeboard height per stage	0.55	0.5	m
total height of adsorber column (incl. windbox and extended freeboard in top stage)	5.4		m
pressure drop			
specific solid pressure drop	30.1	22.5	mbar·m _{bed} ⁻¹
gas distributor pressure drop	1.05	2.11	mbar
total pressure drop over column	42.9	44.3	mbar
total inventory	~100		kg

With the total cooling demand derived from process simulation, the required heat transfer surface can be calculated. For this calculation, the average heat transfer coefficient derived from dedicated tests (see 4.1.2) were used (see Table 5-3). In combination with the fluid-dynamic design tasks, a heat exchange bundle geometry that provides sufficient heat exchange surface within the dense phase of the fluidized beds was derived (see Table 5-4). As can be seen, the heat exchange surface was not evenly distributed to the 5 stages. The reason for that is, that according to the process simulation, the cooling duty of the uppermost stage is higher compared to the other stages, since remaining sensible heat needs to be extracted to reach the desired operating temperature of the adsorber.

The design of the adsorber is presented in Figure 5-2. As mentioned previously, the adsorber design features external downcomer with active aeration to control the sorbent flow from stage to stage. In order to avoid overflowing or emptying of stages, it is important to have good control of the sorbent flow in the downcomer. Several different downcomer geometries have been tested in a cold flow model [98] and an externally aerated downcomer with an inner diameter of 54.5 mm was selected finally. The required gas flow to achieve the desired sorbent flow for design and high load was estimated between 1.5 and 2.1 m³·h⁻¹ (see Table 5-5). The additional benefit of an externally aerated downcomer is the possibility to actively control the inventory. Thus, the adsorber design, principally allows for variation of the total inventory or as well for inventory shifts between the stages. The extraction height of the downcomer is chosen in a way, that a minimum inventory is maintained also when the incoming flow of sorbent to the stage is lower than the theoretically outgoing flow of sorbent. Since the downcomer inlet seemed to limit the overall transport in some cold flow experiments, a cone was attached to the downcomer top, providing a larger cross section for the

sorbent to flow into the downcomer. The height, at which the downcomer introduces the sorbent into the stage on the other hand was chosen relatively low to avoid bypasses of the sorbent. For start-up reasons, a ball valve is installed in the downcomer standpipe to avoid a gas bypass over the downcomer when it is not filled with sorbent material.

Table 5-3: Required heat transfer surface in adsorber

	Design load	High load	Unit
heat transfer			
total cooling requirement (from process simulation)	29.9	42.7	kW
measured average heat transfer rate	203		W·(m ² ·K) ⁻¹
assumed stage HEX wall temperature	32.0	34.0	°C
minimum total heat transfer surface area	8.18	13.14	m ²

Table 5-4: Adsorber heat exchanger design

	Stages 1-4	Stage 5	Unit
stage heat exchanger dimensions			
single tube outer diameter	20.0	20.0	mm
triangular pitch in tube bundle	50.0	50.0	mm
number of tubes per HEX	80	100	-
number of vertical tube rows in bundle	8	10	-
HEX surface per stage	2.58	3.22	m ²
total available heat transfer surface area	13.54		m ²

Table 5-5: Adsorber downcomer design

	Design load	High load	Unit
dimensions			
vertical standpipe inner diameter	54.5		mm
vertical standpipe height	929		mm
horizontal pipe inner diameter	54.5		mm
horizontal pipe length	125		mm
estimated aeration gas flow per L-valve ⁽²⁾	1.5	2.1	m ³ ·h ⁻¹

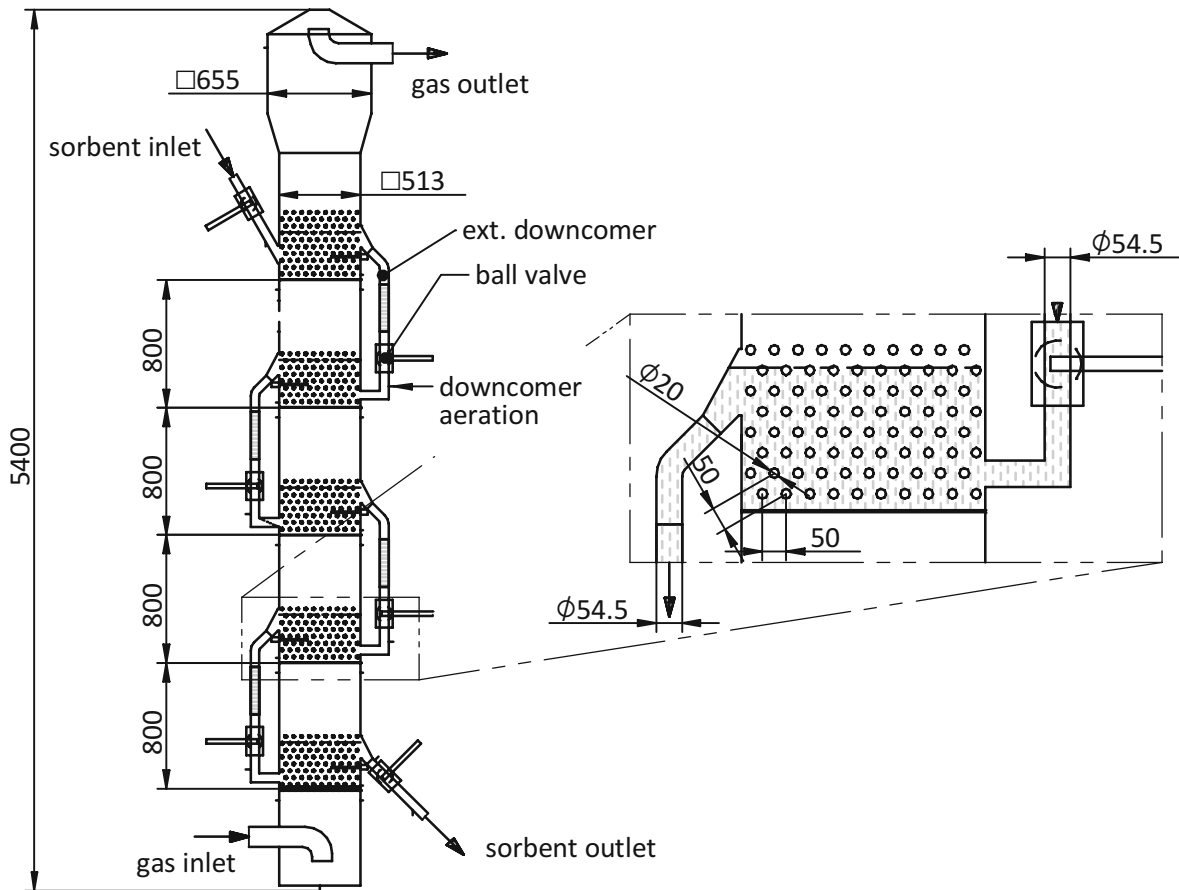


Figure 5-2: Adsorber design

5.3 DESORBER COLUMN

A maximization of the gas throughput at preferably low differential pressure, resulted in (relatively) wide and shallow beds for the adsorber. As can be seen in Figure 5-3, the design of the desorber column deviates strongly from the adsorber design. While the adsorber is designed for a maximization of the gas throughput, the desorber is designed for a certain stripping steam feed rate, which shall represent the optimum from a thermodynamic point of view (see 4.1.4). A parameter variation with the process simulation tool indicated a thermodynamically optimum specific stripping steam flow rate of approximately 0.5 kilogram per kilogram of released CO_2 . However, as design basis a slightly lower value of $0.3 \text{ kg} \cdot \text{kg}_{\text{CO}_2}^{-1}$ was chosen to account for uncertainties (see Table 5-1) and to make sure, that the pilot unit can also be operated below the calculated optimum. At the same time, the pilot unit is designed to allow for broad variation to higher values of the specific stripping steam rate. This very important process parameter has a huge impact on the desorber design. At one hand, the estimated thermodynamically optimum feed rate requires a rather small cross section of the desorber to achieve minimum fluidization condition at all, and on the other hand it results in a high flow gradient over the height of the desorber, due to the amount of CO_2 that is released. If co-adsorption effects are neglected, the flow at the top stage of the column (with released CO_2) would be more than 4 times higher, than at the bottom stage.

Another problem that comes with this low specific stripping steam rate is the limited space in the fluidized bed for heat exchange. The heat required for regeneration of the material is roughly in the same range as the cooling duty in the adsorber. However, since the cross section of the desorber is only a fraction of the cross section of the adsorber, a different strategy to provide this heat needs to be found.

In total, three independent measures have been applied to ensure sufficient heat transfer to regenerate the sorbent:

One way to partially compensate the lower cross section is to design **deeper fluidized beds**. Deeper fluidized beds result in an increased pressure drop over the desorber. This would at least not be an issue for the steam supply, but there are certain limits on the fluid-dynamic design of the desorber. More and more pressure drop over the beds can hinder the transport within the internal downcomers but also complicates the gas sealing between the two columns. In the fluid dynamic design of the downcomers, the increased pressure difference from stage to stage needs to be compensated by sufficient downcomer height (see also adsorber downcomer and freeboard design in section 5.2), Especially at small scale, the small cross section and high height of the downcomer can easily lead to slugging if bubble formation occurs in the downcomer, which would lead to partial blockages and a potential blow out of the downcomers.

A **narrower heat exchange bundle** was selected, which has a higher specific heat exchange surface per bed volume. Furthermore, the desorber is operated at very low gas velocity. A narrower heat exchange bundle increases the local gas velocity within the bundle and can help to improve the fluidization behavior.

Since a rich riser set-up was selected, where released gas in the rich riser is combined with the desorber off-gas anyway, one reasonable way to reduce the load on the desorber is to further heat up and to pre-regenerate the material within the riser. With this measure, **latent and sensible heating load was partially shifted** to the pre-regenerator (see 5.4)

As indicated in Table 5-6, the cross section of the bottom stage of the desorber, was finally selected $150 \times 150 \text{ mm}^2$ which results in a fluidization number of 1.1 just above the first gas distributor of the desorber (CO_2 release and co-adsorption of water is neglected). Over the height of the stages the regeneration of the sorbent causes more and more gas flow. This increase of gas flow was partially compensated with an increasing cross section. However, a trade-off between start-up behavior when almost no gas is released and operation at design or high load when the gas flow potentially quadruples limited this increase of the cross section. Therefore, the fluidization number within the desorber is expected to increase significantly at design or high load over the height of the desorber. For simplicity, an average fluidization number for stage 2-5 was derived (see Table 5-6).

Due to lacking data and confidence, the effect of co-adsorption was not fully considered for the fluid-dynamic design of the desorber. Thus, Table 5-6 represents only the steam flow rate, which is supposed to be available for fluidization purpose. The amount of steam that gets adsorbed by the sorbent needs to be compensated by a higher flow rate of steam. In order to allow for detailed studies on co-

adsorption within the continuous CO₂ capture process, the auxiliary equipment like flow meters, steam supply valves, CO₂ condenser, flue gas condenser are specified with a broad operating range, which shall enable dedicated parameter variations. As mentioned previously, getting a deeper understanding of water co-adsorption is a major goal of the ViennaGreenCO₂ project.

In contrast to the adsorber, the desorber features internal downcomers, which are shown in Figure 5-3. The sorbent material flows over the weir into the downcomer. Depending on the stage pressure drop and the sorbent circulation rate, a certain filling level is established within the downcomer that operates in a moving bed regime in stable operating conditions. Besides a moving bed regime with a stable filling level within the downcomer, also flooding or slugging behavior of the downcomer was observed in a cold flow study [89]. The transport behavior of the downcomer can be significantly affected by the gas distribution below the downcomer. Therefore, the desorber features exchangeable perforated plate gas distributors with a hole pattern, that has been derived from cold flow tests. Furthermore, the freeboard height is a result from the downcomer tests at cold flow as well, since a stability criterion for the moving bed downcomer is, that the filling level of the downcomer stays below the weir. From entrainment point of view, less freeboard height would be sufficient, but the freeboard was chosen with sufficient margin to the maximum filling level of the downcomer observed in the cold flow study.

Table 5-6: Fluid-dynamic key figures and dimensions of desorber column

	design load	high load	unit
fluid-dynamics			
operating gas flow rate (stripping steam feed)	20.8	29.7	m ³ ·h ⁻¹
weighted mean operating gas flow rate ⁽¹⁾	30.4	43.7	m ³ ·h ⁻¹
minimum fluidization velocity (calculated)	0.22	0.22	m·s ⁻¹
fluidization number (stage 1)	1.1	1.6	-
fluidization number (stage 2-5/mean)	1.6	2.3	-
weighted mean gas velocity in desorber	0.33	0.47	m·s ⁻¹
column main dimensions			
total average bed height per stage (stage 1-4)	0.45		m
total average bed height per stage (stage 5)	0.5		m
cross section of empty column (stage 1)	0.0225		m ²
side length of quadratic stage 1 cross section	0.15		m
cross section of empty column (stage 2-4)	0.0255		m ²
width of desorber stages 2-4	0.17		m
depth of desorber stages 2-4 (=tube length)	0.15		m
cross section of empty column (stage 5)	0.027		m ²
width of desorber stages 5	0.18		m
depth of desorber stages 5 (=tube length)	0.15		m
freeboard height in stages 1-4	0.45		m
freeboard height in stage 5	0.5		m
total height of desorber column (incl. windbox and extended freeboard in top stage)	5.17		m
pressure drop			
stage pressure drop incl. gas distributor	26.6	28.0	mbar
total pressure drop over column	133.0	140.0	mbar
total inventory	~28		kg

⁽¹⁾ Gas flow rate excludes adsorption of steam but considers desorption of CO₂ and is weighted by heat released per stage (according to process simulation)

In accordance with the adsorber, the desorber heating duty was derived from process modelling and the required heat exchange surface was determined. To avoid thermal degradation of the sorbent material, the steam condensation temperature was limited to 149 °C by reducing the main steam supply pressure. Since the inner heat transfer coefficient (steam to pipe) and heat conduction in the wall thickness of the pipe plays only a minor role in total heat transfer, its contribution was neglected. Since the material is brought to desorber operating temperature already in the pre-regenerator where it is also partially regenerated, the load on the desorber is strongly reduced (see Table 5-7). Table 5-8 summarizes results of the heat exchanger design calculations.

Table 5-7: Required heat transfer surface in desorber column

	design load	high load	unit
heat transfer			
total heating requirement	11.9	17.4	kW
maximum heat transfer rate (Zabrodsky)	220	220	$W \cdot (m^2 \cdot K)^{-1}$
measured average heat transfer rate	188	200	$W \cdot (m^2 \cdot K)^{-1}$
assumed stage HEX wall temperature	145.0	149.0	$^{\circ}C$
minimum total heat transfer surface area	2.11	2.56	m^2

Table 5-8: Desorber heat exchanger design

	stage 1	stages 2-4	stage 5	unit
stage heat exchanger dimensions				
single tube outer diameter	16.0			mm
triangular pitch in tube bundle	30.0			mm
number of tubes per HEX	80	80	110	-
number of vertical tube rows in bundle	20	20	22	-
HEX surface per stage	0.60	0.60	0.83	m^2
total available heat transfer surface area	3.24			m^2

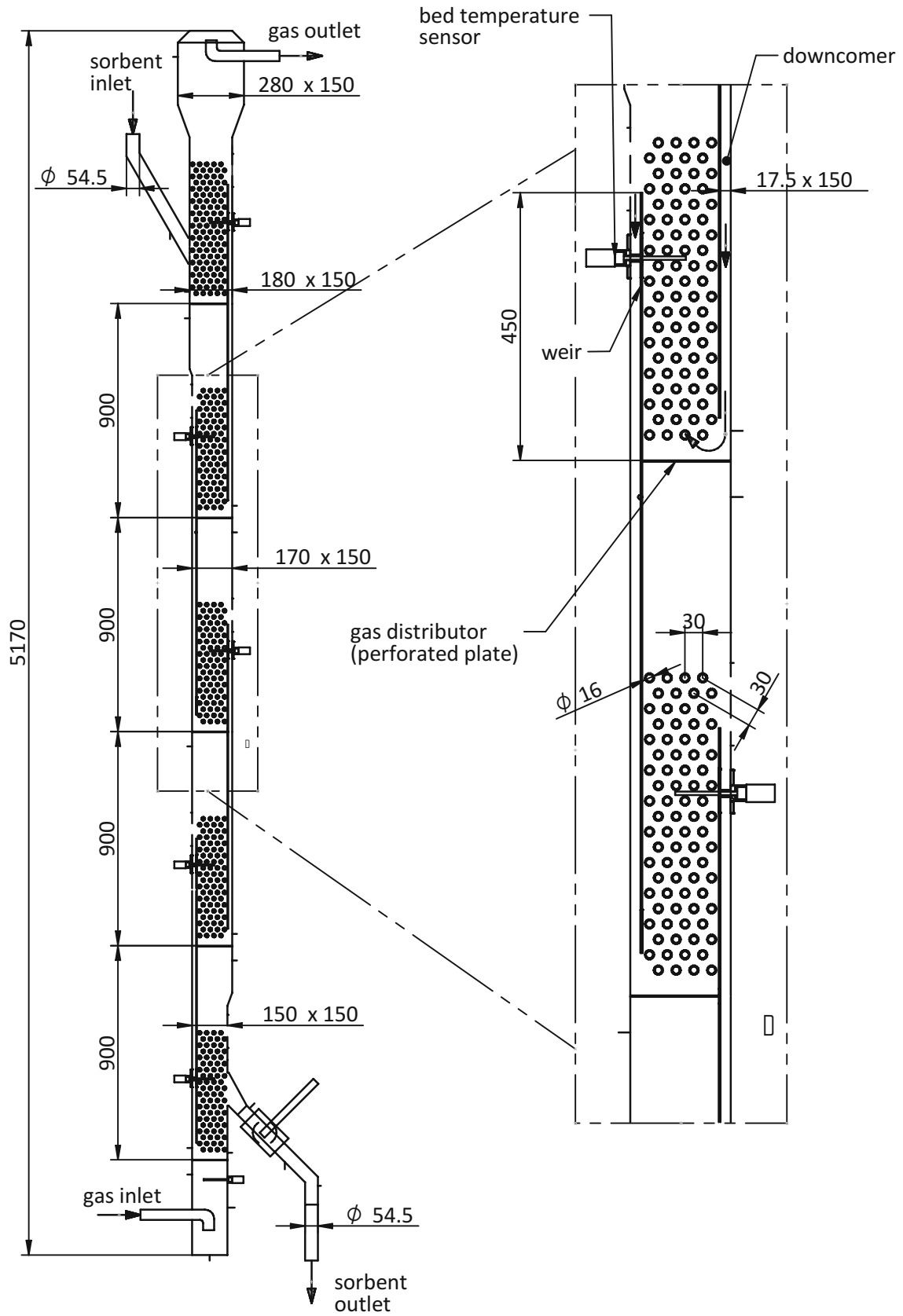


Figure 5-3: Desorber design

5.4 LEAN/RICH HEAT EXCHANGE

It was decided to implement moving bed heat exchangers on the rich and lean sorbent outlet of the two main columns (see considerations in 4.4). Both heat exchangers are shell and tube bundle heat exchangers with horizontal tubes with fins. The sorbent side design of both heat exchangers is identical.

An actual indirect heat exchange between both heat exchangers, as it would be required for heat recovery, was not realized. In order to increase flexibility for the planned experiments, the lean heat exchanger is independently cooled with an internal cooling water loop, which ensures precise flow and temperature of cooling water, while the rich heat exchanger is operated with steam.

By setting the heating and cooling load accordingly, lean/rich heat exchange can be simulated. But for dedicated experiments, it is possible to investigate the heat exchanger performance independently.

As highlighted in section 4.4, a tall heat exchanger with low cross section (and subsequently high solid flux) is expected to deliver better performance compared to a heat exchanger with the same heat exchange surface but less height and more cross section. The ViennaGreenCO₂ lean/rich heat exchanger design is a trade-off between many aspects. But especially the total height of the plant is a limiting factor for lean and rich heat exchanger. Table 5-9 and Table 5-10 summarize the most important design parameters for the two heat exchangers.

Table 5-9: Lean heat exchanger design

	design load	high load	unit
required heat exchanger surface area			
cooling medium	internal cooling water at 20 °C		
inlet adsorbent temperature	115.0	115.0	°C
outlet adsorbent temperature	76.0	76.0	°C
cooling demand	14.6	20.8	kW
assumed heat transfer coefficient	30	30	W·(m ² ·K) ⁻¹
required heat transfer surface area	7.3	10.6	m ²
dimensions and operating parameters (for tested 300FPM finned tubes)			
plane tube outer diameter (w/o fins)	30.0		mm
fin dimensions (height x thickness)	9.0 x 0.4		mm
specific finned tube surface area	0.76		m ² ·m ⁻¹
heat exchanger width	0.325		m
heat exchanger length (=active tube length)	0.325		m
solid flux through open HEX cross section	3.6	5.2	kg·(m ² ·s) ⁻¹
number of finned tubes per horizontal layer	6		-
number of horizontal tube layer	12		-
provided total heat transfer surface area	17.7		m ²
total height of heat exchanger	0.994		m
estimated total adsorbent inventory	~33		kg

Table 5-10: Rich heat exchanger design

	design load	high load	unit
required heat exchanger surface area			
heating medium	saturated steam at 149 °C max.		
inlet adsorbent temperature	50.0	50.0	°C
outlet adsorbent temperature	90.0	90.0	°C
heating demand	14.9	21.3	kW
assumed heat transfer coefficient	30	30	W·(m ² ·K) ⁻¹
required heat transfer surface area	6.8	9.2	m ²

5.5 PRE-REGENERATOR AND RICH RISER

With the previously discussed shift of load from the desorber to the pre-regenerator, a new sorbent regeneration strategy was created. While the desorber can be seen as a counter current flow stripping zone, where the stripping gas steam is utilized to achieve deep regeneration, the pre-regenerator fluidization gas flow rate is uncoupled from the stripping gas flow rate of the desorber, which allows for a different fluid-dynamic design and more bed volume for installation of heat transfer surface. The pre-regenerator is mainly operated with the gas that is released by the sorbent. Thus, a gas mixture containing H₂O and CO₂ (and traces of other species) will be formed. Although, a partial regeneration of the sorbent is possible even in pure CO₂ atmosphere, any dilution with steam and subsequent reduction of the partial pressure of CO₂ helps to regenerate the sorbent deeper. Therefore, it makes sense, not to recycle the rich riser gas directly but to recycle gas from the desorber off gas line which was foreseen in the ViennaGreenCO₂ process set-up (see Figure 5-1) and represents one of the major changes to the process set-up introduced by Pröll et. al [36] (see also 2.3.2).

The estimation of heat exchanger loads derived from process simulation, as well as the most important fluid-dynamic design and heat exchange design figures are summarized in Table 5-11. As can be seen in Table 5-11, the pre-regenerator features the same bundle design as the desorber. However, the available heat exchange surface is almost doubled compared to the desorber. Beside the heat up from rich heat exchanger outlet temperature to a regeneration temperature of 115 °C, the simulations predict, that around 1/3 of total CO₂ release from the sorbent takes place in the pre-regenerator. But these figures need to be confirmed by the upcoming experiments still, since high uncertainties around co-adsorption of water (especially with potential deviations of operating temperatures) are expected.

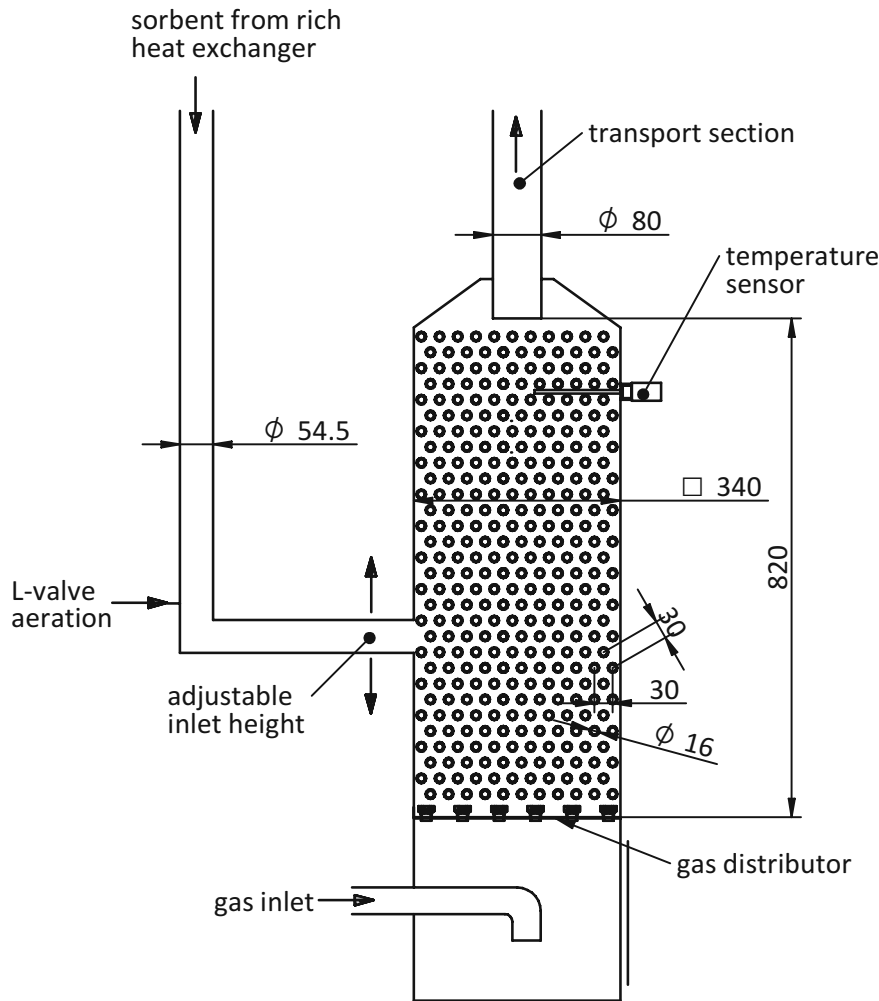


Figure 5-4: Pre-regenerator design

Figure 5-4 shows the design of the pre-regenerator. The sorbent material flows in moving bed regime from the adsorber through the rich heat exchanger into the standpipe of the L-valve, which is used to control the sorbent flow into the pre-regenerator. Similar to the bottom stage of the adsorber, a gas distributor with 36 tuyere nozzles (6 x Ø2.5 mm each) is installed, which avoids a backflow of sorbent during a shutdown of the plant. Within the pre-regenerator a bubbling fluidized bed is established by the flow of recycled off gas from the desorber. At the top of the heat exchange section, the cross section is reduced to achieve gas velocities required for the pneumatic transport with the same gas flow. In order to improve the transport characteristics of sorbent from the bubbling bed section to the transport section, different geometries have been tested, whereby extraction of sorbent directly above the bundle resulted in an acceptable behavior, while conical reductions led to strong fluctuations. Design parameters for the transport section are given in Table 5-12.

In contrast to the lean riser (see Chapter 5.6), the design flux of the rich riser is significantly lower (approx. 50 % of lean riser flux), which is explained by the pre-regenerator design rather than the design of the rich riser itself. In order to achieve the desired operating temperatures, the bed volume of the pre-regenerator had to be increased to fit sufficient heat transfer surface. Since bubble growth in the pre-regenerator would lead to increasing slugging behavior above a certain height of the

bubbling fluidized bed, the bed volume had to be increased by increasing the cross section of the bed, which also results in higher required gas flow. The deviation from the optimum operating conditions of the rich riser and fluidization conditions within the pre-regenerator is seen as a good compromise between both factors.

Table 5-11: Pre-regenerator design figures

	design load	high load	unit
required heat exchanger surface area for pre-regenerator			
inlet sorbent temperature	90.0	90.0	°C
outlet sorbent temperature	115.0	115.0	°C
heating demand	25.4	36.1	kW
heat transfer coefficient (measured)	188	188	W·(m ² ·K) ⁻¹
assumed stage HEX wall temperature	145.0	149.0	°C
required heat transfer surface area	4.49	5.65	m ²
fluid-dynamics			
operating gas flow rate (at pre-regenerator inlet)		84.5	m ³ ·h ⁻¹
minimum fluidization velocity		0.15	m·s ⁻¹
fluidization number (CO ₂ release neglected)		1.3	-
main dimensions pre-desorber			
width of pre-desorber		0.34	m
length of pre-desorber (=tube length)		0.34	m
total bed height		0.8	m
heat exchanger design			
single tube outer diameter		16.0	mm
triangular pitch in tube bundle		30.0	mm
total HEX surface		5.64	m ²
pressure drop			
total pressure drop over pre-desorber		34	mbar
total inventory Pre-desorber		~40	kg

The bubbling fluidized bed in the pre-regenerator is also exploited for balancing of the pressure profile between adsorber sorbent outlet and desorber off gas path. The backpressure from the fluidized bed can be influenced, by introducing the sorbent at a certain height of the pre-regenerator, which can be exploited to reduce the gas slip between the adsorber and this section of the process (see also Chapter 4.3). In particular, the inlet height of the horizontal part of the L-valve has been chosen in a way, that the backpressure from the pre-regenerator and riser compensates most of the pressure gradient in the standpipe. The residual gas slip from the adsorber towards the pre-regenerator is then further avoided by an actively controlled purge gas introduction into the standpipe which is based on a differential pressure measurement over the moving bed section. Without the backpressure from the pre-regenerator, this purge gas stream would need to be significantly higher to achieve the same sealing effect. For later fine adjustment of the back pressure, an adjustable inlet height for the sorbent was foreseen (see Figure 5-4).

Table 5-12: Rich riser design parameters

	design load	high load	unit
dimensions and fluid-dynamics			
inner diameter of riser pipe	80.0		mm
height of riser pipe	7.1		m
transport gas velocity (incl. released CO ₂)	5.5	5.9	m·s ⁻¹
quality of particle transport (u_{riser}/u_t)	2.17	2.31	-
pressure drop (estimated from CFM tests)	10.0	14,3	mbar

5.6 LEAN TRANSPORT SECTION

Within the rich transport section including rich heat exchanger, L-valve, pre-regenerator, rich riser and particle separator, not only sensible heat is provided to reach the target temperature of 115 °C (see Table 5-1). A significant share of total heat provided to reach 115 °C is latent heat for the release of water and CO₂ within this section. Although, adsorption of CO₂ within the lean riser is enabled by extracting adsorber off gas for fluidization of the riser, a significant advantage of providing a dedicated heat exchange section as at the rich transport riser bottom (pre-regenerator) is not expected.

However, since adsorber and desorber gas outlets are approximately at equal pressure levels the pressure drop of the whole desorber column, which is roughly 130-140 mbar (see Table 5-6) needs to be dissipated within desorber sorbent outlet and lean particle separator to minimize the slip of steam from the desorber to the lean riser. A pneumatic L-valve, if designed properly, can balance a certain pressure drop in flow direction. However, experiments at lab scale indicated increasing loss of controllability if the pressure difference gets too high. Depending on the standpipe and L-valve geometry, the gas flow, which results from the pressure difference, at some point causes the L-valve to transport sorbent even without any external aeration. Therefore, in a first design proposal, this pressure difference was partially dissipated by formation of a deep dense phase at the bottom of the lean riser, in order to avoid this behaviour. However, this had several negative effects, like strong fluctuations of the sorbent flow rate within the transport section of the riser, which is explained by the required deep fluidized bed and subsequent formation of slugs. Furthermore, the fluidized bed led to an undesired increase of the total sorbent inventory.

Therefore, a combination of a mechanical slide valve with an actively controlled purge gas introduction was designed and tested within a cold flow model. With this set-up, it has been shown, that the sorbent circulation rate can be precisely controlled by adjusting the opening of the slide valve. Furthermore, the purge gas introduction enables to adopt the pressure profile by creating a high-pressure point, which helps to reduce or avoid a gas slip from the column towards the riser. Although both adjustment possibilities (slide valve opening and purge flow rate) are influencing both parameters (sorbent flow and gas flow), the purge flow has a stronger impact on gas sealing while the slide valve opening has a stronger impact on the sorbent flow. Therefore, with a combined control strategy, it is possible to achieve the desired gas sealing effect and the desired sorbent flow at the same time [89].

Furthermore, the cold flow results also showed, that with this configuration, the pressure drop signal in the transport section of the lean riser is very smooth and thus allows for proper determination of the sorbent circulation rate within the TSA system. The design of the lean riser is summarized in Table 5-13. The design gas velocity of the lean riser is 5.0 m·s⁻¹ which provides enough margin to choking

behaviour, which occurred at around $4 \text{ m}\cdot\text{s}^{-1}$. Choking behaviour would result in a strongly fluctuating transport of sorbent, which also makes the determination of the sorbent flow via the pressure drop of the transport riser inaccurate. A too high gas velocity on the other hand would require more blower power and would result in less sensitivity of the riser pressure differential signal as well. Furthermore, higher gas velocities would lead to an increased attrition rate of the sorbent. Depending on the load condition, the lean riser is operated at a flux in the approximate range between 50 and $120 \text{ kg}\cdot\text{m}^{-2}\cdot\text{s}^{-1}$. For more detailed results from cold flow modelling of this section, it is referred to the work of Zehetner [89].

Table 5-13: Lean riser key figures

	design load	high load	unit
dimensions and fluid-dynamics			
ID of riser pipe	54.5	54.5	mm
Height of riser pipe	7.93		m
Transport gas velocity	5.0		$\text{m}\cdot\text{s}^{-1}$
Quality of particle transport (u_{riser}/u_t)	1.75		-
Pressure drop (estimated from CFM tests)	27	36	mbar

5.7 REACTOR DESIGN OVERVIEW

In the previous sections, several design aspects have been discussed and a reactor design was elaborated. Besides the equipment, which has already been described in detail, also the transport risers and particle separators are shown in Figure 5-5. On the left side an isometric view on a 3d model of the reactor design is depicted. On the right side a cross sectional view through the main process equipment is presented in an unfolded view. In contrast to Figure 5-1, the cross sectional view of the reactor design (Figure 5-5) is a scaled drawing, thus, size proportions are presented correctly.

Figure 5-5 shows, that the total height of the main reactor design is not only depending on adsorber and desorber but also on the design of remaining equipment. The lean/rich heat exchange strategy for example, does not foresee dedicated transport risers for the moving bed heat exchangers, which means, that they have to be installed below the columns. But also the way, how horizontal transport of the sorbent is achieved (by $45 \text{ }^\circ\text{C}$ pipe sections in this case) can significantly increase the total height of the plant.

Table 5-14 summarizes the most important pressure differences in the system. The corresponding locations (P1-P9) are shown in Figure 5-5.

Table 5-14: Estimated pressure differences at design load

	design load	unit
Approx. off-gas pressure difference (P2-P4)	0	mbar
Adsorber total pressure drop (P1-P2)	43	mbar
Desorber total pressure drop (P3-P4)	133	mbar
Pre-regenerator total pressure drop (P5-P6)	33	mbar
Rich transport riser pressure drop (P6-P7)	10	mbar
Lean transport riser pressure drop (P8-P9)	27	mbar

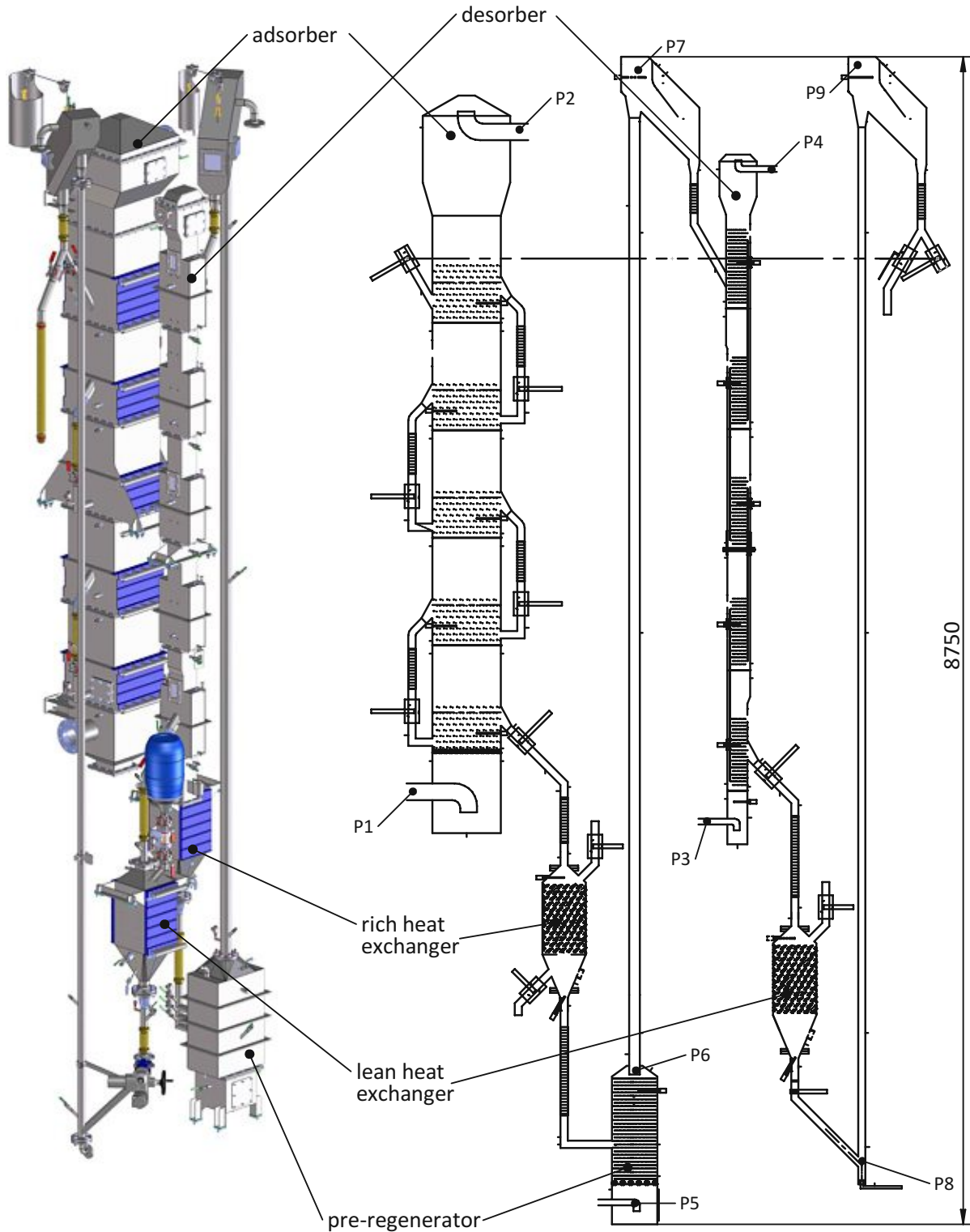


Figure 5-5: Reactor design overview

5.8 DETAILED ENGINEERING

After dimensioning of main process equipment was finished, remaining specifications of the plant including the auxiliary systems like steam supply, cooling water supply, flue gas cooler, and others were

made. Besides the main equipment, several heat exchangers, blowers and pumps, in total, more than 300 valves, 55 flow indicators, 29 pressure sensors and 81 temperature indicators have been specified in a detail design package. Furthermore, a 3d model of the plant (see Figure 5-6) was elaborated, which was the further basis for required manufacturing drawings. In the following, a short summary of detailed process engineering will be given.

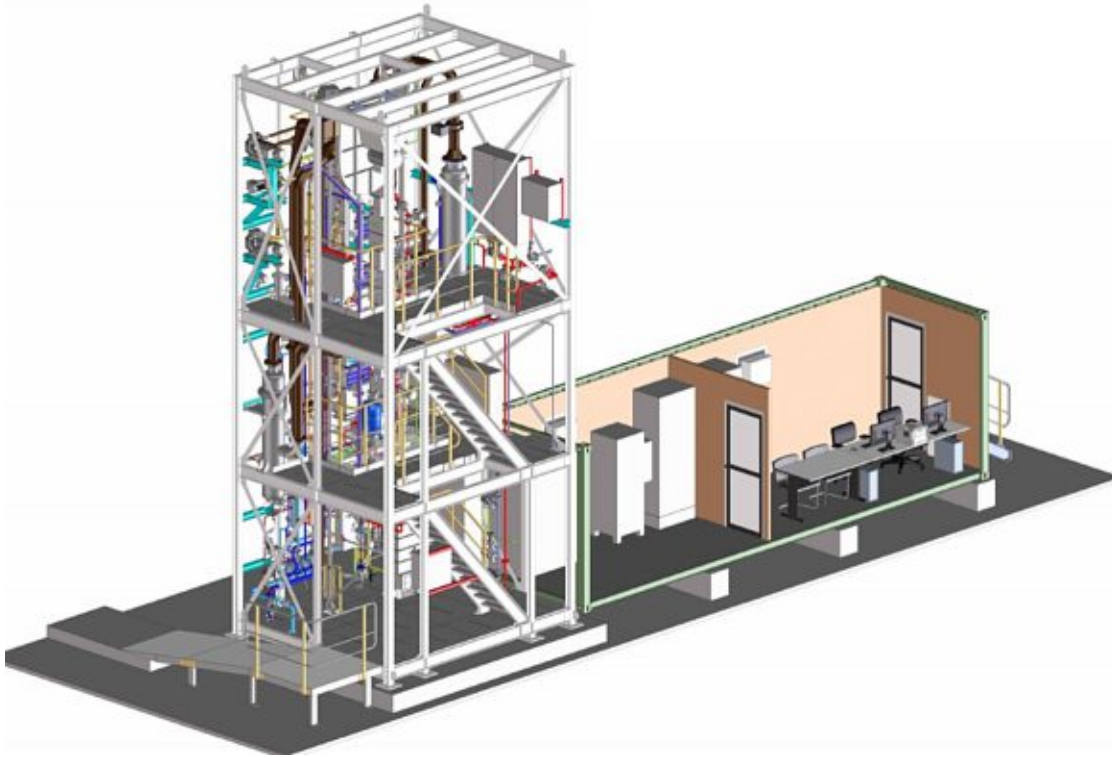


Figure 5-6: 3d model of pilot plant

5.8.1 Process instrumentation

Precise knowledge of operating conditions is crucial for a successful experimental campaign, as well as for the validation of the process model. Therefore, the ViennaGreenCO₂ pilot plant has been equipped with sufficient process instrumentation.

Temperature sensors

Adsorption of CO₂ and water moisture is strongly affected by the operating temperatures. Accurate measurements are important not only for operation of the plant, but also for later data evaluation. Besides 16 most important temperature probes, which are directly measuring sorbent temperatures at different locations within the sorbent cycle, 65 sensors are installed in the cooling water system, flue gas cooling, CO₂ product cooler and condenser, as well as in steam supply and trace heating.

Pressure sensors

For fluidized beds, which cannot be monitored visually, pressure measurements are the most important feedback for the operator. Within a fluidized bed, the pressure drop is approximately proportional to the inventory of a fluidized bed, which can be exploited for example for inventory

control. However, differential pressure measurements are also used for the measurement of sorbent flow within the transport risers or to control the amount of purge gas required to achieve gas sealing in the standpipes.

Besides some pressure sensors in the auxiliary systems, in total 20 differential pressure sensors with high sensitivity are installed to continuously monitor the state of the fluidized beds and the transport systems.

Flow sensors

In order to allow for evaluation of the process mass balance, each incoming and outgoing stream as well as recycled streams of the process are measured either with an online measurement (steam flows, flue gas flow, purge gas flows, riser fluidization flows and CO₂ product flow) or with an offline measurement (measurement of pressure sensor purge gas flows).

5.8.2 Analytical equipment and sampling

Table 5-15 summarizes analytical equipment which comes to use to derive gas compositions at certain sampling locations.

Table 5-15: Online measurement of gas compositions

analyzer	sampling location	detected components
<i>Siemens Ultramat 23</i> (Channel 1 of 2)	adsorber feed	CO ₂
<i>Siemens Ultramat 23</i> (Channel 2 of 2)	switchable to: adsorber feed / freeboard of adsorber Stage 1-5	CO ₂ , O ₂
<i>Siemens Oxymat 61</i>	Adsorber feed	O ₂
<i>CAI FTIR 700</i>	switchable to: adsorber feed / freeboard of adsorber stage 5 / CO ₂ product	amine and amine degradation products
<i>Orbisphere M1100</i>	CO ₂ product	O ₂ (ppmv level)

Besides these online measurements, the pilot unit features several sampling nozzles, where a small sample of sorbent can be extracted for further lab analyses (e.g.: water content, CO₂ loading, CO₂ capacity etc.). In order to freeze the state of the sorbent to some extent, a sorbent sampling device was designed, which allows to extract a sorbent sample without exposure to ambient air. The device (see Figure 5-7) is connected to one of the sampling locations in the process and the valves are opened. Stagnant sorbent from the nozzle itself flows into the purge container first, until the lower most valve gets closed. After this initial purge of the sampling nozzle, the actual sample tube gets filled by closing the valves in the right order. Optionally, a valve for nitrogen introduction can be used to back pulse the sampling nozzle before and after taking the sample. The sample remains in the steel tube between the two valves until it is further analysed, therefore not only the sorbent gets sampled, but also the surrounding gas in the void of the particles, which makes the sorbent samples more representative to

the conditions inside the process. Furthermore, liquid samples are taken for further analyses of process effluents.

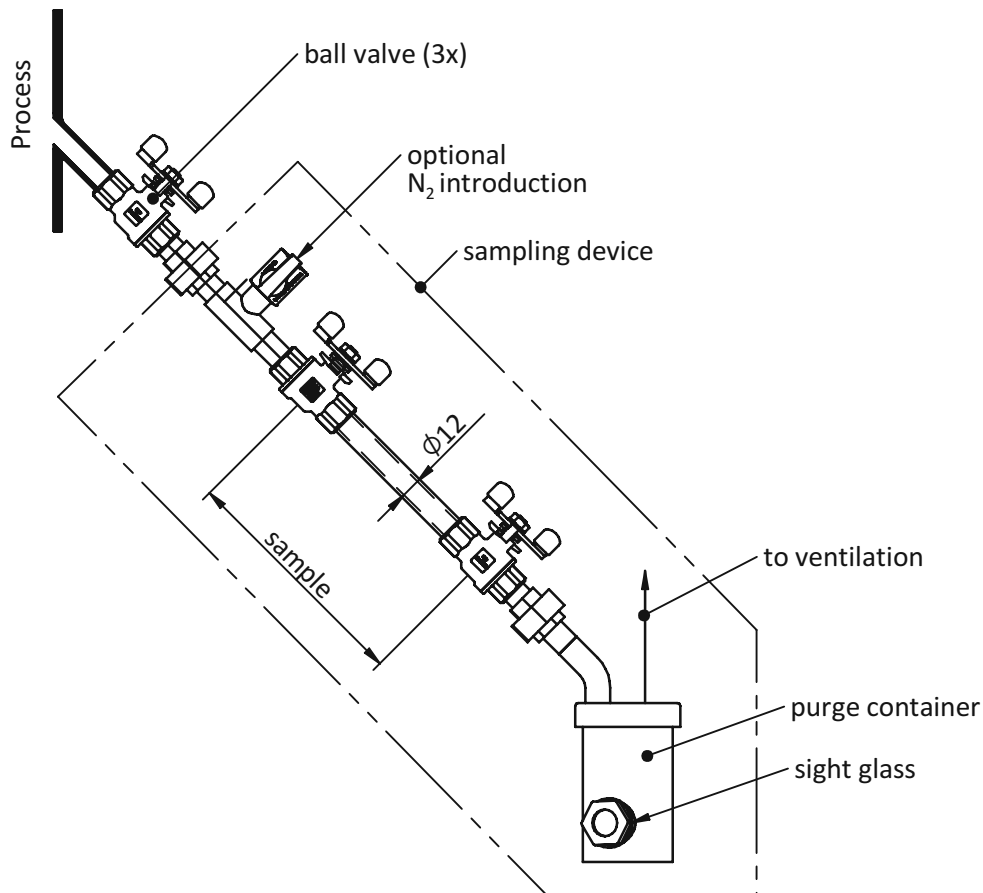


Figure 5-7: Sorbent sampling device

5.8.3 Corrosion test coupons

For absorption with aqueous amine solutions corrosion is a frequently reported issue, which is expected to be less critical for solid sorbents. However, it is not clear yet, which material of construction is compatible. In order to gain first experience in this topic, the pilot plant has been equipped with corrosion test coupons. While the main process equipment was constructed with stainless steel (mainly 1.4301), corrosion test coupons with different steel grades (see Figure 5-8) were installed in the heat exchange zone of adsorber stage 1, in the freeboard of the adsorber, as well as in the freeboard of the desorber. After the experimental campaign, an analysis of the coupons shall deliver first results for the corrosion behaviour and potentially allows for application of lower grade steel in a next scale TSA plant.

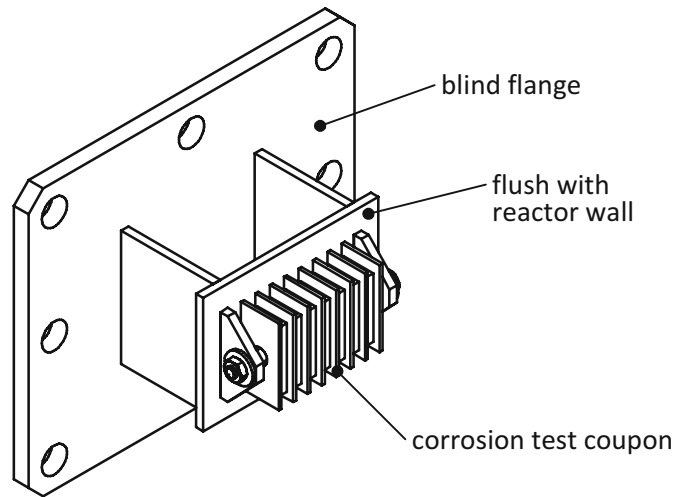


Figure 5-8: Corrosion test coupons

5.8.4 Process control system

The pilot unit is intended to be operated automatically as it will be partially unattended during nights and weekends . Therefore, all relevant process functions are controlled by a Siemens PCS7 programmable logic controller (PLC), which is located in the office container of the pilot unit. The PLC is equipped with an operator station which is used to record all relevant process data and allows for operator interactions. The PLC automatically alarms when operating conditions fall outside the pre-determined operating ranges and interlocks are defined to stop some or all of the equipment in the process, should operating conditions reach unsafe limits. A basic overview drawing of the electrical and process control system is given in Appendix B.

6. ERRECTION OF PILOT PLANT AND FIRST RESULTS

Construction of the pilot plant started in 2017 and has been finished in Q1 2018 when the pre-manufactured pilot plant was delivered in two containers to the power plant host site at Wien Energie in Vienna, Austria (see Figure 6-1). After delivery of the pilot, remaining tasks like the electrical connections, piping from and to the host site, installation of gas analyses etc. have been completed at site.

In parallel to the construction tasks, an operating manual was produced and procedures for operation have been elaborated. Furthermore, an operating team was set up and trained for operation. After the handover between the plant manufacturer and the operating team, final acceptance tests and a pre start-up safety review took place. In addition to 3 factory acceptance tests, several pre start-up tests like an as built documentation check, check of safety interlocks, a gas leakage test, equipment and instrumentation checks and others have been conducted at site in Wien Simmering to ensure safe operation and high quality of the gained results.



Figure 6-1: Erection of pilot unit in Wien Simmering

After completion of the erection phase and the subsequent acceptance tests, the cold commissioning phase started. Cold commissioning in this context means actual operation of the plant at ambient temperatures with a recycled gas (N_2 and flue gas) instead of steam and flue gas. With this mode of operation, operating experience with the process and its sub-systems could be gained whilst the risk to damage the sorbent material is relatively low. Especially the fluid-dynamic behavior of the plant was studied during this phase.

Sorbent circulation at ambient temperature

After commissioning of auxiliary systems and filling of sorbent, the next step was to establish sorbent circulation. Therefore, the required gas flow for the columns and transport risers was set in accordance with design calculations and the sorbent circulation rate was slowly ramped up. The sorbent cycle between adsorber and desorber builds a closed loop. However, this cycle is in a very sensitive balance. Since there are several critical locations in the sorbent path, but the overall sorbent transport rate needs to be constant, any deviation at any point limits the overall transport rate, or at least disturbs the inventory distribution within the system. During cold commissioning of the plant, the following problem with the desorber's transport behavior was identified:

As the sorbent circulation rate was increased, sorbent from desorber stage 5 was not transported down fast enough, overfilled the uppermost stage and sorbent was entrained to the filter which forced a shutdown of the plant. A slugging behavior in the downcomer could be observed through the sight glass, which indicates too much gas flow in the downcomer area. The relative sorbent inventory of each stage was monitored by measurement of the desorber pressure drop over each stage. The described behavior is reflected by the exemplary measured data of the desorber shown in Figure 6-2. One can see, that as the sorbent circulation rate is increased, stage 1 empties, while stage 5 of the desorber overfills, which clearly indicates a limitation of sorbent flow in the desorber. Although, the control strategy was later revised, which avoided emptying of stage 1 at least, the overall sorbent flow through the desorber was still limited.

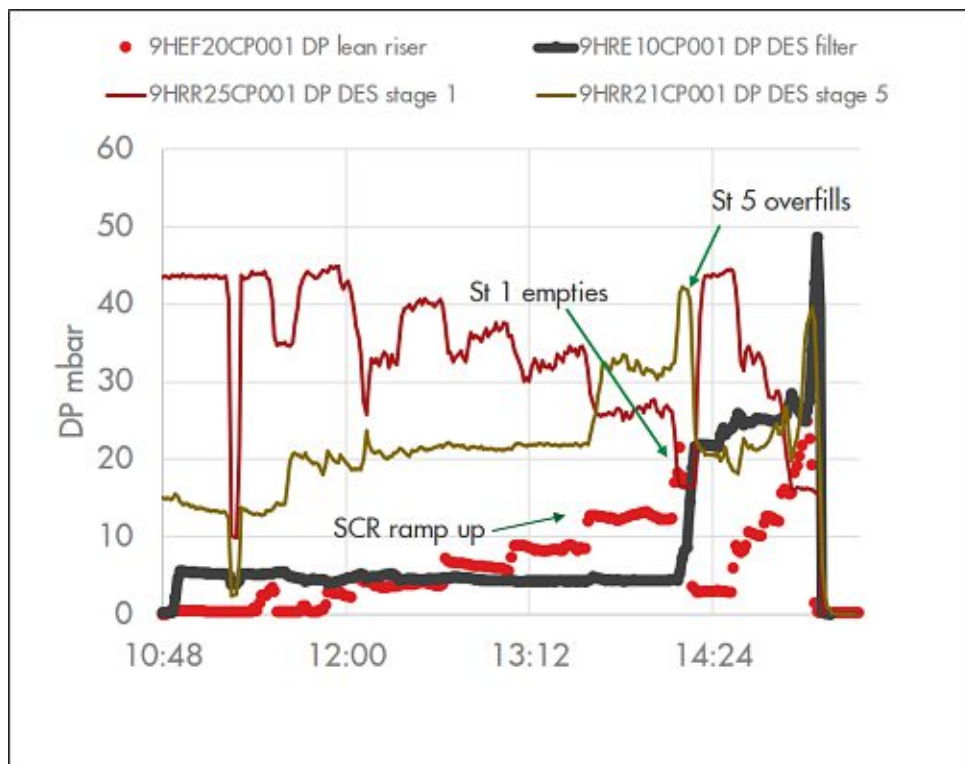


Figure 6-2: Desorber sorbent transport limitation (observed on Sept. 4th 2018)

By closing holes of the perforated plate gas distributors, the gas flow in the downcomer area was reduced in several steps. Figure 6-3 shows the modified area of the desorber gas distributors. In several steps, up to 50 % of the holes in this area were closed. With this measure, the transport behavior of

the desorber was significantly improved at cold conditions, so that the target sorbent flow was finally achieved.

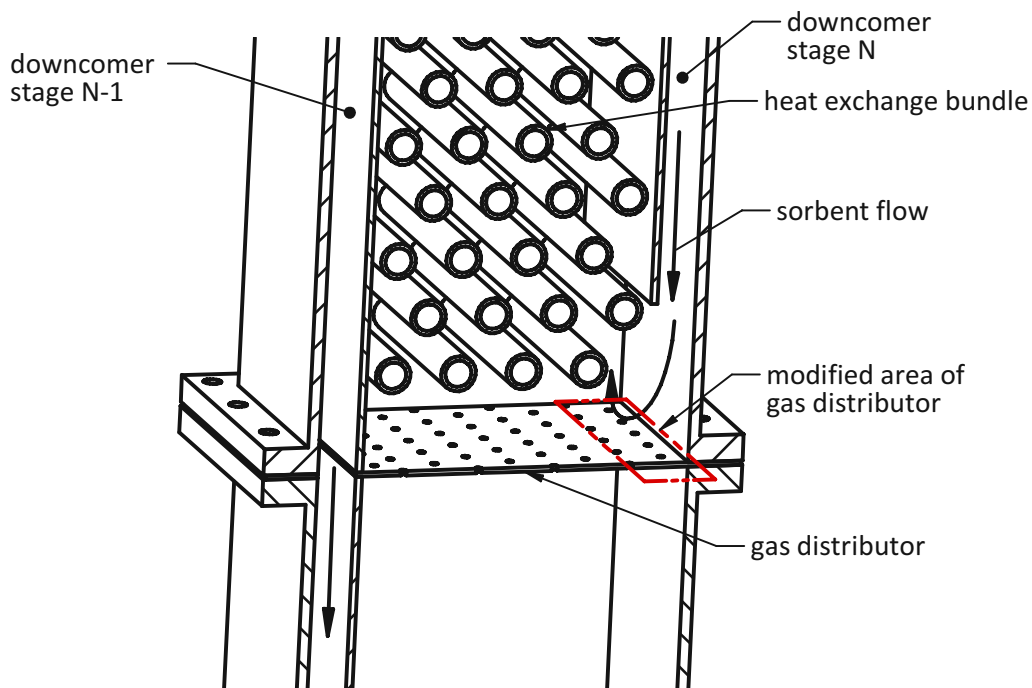


Figure 6-3: Modification of desorber gas distributors

After successful cold commissioning, first tests at elevated temperature, and later with steam as fluidization gas for the desorber, were conducted. During hot commissioning, the plant showed satisfying controllability of most subsystems like the heat exchangers, the steam and condensate system, internal and external cooling water system. But also, several challenges for example with entrainment of sorbent material and subsequent malfunctions on downstream equipment of the pilot plant were faced. Despite excellent fluid-dynamic behavior of the adsorber, as well as the pre-desorber and the riser system, the desorber again showed sorbent throughput limitations at hot conditions, which was the main challenge for the remaining campaign. With further modifications of the gas distributor, this limitation was at least partially overcome and first CO₂ capture operation at reduced capacity was established in October 2018. A preliminary evaluation of data clearly indicated that the overall capture capacity was limited by the reduced sorbent circulation rate, since apart from the desorber transport behavior, the pilot unit showed excellent performance of equipment and good controllability of the most important remaining process parameters.

Although, a detailed description of the further troubleshooting and experimental campaign is outside the scope of this thesis and is to be expected in future publications, a short summary is given here: To understand the throughput limitation of the desorber, a 1:1 copy of 4 desorber stages was manufactured out of Perspex to allow for observation of the sorbent flow within the column and the behavior was studied with different gas distributors and operating conditions. From these experiments, stable operating conditions were derived and transferred to hot conditions in the pilot

unit. Furthermore, the desorber downcomers were equipped with an additional controlled steam aeration which is introduced for certain operating conditions. Since the process temperatures have a strong influence on water co-adsorption and therefore on the gas velocity profile of the desorber, a further approach was the modification of desorber and pre-regenerator temperatures. Another improvement of the overall transport behavior was achieved by a different sorbent flow control strategy, which created less fluctuations in the flow of sorbent to and from the desorber. Although, the throughput limitations still could not be eliminated fully, the desorber transport behavior was significantly improved. In the further scope of the project, the general operability of the plant was proven in more than 1000 hours of operation. In these 1000 hours, more than 30 datapoints have been recorded (see Figure 6-4). The ViennaGreenCO₂ pilot unit was able to separate more than 90% of CO₂ from a flue gas with 4 Vol-% feed concentration. The maximum capture capacity measured was in the range of 700kg/day. In addition to the recorded online measurements, several samples of sorbent from various location for each datapoint and effluents from the process have been taken for further analyses. As already indicated, data evaluation and a detailed presentation of experimental results is to be expected in upcoming publications.

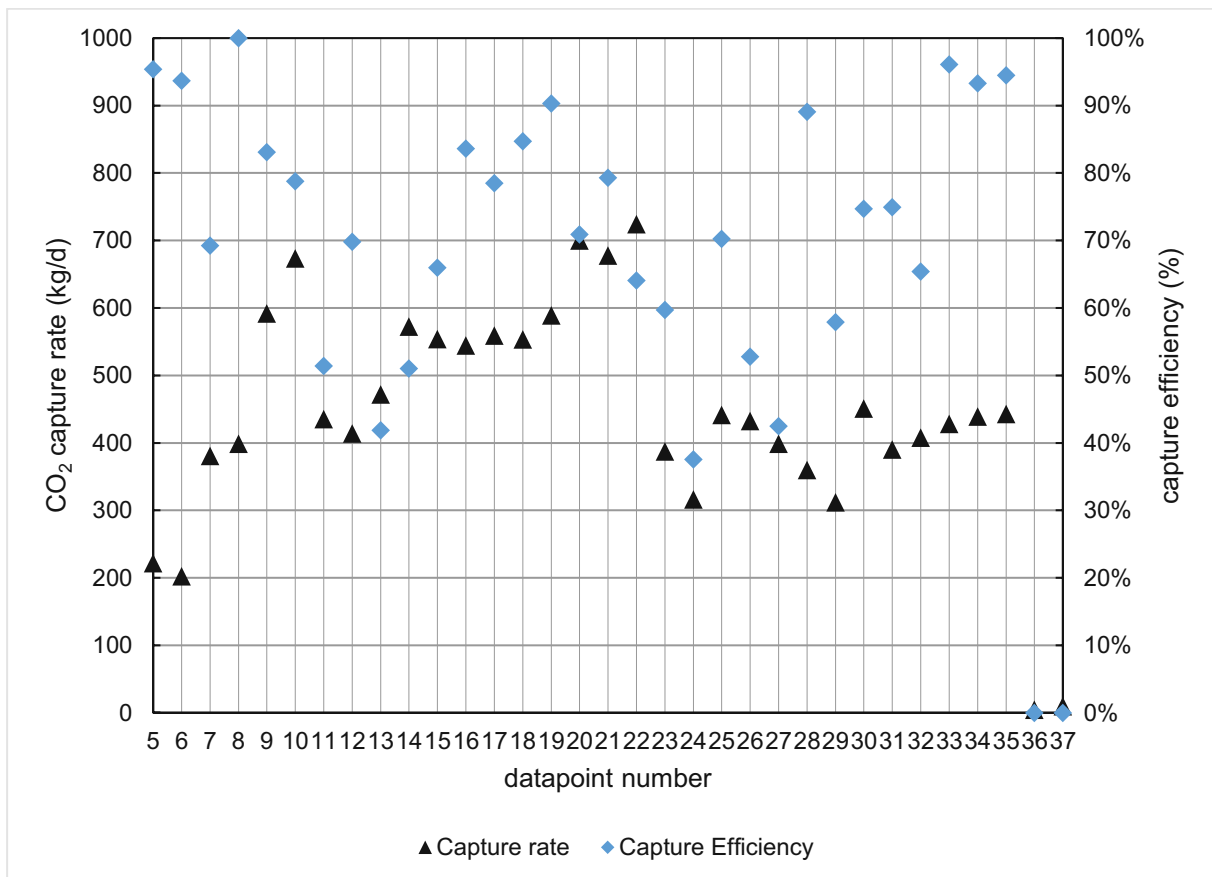


Figure 6-4: Datapoint overview

7. SUMMARY AND CONCLUSIONS

Carbon capture and storage is still seen as a key technology to limit global warming and to achieve the targets of the Paris Agreement. Especially with delays in reaching targeted reductions of CO₂ emissions, CCS becomes even more important, so that at one point in future, it might be the only chance to limit the global temperature increase to acceptable values. It is broadly accepted, that the main challenge of CCS lies in the capture part. Reported energy demands for the capture of CO₂ are still very high. Furthermore, CO₂ scrubbing with aqueous amines, which is seen as the state of the art technology suffers from several other drawbacks like: process related emissions of volatile organic compounds, high specific plant size and subsequent high capital expenses, as well as foaming, fouling and corrosion issues, which are reported in literature.

Adsorption with solid sorbents has the potential to overcome the above-mentioned drawbacks at least partially as well as to reduce the energy demand required for separation of CO₂. However, adsorbent as well as process and reactor development for CO₂ adsorption from large sources are still in an early stage.

A promising process design based on multistage fluidized bed temperature swing adsorption was elaborated and tested at lab scale. Within an extensive parameter variation and several hundred hours of operation at lab scale, the proof of concept was clearly given, and the plant showed highly promising CO₂ capture performance. However, due to the small size of the lab plant, not all relevant questions could be answered. At bench scale, the major limitation which hindered an increase of the overall capture performance was a thermodynamic limitation due to insufficient heat transfer surface. Furthermore, the relatively high heat losses, which are based on the high surface to volume ratio of small-scale plants led to high uncertainties for the determination of the process energy demand. Also, the bench scale unit was simply not designed for long term operation and was not equipped with adequate instrumentation to further assess the process on a higher level. Therefore, the decision was taken, to assess the process at an increased scale.

Within this thesis, the full-scale target application is defined and an intermediate scaling step with its dedicated requirements is elaborated in a design basis.

In order to maximize the output from the pilot experimental campaign, objectives and key requirements on the pilot unit are defined. Besides the elimination of limitations observed at bench scale, the focus for the pilot unit design lies on process development in the view of the whole development chain from lab scale to full scale.

For the design of a multistage fluidized bed temperature swing adsorption process countless aspects have to be considered. Within the design philosophy section of this thesis the crosslinks between some of these aspects are discussed. Furthermore, it is shown that especially the process heat management is a key factor. Although, fluidized beds feature high heat transfer coefficients, the actual figures are strongly depending on sorbent properties and fluidization conditions. Therefore, dedicated heat transfer measurements at design conditions with the selected sorbent material have been conducted. The advantages of a counter-current flow pattern, which is achieved with the multistage fluidized bed columns are evident. However, especially what happens outside of the two main reactors will be extremely important for the overall process performance. One frequently claimed advantage of solid

sorbents is the reduced heat capacity of a solid vs. aqueous amines, which results in less energy demand to achieve the temperature swing between the two columns. But this is only half the truth. While heat recovery between two liquids is achieved at relatively low costs and is highly efficient, heat recovery between two bulk material streams is much more complicated. Nevertheless, heat recovery from the hot lean sorbent stream to the colder rich sorbent stream was investigated and several potential heat recovery set-ups have been compared. Finally, a promising heat exchanger design, which was tested within the pilot unit, was elaborated.

However, not only heat recovery between lean and rich sorbent streams is more difficult compared to CO₂ scrubbing. Also, the transport of sorbent between the columns and the avoidance of a gas slip between both reactors is challenging. Furthermore, adsorption and desorption reactions are not stopped during transport between the columns. Sorbent and surrounding gas phase will always aim for equilibrium, which can be a big issue if not considered in design. In Chapter 4, a thermodynamically optimized transport riser set-up is elaborated. By extracting gas from the column off gas streams, instead of recirculating the riser fluidization gas itself, adsorption and desorption activities within the transport sections are utilized advantageously. Within Chapter 4 also gas sealing requirements are discussed, and appropriate measures are elaborated.

Based on the elaborated design philosophy, a reactor design strategy is presented and the geometry of the main process equipment is derived. While the design of the adsorber aims for a maximization of the gas throughput, the desorber fluidized bed design shall achieve the opposite. Based on simulations, an optimum specific stripping steam flow rate of less than 1 kilogram steam per kilogram CO₂ captured was identified. However, this relatively low steam flow compared to the amount of CO₂ released in the desorber, results in a high flow gradient over the height at one hand, and low bed volume available for heat exchange. Therefore, a significant share of the total heat demand for regeneration was shifted towards the heat exchange zone in the rich riser. The pre-regenerator then turned out to be advantageous also with respect to regeneration of the sorbent. Recirculation of desorber off gas and rich riser gas, partially uncouples the steam supply to the desorber from the overall heat transfer surface and enables to allow for a significant gas release in the pre-regenerator and the following rich riser.

Furthermore, a summary of detail engineering, erection and commissioning of the pilot plant is presented. First results showed good controllability of the process at cold conditions. However, operation at design load was not achieved, due to sorbent throughput limitations in the desorber. In the further scope of the project, this limitation was mostly overcome which enabled a thorough experimental campaign from which first results were presented.

8. OUTLOOK

8.1 PRELIMINARY IMPLICATIONS ON FURTHER SCALE UP

Although extensive tests with the pilot unit, as well as required evaluation of data are outside the scope of this work, some preliminary implications on the further scale up of the technology are possible already and summarized in the following.

- Adsorbent selection

Lewatit VP OC1065, which came to use in the ViennaGreenCO₂ pilot unit showed satisfying performance with the additional benefit of low degradation rates and high mechanical stability. Furthermore, analyses of process off-gas streams and effluents showed promisingly low sorbent related emissions. However, the elaborated pilot design was strongly dependent on this sorbent selection. Especially the particle size of the sorbent had a strong impact on the fluid-dynamic design and heat exchanger design of the plant. With the technological advances in adsorbent development and the increasing inventory demand of large-scale plants custom made solutions are more likely, which brings an additional degree of freedom in reactor and process design.

- Sorbent and gas distribution at large scale

As mentioned in Chapter 3, pilot scale is not the target of technology development but a required intermediate step towards commercialisation of the technology. Since commercial scale is still out of reach, a further scaling step between pilot scale and commercial scale is seen reasonable. Under the assumption, that sorbent throughput limitations can be eliminated, and the pilot unit achieves its design capture capacity, the scaling step (related to capture rate) from pilot scale to commercial scale is roughly 2700. With this scaling factor, a directly scaled pilot adsorber would have a fluidized bed cross section with a quadratic side length of more than 25m but less than a meter of bed height per stage. Since this extreme aspect ratio is very likely to cause major problems in gas and sorbent distribution, the required cross section needs to be divided into individual modules. At demonstration scale it would therefore make sense to prove operability of one single module at only slightly smaller scale (compared to a commercial scale module). Since sorbent distribution will remain challenging even with the modular design, multiple downcomers per module stage should be considered.

- Adsorber design

A preliminary evaluation of experimental results and raw data confirmed the general operability of the pilot unit adsorber. Within the tested range of operating conditions, the main parameters (e.g.: sorbent flow, inventory control and stage temperatures) showed satisfactory controllability. Therefore, the general design strategy for the adsorber column was confirmed. Nevertheless, experimental data should be used to refine models for heat exchange to allow for more precise calculation of required heat exchange surface. Furthermore, an evaluation of mass transfer at high gas velocities should be conducted, to further reduce the footprint of the adsorber.

- Desorber design

Operation within the possible range of sorbent flow showed excellent control of desorber temperatures, which indicates that the heat exchange limitation observed at bench scale was overcome. However, the fluid-dynamic design of the desorber caused a major limitation of the pilot units capture performance. Deviations from design in terms of the gas velocity and composition profile over the height of the desorber caused a malfunction of the internal downcomers. These deviations mainly come from H₂O co-adsorption effects, which have not been considered sufficiently. Furthermore, the internal downcomers do not feature enough flexibility for operation at different load cases. In order to avoid a limitation of the sorbent throughput at larger scale, it is important to further assess the limitation at pilot scale. To fully understand the mechanisms leading to the observed deviations, the existing models for water co-adsorption should be refined with the aid of sorbent and gas sample analyses from the individual desorber stages. Finally, a design strategy for internal downcomers dependent on the range of gas flows in the individual stages should be elaborated. However, also a switch to external downcomers, which would resemble a more robust solution with more operating flexibility should be considered.

- Lean/rich heat exchange

Although both moving bed heat exchangers caused initial problems with condensation, their general operability could be proven. However, for the large-scale design of these heat exchangers further investigations are necessary. Especially the actual heat transfer coefficients have to be derived under varying operating conditions in continuous operation of the pilot unit. Finally, a techno-economical investigation should allow for calculation of an (total cost) optimum heat recovery approach.

- Material of construction

The ViennaGreenCO₂ pilot unit was built out of stainless steel and equipped with corrosion test coupons (see Figure 5-8). A full metallurgical assessment of these test plates is not yet available. However, a preliminary visual inspection after several hundred hours of operation did not show significant corrosion, which indicates that steel with a lower grade could be used for a large scale TSA plant.

8.2 OUTLOOK PILOT OPERATION AND DATA EVALUATION

The conduction of a comprehensive test plan shall allow to validate the process model which is a key factor for further scale up as well as to gain a deepened understanding of the process in general and the interactions between certain process sub-systems.

In the first part of the experimental campaign, the pilot plant shall be operated at design conditions. By adaptation of operating parameters, a data point with 90 % capture efficiency at design load shall be found and hold for enough time to derive sufficient data to evaluate the process energy demand, sorbent degradation, emissions, and other key performance indicators. This data point is then defined

as base case and shall allow to compare sorbent performance after certain variations with the initial performance by setting the operating conditions accordingly.

In the further scope of the experimental campaign, the plant performance shall be further studied at varying operating conditions with the focus on following points:

- Plant behaviour at varying load conditions
By variation of the absolute and relative CO₂ feed, the effect of fluctuations coming from the flue gas source shall be studied. Furthermore, operation at high load conditions shall allow to identify potential limitations and to assess the impact of the plant load on certain key performance indicators.
- Investigation of water co-adsorption
The pilot unit design features the possibility to study the impact of water co-adsorption on the process. A variation of the dewpoint of the adsorber feed gas as well as a variation of the relative humidity in the desorber is expected to have a huge impact on the process heat management. Within a dedicated parameter variation, this impact shall be studied and an optimized operation strategy which considers water co-adsorption effects shall be found.
- Variation of the simulated heat recovery rate
Through implementation of independently heated and cooled lean and rich heat exchangers, the pilot unit enables a broad variation of the simulated heat recovery between lean and rich sorbent stream. Focussed tests, shall identify optimum operating parameters especially with regard to the rich heat exchanger, where a significant amount of gas is potentially released from the sorbent. Furthermore, heat exchange coefficients in dependence on operating conditions shall be derived from these tests.
- Assessment of gas sealing measures
As discussed in chapter 4.3, gas sealing between adsorption and regeneration side of the process is crucial. An oxygen slip towards the desorber can cause sorbent degradation at one side and can be an issue for subsequent liquefaction and transport of the separated CO₂ on the other side. Furthermore, a steam slip from the desorber towards colder sections of the process can lead to condensation and blocking in sorbent transport. Therefore, the pilot unit features several counter measures to avoid or reduce a gas slip from one side towards the other. Some of these are design measures without any control requirements, while the purge gas flows in lean and rich standpipe require precise control during operation. Furthermore, other operating parameters can influence gas sealing between the columns. With the aid of analytical equipment, a strategy for minimization of an oxygen slip as well as for condensation avoidance shall be defined.

Since the fluid dynamic design of the desorber caused major problems in operation of the pilot unit, the underlying effects should be further assessed in detail to avoid costly limitations at larger scale.

NOTATION

List of symbols:

Symbol	Description	Unit
A	cross section	[m ²]
A _{FB}	cross section of fluidized bed	[m ²]
A _p	particle surface	[m ²]
Ar	Archimedes number	[-]
c	volumetric gas concentration	[Vol-%]
c _p	particle heat capacity	[J·(kg·K) ⁻¹]
D, d	pipe/reactor diameter, diameter	[m]
d _p	sieve diameter	[m]
\bar{d}_p	mean particle size	
d _s	surface equivalent diameter	[m]
d _{SV}	Sauter diameter	[m]
d _v	volume equivalent diameter	[m]
dSL	dynamic sorbent loading	[% _w]
g	acceleration due to gravity	[m·s ⁻²]
G _s	solids flux	[kg·(m ² ·s) ⁻¹]
H	height	[m]
h	heat transfer coefficient	[W·(m ² ·K) ⁻¹]
h _{FB}	fluidized bed heat transfer coefficient	[W·(m ² ·K) ⁻¹]
h _{max}	maximum heat transfer coefficient	[W·(m ² ·K) ⁻¹]
L _m , L _{mf} , L _f	height of fixed bed, bed at minimum fluidization and bubbling bed	[m]
\dot{m}	mass flow rate	[kg·s ⁻¹]
m _p	particle mass	[kg]
m _{FB}	mass of fluidized bed inventory	[kg]
p	pressure	[mbar]; [Pa]
p _i	partial pressure	[bar]; [Pa]
RH	relative humidity	[%]
q	adsorbent loading	[mol·kg ⁻¹]
q	heat transfer rate	[W]
T	temperature	[K]; [°C]
u	superficial gas velocity	[m·s ⁻¹]
u _{MF}	minimum fluidization velocity	[m·s ⁻¹]
u _t	terminal velocity	[m·s ⁻¹]
V _p	particle volume including pore volume	[m ³]
V _{pore}	pore volume	[m ³]
\dot{V}	volumetric flow rate	[m ³ ·s ⁻¹]
V _s	volume of solid substance (excl. pore volume)	[m ³]
Δp	pressure difference	[mbar]; [Pa]

Greek symbols:

Symbol	Description	Unit
β	adsorbent loading	$[\text{mol}\cdot\text{kg}^{-1}]$
η_{captured}	CO ₂ capture efficiency	[%]
η_{HR}	heat recovery rate	[%]
λ_{G}	thermal conductivity of gas	$[\text{W}\cdot(\text{m}\cdot\text{K})^{-1}]$
ρ_{true}	(true) particle density	$[\text{kg}\cdot\text{m}^{-3}]$
$\rho_{\text{P}}, \rho_{\text{S}}$	apparent density	$[\text{kg}\cdot\text{m}^{-3}]$ $[\text{gm}\cdot\text{cm}^3]$
ρ_{g}	gas density	$[\text{kg}\cdot\text{m}^{-3}]$
ϕ_{P}	particle form factor	[-]

Abbreviations:

Symbol	Description
ADS	adsorber
AFOLU	agriculture, forestry, and other land use
AMP	aminomethylpropanol
BSC	bottom screw conveyor
BSU	bench scale unit
CAPEX	capital expenditure
CCS	carbon capture and storage
CFM	cold flow model
CHP	combined heat and power
CW	cooling water
DEA	diethanolamine
FB	fluidized bed
FTIR	fourier transform infrared analyzer
GHG	greenhouse gas
HEX	heat exchanger
HMB	heat and material balance
HSE	health, safety, security, and environment
ID	inner diameter
LRHX	lean/rich heat exchange
MB	moving bed
MDEA	methyldiethanolamine
MEA	monoethanolamine
MStFB	multistage fluidized bed
MOF	metal organic framework
OD	outer diameter
OPEX	operational expenditure
PLC	programmable logic controller
PEI	polyethylenimine
PFD	process flow diagram
PMMA	polymethylmethacrylat
PSD	particle size distribution
RH	relative humidity
SCR	sorbent circulation rate
SCR	selective catalytic reduction
TGA	thermogravimetric analysis
TSA	temperature swing adsorption
VOC	volatile organic compound

LIST OF FIGURES

Figure 1-1: Observed and projected temperature change between 1900 and 2100 (taken from [3])... 6	6
Figure 1-2: GHG emissions by economic sectors (taken from [7])..... 8	8
Figure 1-3: Overview of CO ₂ capture processes (taken from [13]) 9	9
Figure 1-4: Cansolv process line-up for the SaskPower BD3 CCS project (taken from [14])..... 11	11
Figure 2-1: liquidlike behaviour of a fluidized bed (taken from [40]) 16	16
Figure 2-2: Fixed bed, fluidized bed, pneumatic/hydraulic transport (taken from [40])..... 17	17
Figure 2-3 Geldart particle classification (taken from [40]) 20	20
Figure 2-4 pressure drop of a fixed/fluidized bed..... 20	20
Figure 2-5: effect of the particle size on fluidized bed heat transfer (adapted from [40])..... 22	22
Figure 2-6: Definition of terms..... 23	23
Figure 2-7: Overview of sorbent CO ₂ capacities and operating temperature range (taken from [25]) 25	25
Figure 2-8: CO ₂ Adsorption isotherms for zeolite 13X (taken from [62])..... 26	26
Figure 2-9: Carbamate formation by reaction of CO ₂ with primary, secondary or hindered amines (taken from [25]) 27	27
Figure 2-10: Mechanism for the reaction of CO ₂ and tertiary amines (taken from [25]) 27	27
Figure 2-11: Comparison of adsorption-desorption performance with 100 % CO ₂ feed gas between zeolite 13X and 50 % PEI impregnated porous silica. ((a): zeolite 13X at 25 °C; (b): KIT-60-PEI-50 at 75 °C; (c): zeolite 13X at 75 °C; (d): KIT-60-PEI-50 at 25 °C) (taken from [65]) 28	28
Figure 2-12: CO ₂ capacity loss of amine functionalized sorbents as a function of exposure time and temperature in presence of oxygen (taken from [66]) 28	28
Figure 2-13: Adsorption isotherms..... 29	29
Figure 2-14: Classification of isotherms (taken from [68])..... 30	30
Figure 2-15: Counter current adsorption 31	31
Figure 2-16: Lewatit VP OC1065 adsorption isotherms: Regeneration in CO ₂ atmosphere (adapted from [71]) 32	32
Figure 2-17: Basic scheme of double loop staged fluidized bed system for continuous TSA (taken from [36]) 34	34
Figure 2-18: Illustration of CO ₂ loadings in a multistage fluidized bed TSA process for adsorption at 75°C and regeneration at 120°C, at approx. 10 Vol-% CO ₂ , utilizing an amine impregnated silica sorbent (taken from [36]) 35	35
Figure 2-19: Multistage fluidized bed TSA bench scale unit (taken from [37])..... 36	36
Figure 2-20: Bench scale unit: adsorber stage design..... 37	37
Figure 2-21 Bench scale unit: desorber stage design..... 38	38
Figure 2-22 Bench scale unit: sorbent transport section design..... 39	39
Figure 2-23: Data log of BSU experiment with N ₂ /CO ₂ mixture (taken from [37]) 41	41
Figure 2-24: Variation of sorbent circulation rate under dry conditions (desorber operated with nitrogen) at bench scale (taken from [38]) 42	42
Figure 2-25: Variation of CO ₂ content in adsorber at bench scale (taken from [38]) 43	43
Figure 3-1: ViennaGreenCO ₂ project..... 50	50
Figure 3-2: Simmering biomass power plant (adapted from [81])..... 57	57

Figure 3-3: Flue gas H ₂ O, CO ₂ and O ₂ concentration at Simmering biomass power plant (measured between Feb. 2015 and Mar. 2016).....	58
Figure 4-1: Exemplary calculation of heat transfer rates using literature equations ([44], [84], [85]), calculated for copper particles with a mean diameter of 50µm and air as fluidization gas at ambient conditions.....	63
Figure 4-2: Heat transfer measurement test rig	64
Figure 4-3: Heat transfer probe.....	65
Figure 4-4: Measured heat transfer rates for varying superficial gas velocities at indicated locations of adsorber stage heat exchanger	66
Figure 4-5: Measured heat transfer rates for varying superficial gas velocities at indicated locations of desorber stage heat exchanger.....	68
Figure 4-6: Downcomer configurations (taken from [40]).....	71
Figure 4-7: Specific stripping steam demand at optimal total energy demand dependent on number of stages in adsorber and desorber (taken from [72])	72
Figure 4-8: Influence of lean/rich heat exchange and stripping steam rate on the total energy demand (taken from [72])	73
Figure 4-9: Effect of stage configurations on process energy demand (taken from [72])	74
Figure 4-10: H ₂ O adsorption capacity of Lewatit VP OC 1065 plotted against the relative humidity (RH) in the gas phase (taken from [71])	75
Figure 4-11: Basic TSA process set-up.....	77
Figure 4-12: Different sorbent inlet details.....	78
Figure 4-13: Superimposed gas flow in moving bed regime	80
Figure 4-14: Transport risers as dedicated adsorption/desorption stages	83
Figure 4-15: Standpipe pressure profiles with and without purge gas introduction	87
Figure 4-16: Moving bed lean/rich heat exchange	90
Figure 4-17: Combination of moving bed and fluidized bed lean/rich heat exchanger	91
Figure 4-18: Experimental setup for single pipe moving bed heat transfer measurements	94
Figure 4-19: Summary of results gained from single pipe moving bed heat transfer measurements .	96
Figure 4-20: Moving bed plate heat exchanger (taken from [97]).....	97
Figure 4-21: Vertical tube bundle moving bed heat exchanger	99
Figure 4-22: Finned tube moving bed heat exchanger	100
Figure 4-23: Finned tube moving bed heat exchanger cold flow model.....	104
Figure 5-1: Final ViennaGreenCO ₂ process scheme (simplified)	108
Figure 5-2: Adsorber design	113
Figure 5-3: Desorber design	118
Figure 5-4: Pre-regenerator design	121
Figure 5-5: Reactor design overview	126
Figure 5-6: 3d model of pilot plant.....	127
Figure 5-7: Sorbent sampling device	129
Figure 5-8: Corrosion test coupons	130
Figure 6-1: Erection of pilot unit in Wien Simmering.....	131
Figure 6-2: Desorber sorbent transport limitation (observed on Sept. 4 th 2018).....	132
Figure 6-3: Modification of desorber gas distributors	133

Figure 6-4: Datapoint overview..... 134

Die approbierte gedruckte Originalversion dieser Dissertation ist an der TU Wien Bibliothek verfügbar.
The approved original version of this doctoral thesis is available in print at TU Wien Bibliothek.



REFERENCES

- [1] IPCC, "Summary for Policymakers. In: Climate Change 2013: The Physical Science Basis. Contribution of Working Group I to the Fifth Assessment Report of the Intergovernmental Panel on Climate Change [Stocker, T.F., D. Qin, G.-K. Plattner, M. Tignor, S.K. Allen, J.," *Cambridge Univ. Press. Cambridge, United Kingdom New York, NY, USA*, 2013.
- [2] IPCC, "Summary for policymakers. In: Climate Change 2014: Impacts, Adaptation, and Vulnerability. Part A: Global and Sectoral Aspects. Contribution of Working Group II to the Fifth Assessment Report of the Intergovernmental Panel on Climate Change [Field, C.B.," *Cambridge Univ. Press. Cambridge, United Kingdom New York, NY, USA*, 2014.
- [3] IPCC, "Summary for Policymakers. In: Global Warming of 1.5°C. An IPCC Special Report on the impacts of global warming of 1.5°C above pre-industrial levels and related global greenhouse gas emission pathways, in the context of strengthening the global response to," 2018.
- [4] European Commission, "Energy Roadmap 2050," 2011.
- [5] European Environment Agency, "Trends and drivers of EU greenhouse gas emissions," 2020.
- [6] IEA, *Energy Technology Perspectives 2012: Pathways to a Clean Energy System (Paris: OECD/IEA, 2012)*. 2012.
- [7] IPCC, "Summary for Policymakers. In: Climate Change 2014: Mitigation of Climate Change. Contribution of Working Group III to the Fifth Assessment Report of the Intergovernmental Panel on Climate Change [Edenhofer, O., R. Pichs-Madruga, Y. Sokona, E. Farahani," *Cambridge Univ. Press. Cambridge, United Kingdom New York, NY, USA*, 2014.
- [8] European Commission, "Submission by Lithuania and the European Commission on behalf of the European Union and its member states," vol. 2019, no. March, pp. 1–7, 2020, [Online]. Available: [http://www4.unfccc.int/submissions/INDC/Published Documents/Latvia/1/LV-03-06-EU INDC.pdf](http://www4.unfccc.int/submissions/INDC/Published_Documents/Latvia/1/LV-03-06-EU_INDC.pdf).
- [9] S. Shackley, D. Reiner, P. Upham, H. de Coninck, G. Sigurthorsson, and J. Anderson, "The acceptability of CO₂ capture and storage (CCS) in Europe: An assessment of the key determining factors. Part 2. The social acceptability of CCS and the wider impacts and repercussions of its implementation," *Int. J. Greenh. Gas Control*, vol. 3, no. 3, pp. 344–356, 2009.
- [10] M. Odenberger, J. Kjärstad, and F. Johnsson, "Prospects for CCS in the EU energy roadmap to 2050," *Energy Procedia*, vol. 37, pp. 7573–7581, 2013.
- [11] H. de Coninck, T. Flach, P. Curnow, P. Richardson, J. Anderson, S. Shackley, G. Sigurthorsson, and D. Reiner, "The acceptability of CO₂ capture and storage (CCS) in Europe: An assessment of the key determining factors. Part 1. Scientific, technical and economic dimensions," *Int. J. Greenh. Gas Control*, vol. 3, no. 3, pp. 333–343, 2009.
- [12] P. H. M. Feron, "Challenges in capture processes: The way forward," *Oil Gas Sci. Technol.*, vol. 60, no. 3, pp. 509–510, 2005.
- [13] J. D. Figueroa, T. Fout, S. Plasynski, H. McIlvried, and R. D. Srivastava, "Advances in CO₂ capture technology-The U.S. Department of Energy's Carbon Sequestration Program," *Int. J. Greenh. Gas Control*, vol. 2, no. 1, pp. 9–20, 2008.
- [14] K. Stéphenne, "Start-up of world's first commercial post-combustion coal fired ccs project: Contribution of shell consolv to saskpower boundary dam iccs project," *Energy Procedia*, vol. 63, pp. 6106–6110, 2014.
- [15] N. MacDowell, N. Florin, A. Buchard, J. Hallett, A. Galindo, G. Jackson, C. S. Adjiman, C. K. Williams, N. Shah, and P. Fennell, "An overview of CO₂ capture technologies," *Energy Environ. Sci.*, vol. 3, no. 11, p. 1645, 2010.
- [16] S. A. Mazari, B. Si Ali, B. M. Jan, I. M. Saeed, and S. Nizamuddin, "An overview of solvent management and emissions of amine-based CO₂ capture technology," *Int. J. Greenh. Gas Control*, vol. 34, pp. 129–140, 2015.

- [17] J. N. Knudsen, J. N. Jensen, P. J. Vilhelmsen, and O. Biede, "Experience with CO₂ capture from coal flue gas in pilot-scale: Testing of different amine solvents," *Energy Procedia*, vol. 1, no. 1, pp. 783–790, 2009.
- [18] W. Zhang, H. Liu, Y. Sun, J. Cakstins, C. Sun, and C. E. Snape, "Parametric study on the regeneration heat requirement of an amine-based solid adsorbent process for post-combustion carbon capture," *Appl. Energy*, vol. 168, pp. 394–405, 2016.
- [19] K. Goto, K. Yogo, and T. Higashii, "A review of efficiency penalty in a coal-fired power plant with post-combustion CO₂ capture," *Appl. Energy*, vol. 111, pp. 710–720, 2013.
- [20] B. Dutcher, M. Fan, and A. G. Russell, "Amine-based CO₂ capture technology development from the beginning of 2013-A review," *ACS Appl. Mater. Interfaces*, vol. 7, no. 4, pp. 2137–2148, 2015.
- [21] C. Gouedard, D. Picq, F. Launay, and P. L. Carrette, "Amine degradation in CO₂ capture. I. A review," *Int. J. Greenh. Gas Control*, vol. 10, pp. 244–270, 2012.
- [22] M. Wilson, P. Tontiwachwuthikul, A. Chakma, R. Idem, A. Veawab, A. Aroonwilas, D. Gelowitz, J. Barrie, and C. Mariz, "Test results from a CO₂ extraction pilot plant at boundary dam coal-fired power station," *Energy*, vol. 29, no. 9–10, pp. 1259–1267, 2004.
- [23] C. M. Quintella, S. A. Hatimondi, A. P. S. Musse, S. F. Miyazaki, G. S. Cerqueira, and A. De Araujo Moreira, "CO₂ capture technologies: An overview with technology assessment based on patents and articles," *Energy Procedia*, vol. 4, pp. 2050–2057, 2011.
- [24] B. Li, Y. Duan, D. Luebke, and B. Morreale, "Advances in CO₂ capture technology: A patent review," *Appl. Energy*, vol. 102, pp. 1439–1447, 2013.
- [25] S. Choi, J. H. Drese, and C. W. Jones, "Adsorbent materials for carbon dioxide capture from large anthropogenic point sources," *ChemSusChem*, vol. 2, no. 9, pp. 796–854, 2009.
- [26] A. Samanta, A. Zhao, G. K. H. Shimizu, P. Sankar, and R. Gupta, "Post-combustion CO₂ capture using solid sorbents: A review," *Ind. Eng. Chem. Res.*, vol. 51, no. 4, pp. 1438–1463, 2012.
- [27] T. O. Nelson, L. J. I. Coleman, A. Kataria, M. Lail, M. Soukri, D. V. Quang, and M. R. M. A. Zahra, "Advanced solid sorbent-based CO₂ capture process," *Energy Procedia*, vol. 63, pp. 2216–2229, 2014.
- [28] J. C. Glier and E. S. Rubina, "Assessment of solid sorbents as a competitive post-combustion CO₂ capture technology," *Energy Procedia*, vol. 37, pp. 65–72, 2013.
- [29] H. Krutka, S. Sjoström, T. Starns, M. Dillon, and R. Silverman, "Post-combustion CO₂ capture using solid sorbents: 1 MW e pilot evaluation," *Energy Procedia*, vol. 37, pp. 73–88, 2013.
- [30] G. D. Pirngruber, F. Guillou, A. Gomez, and M. Clausse, "A theoretical analysis of the energy consumption of post-combustion CO₂ capture processes by temperature swing adsorption using solid sorbents," *Int. J. Greenh. Gas Control*, vol. 14, pp. 74–83, 2013.
- [31] R. Veneman, T. Hilbers, D. W. F. Brilman, and S. R. A. Kersten, "CO₂ capture in a continuous gas-solid trickle flow reactor," *Chem. Eng. J.*, vol. 289, pp. 191–202, 2016.
- [32] E. E. Ünveren, B. Ö. Monkul, Ş. Sarioğlan, N. Karademir, and E. Alper, "Solid amine sorbents for CO₂ capture by chemical adsorption: A review," *Petroleum*, vol. 3, no. 1, pp. 37–50, 2017.
- [33] S. Sjoström, H. Krutka, T. Starns, and T. Campbell, "Pilot test results of post-combustion CO₂ capture using solid sorbents," *Energy Procedia*, vol. 4, pp. 1584–1592, 2011.
- [34] T. Starns, S. Sjoström, H. Krutka, C. Wilson, and M. Ivie, "Solid Sorbents as a Retrofit CO₂ Capture Technology: Update on 1 MWe Pilot Progress," pp. 1–12, 2012.
- [35] T. O. Nelson, A. Kataria, P. Mobley, M. Soukri, and J. Tanthana, "RTI's Solid Sorbent-Based CO₂ Capture Process: Technical and Economic Lessons Learned for Application in Coal-fired, NGCC, and Cement Plants," *Energy Procedia*, vol. 114, no. November 2016, pp. 2506–2524, 2017.
- [36] T. Pröll, G. Schöny, G. Sprachmann, and H. Hofbauer, "Introduction and evaluation of a double loop staged fluidized bed system for post-combustion CO₂ capture using solid sorbents in a continuous temperature swing adsorption process," *Chem. Eng. Sci.*, vol. 141, pp. 166–174, 2016.
- [37] G. Schöny, "Post Combustion CO₂ Capture based on Temperature Swing Adsorption – from Process Evaluation to Continuous Bench Scale Operation," *PhD Thesis, Inst. Chem. Eng. Vienna*

- Univ. Technol. Vienna, Austria, 2015.*
- [38] F. Dietrich, "A novel system for continuous temperature swing adsorption: parameter study at bench scale," *Master thesis, Inst. Chem. Eng. Vienna Univ. Technol. Vienna, Austria, 2014.*
- [39] T. Ringhofer, "First Operation of a Novel Fluidized Bed Reactor System for Continuous Solid-Sorbent CO₂ Capture," *Master thesis, Inst. Chem. Eng. Vienna Univ. Technol. Vienna, Austria, 2014.*
- [40] D. Kunii and O. Levenspiel, *Fluidization Engineering (2nd Edition)*. 1991.
- [41] D. Geldart, "Types of Gas Fluidization," *Powder Technol.*, vol. 7, pp. 285–292, 1973.
- [42] O. Molerus, "Heat transfer in gas fluidized beds part 1.," *Powder Technol.*, vol. 70, no. 1, pp. 1–14, 1992.
- [43] O. Molerus and W. Mattmann, "Heat transfer in gas fluidized beds part 2. Dependence of heat transfer on gas velocity," *Powder Technol.*, vol. 70, no. 1, pp. 15–20, 1992.
- [44] S. S. Zabrodsky, "Hydrodynamics and Heat Transfer in Fluidized Beds," *MIT Press*, 1966.
- [45] H. Martin, "Heat transfer between Gas Fluidized Beds of Solid Particles and the Surfaces of Immersed Heat Exchanger Elements, Part 1," *Chem. Eng. Process.*, vol. 18, no. 3, pp. 157–169, 1984.
- [46] S. W. Kim, J. Y. Ahn, S. D. Kim, and D. Hyun Lee, "Heat transfer and bubble characteristics in a fluidized bed with immersed horizontal tube bundle," *Int. J. Heat Mass Transf.*, vol. 46, no. 3, pp. 399–409, 2003.
- [47] J. C. Chen, J. R. Grace, and M. R. Golriz, "Heat transfer in fluidized beds: Design methods," *Powder Technol.*, vol. 150, no. 2 SPEC. ISS., pp. 123–132, 2005.
- [48] H. S. Mickley and D. F. Fairbanks, "Mechanism of heat transfer to fluidized beds," *AIChE J.*, vol. 1 (3), pp. 374–384, 1955.
- [49] D. Bathen and M. Breitbach, *Adsorptionstechnik*. Springer-Verlag Berlin Heidelberg GmbH, 2001.
- [50] E. Sonnleitner, G. Schöny, and H. Hofbauer, "Assessment of zeolite 13X and Lewatit® VP OC 1065 for application in a continuous temperature swing adsorption process for biogas upgrading," *Biomass Convers. Biorefinery*, vol. 8, no. 2, pp. 379–395, 2018.
- [51] N. Hedin, L. Andersson, L. Bergström, and J. Yan, "Adsorbents for the post-combustion capture of CO₂ using rapid temperature swing or vacuum swing adsorption," *Appl. Energy*, vol. 104, pp. 418–433, 2013.
- [52] A. D. Ebner, M. L. Gray, N. G. Chisholm, Q. T. Black, D. D. Mumford, M. A. Nicholson, and J. A. Ritter, "Suitability of a solid amine sorbent for CO₂ capture by pressure swing adsorption," *Ind. Eng. Chem. Res.*, vol. 50, no. 9, pp. 5634–5641, 2011.
- [53] S. Sjostrom and H. Krutka, "Evaluation of solid sorbents as a retrofit technology for CO₂ capture," *Fuel*, vol. 89, no. 6, pp. 1298–1306, 2010.
- [54] W. Zhao, Z. Zhang, Z. Li, and N. Cai, "Investigation of thermal stability and continuous CO₂ capture from flue gases with supported amine sorbent," *Ind. Eng. Chem. Res.*, vol. 52, no. 5, pp. 2084–2093, 2013.
- [55] J. C. Abanades, E. S. Rubin, and E. J. Anthony, "Sorbent Cost and Performance in CO₂ Capture Systems," *Ind. Eng. Chem. Res.*, vol. 43, pp. 3462–3466, 2004.
- [56] S. Lee, T. P. Filburn, M. Gray, J. W. Park, and H. J. Song, "Screening test of solid amine sorbents for CO₂ capture," *Ind. Eng. Chem. Res.*, vol. 47, no. 19, pp. 7419–7423, 2008.
- [57] M. L. Gray, Y. Soong, K. J. Champagne, H. Pennline, J. P. Baltrus, R. W. Stevens, R. Khatri, S. S. C. Chuang, and T. Filburn, "Improved immobilized carbon dioxide capture sorbents," *Fuel Process. Technol.*, vol. 86, no. 14–15, pp. 1449–1455, 2005.
- [58] M. L. Gray, J. S. Hoffman, D. C. Hreha, D. J. Fauth, S. W. Hedges, K. J. Champagne, and H. W. Pennline, "Parametric study of solid amine sorbents for the capture of carbon dioxide," *Energy and Fuels*, vol. 23, no. 10, pp. 4840–4844, 2009.
- [59] C. Dhoke, S. Cloete, S. Krishnamurthy, H. Seo, I. Luz, M. Soukri, Y. Park, R. Blom, S. Amini, and A. Zabout, "Sorbents screening for post-combustion CO₂ capture via combined temperature and pressure swing adsorption," *Chem. Eng. J.*, 2019.

- [60] J. Wang, L. Huang, R. Yang, Z. Zhang, J. Wu, Y. Gao, Q. Wang, D. O'Hare, and Z. Zhong, "Recent advances in solid sorbents for CO₂ capture and new development trends," *Energy Environ. Sci.*, vol. 7, no. 11, pp. 3478–3518, 2014.
- [61] M. Hefti, L. Joss, D. Marx, and M. Mazzotti, "An Experimental and Modeling Study of the Adsorption Equilibrium and Dynamics of Water Vapor on Activated Carbon," *Ind. Eng. Chem. Res.*, vol. 54, no. 48, pp. 12165–12176, 2015.
- [62] J. S. Lee, J. H. Kim, J. T. Kim, J. K. Suh, J. M. Lee, and C. H. Lee, "Adsorption equilibria of CO₂ on zeolite 13X and zeolite X/activated carbon composite," *J. Chem. Eng. Data*, vol. 47, no. 5, pp. 1237–1242, 2002.
- [63] T. C. Drage, A. Arenillas, K. M. Smith, and C. E. Snape, "Thermal stability of polyethylenimine based carbon dioxide adsorbents and its influence on selection of regeneration strategies," *Microporous Mesoporous Mater.*, vol. 116, no. 1–3, pp. 504–512, 2008.
- [64] F. Rezaei and C. W. Jones, "Stability of supported amine adsorbents to SO₂ and NO_x in postcombustion CO₂ capture. 2. Multicomponent adsorption," *Ind. Eng. Chem. Res.*, vol. 53, no. 30, pp. 12103–12110, 2014.
- [65] W. J. Son, J. S. Choi, and W. S. Ahn, "Adsorptive removal of carbon dioxide using polyethyleneimine-loaded mesoporous silica materials," *Microporous Mesoporous Mater.*, vol. 113, no. 1–3, pp. 31–40, 2008.
- [66] F. Dietrich, "Experimental Studies on a Multi-Stage Fluidized Bed System for Post-Combustion CO₂ capture," *PhD Thesis, Inst. Chem. Eng. Vienna Univ. Technol. Vienna, Austria*, 2019.
- [67] A. H. Berger and A. S. Bhowan, "Optimizing solid sorbents for CO₂ capture," *Energy Procedia*, vol. 37, no. 650, pp. 25–32, 2013.
- [68] K. S. W. Sing, D. H. Everett, R. A. W. Haul, L. Moscou, R. A. Pierotti, J. Rouquerol, and T. Siemieniowska, "Reporting physisorption data for gas/solid systems with special reference to the determination of surface area and porosity," *Pure Appl. Chem.*, vol. 57, no. 4, pp. 603–619, 1985.
- [69] S. Sjöström, "Evaluation of Solid Sorbents As a Retrofit Technology for CO₂ Capture From Coal-Fired Power Plants," no. 05649, 2011.
- [70] W. C. Yang and J. Hoffman, "Exploratory design study on reactor configurations for carbon dioxide capture from conventional power plants employing regenerable solid sorbents," *Ind. Eng. Chem. Res.*, vol. 48, no. 1, pp. 341–351, 2009.
- [71] R. Veneman, N. Frigka, W. Zhao, Z. Li, S. Kersten, and W. Brilman, "Adsorption of H₂O and CO₂ on supported amine sorbents," *Int. J. Greenh. Gas Control*, vol. 41, pp. 268–275, 2015.
- [72] J. Pirklbauer, G. Schöny, T. Pröll, and H. Hofbauer, "Impact of stage configurations, lean-rich heat exchange and regeneration agents on the energy demand of a multistage fluidized bed TSA CO₂ capture process," *Int. J. Greenh. Gas Control*, vol. 72, no. March, pp. 82–91, 2018.
- [73] G. Schöny, E. Zehetner, J. Fuchs, T. Pröll, G. Sprachmann, and H. Hofbauer, "Design of a bench scale unit for continuous CO₂ capture via temperature swing adsorption — Fluid-dynamic feasibility study," *Chem. Eng. Res. Des.*, vol. 106, pp. 155–167, 2015.
- [74] J. C. Abanades, B. Arias, A. Lyngfelt, T. Mattisson, D. E. Wiley, H. Li, M. T. Ho, E. Mangano, and S. Brandani, "Emerging CO₂ capture systems," *Int. J. Greenh. Gas Control*, vol. 40, pp. 126–166, 2015.
- [75] B. Metz and L. A. M. (eds. . O. Davidson, H. C. de Coninck, M. Loos, "IPCC, 2005: IPCC Special Report on Carbon Dioxide Capture and Storage. Prepared by Working Group III of the Intergovernmental Panel on Climate Change," *Cambridge Univ. Press*, 2005.
- [76] Y. C. Park, S. H. Jo, C. K. Ryu, and C. K. Yi, "Demonstration of pilot scale carbon dioxide capture system using dry regenerable sorbents to the real coal-fired power plant in Korea," *Energy Procedia*, vol. 4, pp. 1508–1512, 2011.
- [77] M. Heftia, D. Marx, L. Jossa, and M. Mazzottia, "Model-based process design of adsorption processes for CO₂ capture in the presence of moisture," *Energy Procedia*, vol. 63, pp. 2152–2159, 2014.
- [78] J. Pirklbauer, "The development and application of a multi-component adsorption model for a

- temperature swing adsorption process in the field of post combustion CO₂ capture - From Particle to Process Integration," *PhD Thesis, Inst. Chem. Eng. Vienna Univ. Technol. Vienna, Austria*, 2019.
- [79] R. Serna-Guerrero, Y. Belmabkhout, and A. Sayari, "Modeling CO₂ adsorption on amine-functionalized mesoporous silica: 1. A semi-empirical equilibrium model," *Chem. Eng. J.*, vol. 161, no. 1–2, pp. 173–181, 2010.
- [80] Q. Yu, J. D. L. P. Delgado, R. Veneman, and D. W. F. Brilman, "Stability of a Benzyl Amine Based CO₂ Capture Adsorbent in View of Regeneration Strategies," *Ind. Eng. Chem. Res.*, vol. 56, no. 12, pp. 3259–3269, 2017.
- [81] Website_Wien_Energie, "Wien Energie Webpage," 2020. <https://www.wienenergie.at/eportal3/ep/channelView.do/pageTypeld/67831/channelId/-48494> (accessed May 25, 2020).
- [82] E-Control, "Ökostrombericht 2018," 2018.
- [83] H. J. Natusch, B. Neukirchen, and R. Noack, "Lokale Wärmeübergangskoeffizienten für ein Einzelrohr und für Rohrbündel verschiedener Anordnung in Wirbelschichten," *Forschungs-Gesellschaft Verfahrenstechnik e.V.*, 1975.
- [84] O. Molerus, A. Burschka, and S. Dietz, "Particle migration at solid surfaces and heat transfer in bubbling fluidized beds-II. Prediction of heat transfer in bubbling fluidized beds," *Chem. Eng. Sci.*, vol. 50, no. 5, pp. 879–885, 1995.
- [85] H. Martin, "Wärmeübergang in der Wirbelschicht," in *VDI Wärmeatlas*, VOL. 52., Springer Berlin Heidelberg, 2010, pp. 1301–1310.
- [86] G. Hofer, J. Fuchs, G. Schöny, and T. Pröll, "Heat transfer challenge and design evaluation for a multi-stage temperature swing adsorption process," *Powder Technol.*, vol. 316, pp. 512–518, 2017.
- [87] G. Hofer, G. Schöny, J. Fuchs, and T. Pröll, "Investigating wall-to-bed heat transfer in view of a continuous temperature swing adsorption process," *Fuel Process. Technol.*, vol. 169, no. June 2017, pp. 157–169, 2018.
- [88] G. Hofer, "Fluidized bed heat transfer and solids mixing in view of a post-combustion carbon capture process," *PhD Thesis, Univ. Nat. Resour. Life Sci. Vienna, Austria*, vol. 69, no. 1, pp. 134–136, 2017.
- [89] E. Zehetner, "Cold Flow Model Study on a Sorbent Based Multistage Fluidized Bed System for Continuous CO₂ Capture," *PhD Thesis, Inst. Chem. Eng. Vienna Univ. Technol. Vienna, Austria*, 2017.
- [90] G. Hofer, G. Schöny, and T. Pröll, "Acting on hydrodynamics to improve the local bed-to-wall heat transfer in bubbling fluidized beds," *Chem. Eng. Res. Des.*, vol. 134, pp. 309–318, 2018.
- [91] S. Lechner, M. Merzsch, and H. J. Krautz, "Heat-transfer from horizontal tube bundles into fluidized beds with Geldart A lignite particles," *Powder Technol.*, vol. 253, pp. 14–21, 2014.
- [92] H. Löfstrand, A. E. Almstedt, and S. Andersson, "Dimensionless expansion model for bubbling fluidized beds with and without internal heat exchanger tubes," *Chem. Eng. Sci.*, vol. 50, no. 2, pp. 245–253, 1995.
- [93] E. Zehetner, G. Schöny, and H. Hofbauer, "L-valve design study for a continuous temperature swing adsorption CO₂ capture unit," *12th Int. Conf. Fluid. Bed Technol. CFB 2017*, pp. 199–206, 2017.
- [94] R. S. Franchi, P. J. E. Harlick, and A. Sayari, "Applications of pore-expanded mesoporous silica. 2. Development of a high-capacity, water-tolerant adsorbent for CO₂," *Ind. Eng. Chem. Res.*, vol. 44, no. 21, pp. 8007–8013, 2005.
- [95] G. Schöny, F. Dietrich, J. Fuchs, T. Pröll, and H. Hofbauer, "A multi-stage fluidized bed system for continuous CO₂ capture by means of temperature swing adsorption – First results from bench scale experiments," *Powder Technol.*, vol. 316, pp. 519–527, 2017.
- [96] J. Niegsch, D. Köneke, and P. M. Weinspach, "Heat transfer and flow of bulk solids in a moving bed," *Chem. Eng. Process.*, vol. 33, no. 2, pp. 73–89, 1994.
- [97] Website_Solex, "Commercial Heat Exchanger - Efficient Bulk Solids Heating | Solex - Solex,"

-
2020. <https://www.solexthermal.com/products-solutions/heating/> (accessed May 26, 2020).
- [98] E. Zehetner, G. Schöny, J. Fuchs, T. Pröll, and H. Hofbauer, "Fluid-dynamic study on a multistage fluidized bed column for continuous CO₂ capture via temperature swing adsorption," *Powder Technol.*, vol. 316, pp. 528–534, 2017.
- [99] F. Dietrich, G. Schöny, J. Fuchs, and H. Hofbauer, "Experimental study of the adsorber performance in a multi-stage fluidized bed system for continuous CO₂ capture by means of temperature swing adsorption," *Fuel Process. Technol.*, vol. 173, no. January, pp. 103–111, 2018.
- [100] H. T. Bi and J. R. Grace, "Flow regime diagrams for gas-solid fluidization and upward transport," *Int. J. Multiph. Flow*, vol. 21, no. 6, pp. 1229–1236, 1995.

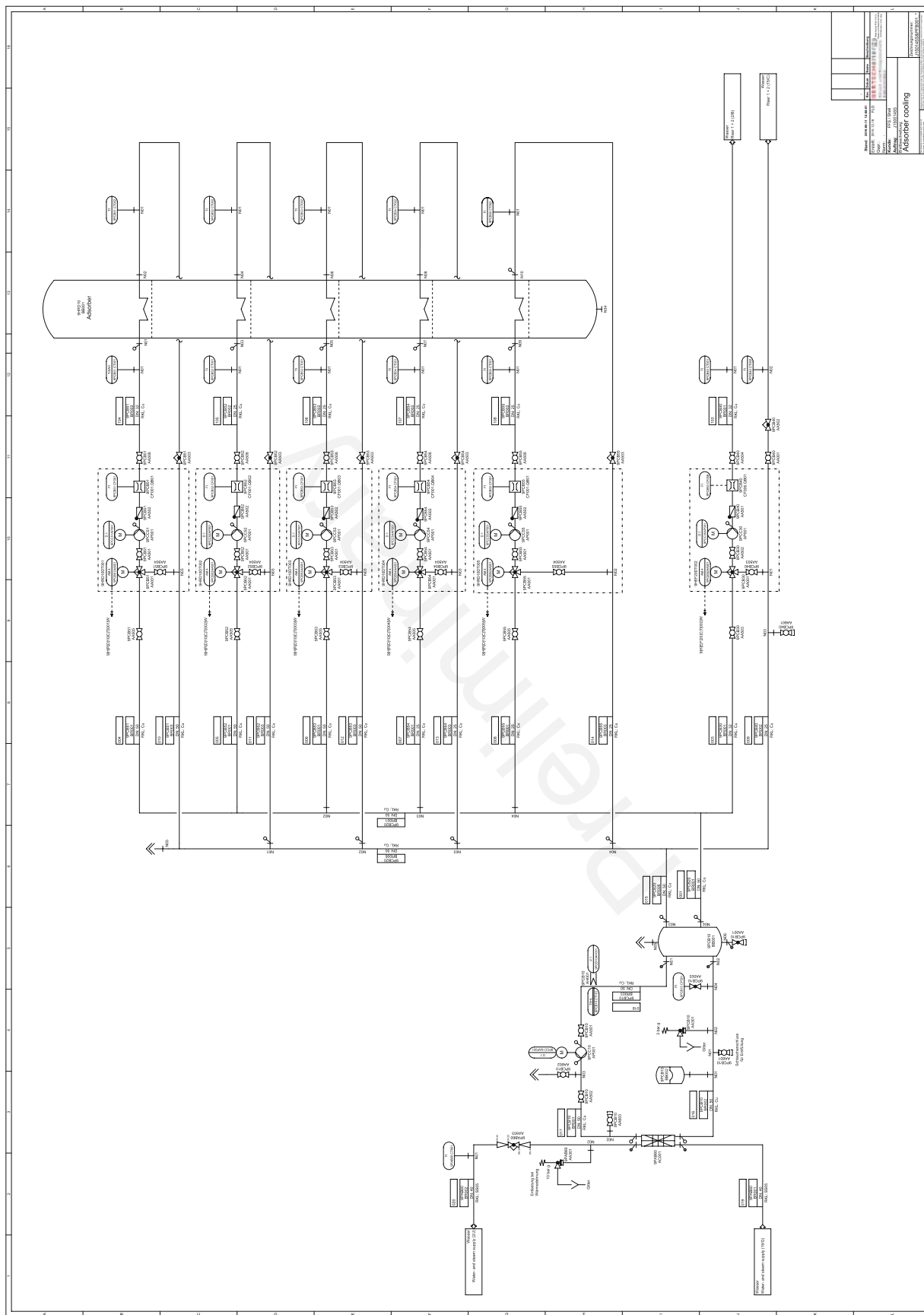
LIST OF PUBLICATIONS

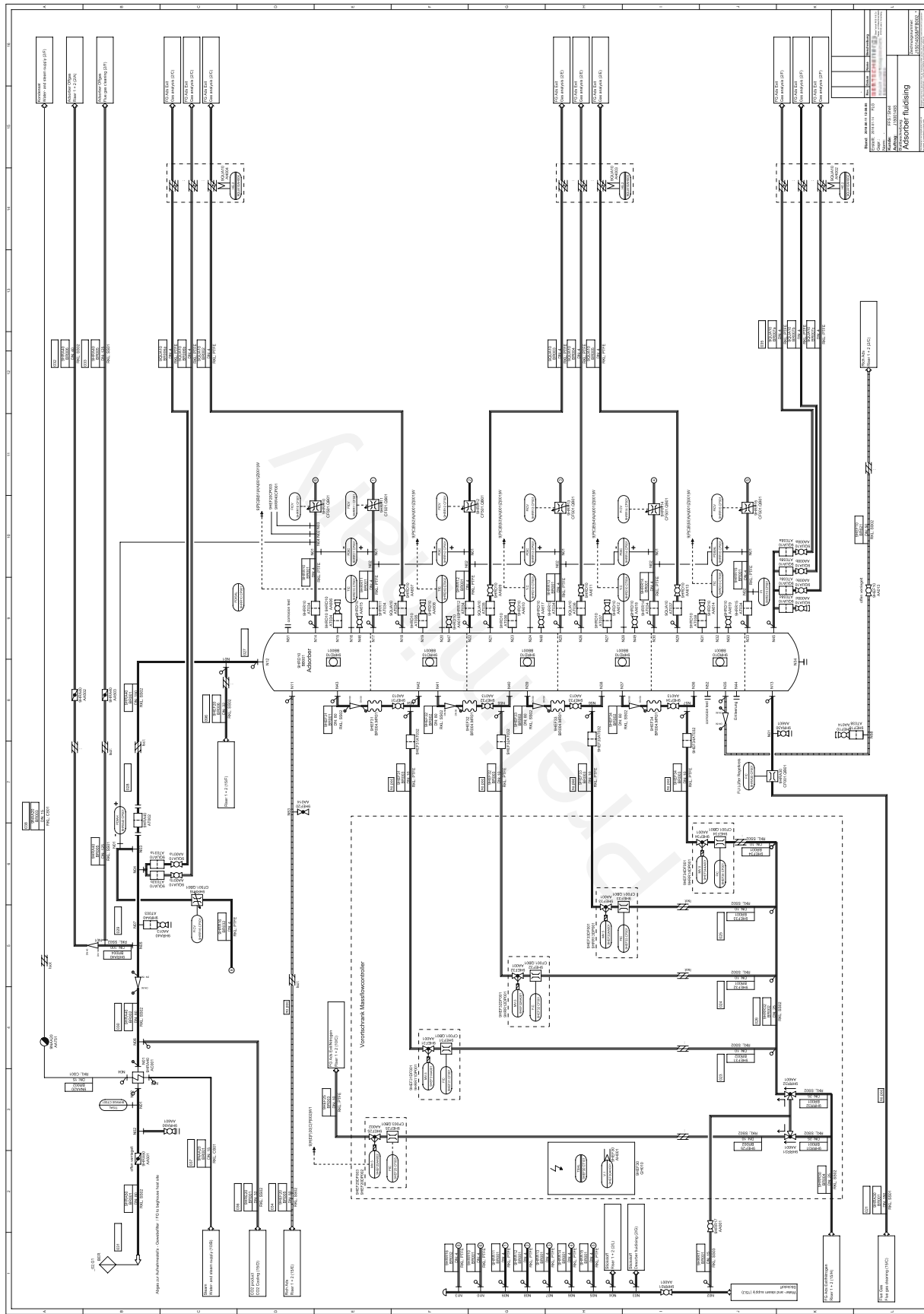
- I. G. Hofer, J. Fuchs, G. Schöny, and T. Pröll, "Heat transfer challenge and design evaluation for a multi-stage temperature swing adsorption process," *Powder Technol.*, vol. 316, pp. 512–518, 2017.
- II. G. Schöny, E. Zehetner, J. Fuchs, T. Pröll, G. Sprachmann, and H. Hofbauer, "Chemical Engineering Research and Design Design of a bench scale unit for continuous CO₂ capture via temperature swing adsorption — Fluid-dynamic feasibility study," *Chem. Eng. Res. Des.*, vol. 106, pp. 155–167, 2015.
- III. G. Hofer, G. Schöny, J. Fuchs, and T. Pröll, "Investigating wall-to-bed heat transfer in view of a continuous temperature swing adsorption process," *Fuel Process. Technol.*, vol. 169, pp. 157–169, 2018.
- IV. F. Dietrich, G. Schöny, J. Fuchs, and H. Hofbauer, "Experimental study of the adsorber performance in a multi-stage fluidized bed system for continuous CO₂ capture by means of temperature swing adsorption," *Fuel Process. Technol.*, vol. 173, no. January, pp. 103–111, 2018.
- V. E. Zehetner, G. Schöny, J. Fuchs, T. Pröll, and H. Hofbauer, "Fluid-dynamic study on a multistage fluidized bed column for continuous CO₂ capture via temperature swing adsorption," *Powder Technol.*, vol. 316, pp. 528–534, 2017.
- VI. G. Hofer, G. Schöny, J. Fuchs, and T. Pröll, "Investigating wall-to-bed heat transfer in view of a continuous temperature swing adsorption process," *Fuel Process. Technol.*, vol. 169, no. June 2017, pp. 157–169, 2018.
- VII. G. Hofer, J. Fuchs, G. Schöny, and T. Pröll, "Heat transfer challenge and design evaluation for a multi-stage temperature swing adsorption process," *Powder Technol.*, vol. 316, pp. 512–518, 2017.
- VIII. G. Schöny, F. Dietrich, J. Fuchs, T. Pröll, and H. Hofbauer, "A multi-stage fluidized bed system for continuous CO₂ capture by means of temperature swing adsorption – First results from bench scale experiments," *Powder Technol.*, vol. 316, pp. 519–527, 2017.
- IX. G. Schöny, J. Fuchs, M. Infantino, J. Van De Graaf, S. Van Paasen, and H. Hofbauer, "Pilot scale demonstration of solid sorbent CO₂ capture technology at a biomass power station SUCCESS View project Post Combustion CO₂ Capture View project Pilot scale demonstration of solid sorbent CO₂ capture technology at a biomass power station," in 14th Greenhouse Gas Control Technologies Conference Melbourne 21-26 October 2018 (GHGT-14).

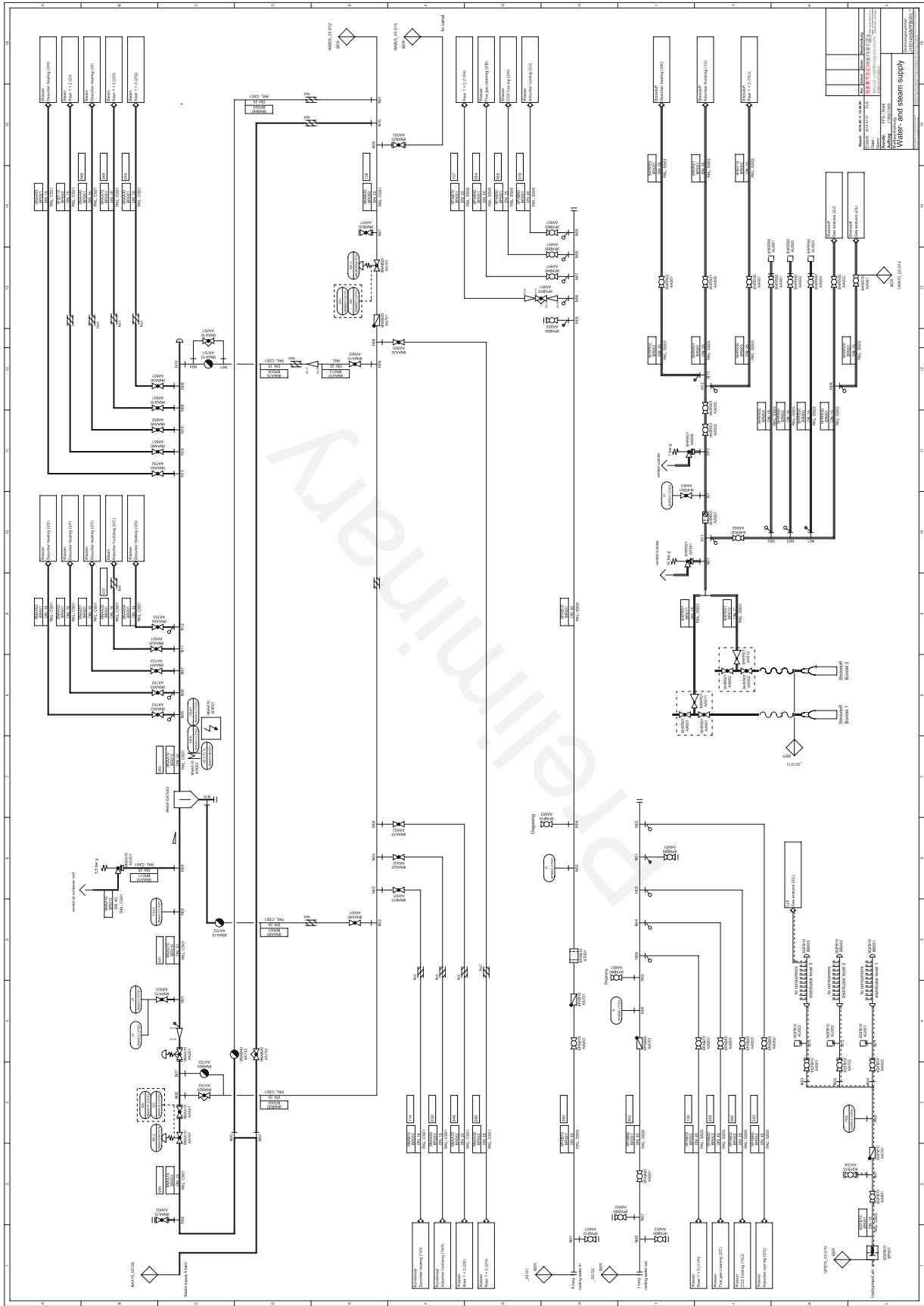
APPENDIX A – VIENNAGREENCO₂ P&IDS

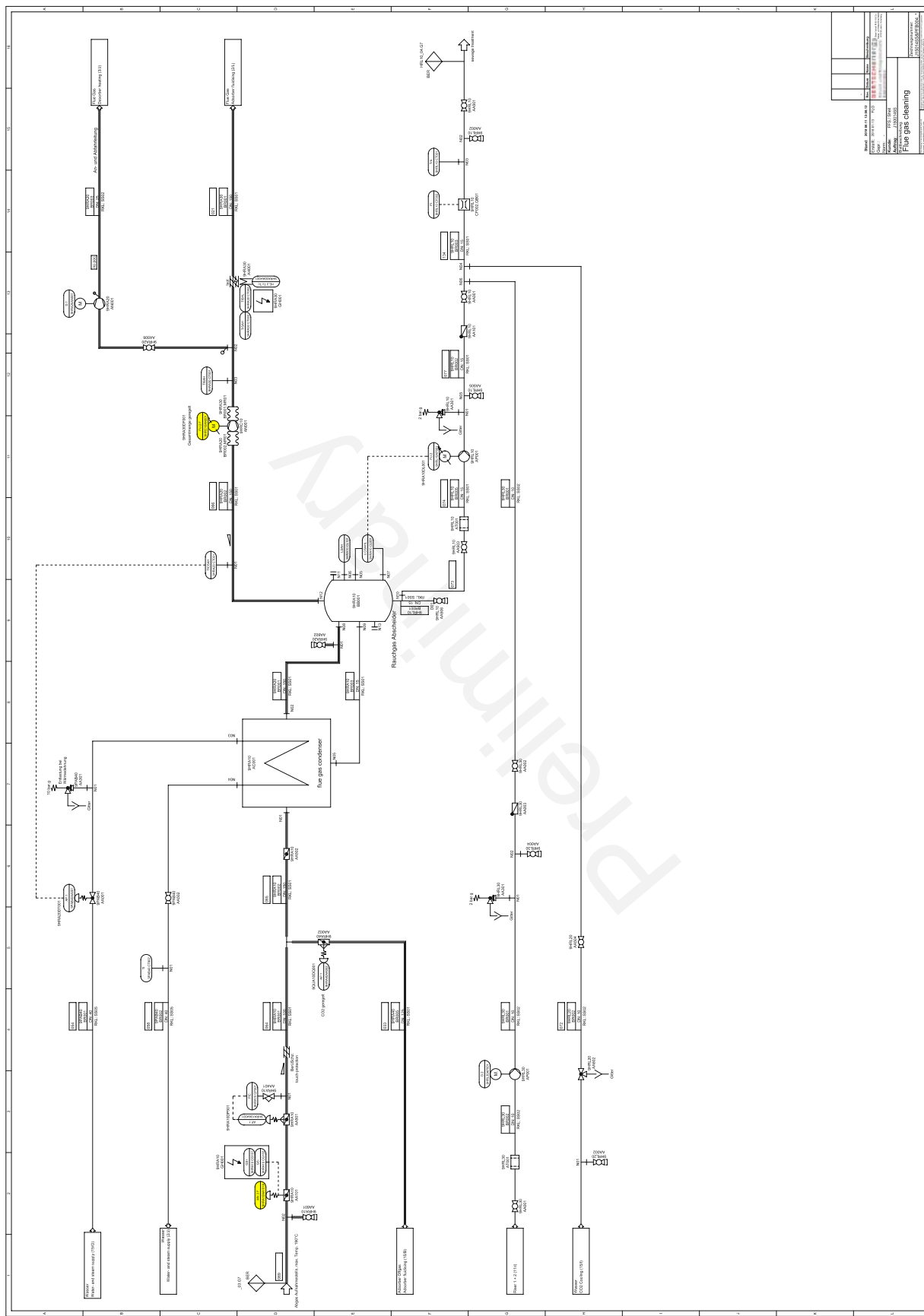
Die approbierte gedruckte Originalversion dieser Dissertation ist an der TU Wien Bibliothek verfügbar.
The approved original version of this doctoral thesis is available in print at TU Wien Bibliothek.

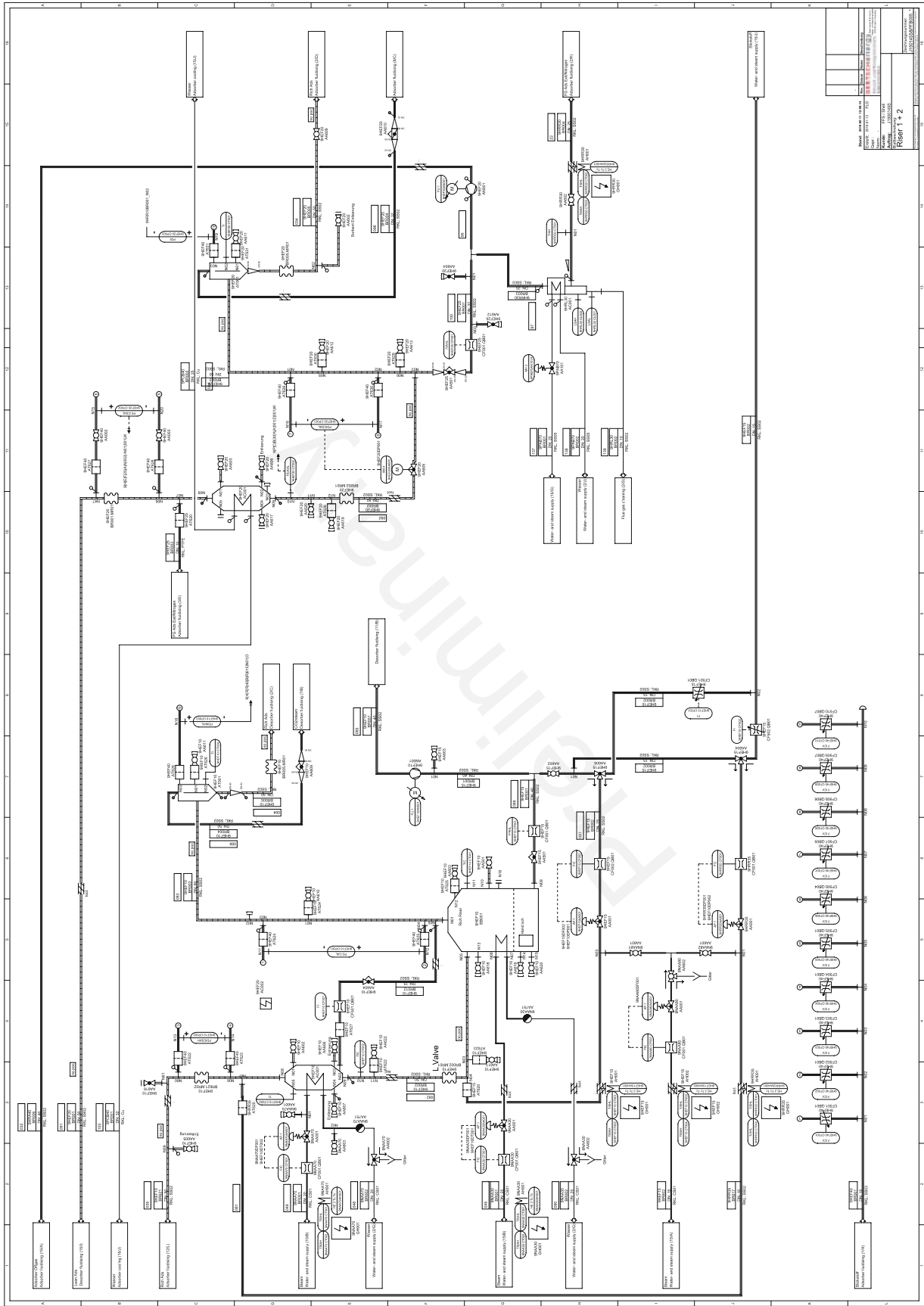


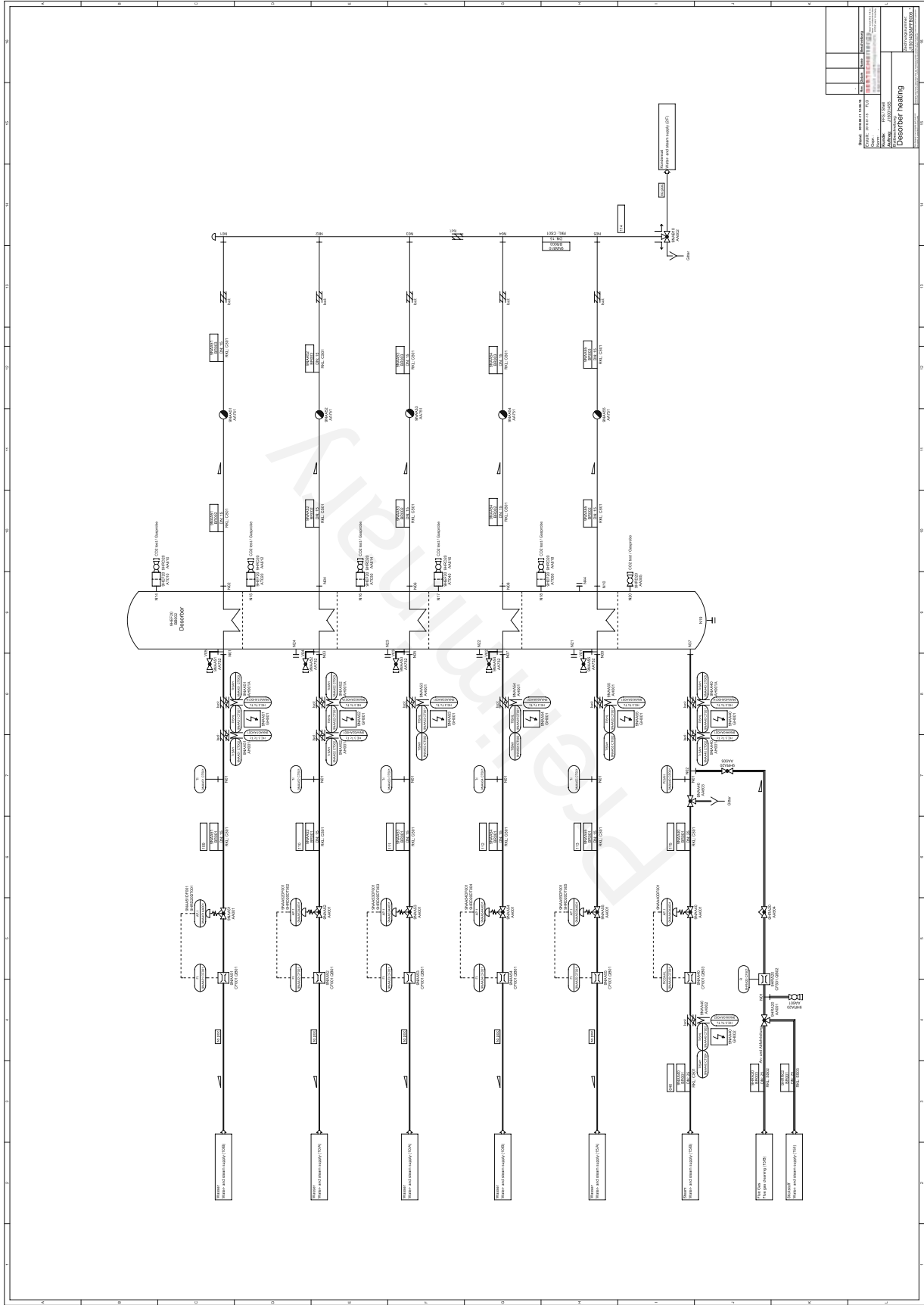


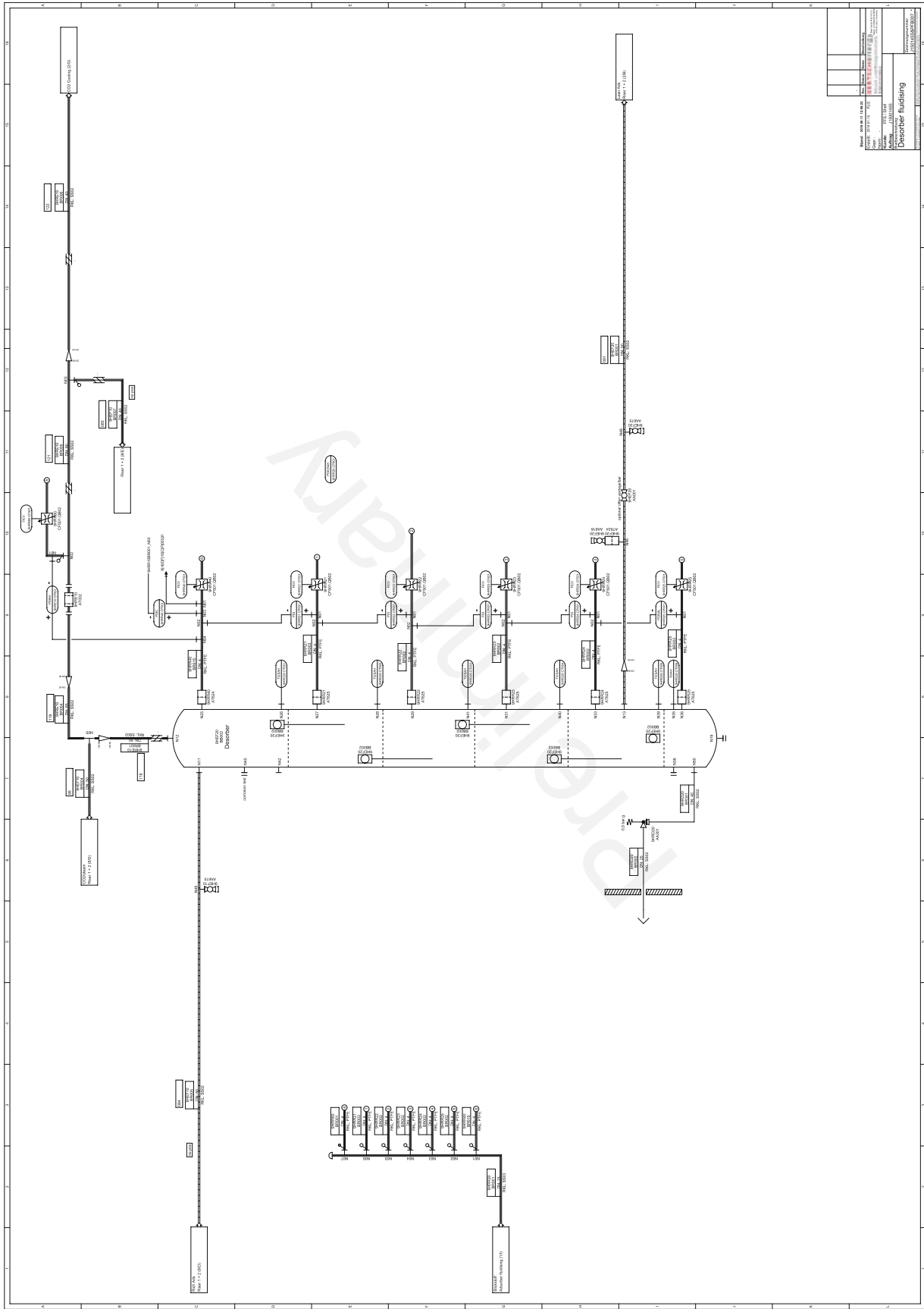


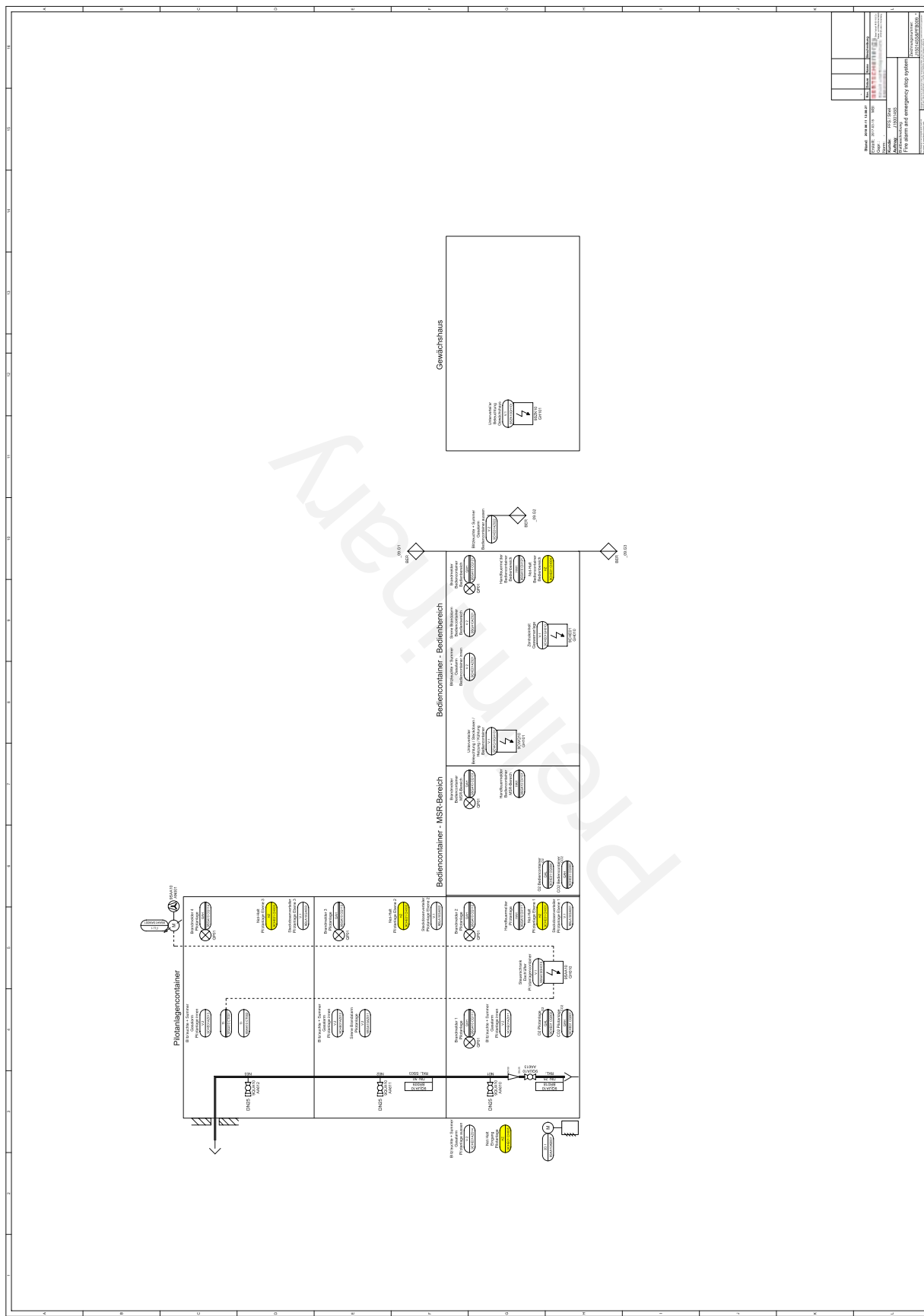


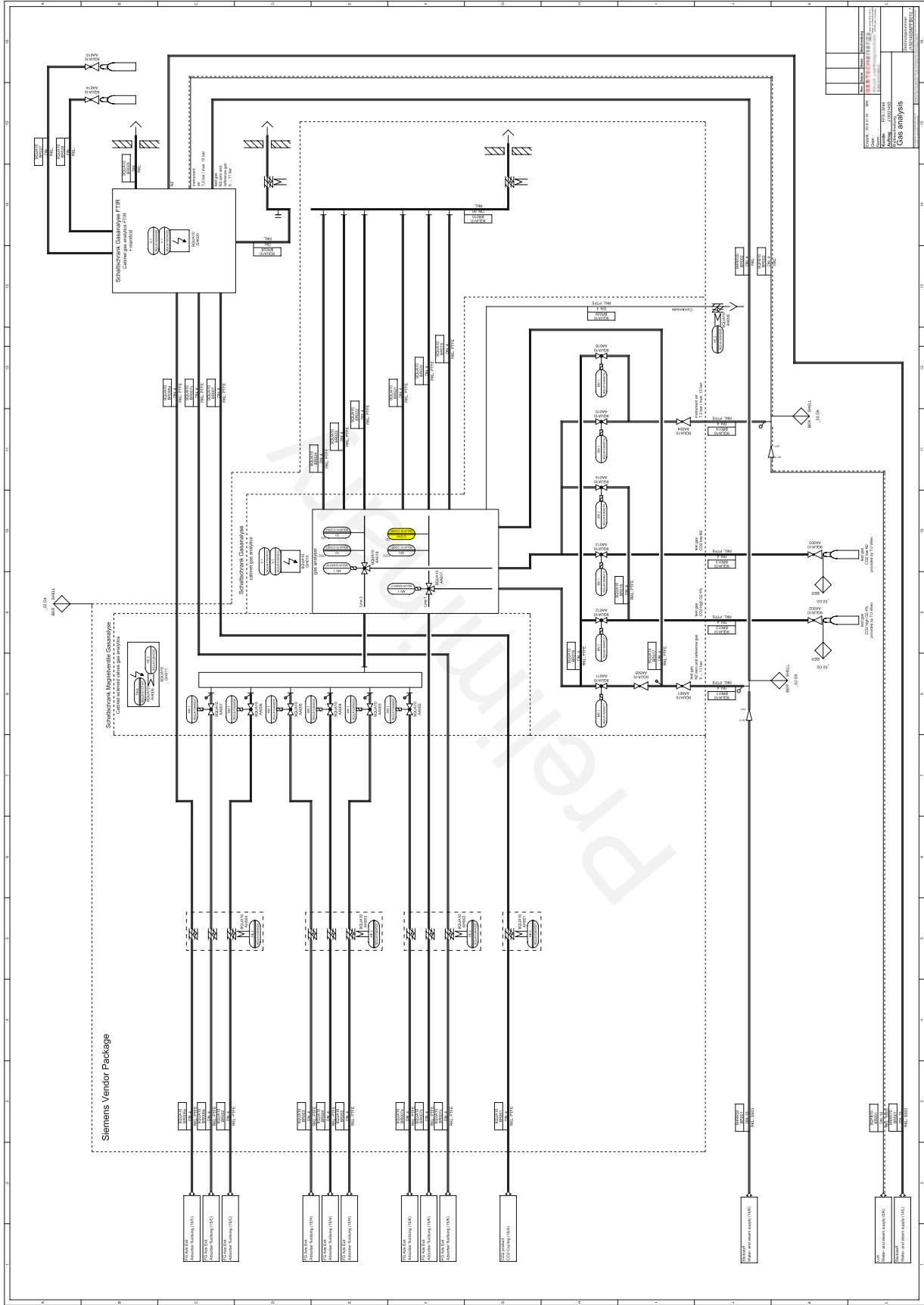


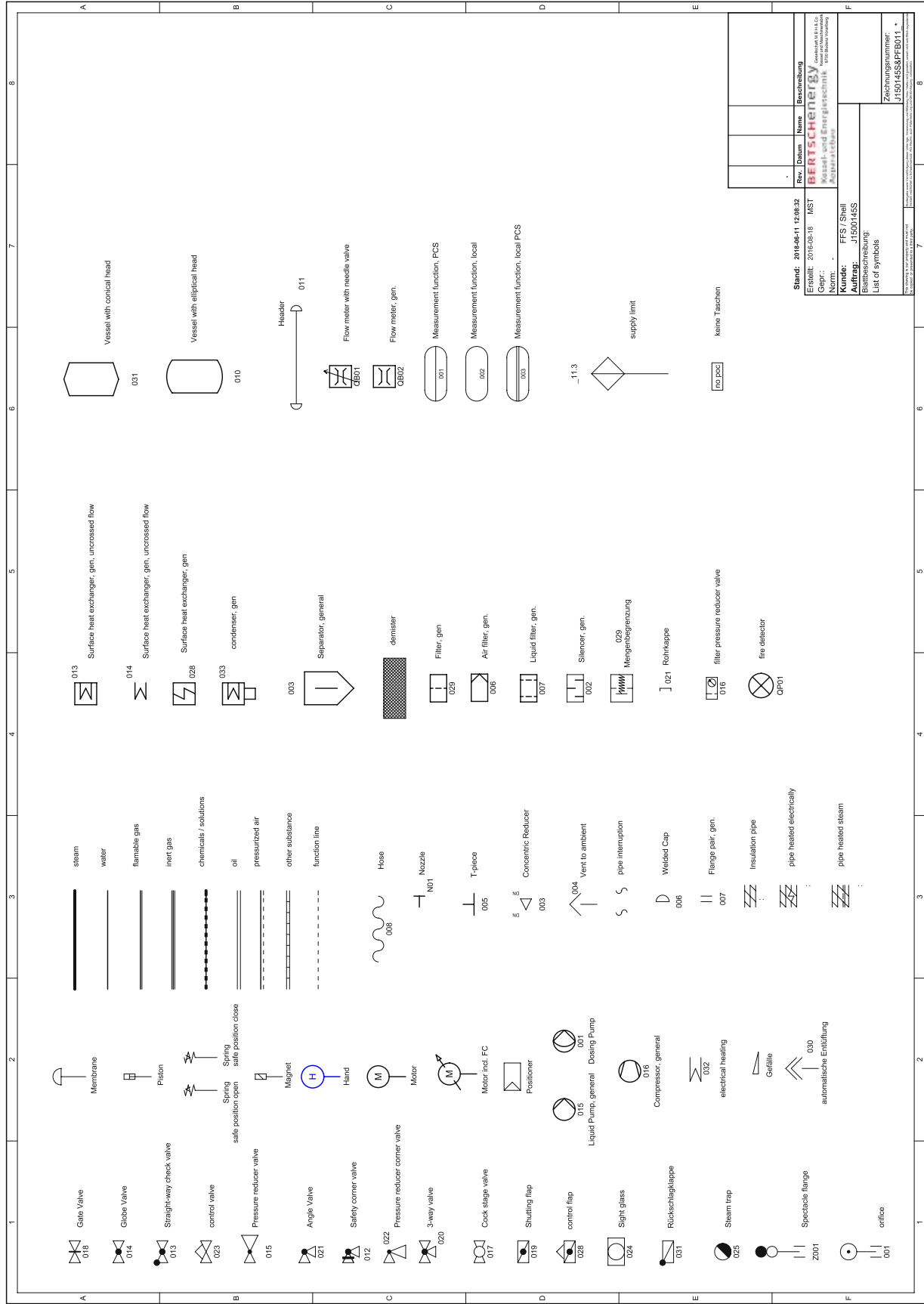




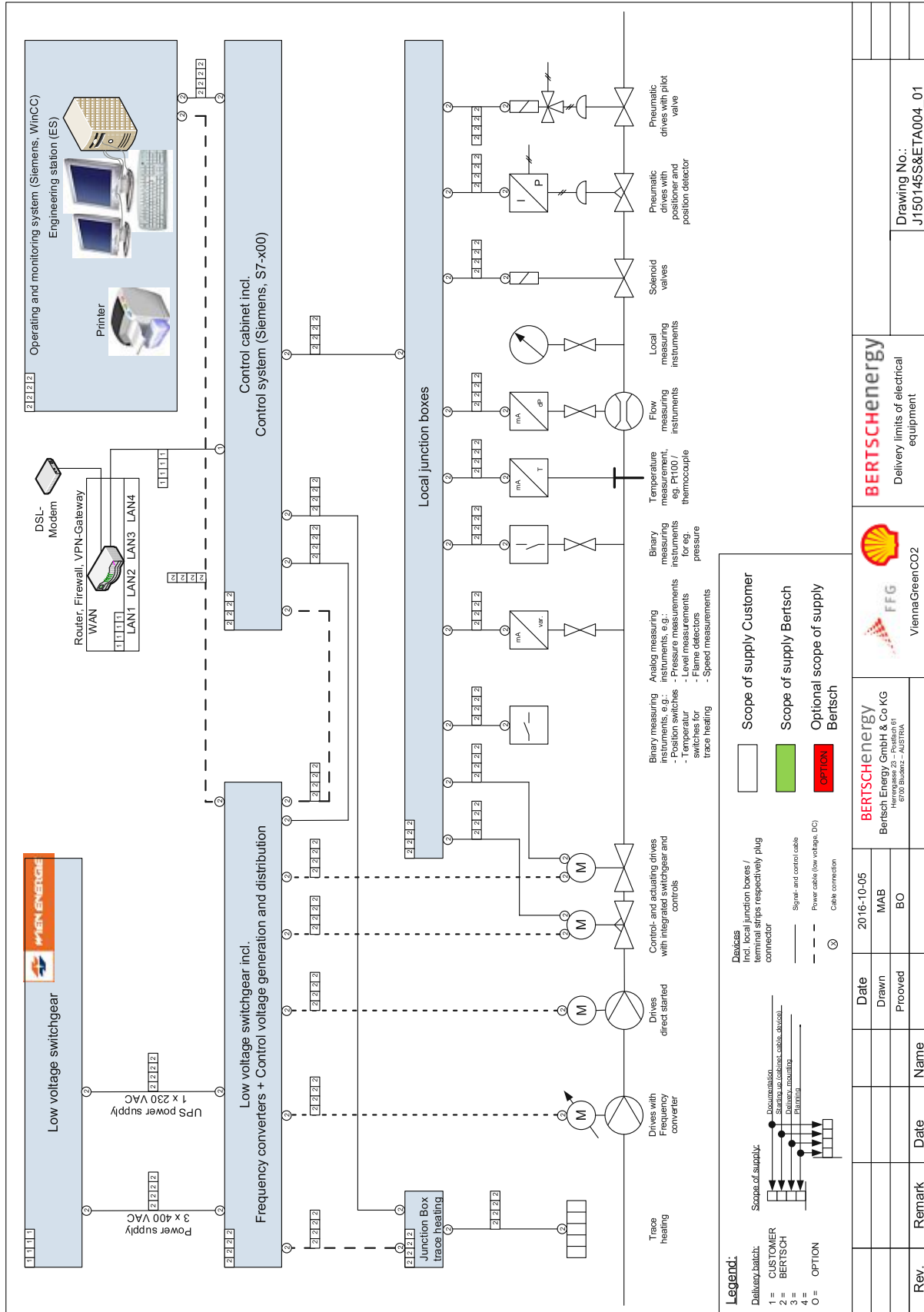


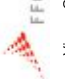







APPENDIX B – PROCESS CONTROL SYSTEM



Rev.	Remark	Date	Name	Date	2016-10-05
			MAB		
			BO		
BERTSCHENERGY Bertsch Energy GmbH & Co KG Hüttelstraße 10 1070 Wien - AUSTRIA					
 ViennaGreenCO2					
 BERTSCHENERGY Delivery limits of electrical equipment					
					Drawing No.: J150145S&ETA004_01